UNIVERSITY OF NEWCASTLE UPON TYNE

DEPARTMENT OF MINING ENGINEERING

NEWCASTLE UNIVERSITY LIBRARY

086 11596 3

Thesis L3118

LABORATORY WATER JET ASSISTED DRAG TOOL ROCK CUTTING STUDIES AT HIGH TRAVERSE SPEEDS

CHUN KEUNG IP

Thesis submitted for the degree of
Doctor of Philosophy of the
University of Newcastle upon Tyne

MAY 1986

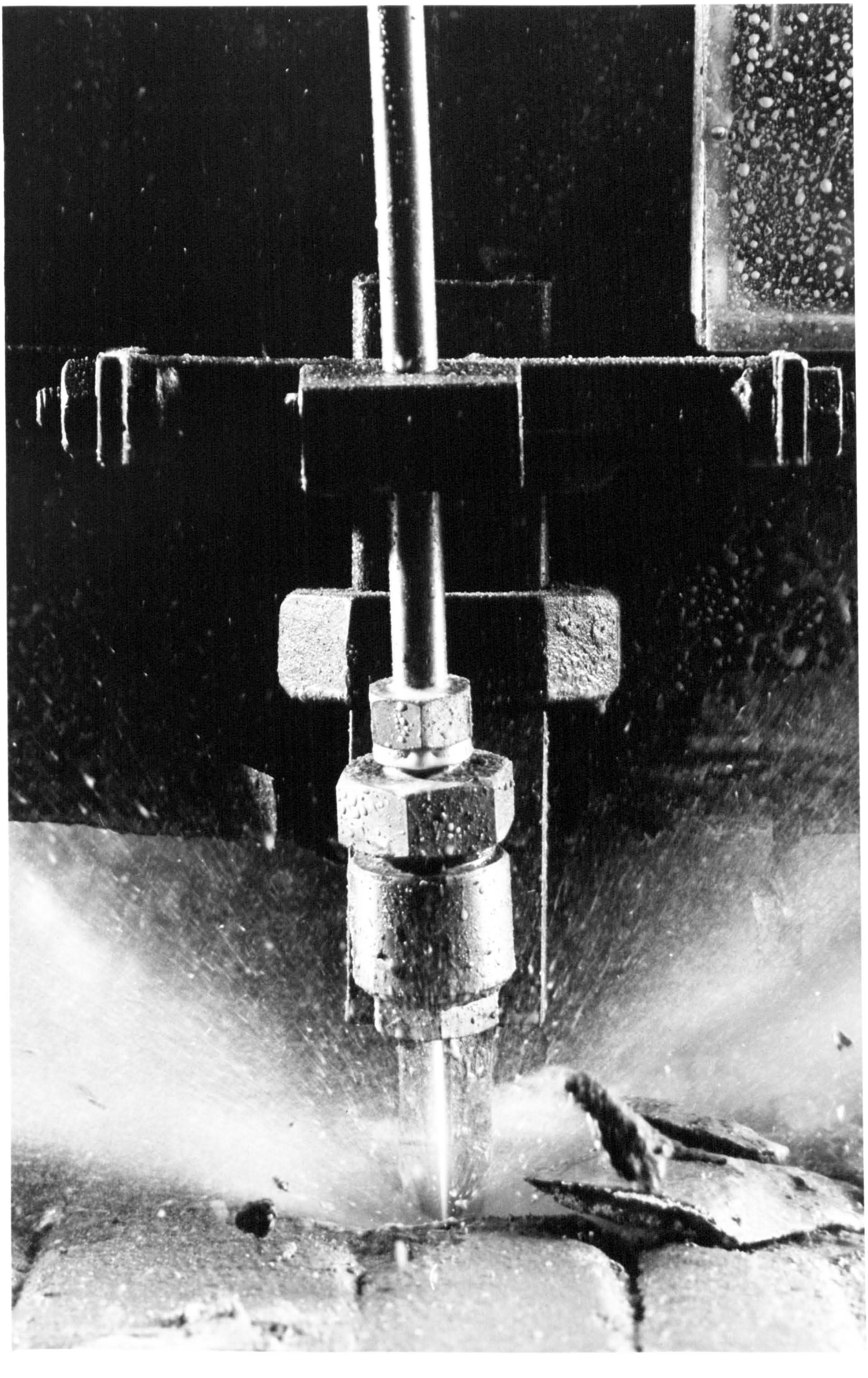

ACKNOWLEDGEMENTS

The author would like to express his gratitude to the following people without whose help much of the research work would not have been possible:

Professor J.F. Tunnicliffe, Head of Department of Mining Engineering and Professor W.R. Dearman, Head of Department of Geotechnical Engineering, University of Newcastle upon Tyne, for providing the opportunity and facilities to carry out this research.

Dr. R.J. Fowell, Reader in Excavation Engineering, for his help, advice and enthusiasm whilst supervising the project.

Dr. C. Morris, the Engineer, for this Project; Dr. K.Hurt, and Dr. K. MacAndrew, of MRDE, NCB, for many valuable and useful discussions.

Dr. S.T. Johnson, for his assistance.

Mr. R. Mahon,previously of the Computing Laboratory of this University, for his advice on the digital data logging program.

Mr. M. McKenna, Laboratory/Workshop Supervisor of the Department of Mining Engineering, and Mr. T. Shepherdson, Laboratory Superintendent of the Department of Geotechnical Engineering and their technical staff, in particular Mr. C. Dixon, for their technical assistance during the laboratory experiments.

Mr. M. Paisley for producing excellent photographs.

Mrs. Edna Gannie for the finest typing obtainable, with kindness and concern as extra, without mentioning the delicious coffee and biscuits.

Mr. D. Panich, Mr. P. Round, Dr. R.Irwin, Mr. L-X Kong, Mr. G-C. Xiao, Mr. S. Minett, Dr. P. Garritty, Dr.O.Hekimoglu, Mr. G. Stripp, Dr. M.L. Athorn, Mr. G. Peace and other research colleagues for their humour and friendship.

Last, but not least, my wife, Christine, for her patience, understanding, help and love to keep me going for the three years of the research.

The author wishes to gratefully acknowledge the National Coal Board, Science and Engineering Research Council and the European Coal and Steel Community, for the financial assistance which has made this work possible.

* * *

CONTENTS

PAGE

PAGE

PAGE

PAGE

PAGE

PAGE

* * *

ABSTRACT

Water jet assistance has shown many promising benefits to drag tool rock cutting. However, the basic failure mechanism of hybrid cutting is not well understood. In addition, most previous laboratory investigations have been carried out with cutting speeds of less than 0.25 m/s, whilst typical tool speeds for a production boom-type tunnelling machine cutting hard rock is over 1.0 m/s. Potentially erroneous conclusions may be obtained unless laboratory cutting speeds are comparable with those used in the practical situation.

Based on the research work carried out under a three-year contract sponsored jointly by the Science and Engineering Research Council and the European Coal and Steel Community, this thesis examines the cutting mechanisms when a water jet and a drag tool are acting together.

Over one thousand cuts have been carried out in five rock types which cover a wide range of strength and abrasivity. A linear cutting rig was modified to enable cutting speeds up to 1.10 m/s to be obtained. Jet pressures up to 70 MPa were provided by a 75-kW water pump.

Based on the cutting mechanisms of the drag tool and the effect of the water jet action, a hybrid cutting model is proposed. To obtain significant tool force reductions, the jet power must be greater than either the threshold jet power for slotting, or a critical jet power for hydraulic fracturing. Depending on the jet power,

rocks can be separated into two groups, one with significant jet penetration and the other without. For rocks with significant jet penetration, the force reductions with water jet assistance can be estimated from the jet penetration characteristic. An optimum jet penetration was found to exist which provided the maximum force reductions. For rocks without jet penetration, the force reduction is marginal except when the jet power exceeds the critical jet power for hydraulic fracturing.

An expression is given which characterises the functional relationship between force reduction and jet penetration. When the jet penetration for the rock is insignificant, an equation is proposed to estimate the critical jet power required.

* * *

PAPERS PUBLISHED

The following papers, which summarise part of the intermediate findings, were published during the period of the research project:

Fowell, R.J. Johnson, S.T. Ip, C.K.	"Further Studies in the Drag Tool Cutting of Rock" 3rd US Water Jet Symposium, Pittsburgh. May 1985.
Ip, C.K. Johnson, S.T. Fowell, R.J.	"Water Jet Rock Cutting and its Application to Tunnelling Machine Performance" 27th US Symposium on Rock Mechanics. Alabama. June 1986.
Fowell, R.J. Ip, C.K. Johnson, S.T.	"Water Jet Assisted Drag Tool Cutting : Parameters for Success" 8th International Symposium on Jet Cutting Technology. Durham, England. Sept. 1986.

* * *

LIST OF FIGURES

PAGE

PAGE

CHAPTER SEVEN -

PAGE

PAGE

PAGE

PAGE

CHAPTER NINE -

* * *

LIST OF TABLES

PAGE

PAGE

* * *

LIST OF PLATES

* * *

NOMENCLATURE

C_d	- Nozzle discharge coefficient
d	- Mechanical Depth of Cut
d_o	- Nozzle Diameter
F	- Force
F_c	- Cutting Force
F_N	- Normal Force
F_R	- Force Reduction
F_{Rmax}	- Maximum Force Reduction
F(m)	- Mechanical Tool Force
F(h-m)	- Hydromechanical Tool Force
h	- Jet Penetration
h_k	- Optimum Jet Penetration
k	- Permeability
MCF	- Mean Cutting Force
MNF	- Mean Normal Force
MPCF	- Mean Peak Cutting Force
MPNF	- Mean Peak Normal Force
P,p	- Jet (nozzle) Pressure
P_o	- Staganation Pressure
P_{th}	- Threshold Jet Pressure
S	- Shear Strength
T	- Time of Exposure
T_o	- Critical Time of Exposure
V	- Traverse Speed

V_o	-	Jet Speed
ρ	-	Water Density
γ	-	Rock Density
σ_c	-	Uniaxial Compressive Strength (UCS)
σ_t	-	Uniaxial Tensile Strength
σ_y	-	Yield Strength
ϕ	-	Angle of Internal Friction
μ	-	Viscosity of Water

(<u>NOTE</u> : Other, more specific, symbols will be deailed in the text.)

*   *   *

CHAPTER ONE

CHAPTER ONE

INTRODUCTION

Currently about 60% of underground roadways in Britain are driven by boom-type roadheaders and coal heading machines equipped with drag tools. Whilst light and medium size roadheaders are still enjoying success in most types of Coal Measures strata, an extension of their application to harder and more abrasive rocks has revealed the shortcomings of these machines due to lack of stability and power in the cutting head. The trend has been to increase the rock cutting ability of roadheaders by building even heavier machines of greater stability and power. As a result, a caterpillar-tracked machine can weigh from 25t to 120t with cutter head motor power from 25 to 150 kW. A summary of roadheaders used for tunnel drivage in National Coal Board (NCB) mines is tabulated in Table 1.1. The trend of increased roadheader power on a chronological scale is shown in Figure 1.1.

While the heavier and stiffer machines can ensure the transmission of power to the tool/rock interface, these suffer from two main drawbacks:

(1) loss of operational flexibility and manoeuvrability due to the wider and larger machine body; and

(2) high tool consumption rates due to excessive pick force causing tool destruction and/or rapid wear.

Type of Machine	Weight (tonne)	Installed Power (kW)	Cutting Head Power (kW)
Dosco			
SL120	33	164	82
MK2A	27	150	67
MK2B	41	194	82
MK3	83	254	142
LH1300	48	335	141
TB600	81	625-750	2 @ 93-225
TB2000	75	426	2 @ 120
Anderson Strathclyde			
RH22	40	180/224	90
RH1-3	50	180	90
RH1-4	66	224	113
Anglo-Soviet	85	300	150
Thyssen			
E169	30-50	165	83
E134	65	290	195
Eimco			
NCB/Eimco	110	300	150

Table 1.1 A summary of roadheaders used for tunnel drivage in NCB (UK) mines.

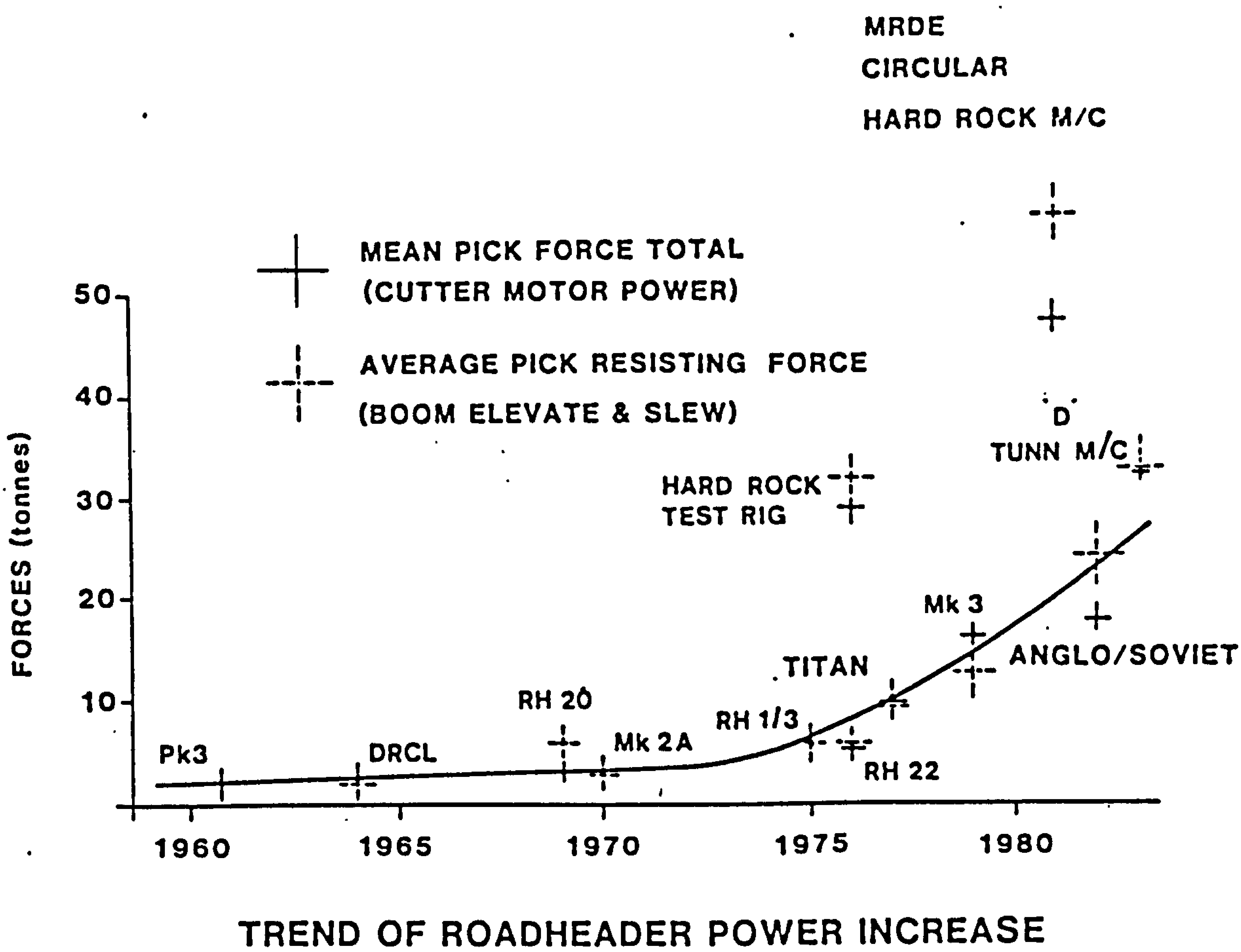

<u>Figure 1.1</u> The trend of Power Increase in Roadheaders (after Barnes 1981).

In order to extend the ability of the roadheader to cut harder rock without paying the penalty of an excessive tool consumption rate and bulky machine body, a means of applying significant extra energy at the cutting head without increasing machine weight and size is sought. A very promising approach is to provide high pressure water jet assistance to the drag tools on the cutting head which generates no significant reactive force.

Following earlier research conducted by the South African Chamber of Mines (Hood 1976), there has been a surge of research interest on a worldwide scale in investigating the effects of using high pressure water jets together with conventional rock cutting tools. So far, all results indicate unanimous approval of this novel technique and have recommended further research in this field. The encouraging South African findings resulted in an in-situ trial of a light duty roadheader (Dosco MK2A) using jet pressures up to 70 MPa (Plumpton and Tomlin 1982). The trial showed improvement, not only in excavation rate, but also in dust suppression and cutting tool consumption. However, the basic failure mechanism of hybrid cutting is not well understood. Laboratory results with nozzle diameter ranging from 0.2mm to 1.2mm and jet pressure from 15 MPa to 300 MPa have been undertaken and the results claimed as successful. Confusing results have delayed rapid commercialisation of the roadheader equipped with high pressure jets as the roadheader manufacturers experienced difficulty in determining the optimum selection with respect to variables such as nozzle diameter, jet pressure, flow rate and jet position. The situation was not improved when most of the laboratory experiments were carried out at a slow traverse speed (in the range 0.1 to 0.25 m/s), whilst almost all boom-type tunnelling machines have tool traverse speeds exceeding 1.0 m/s (Table 1.2). Direct extrapolation and application of this experimental data is doubtful and may lead to erroneous results.

Manufacturer	Type	Cutting Head		Circumferential Tool Speed (m/s)
		Head Diameter (mm)	Revolution (rpm)	
USSR	PK-3	650	98/182	3.33/6.66
Greenside-McAlpine	Rock Tunneller	1220	18	1.17
Mitsui Miike	MRH-S40C	740	45/52	1.75/2.02
Mavor & Coulson	RH20	865	37/85	1.68/3.85
Eickoff	EV100	1000	27/67	1.40/3.50
Paurate	Roboter	906	13.7/41.3	0.65/1.98
Mitsui Miike	MRH-S90	900	54/65	2.55/3.07
Eickoff	EVR-200	2000	40	3.0
Thyssen	E134	to 1400	20.6/41.3	1.3/2.5
	E169	1240	20/40	1.3/2.6
Anderson Strathclyde	RH 1/3	812/1067	30/50	1.28/2.79
	RH22	813/1067	30/50	1.28/2.79
Dosco	MK2	483	50/75	1.26/1.93
	MK2A	500/620	44/60	1.22/1.67
	MK2B	600	58	1.9
	MK3	1000	27/50	1.31/2.62
	TB600	to 914	27/50	1.22/1.67

Table 1.2 Examples of the tool speed of Boom Type Tunnelling Machines (partly adopted from Nishimatsu 1979).

Previous valuable experience and expertise gained by the Department of Mining Engineering in the University of Newcastle upon Tyne on this subject led to a research contract to further investigate hybrid cutting on a much larger scale. This contract is sponsored jointly by the Science and Engineering Research Council (SERC) and the European Coal and Steel Community (ECSC), with a contract through the National Coal Board (NCB).

This work will describe the research which has been carried out during the last three years. The aim of the project is to investigate the cutting mechanism of high pressure water jet assisted drag tools cutting in rock materials.

A large 50-tonne linear cutting rig, previously used for disc cutting research (Fauvel 1981) has been extensively modified to provide cutting speeds of up to 1.1 m/s. A 75-kW pump with double-acting intensifier is used to provide a water jet at pressures up to 70 MPa and a flow rate of 45 litre/min.

The research programme was divided into two phases:

The primary experimental programme was designed to investigate three major variables which were identified as jet pressure, mechanical depth of cut and traverse speed. The latter variable is of particular importance. The main thrust of this project was to carry out laboratory tests at traverse speeds over 1 m/s, which is a typical practical tool speed used on production machines in hard rock. Cuts of 0.27 m/s tool speed are also included with the aim of providing an explanation for the difference, if any, between water jet assisted cutting at fast and slow traverse speeds.

Five rock types were examined, which covered a wide range of strengths and abrasivities. A factorial experiment was applied to all five rocks in order to obtain a general picture of the effect of water jet assistance in different rocks in the same conditions. Possible interactions between variables were also investigated.

In the secondary experimental programme, other variables important to the application of water jet assistance in a tunnelling machine were investigated. The size of the research design was reduced in order to allow more variables to be studied in the limited time scale. The typical traverse speed is 1.10 m/s and the typical depth of cut 10mm, representing field conditions for a production tunnelling machine cutting at an economical rate in hard rock. The variables included nozzle diameter, nozzle position, tool bluntness, wear rate, mode of cutting and the effect of slot depth.

Based on careful observations of drag tool cutting and a study of jet action, a phenomenological model of hybrid cutting mechanisms was proposed. The validity of the proposed model was examined by comparing the model with the experimental results.

* * *

CHAPTER TWO

CHAPTER TWO

LITERATURE REVIEW

2.1 Introduction

Since water jet assisted drag tool rock cutting is essentially drag tool cutting with a superimposed water jet, it is logical to review the studies on the drag tools and water jet rock cutting individually before their combined effects are investigated.

Mechanical rock cutting involves the use of roller cutters or drag tools. For water jet cutting the spectrum is even wider, including steady jets, unsteady jets, pulsed jets and cavitational jets. The jet pressure can be more than 400 MPa in an ultra-high pressure system. To limit the scale of this review, only studies relevant to the laboratory conditions for this project are covered. Only wedge-tipped drag tools and continuous steady jets were used during the project, with jet pressures up to 70 MPa.

For drag tool rock cutting, three theories are examined. For water jet rock cutting, priority is given to those theories predicting the jet penetration by a travelling continuous steady jet. Finally, published works on water jet assisted drag tool rock cutting are reviewed. The review includes both laboratory investigations and in-situ trials using full size machines.

2.2 Drag Tool Rock Cutting

There are three theories commonly quoted relating the performance of drag picks to the strength of the material to be excavated.

2.2.1 Merchant's Theory

Merchant (1945) derived an expression predicting the tool force required to cut a continuous strip from the plane surface of a block of metal. The geometry of Merchant's model is illustrated in Figure 2.1.

The theory is based on two assumptions:

(a) the depth of cut is small compared with the width of tool to ensure the condition of plane strain; and

(b) shear failure takes place over a straight line making an angle, Θ, with the direction of cut.

Considering the equilibrium of the chip and applying the hypothesis of minimum work, the value of cutting force at chip failure is given by:

$$Fc = 2.d.S.\tan \frac{(\beta+\phi)}{2}$$

where d = depth of cut

ϕ = angle of friction between tool and chip

β = angle between wedge front face and direction of cut

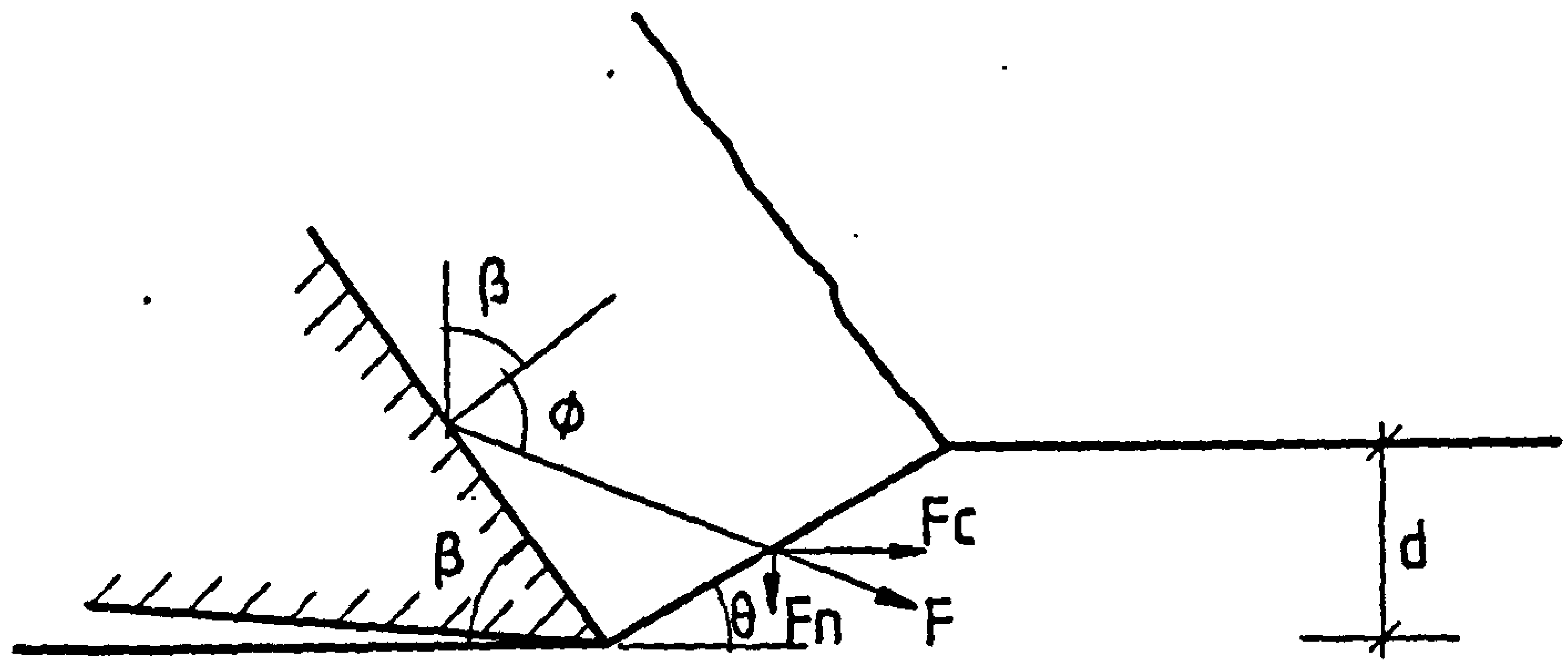

Figure 2.1 Illustration of Merchant's Theory Metal Cutting.

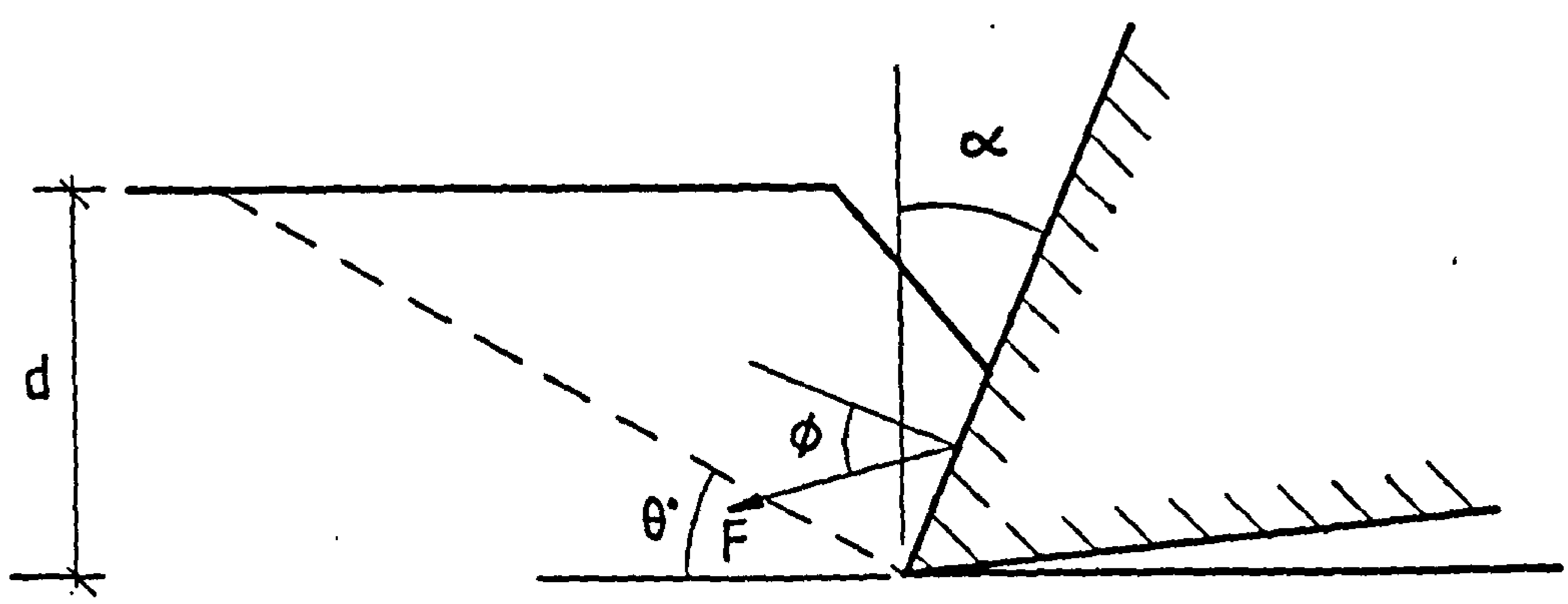

Figure 2.2 Illustration of Nishimatsu's Theory of Rock Cutting.

S = shear strength of the material.

2.2.2 Nishimatsu's Theory

Nishimatsu (1972) observed a recompacted crushed zone which sticks to the rake face of the cutting tool during the rock cutting. The crushed zone acts as a built-up edge in rock cutting, and initiates a macroscopic failure crack which leads to the formation of a coarse cutting chip at the peak value of cutting force (Figure 2.2).

Based on this observation and assuming:

(a) the failure surface is plane;

(b) the stress varies along the plane according to a specified function; and

(c) Mohr's failure criterion is valid,

the resultant cutting force, F, is given by:

$$F = \frac{2}{n+1} \cdot S.d. \frac{\operatorname{Cos} k}{1-\sin(k-\alpha+\phi)}$$

where ϕ = angle between resultant force and normal plane of the wedge front face

n = stress distribution factor

S = shear strength of rock

d = depth of cut

k = angle of internal friction

α = rake angle of cutting tool.

2.2.3 Evans' Theory

Based on his observations of the penetration of wedges into rock, Evans (1962) concluded that the rock is failed in tension, and proposed the most widely accepted rock cutting theory. The basic theory for the penetration of a buttock of rock by a simple symmetrical wedge, and an asymmetric wedge, is shown in Figure 2.3.

Assuming:

(a) the failure surface is a circular arc; and

(b) depth of cut is small compared with the width of tool,

the cutting force, Fc, was derived.

For symmetrical wedge:

$$Fc = \frac{2.t.d \sin(\theta+\phi)}{1-\sin(\theta+\phi)}$$

For asymmetrical wedge:

$$Fc = \frac{2.t.d.\sin\left[\frac{1}{2}(\frac{\pi}{2}-\varepsilon)+\phi\right]}{1-\sin\left[\frac{1}{2}(\frac{\pi}{2}-\varepsilon)+\phi\right]}$$

where: d = depth of cut

t = tensile strength of rock

ϕ = angle of friction between wedge and rock

θ = half angle of the wedge

η = angle between the wedge centre and line and the rock surface

ε = $90 - \eta - \theta$

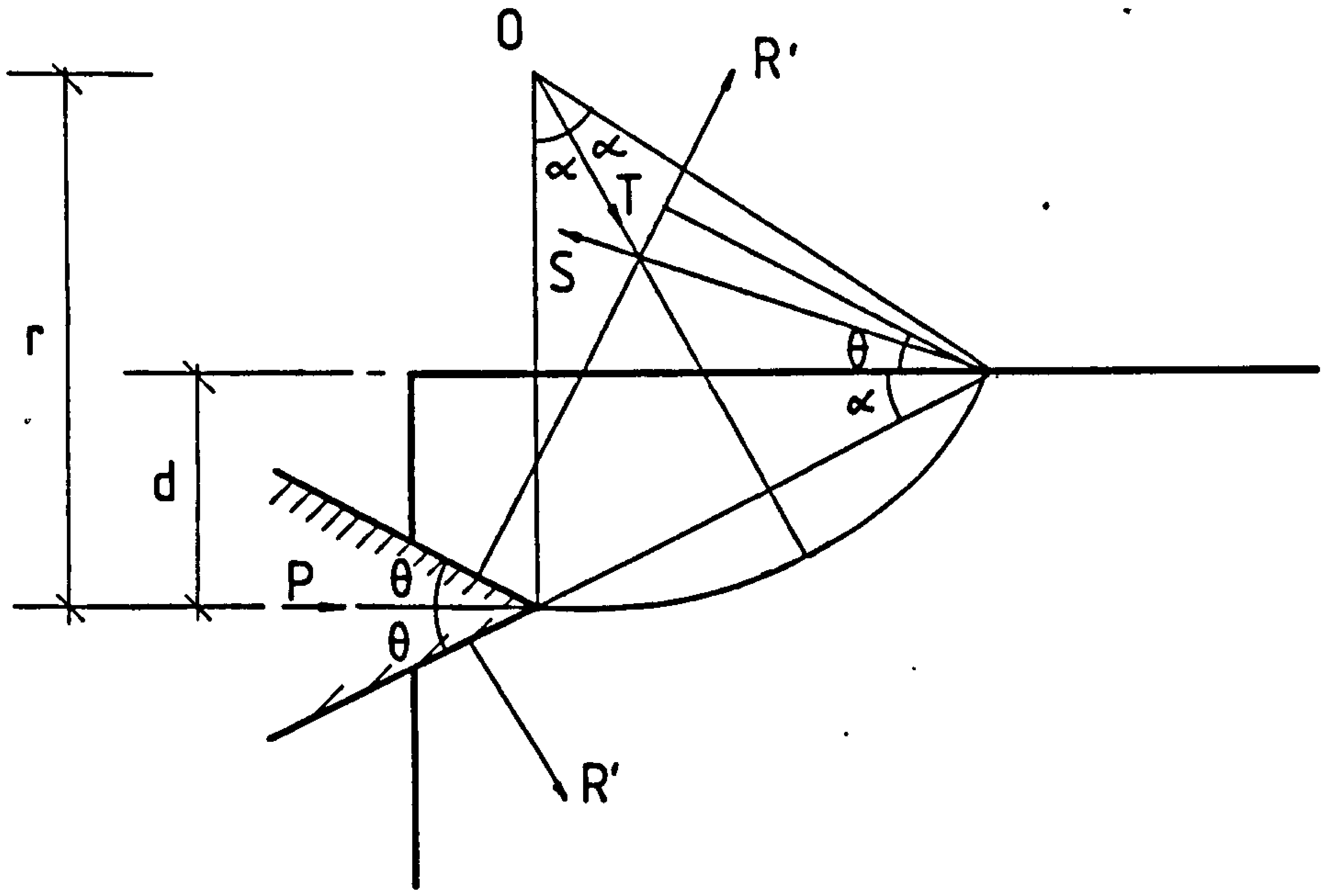

Symmetric Wedge

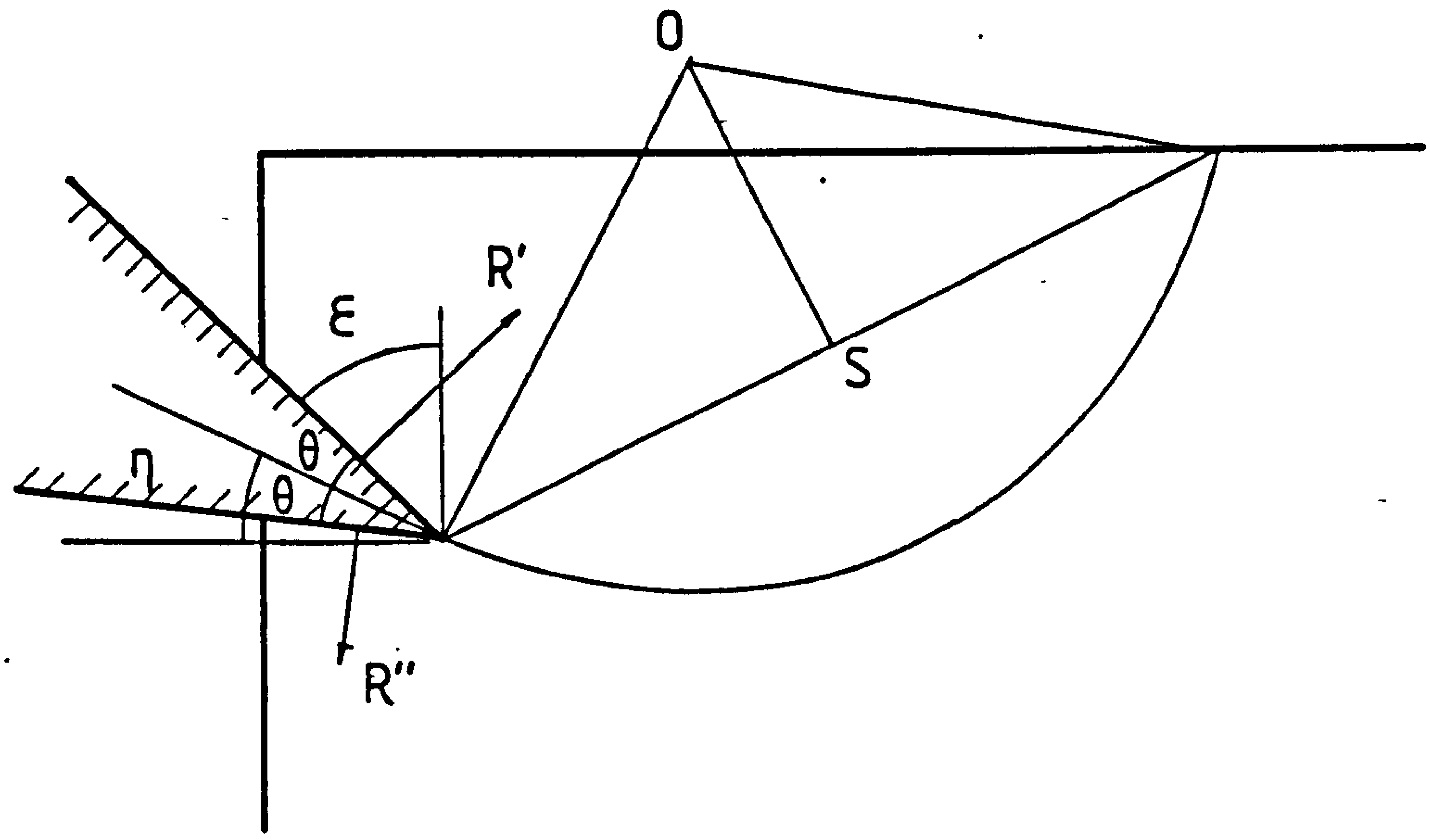

Asymmetric Wedge

Figure 2.3 Illustration of Evans' Tensile Breakage Theory.

2.2.4 Discussion

Merchant's theory is generally only applicable to situations where a wedge-shaped chisel tool is cutting a plastic material. However, this theory is considered inadequate for rock cutting as most rocks behave in a brittle manner. Nishimatsu's theory is based mainly on the metal cutting theory of Merchant. However, whereas Merchant used a single value for the shear strength of the material, Nishimatsu invoked Mohr's failure envelope to define the strength of the rock. Evans' theory pointed out the fact that most rocks have a much lower tensile strength than shear strength (hence the rock fails in tension before failing in shear). However, he did suggest that some indication of whether the rock will fail in tension or shear can be obtained from triaxial test results. If the angle of internal friction is high, tensile strength is low relative to the shear strength in which case tensile failure is more likely.

Recent additions to the field of rock fragmentation models include Lebrun (1978) and Ranman (1985). The former model takes a three-dimensional shear approach, whilst the latter concentrates on the action of conical-shaped picks (point attack tools), using an energy approach based on empirical laboratory studies of the chipping process.

Amongst the above theories, Evans' theory is most widely accepted in the field of rock and coal cutting. Practical application of this theory can be found elsewhere (Roxborough 1973;

Roxborough and Rispin 1973). The theory was later extended to cover the action of point attack tool cutting and the effect of bluntness on tool force (Evans 1965, 1984; Hurt and Evans 1981).

2.3 Water Jet Rock Cutting

2.3.1 Introduction

The water jet cutting theory involves the interaction between the jet and the material being cut and the problem is extremely complex in itself. No single theory can claim to solve it. Basically, there are two types of water jet loadings in the jet-material interface:

(1) a continuous, steady jet load, which cuts by shearing out a slot; and

(2) an interrupted jet impact which exposes the material to a series of blows.

All the works described in this thesis have used a continuous steady jet. Hence only the steady jet cutting theory will be considered here in depth. A detailed reference on drop impact and pulsating jets has been summarised by Brown (1981).

Laboratory continuous jet test results on various rocks have been reported (Brook and Summers 1969; Brook and Page 1972; Harris and Mellor 1974; Labus 1976). However, the vast number of variables and unknowns render the theoretical approach an extremely difficult task. As an example, the 'general'water jet cutting equation proposed by Hashish (1981) includes the following parameters:

(a) Jet Parameters

- nozzle diameter
- jet pressure
- spreading coefficient
- nozzle friction losses.

(b) Operational Parameters

- stand-off distance
- traverse speed
- number of passes.

(c) Material Properties

- compressive strength
- yield strength
- material rheological property
- hydrodynamic coefficient of friction between jet and solid target.

Extra parameters are included, based on different cutting mechanisms which depend on the traverse rate.

Basically, three water jet cutting theories have been proposed which are derived based on different cutting mechanisms of rock under the loading of a water jet. Empirical formulae are also suggested by correlating result data with several major parameters.

2.3.2 Crow's Theory

Crow (1973, 1974, 1975) considered the mechanics of hydraulic rock cutting when a continuous high speed water jet is traversing across a rock. It is suggested that the jet curves against the granular surface of the rock and induces a high average surface pressure on the upstream faces of the exposed grains. The state of flow is such that cavitation bubbles form behind the grains causing the downstream faces to generally experience the vapour pressure of the water. The surface erodes under a combination of Coulomb friction between the jet stream and the granular cutting surface, and internal pore pressure resulting from sub-surface permeation. The basic mechanisms are best illustrated in Figure 2.4.

Assuming jet diameter is large compared with the grain size of the rock, Crow proposed a theory that predicted the depth of jet slot:

$$h = 2\mu w \frac{d_o P_o}{\tau_o} \int_0^{\Theta_o} \frac{e^{\mu w(\Theta - \Theta_o)} \sin\Theta}{1 + \frac{V}{c}\sin\Theta} \, d\Theta$$

where c = intrinsic speed = $\frac{k\tau_o}{n f \mu_r g}$

P_o = initial total pressure of jet

Θ_o = instantaneous angle between direction of jet stream and direction of rock motion

μw = coefficient of Coulomb friction between water and rock under cavitation conditions

τ_o = inherent shear strength of rock

k = permeability of rock

d_o = jet diameter

f = porosity

μr = coefficient of internal friction of rock

g = typical grain diameter

η = coefficient of viscosity of cutting fluid

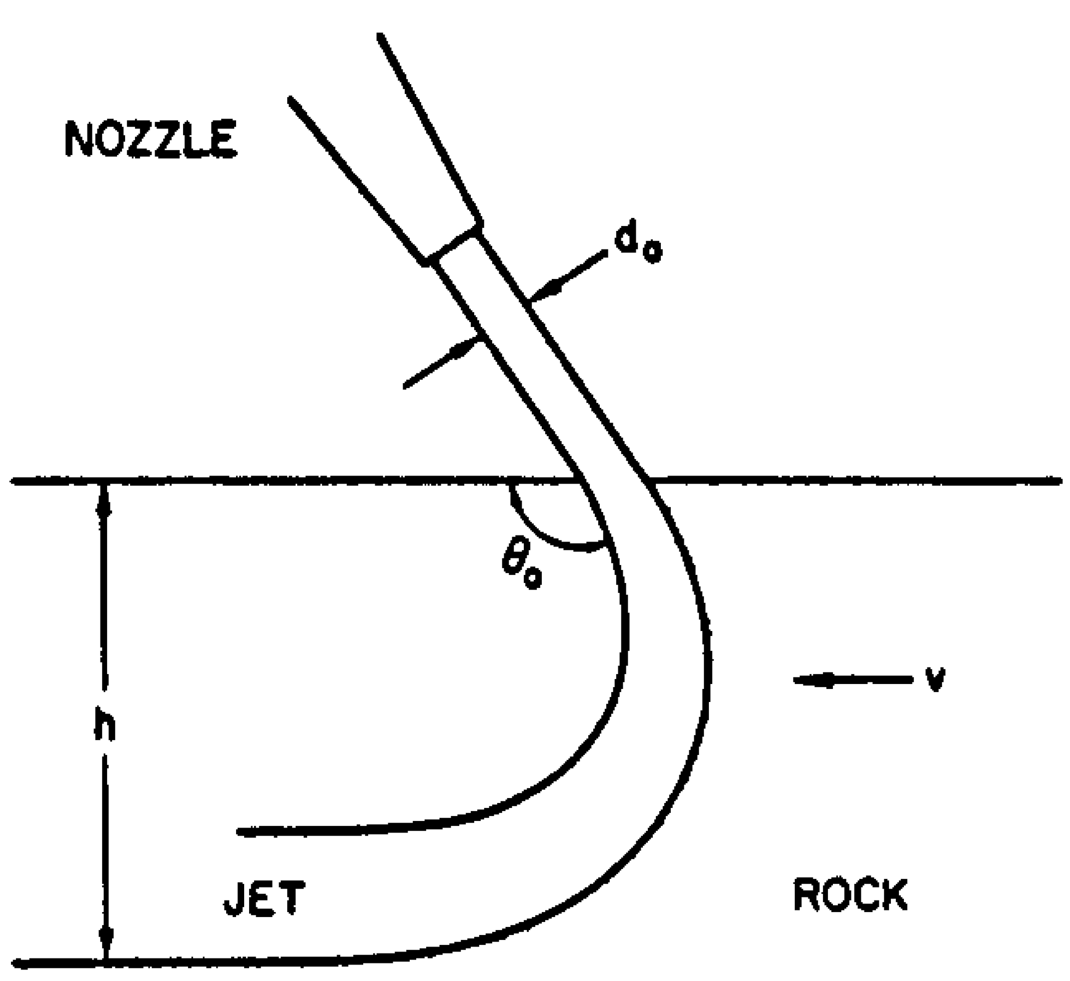

Cutting by a Steady High Speed Water Jet

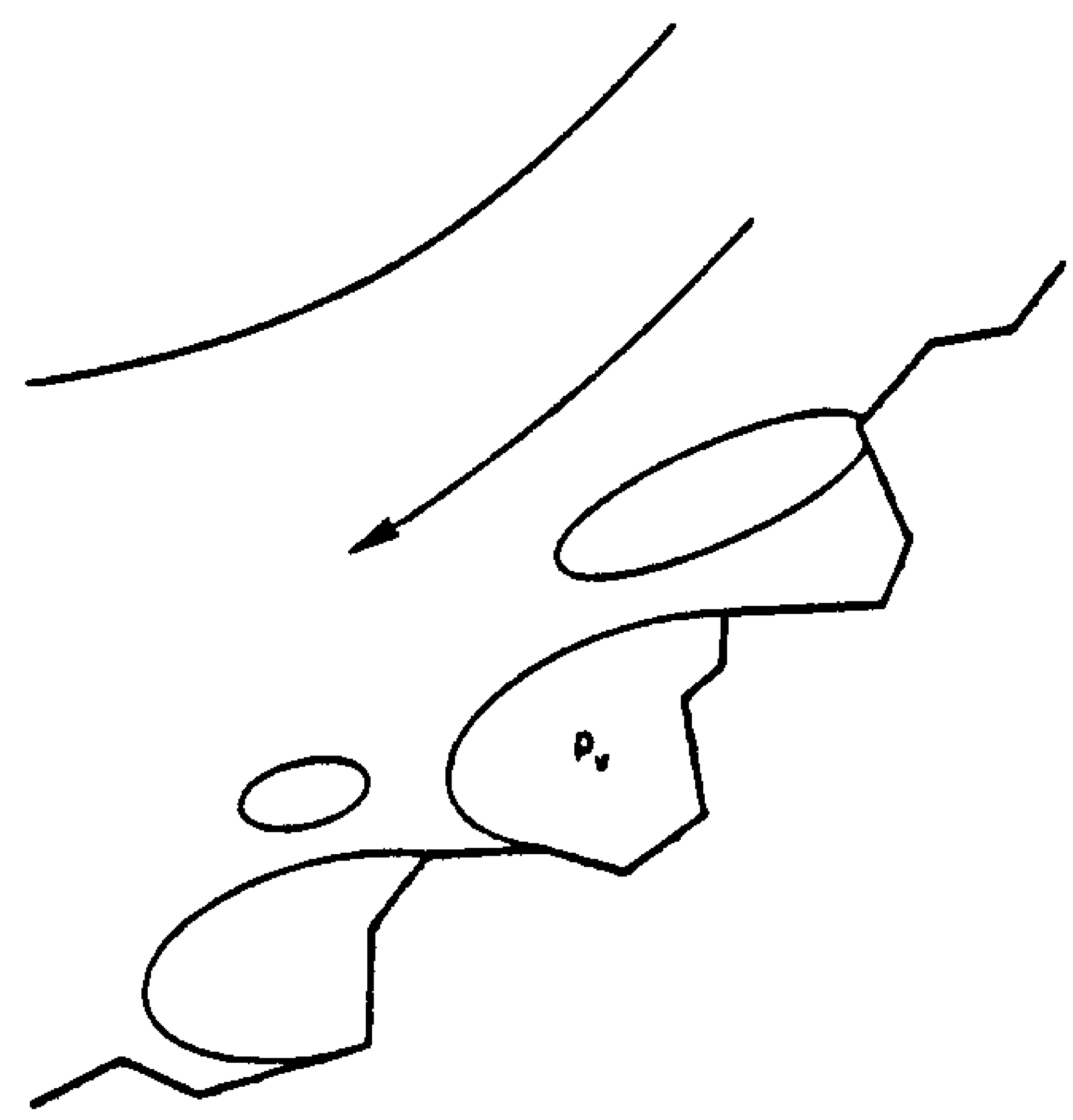

The Origin of Cavitation Stess on a Granular Surface

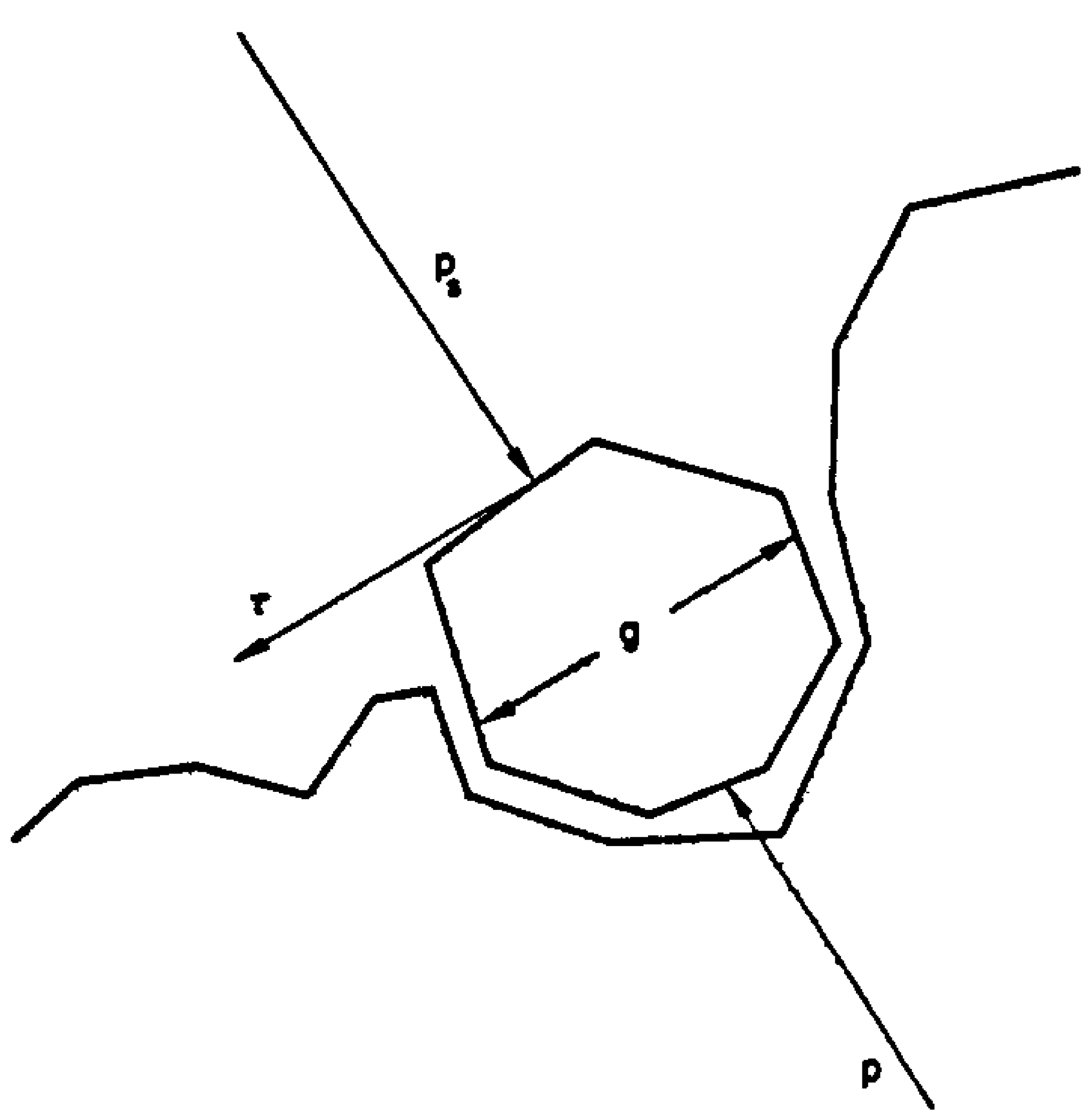

Balance of Forces on a Grain

Figure 2.4 Illustration of Crow's Jet Cutting Theory (after Crow *et al*. 1974).

The accuracy of this theoretical model was examined by Crow *et al.* (1975), who compared the measured slot depths and predicted slot depths on four rocks. It was found that the major effect of permeability on the theoretically predicted depth of slot was not reflected by the experimental results in all four rocks except one.

A modified model is tentatively proposed by Crow *et al.*:

$$\eta = \frac{do\ (Po - Pc)}{\tau_o} F\left(\frac{V}{ce}\right)$$

where F = universal function of V/c_e

c_e = effective intrinsic speed of hydraulic rock cutting that does not depend so strongly on permeability as does the original definition.

No further work has been published to substantiate or prove this modified model.

2.3.3 Rehbinder's Theory

Rehbinder (1976, 1977, 1978, 1980) investigated the parameters of the rock that controlled the cuttability of the rock during the continuous, steady jet slotting tests. It was claimed that the jet slotting process is essentially an erosion by drag force rather than 'stress and fracture' action, and a simple model of erosion of rock based on flow of water in a porous medium is proposed. Depending on the relative magnitude of jet pressure and threshold pressure, two different cases are distinguished. In the first case, the stagnation pressure of the jet, Po, is less than the threshold pressure of the rock, Pth, which resulted in no damage to the rock (Figure 2.5(a)). In the second case, the stagnation pressure of the jet is greater than the threshold pressure of the rock; the grains are spalled at a rate equal to the mean rate at which the water passes a grain (Figure 2.5(b)). Based on several assumptions, the depth of slot was expressed as:

$$\frac{h}{d_o} \begin{cases} \dfrac{D}{d_o \beta} \ln\left(1 + \dfrac{\beta k p P o}{\mu \bar{\ell} D} T\right) & T < To = \dfrac{\mu \bar{\ell} D}{\beta k p P o}\left(\dfrac{Po}{P_{th}} - 1\right) \\[2ex] \dfrac{D}{d_o \beta} \ln \dfrac{Po}{Pth} & T > To = \dfrac{\mu \bar{\ell} D}{\beta k p P o}\left(\dfrac{Po}{P_{th}}\right) - 1) \end{cases}$$

where: D	=	width of slot ($D \simeq 2.5d$)	(mm)
do	=	diameter of jet	(mm)
h	=	slot depth	(mm)
$\bar{\ell}$	=	average grain size of rock	(mm)
Po	=	stagnation pressure of jet	(Pa)
Pth	=	threshold pressure of rock	(Pa)
T	=	time of explosure $^{do}/v$	(s)
To	=	critical time of exposure	(s)
v	=	traversing speed of jet	(m/s)
β	=	coefficient of pressure drop in a slot	
kp	=	modified permeability referring to average pore velocity	(m^2)
μ	=	viscosity of water	(Ns/m^2)

This equation is valid so long as the pressure at the bottom of the slot p(h) exceeds threshold pressure of rock, Pth, and the rock is not coarse grained, i.e. $^{d}/_{\bar{\ell}}$ >>1.

(a)

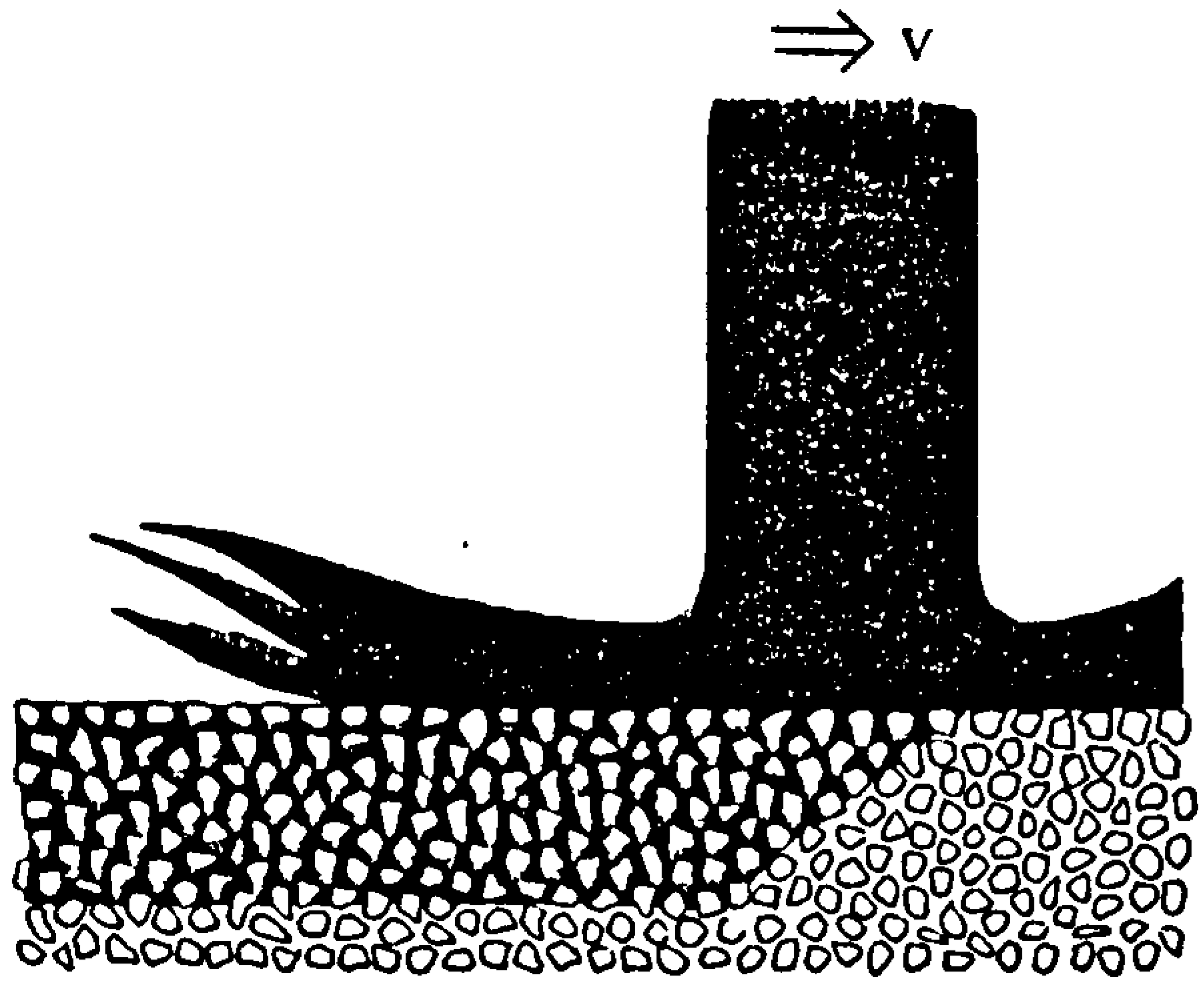

(b)

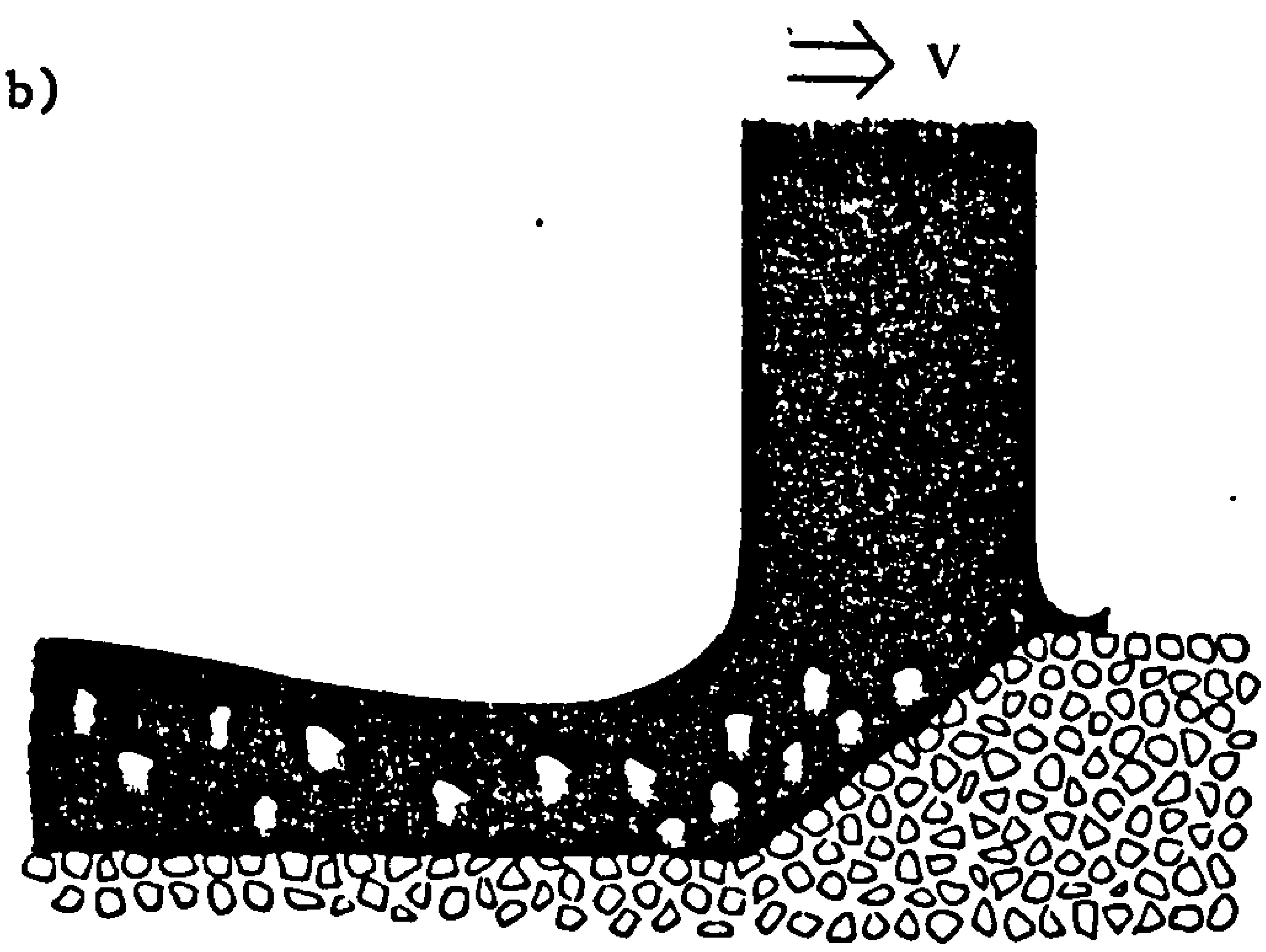

Figure 2.5 Illustration of Rehbinder's Jet Cutting Theory (after Rehbinder 1980).

It was found that the rock is characterised by its threshold pressure, Pth, and its erosion resistance, $\bar{\ell}$/kp. The threshold pressure is a measure of 'microscale' tensile strength of the rock and is thus a lower limit of the pressure of a jet at which erosion occurs. The erosion resistance, however, is a measure of how rapidly a slot grows if the pressure of the jet exceeds threshold pressure.

From an application viewpoint, the fundamental idea is to determine the unknown quantities, Pth and $\frac{kp}{\mu \ell}$, by a reference experiment and then the slotting depth can be predicted by the theory for any choice of parameters.

2.3.4 Hashish - du Plessis' Theory

Hashish and du Plessis (1978, 1979, 1980) proposed a general water jet cutting equation to predict depth of cut, width of cut, volume removal and specific energy. The theory is based on a control volume analysis to determine the hydrodynamic forces acting on the solid boundary of the cutting slot (Figure 2.6) and an assumption that the compressive failure of the material is the dominant cutting mechanism. A Bingham model is used to describe the time-dependent stress/strain relationship of the solid material as it flows under the high normal stress of the jet. The non-dimensional cutting equation for depth of cut prediction was expressed as:

$$\frac{h}{do} = \frac{1 - (\frac{\sigma y}{\rho Vo^2})}{(\frac{2Cf}{\sqrt{\pi}})} \left[1 - e^{-(\frac{2Cf}{\sqrt{\pi}})(\frac{\rho Vo}{\eta})(\frac{Vo}{V})}\right]$$

where: h = jet penetration

do = nozzle diameter

Vo = jet speed

V = traverse speed

ρ = fluid density

σy = compressive yield strength

Cf = total skin friction coefficient

η = damping coefficient.

The equation is open to greater accuracy by choosing the optimum rheological model for the material to be cut.

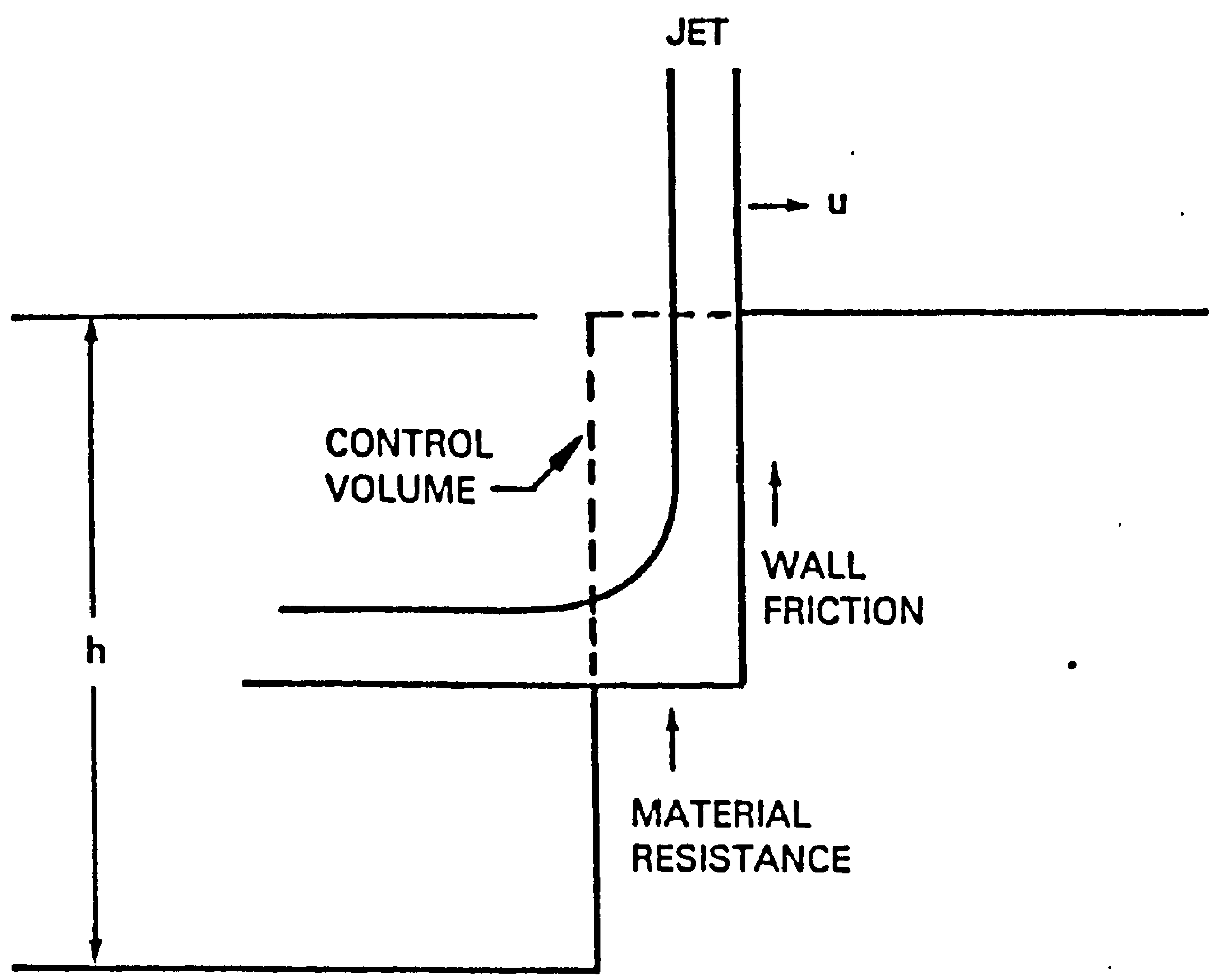

Control Volume of Jet Penetration

Figure 2.6 Illustration of Hashish - du Plessis' Jet Cutting Theory (after Hashish 1981).

2.3.5 Empirical Equations

Due to the dificulties in manipulating the vast number of jet parameters, operation parameters and rock properties in order to form a theoretically sound water jet cutting theory, empirical equations are proposed as an alternative.

Nikonov (1971) and Nikonov and Golden (1972) summarised the Soviet data on slotting cutting of coal by continuous jets and suggested they could be correlated by a dimensionless equation in the form:

$$\frac{h}{do} = 0.5 \left(\frac{Po}{\sigma_c} - 0.2\right) \left(\frac{V}{Vo}\right)^{-0.5}$$

where h = slot depth

do = nozzle diameter

Po = jet pressure

σ_c = unconfined compressive strength of rock

V = traverse speed

V_o = jet speed.

Later Kuzmich et al. (1982) extended the prediction euqation to water jet rock cutting and found it can be used with slight modification:

$$\frac{h}{do} = 0.11 \left(\frac{Po}{\sigma_c}\right)^{0.75} \left(\frac{Vo}{V}\right)^{0.5}$$

Based on a summary of published data by other researchers, Cooley (1974) found that the slot cutting of metals, plastics, rocks and coal by continuous jets can be correlated approximately by an equation of the form proposed by Nikonov:

$$\frac{h}{d_o} = B\left(\frac{P_o}{\sigma_c} - 0.2\right)\left(\frac{V}{V_o}\right)^{-m}$$

where: B = constant for each material

m = constant, equal to 0.5 for coal and generally between 0.5 and 1.0 for other materials.

2.3.6 Discussion

There is no simple theory that can predict the slot depth by water jet cutting with reasonable accuracy using independent parameter inputs without resorting to an actual jet cutting experiment. Three parameters must be determined experimentally to solve the Hashish-du Plesses model, which is regarded as the most comprehensive model so far. Crow (1975) found his model was not a success when compared with theoretical predictions and experimental results. Rehbinder's model can only predict the slot depth to the 'right order of magnitude' and this could be the reason why determination of some of the parameters using a 'reference experiment' has been suggested.

The tendency is regarded as highly reasonable and acceptable. So many parameters and effects are either extremely dificult or impossible to quantify. Using experimentally-determined values can improve the accuracy of predictions by incorporating the theoretical prediction with interpolation and/or extrapolation. Improved predictions have significant implications in engineering applications as the capital investments on high pressure pumps and high traverse speed rigs are very high.

2.4 High Pressure Water Jet Assisted Cutting

2.4.1 Laboratory Investigation

In an attempt to economically excavate the South African gold-bearing rocks with tungsten carbide tipped drag tools, Hood (1976, 1978) carried out laboratory cutting studies with water jet assistance (10-50 MPa) in strong and abrasive norite and quartzite (200-300 MPa). It was reported that the force on the tool was reduced to the extent that depth of cut of the tool could be at least doubled (Figure 2.7). The optimum configuration was suggested to be with two jets, one directed towards each corner of the tool and impinging on the rock approximately 2mm ahead of the leading edge of the tool.

The highly encouraging reports from Hood have promoted much interest worldwide in high pressure water jet assisted rock cutting.

Plumpton and Tomlin (1982) of MRDE/NCB, UK, conducted an investigation on high pressure water jet assisted cutting with the tool cutting a spiral groove in Darley Dale Sandstone. The jet pressure used was up to 70 MPa and the linear cutting speed was 1.27 m/s. Average reductions of 30% and 50% in the

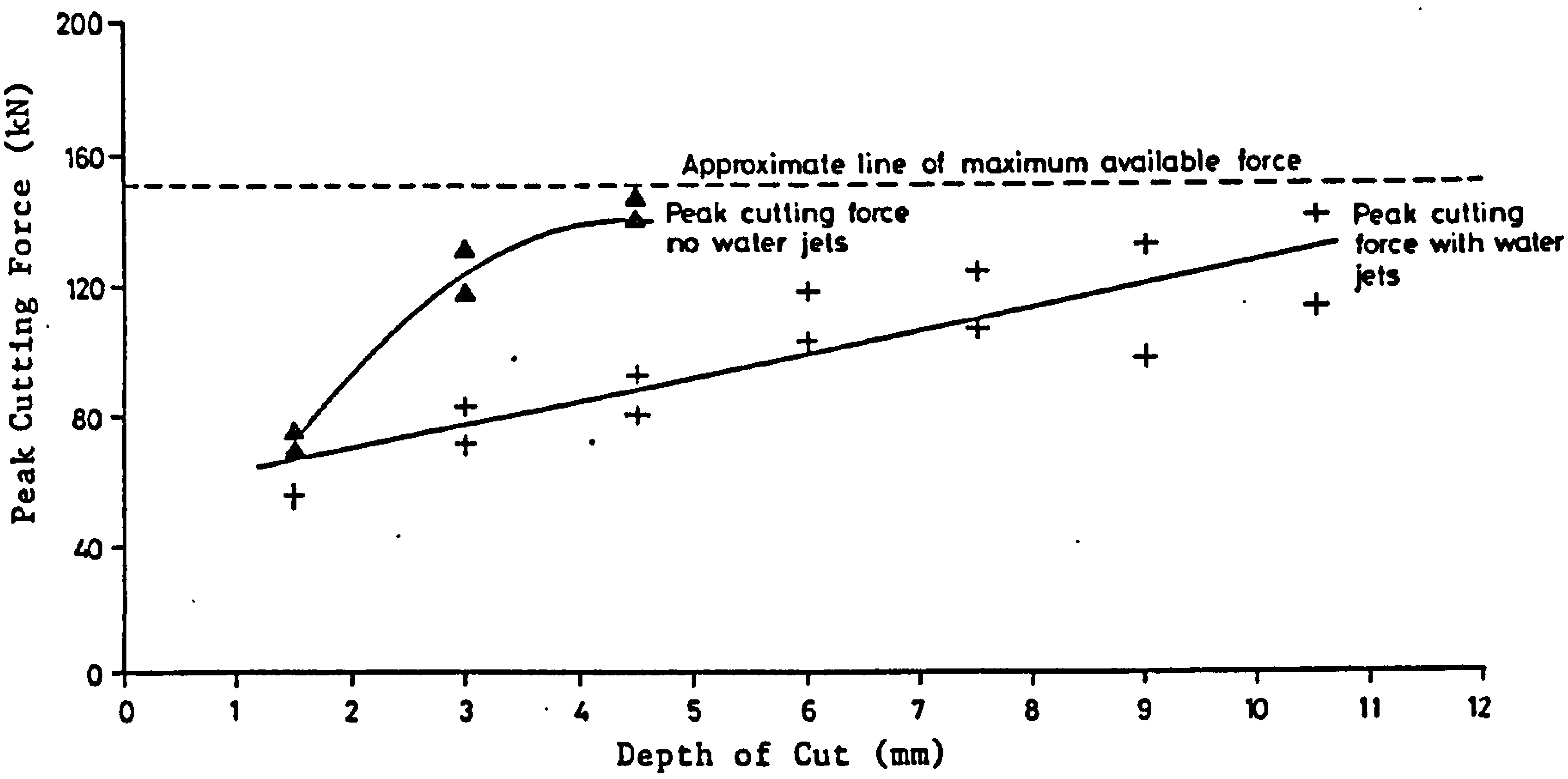

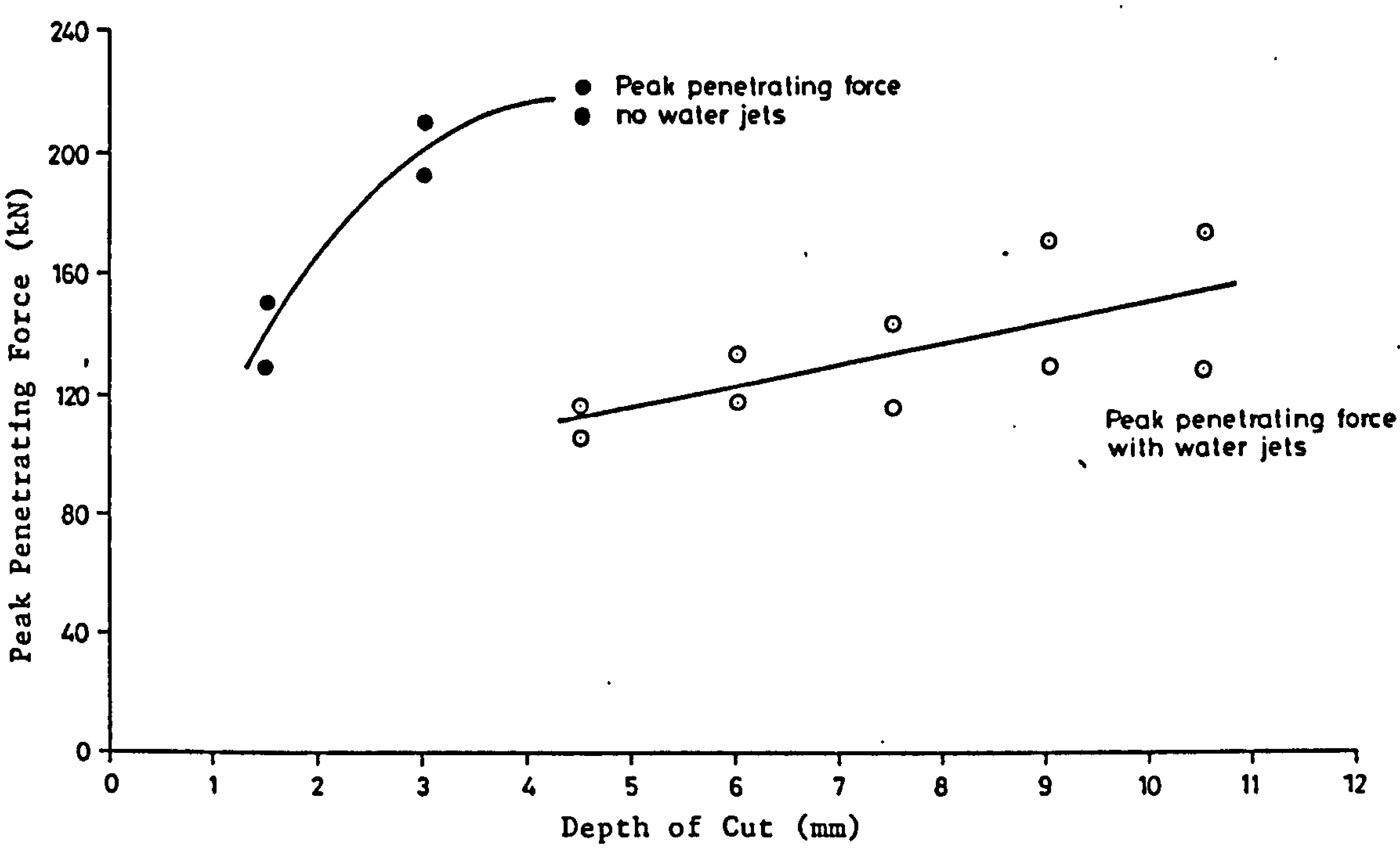

Figure 2.7 Tool Component Forces plotted against depth of cut when 50 MPa water jets were directed outside the corners of the tungsten carbide inserts in the tool (After Hood 1976)

cutting and normal forces respectively were recorded. The results are shown in Figure 2.8. The optimum impingement of the jet was 2mm ahead of the tool tip.

Wang and Wolgamott (1978) of the Colorado School of Mines, USA, examined the possibility of using high pressure water jets to assist rock cutting. A sandstone of uniaxial compressive strength of 50 MPa had been cut using a jet pressure of 25 MPa. Compared with non-assisted cutting, a reduction of 30% in cutting force and up to 75% in normal force was obtained (Figure 2.9). Further studies have been carried out by Ropchan _et al_. (1980) using a jet pressure of up to 70 MPa and the rock types used included hard to soft sandstone, shale and limestone. The general findings were that this technique was more effective with sandstone than with shale or limestone. For the sandstone, the reductions were about 30% to cutting force and 60% to normal force. A typical result is shown in Figure 2.10. The most effective location for the jet was found to be behind the tool. A simple economic analysis revealed that the use of water jets could reduce cost per foot of advance up to 40% with respect to sandstone cutting. Ozdemir _et al_. (1984) furthered the research by using a large drag tool with higher jet pressures on the same test rig. The best result obtained was 50% force reduction in both cutting and normal directions.

Evans _et al_. (1984) of the US Bureau of Mines designed and fabricated a water jet assisted in-seam tester for the purpose of design and development of a water jet assisted rotary drum

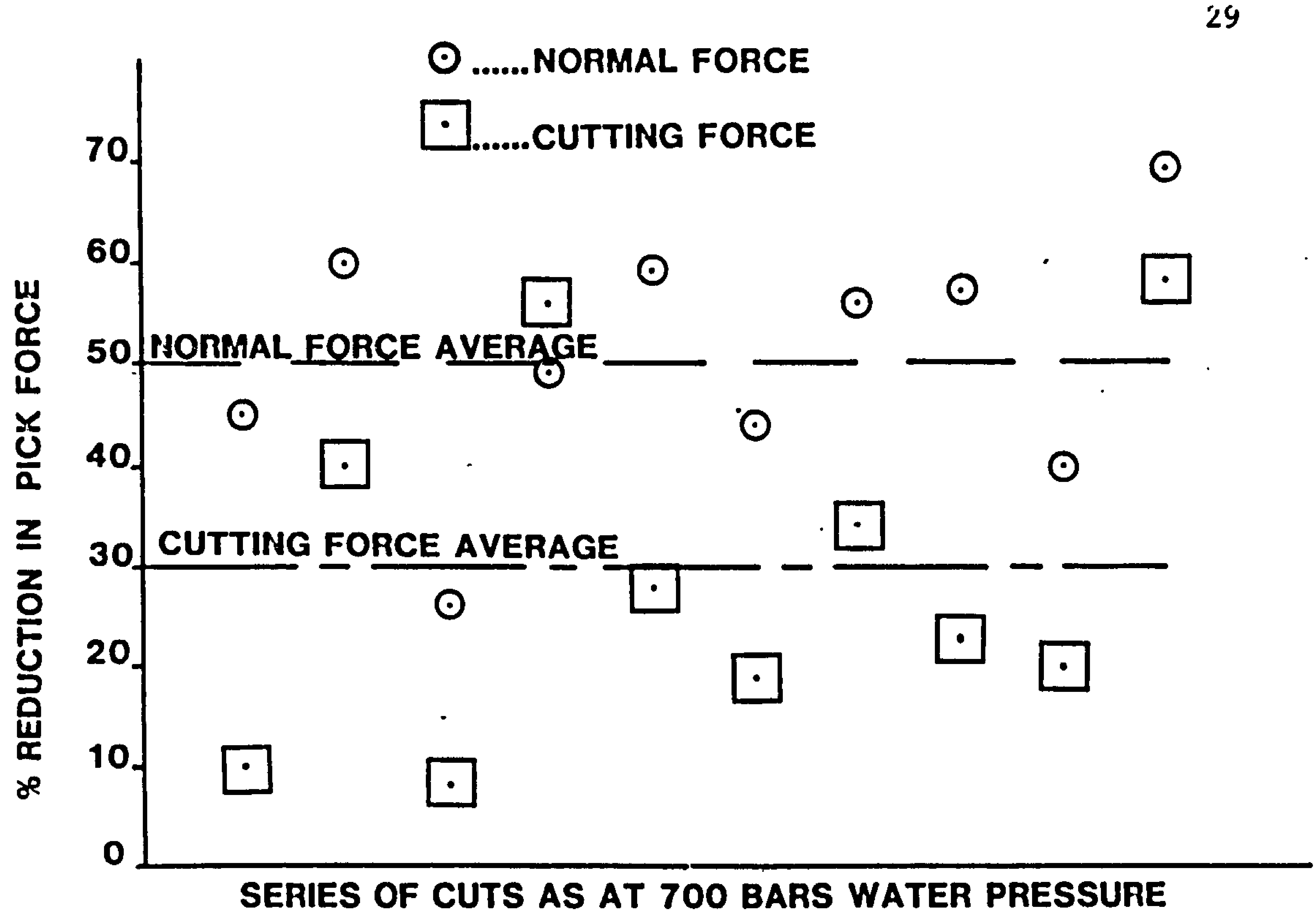

Figure 2.8 Cutting Trials in Darley Dale Sandstone. Jet Pressure up to 70 MPa and 1.27 m/s cutting speed (after Plumpton and Tomlin 1982).

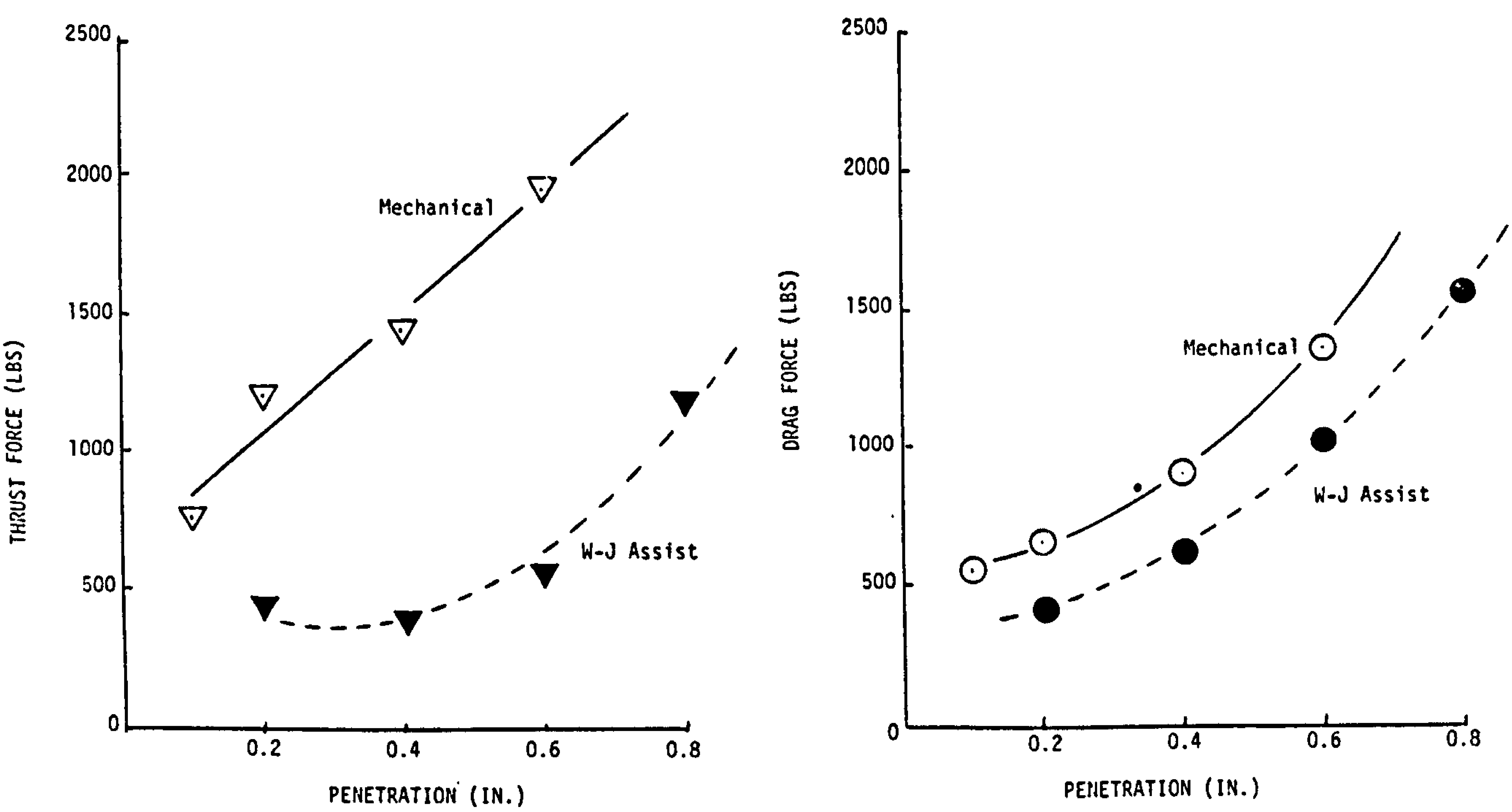

Figure 2.9 Force Reduction due to Water Jet Assisted Wedge Type Drag Tool cutting in Sandstone. Independent Cuts (after Wang and Wolgamott 1978).

Variation in Cutting Forces with Bit Penetration Both With and Without Water Jet Assist from Behind Conical Bit in Dakota Sandstone, Independent Cut Spacing

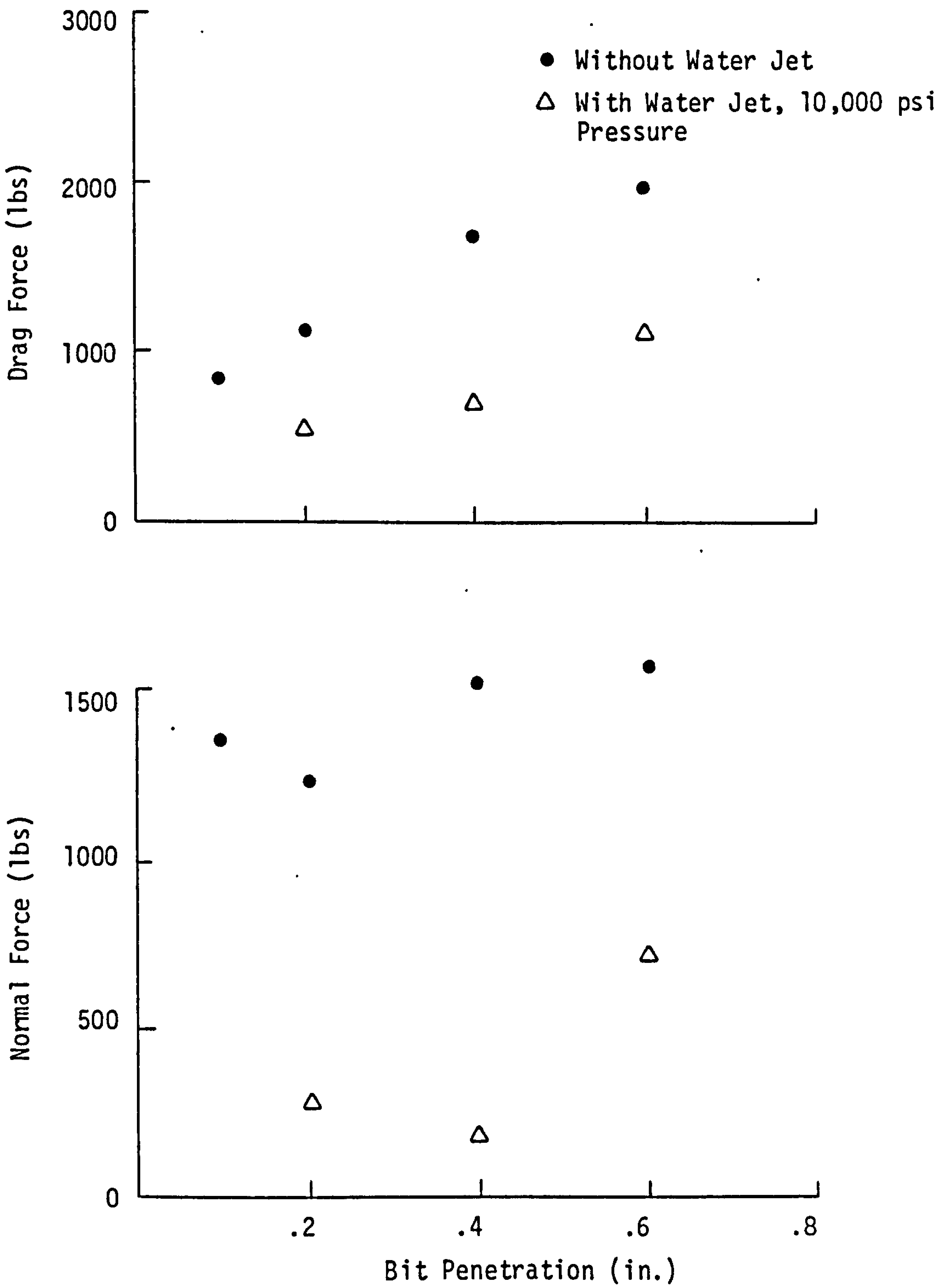

Figure 2.10 Variation in Tool Forces with Bit Penetration With and Without Water Jet Assistance behind a Conical Bit in Dakota Sandstone (after Ropchan 1980).

cutting system. Four types of material had undergone cutting trials, including sandstone, limestone, coalcrete and coal. The best result was obtained for sandstone cutting where a 53% reduction in cutting force was achieved.

Dubugnon (1981) of CERAC, Switzerland, investigated water jet assisted cutting in granite, sandstone and limestone. The cutting and normal forces are progressively reduced down to 35% of the dry value at 65 MPa jet pressure (Figure 2.11). After observation of the rock surface after tests carried out at higher pressures, Dubugnon suggested that water jet assistance is attributed to three processes:

(1) the erosion of the crushed zone underneath the bit;

(2) the hydraulic fracturing; and

(3) pore pressurisation.

Tecen (1982) carried out research on the water jet assisted cutting of two sandstones in the University of Newcastle upon Tyne. The results suggested that the addition of a high pressure water jet to precede the cutting tool significantly reduced the cutting and normal forces on the tool provided a theshold jet pressure was exceeded. Rapid diminishing returns were obtained if jet penetration levels were greater than the mechanical depth of cut. Some results are reproduced in Figure 2.12.

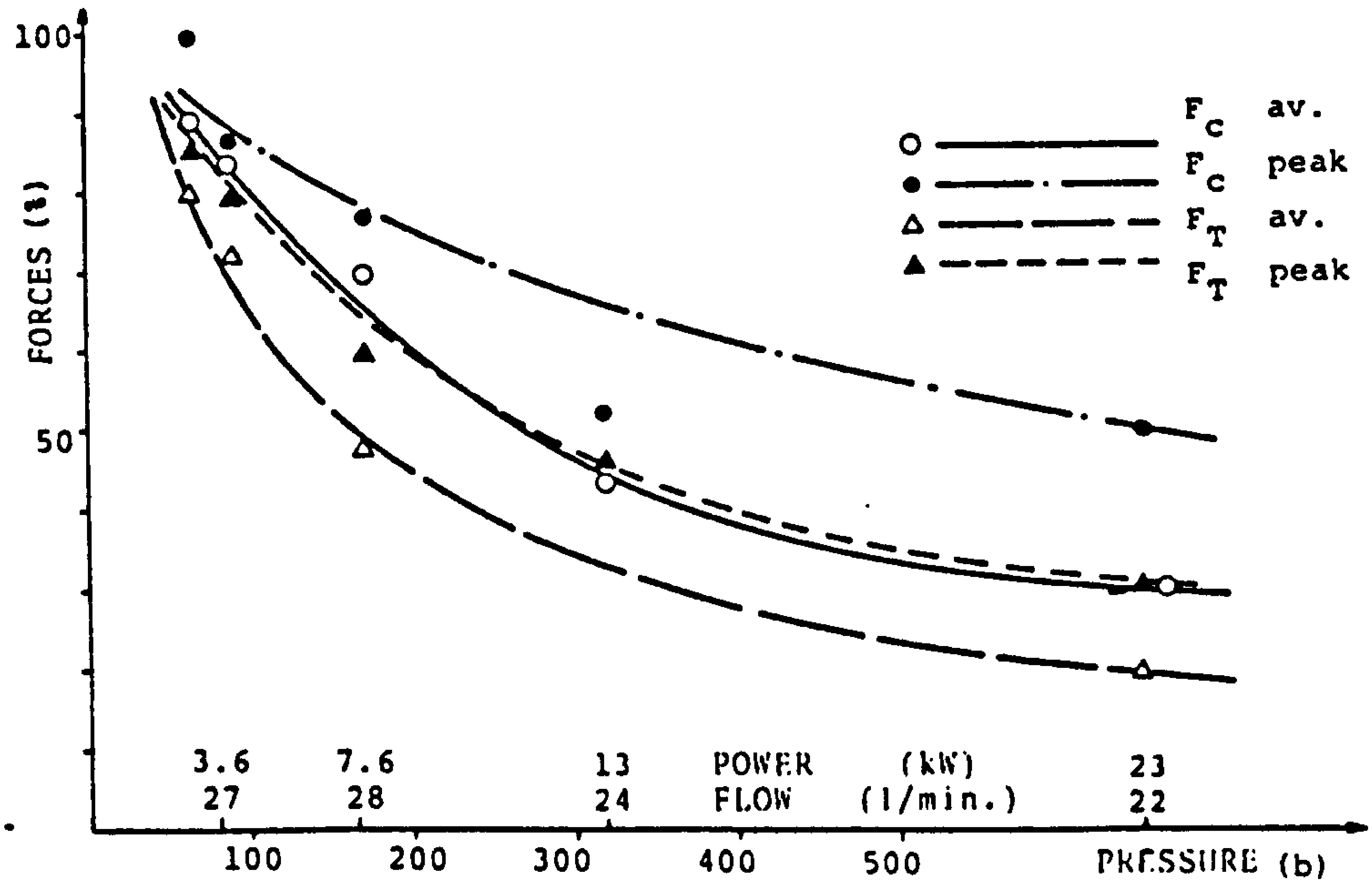

Figure 2.11 Forces (% of the dry cut value) versus Jet Pressure : Bohus Granite, lateral jets, constant flow 25 litre/min (after Dubugnon 1981).

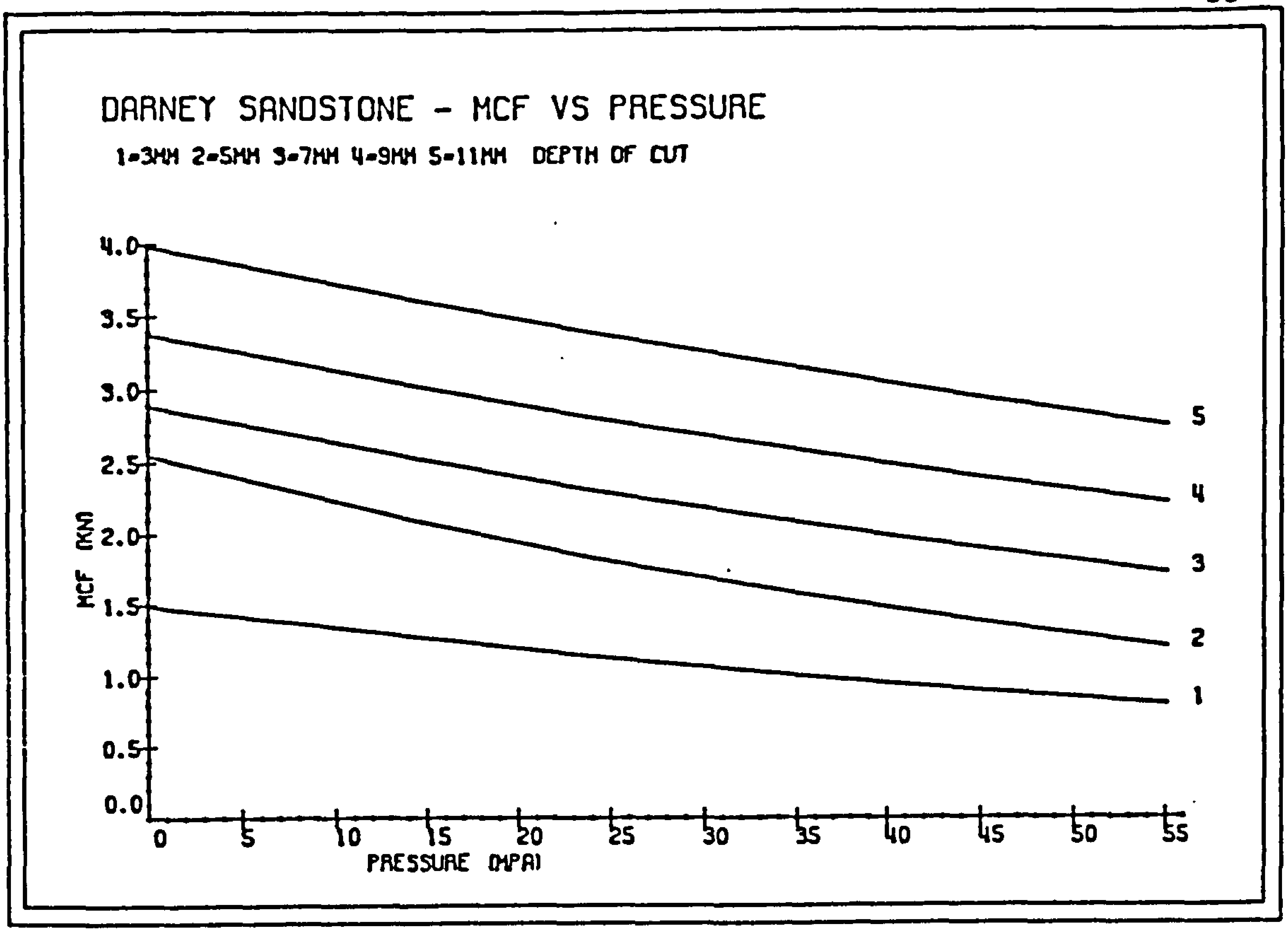

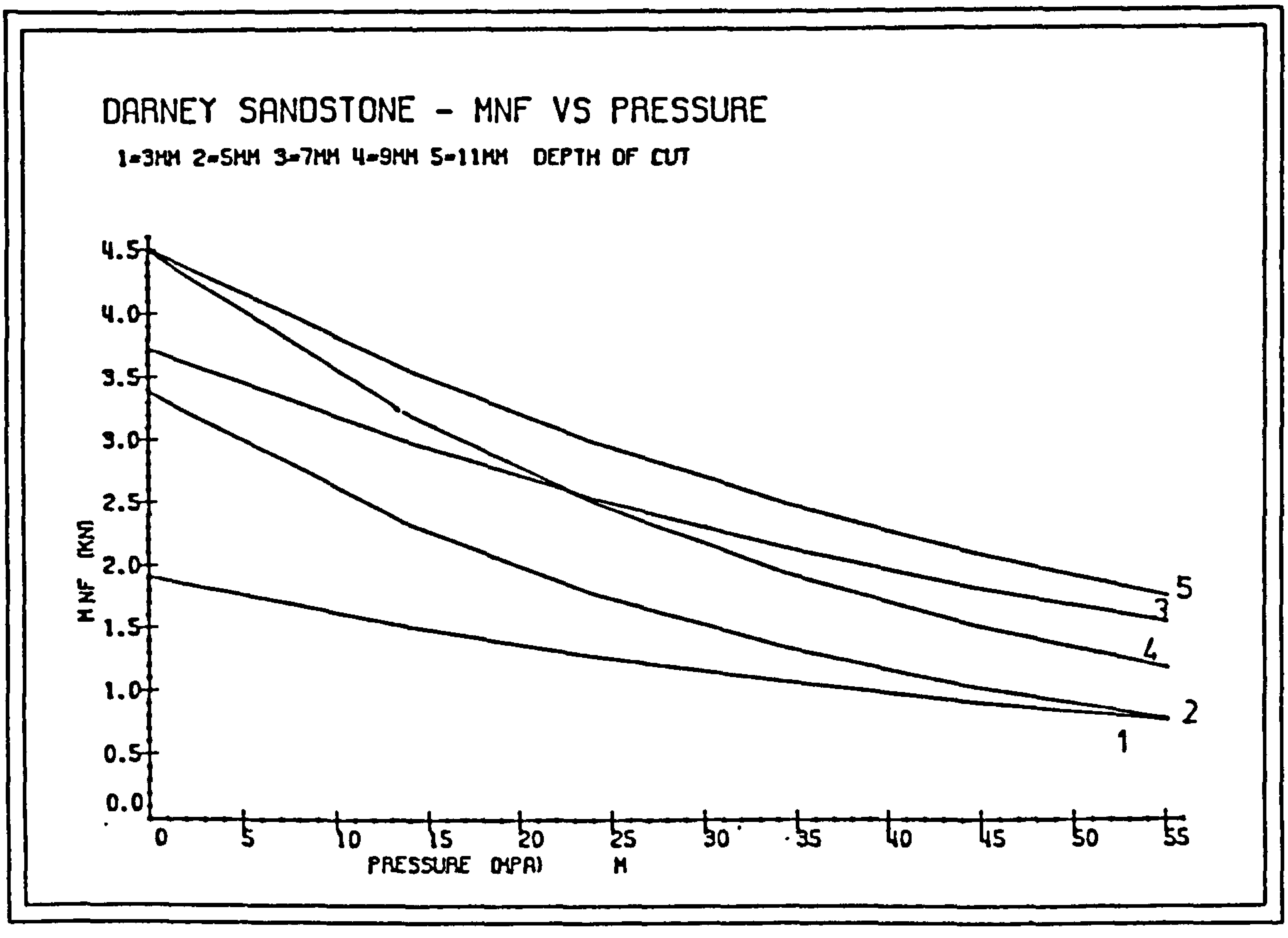

Figure 2.12 Cutting and Normal Force versus Jet Pressure, Front Jet, Darney Sandstone (after Tecen 1982)

Researcher	Rock Type and UCS (MPa)	Depth of Cut (mm)	Cutting Speed (m/s)	Jet Pressure (MPa)	Flow Rate (1/min)	Jet Position	Maximum Force Reduction (%)
Hood (1976)	Norite (300)	1 - 10	0.15	10 - 50	30	1-2mm in front	50% normal 40% cutting
Wang and Walgamott (1978)	Sandstone (49)	15	Unknown	70	45	1-2mm in front	30% normal 70% cutting
Ropchan et al (1980)	Dakota Sandstone (42)	7.5-25	0.05-0.25	33 - 75	40	1-2mm in front & behind	60% normal 30% cutting
Dubugnon (1981)	Bohus Granite (200)	2 - 10	0.03 - 0.2	10 - 85	22	0-4mm in front	80% normal 70% cutting
Tecen (1982)	Darney Sandstone (48)	3 - 11	0.15	55	13	1 mm in front	70% normal 30% cutting
Plumpton & Tomlin (1982)	Darley Dale Sandstone (57)	13	1.27	70	11-90	1-2mm in front	50% normal 30% cutting
Ozdemir & Evans (1983)	German Sandstone (131)	2.5	0.25	138	25	3-12mm in front & behind	50% normal 50% cutting

TABLE 2.1 Summary of Laboratory Findings for Various Researchers.

Hood (1983, 1984) furthered his research in water jet assisted cutting at the University of California, Berkeley, USA. The results suggested that a threshold jet power level existed which had to be exceeded in order to achieve satisfactory results. In addition, the jet power must not exceed an optimum pressure or a reduced force reduction would result. The most important effect of the jet was observed to be the ability to flush out rock fragments from the tool front as soon as these were formed.

A brief summary of the laboratory findings in the field of water jet assisted rock cutting is tabulated in Table 2.1.

2.4.2 In-Situ Trials

The Alpine Miner F6-A was possibly the first roadheader fitted with high pressure water jets. McNary et al.(1976) described the augmentation. A 112 kW triplex pump was used which was capable of delivering 80 litre/min at 69 MPa. This system doubled the rate of production and produced a 70% reduction of respirable dust level to less than ·2 mg/m^3.

In 1978, a collaboration agreement between the US Department of Energy and the Mining Research and Development Establishment (MRDE) of the National Coal Board (NCB) was signed to produce a prototype water jet assisted system suitable for a standard boom-type roadheader. A standard Dosco MK2A roadheader was retrofitted with a 70 MPa water jet assisted system, with a flow rate of 4 litre/min per tool (Plate 2.1). The machine succeeded in cutting Middleton Limestone (UCS = 108-137 MPa), which is normally outside

Plate 2.1

the cutting ability of this type of machine (Figure 2.13). Extra benefits included much reduced machine vibration, prolonged pick life, suppressed dust level and elimination of frictional sparking.

Hood (1976) applied his laboratory findings to underground trials using the slotting machine to cut Witwatersrand Quartzite. With the water jet assisted cutting, the machine demonstrated an average fivefold gain in depth of cut and pick life was improved twofold.

Baumann et al. (1982) described the results of a high pressure water jet assisted roadway profile cutting machine cutting sandstone in a colliery. At a water pressure of approximately 100 MPa, the cutting forces and penetrating forces were reduced by 50% (Figure 2.14).

Based on these successful underground trials, several Europen manufacturers commenced the manufacture of water jet assisted roadheaders. In the UK, Dosco Overseas Engineering updated its popular MK2A roadheader, and the pre-production model completed its surface trials (Anon 1984). Straughan (1985) highlighted the technical development (water jet assisted roadheader) and described the experience of underground trials of both the MK2A and the MK2B in two collieries. Clark (1984) reported the field trials of an Anderson Strathclyde RH22 roadheader equipped with high pressure water jets and claimed that specific energy was reduced by approximately 30% and the cutting rate increased by approximately 50%. Similar developments were in progress in West Germany by Eickhoff and Paurat.

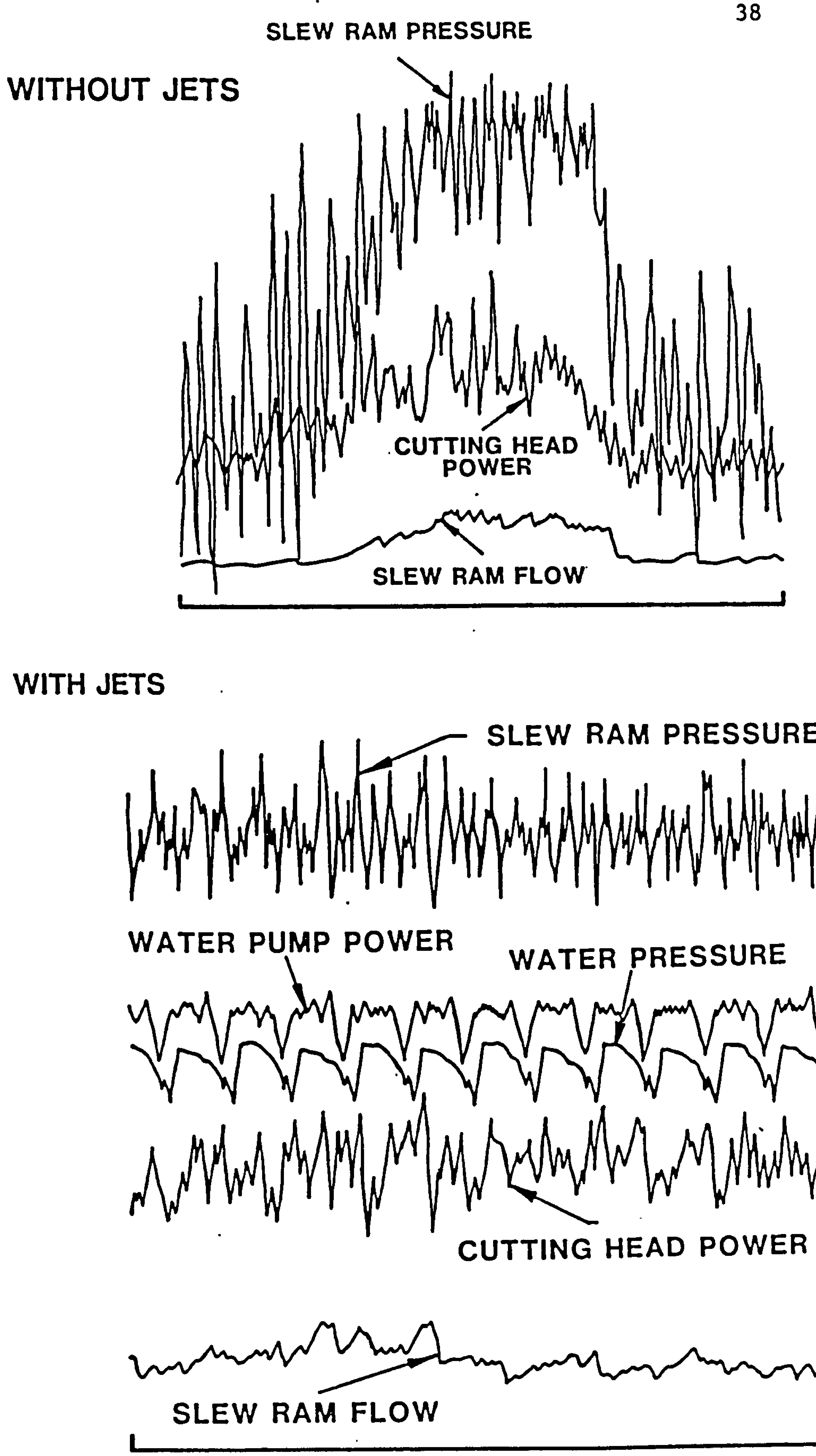

Figure 2.13 Cutting in Middleton Limestone with and without jets, using Dosco MK2A Roadheader (after Plumpton and Tomlin 1982).

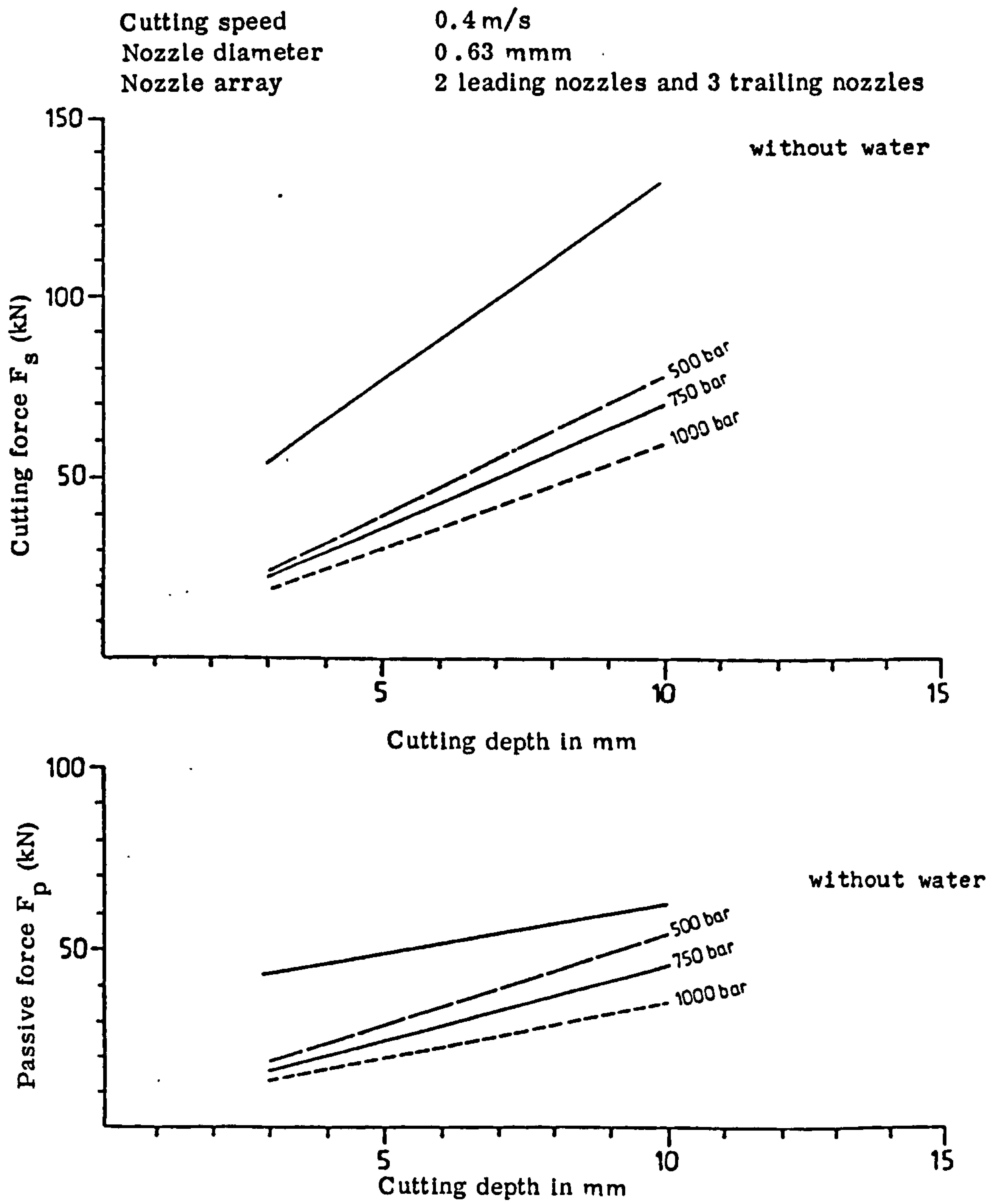

Figure 2.14 Water Jet Assisted Road Profile Profile Cutting. Jet Pressure up to 1000 Bar (after Baumann and Koppers 1982)

Other applications of high pressure water jet technology in related fields include ploughs, shearers and continuous miners. The jet assisted plough has been investigated by Summers et al. (1978) and by Henkel (1980). Adam (1985) discussed the retro-fitting of high pressure water jet systems to shearers and continuous miners to aid in coal production while Kovscek et al. (1985) reported on in-situ tests of longwall shearer retrofitted with water jets.

2.4.3 Empirical Equation

Kuzmich et al. (1982) are possibly the only workers so far who have proposed an expression that can be used to predict force reductions in the mode of hybrid cutting compared with the purely mechanical tool cutting. Based on the analysis of experimental data, a general formula was proposed to characterise the cutting force reduction which was dependent on the mode of cut (Figure 2.15).

(1) Unrelieved Cutting

$$\frac{Fc\ (h-m)}{Fc\ (m)} = 1 - 0.4 \left(\frac{h}{d}\right)^{0.5}$$

(2) Relieved Cutting

$$\frac{Fc(h-m)}{Fc(m)} = 0.18 \frac{t}{d} + 0.3 \left(1-\frac{h}{d}\right)$$

where: h = depth of slot (mm)

d = depth of cut (mm)

Fc(m) = cutting force for mechanical breakage (kN)

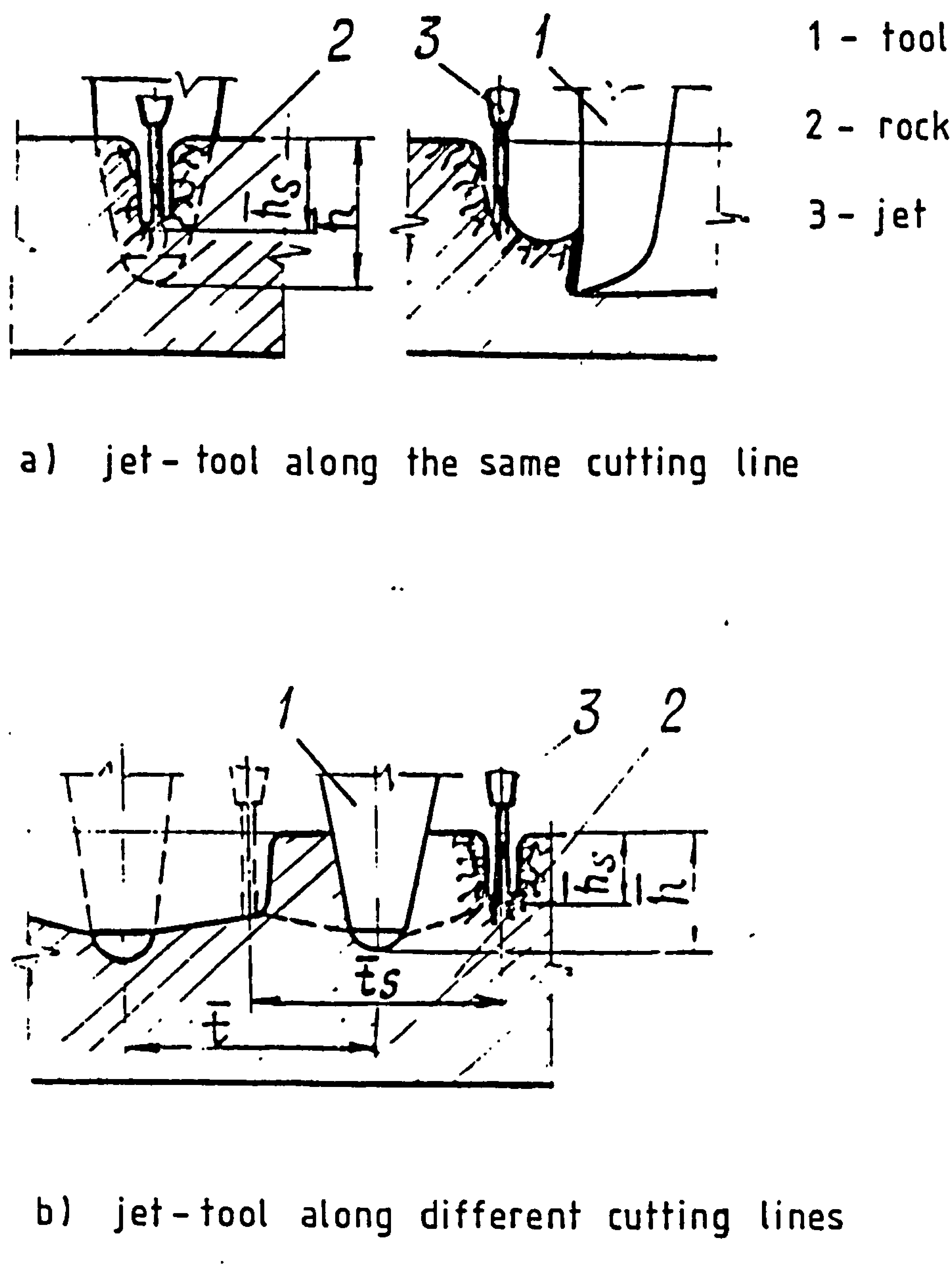

Figure 2.15 Schemes of Hydromechanical Rock Breakage (Kuzmich et al. 1982).

Fc(h-m) = cutting force for hydro-mechanical cutting (kN)

t = mechanical cutting pitch (mm)

Both of the above equations are based on experiments carried out on rocks with uniaxial compressive strength = 20-25 MPa.

2.4.4 Discussion

A common denominator throughout the various laboratory hybrid cutting studies is a cutting traverse speed of generally less than 0.25 m/s. The effect of traverse speed on dry rock cutting is always a point of argument, although it is generally agreed that the speed effect is insignificant with respect to the cutting force component within laboratory conditions which is in the range 0.15 to 0.46 m/s (Roxborough *et al*. 1975). Nishimatsu (1979) concluded that tool speed has no practical effect on cutting force, based on consideration of crack propagation speed and rate of strain, without proof from laboratory experiments. There is a scarcity of literature on this aspect and even less work has been published on normal force. However, in water jet assisted cutting, the impact of the water jet is highly dependent on exposure time (i.e. jet diameter/traverse speed) which is dependent on traverse speed. Hence there arises a previous doubt about the direct interpretation of laboratory findings to practical application in roadheaders which have a tool speed greater than 1 m/s (Table 1.2)

* * *

CHAPTER THREE

CHAPTER THREE

OBJECTIVE OF THE RESEARCH AND EXPERIMENTAL DESIGN

3.1 Object of the Reseach

The research project entitled, 'The Effect of High Pressure Water Jets on the Performance of Boom-Type Tunnelling Machines' is jointly sponsored by the European Coal and Steel Community (ECSC) and the Science and Engineering Research Council (SERC) for a period of three years. As part of the project, the Department of Mining Engineering of the University of Newcastle engaged in the research with the following terms of reference:

> "To investigate, through laboratory experiment, the fundamental mechanics of water jet action on rock surfaces, and the way in which such action affects the reaction of rock surfaces in pick cutting."

In line with the agreement with the Project Engineer, who is represented by the Mining Research and Development Establishment (MRDE) of the National Coal Board (NCB), the subject was studied in two phases. The first phase involved a quantitative approach to investigate the effect of jet pressure, depth of cut and traverse speed on the performance of water jets in hybrid cutting in five rock types. The secondary phase furthered the investigation by including other parameters, such as nozzle diameter, tool bluntness, wear rate, jet position and cutting mode in selected rock types.

The main theme of the project was to carry out laboratory rock cutting tests at traverse speeds over 1.0 m/s to simulate actual production machines in rock tunnelling. It is anticipated that the research results will provide a rational basis to predict pick force reduction under the assistance of high pressure water jets. This work summarises the research findings during the three-year life of the project.

As part of the same research contract, a research programme was carried out at MRDE to investigate the effects of high pressure water jet assistance on the wear rate of tungsten carbide tipped tools. This investigation ran parallel with the research carried out at Newcastle, with the main variables being jet pressure and traverse speed.

3.2 Scope of Work and Experimental Design

3.2.1 Experimental Variables

3.2.1.1 Independent Variables

There is a considerable number of parameter combinations that can be varied during a laboratory hybrid cutting test. Table 3.1 shows some possible independent parameters that can influence the assistance of the water jet in rock cutting. Depending on the interests of investigation, different parameters will be tested at different levels. For those parameters not covered in the present investigation, a brief description is provided in Section 3.3.

Variable	Levels	Value
(a) Jet		
(1) Jet Pressure	4	0,18,44,70 MPa
(2) Nozzle Diameter	4	0.6, 0.9, 1.2, 1.5 mm
(3) Nozzle Design	2	MRDE/Newcastle Nozzle
(4) Nozzle Material	2	Tungsten Carbide/Brass
(5) Additive	1	No additive
(6) Jet Type	1	Continuous, steady
(7) Jet Fluid	1	Water
(b) Operational		
(8) Depth of Cut	3	5, 10, 15 mm
(9) Traverse Speed	2	0.27, 1.10 m/s
(10) Tool Type	1	Wimet Swiftsure SS41/2HW
(11) Tool Bluntness	2	Sharp, Blunt
(12) Cutting Mode	2	Unrelieved, Relieved
(13) Stand-off Distance	1	64/80 mm
(14) Lead-on Distance	1	1-2 mm
(15) Jet Position	2	Jet Before/Jet Behind
(c) Rock		
(16) Rock Type	5	Sandstone: Dumfries, Grindleford, Penrith, Pennant; Limestone: Middleton.

Table 3.1 Independent Variables.

3.2.1.2 Dependent Variables

The parameters of performance fall into two categories, referred to as 'Primary' and 'Secondary'. The primary parameters can be measured directly, while the secondary parameters involve calculations based on the primary parameter values. The following list sets out the general parameters measured in the rock cutting tests:

Primary

- Mean Cutting Force
- Mean Peak Cutting Force
- Mean Normal Force
- Mean Peak Normal Force

Secondary

- Mean Cutting Force Reduction
- Mean Normal Force Reduction
- Mean Peak Cutting Force Reduction
- Mean Peak Normal Force Reduction

Mean force is defined as the arithmatic mean of the digitally logged data (Section 4.3.1.3):

$$\text{Mean Force } \bar{F} = \frac{\sum_{i=1}^{n} Fi}{n}$$

Mean peak force is defined as the 95 percentiles of the total digital force data. This definition is preferred as a fair estimation of chipping force can be made which is relatively unaffected by the choice of sampling time on cutting length.

The proposal to base the definition on the normal distribution was dropped as the data distribution is heavily skewed and cannot be adjusted using normalisation.

Mean cutting and normal forces are the main factors affecting the roadheader's performance in terms of power, arcing force and advance rate. The mean peak cutting and normal forces measure the mean chipping forces which are usually related to pick strength and pick box design. To evaluate the water jet assistance, force reductions are calculated with respect to the corresponding unassisted rock cutting. Because of the importance of the mean forces to the performance of the roadheader, the results are mostly expressed with mean cutting and mean normal force reductions plotted against jet pressure.

Rock yield is not normally measured, as specific energy is no longer an important criterion in hybrid cutting. The calculation of coarseness index was not attempted because of difficulties in collecting the debris, especially for hybrid cutting, as well as its irrelevance to cutting efficiency (Hurt and Laidlaw 1979).

3.2.2. Full Factorial versus Partial Factorial Experimental Design

A full factorial design is always preferred so long as the experiment size is manageable. A factorial experiment can estimate not only the main effects of variables, but also their interactions. However, a major disadvantage of a factorial approach is the great number of experiments involved. Even when all 16 variables are tested at two levels, one replication in a full factorial coverage requires:

$$2^{(16)} = 65536 \text{ tests.}$$

Obviously the size of this test is too large, without taking into account the replications required in order to provide meaningful results.

One method of reducing the number of tests required is by use of a partial factorial design. Protodyakonov et al. (1971) described a rational planning method by systematic variation of all factors. Using this method, the effect of levels of each factor can be obtained with a much smaller test size. Roxborough (1973), Roxborough et al. (1973) and Rispin et al. (1977) successfully applied this technique in rock cutting research.

Although the effect of levels of each factor can be estimated, the estimation is based on the mean effects of other variables. While it may be acceptable for variables without too much interaction, or for the magnitude estimation, it is surely not suitable for this project's purpose to investigate the cutting mechanism of hybrid cutting, as so many variables are potentially interacting. Tecen (1982) used this popular approach and found his results too insensitive for the detailed interpretation required.

The experimental programme in this project is divided into (a) a primary programme and (b) a secondary programme. A full factorial design is applied to a reduced number of variables in order to reduce the number of tests without jeopardising the full information on several important variables. Jet pressure is the principal parameter to be investigated in both the primary and secondary experimental programmes.

3.2.3 Primary Experimental Programme

This programme is designed to provide a full factorial investigation into the effects of jet pressure, depth of cut, and traverse speed on the measured tool forces. The same experimental design is applied to all five rock types so that comparable results are obtained. Other parameters are held constant for the benefit of smaller experiment size. The value of parameters chosen are shown in Table 3.2.

As an exception, the factorial experiment in Pennant Sandstone has been modified. Due to the rapid wear rate, separate tools are used for different traverse speeds. One tool is used for the slow traverse speed, and two tools for the fast traverse speed at 5mm and 10mm depths of cut. No test is carried out at 15mm depth of cut at 1.10 m/s traverse speed because of excessively high force components expected.

All the cuts carried out, both water jet assisted and unassisted, are unrelieved and independent of each other. This mode of cutting has the advantage of being unaffected by the spacing

Variable	Level	Value
1. Jet Pressure	4	0, 18, 44, 70 MPa
2. Depth of Cut	3	5, 10, 15 mm
3. Traverse Speed	2	0.27, 1.10 m/s
4. Nozzle Diameter	1	0.9 mm
5. Tool Bluntness	1	Sharp
6. Cutting Mode	1	Unrelieved
7. Jet Position	1	Jet before tool
8. Rock Type	5	Sandstone Dumfries, Grindleford Penrith, Pennant Limestone Middleton

Table 3.2 Primary Experimental Design.

effect, even when the water jet is operating. Thus the asistance from the water jet can be evaluated under fair and equal conditions. Moreover, the effect of jet penetration on tool force reduction can be identified and estimated. Before cutting commenced, the rock was trimmed flat using a large chisel tool. For the cuts to be independent, the spacing between successive cuts must be wide enough. A spacing of 5cm, 8cm and 12 cm were observed to be sufficient for mechanical depths of cut of 5mm, 10mm and 15mm respectively.

3.2.4 Secondary Experimental Programme

After the primary experimental programme, a general picture of water jet assisted cutting is obtained. The secondary experimental programme aimed at using smaller and discrete experiment designs to investigate the effects of other important parameters in selected rock types.

Mostly the effects of other parameters on water jet assistance are investigated with a depth of cut set equal to 10mm, which is based on the recommended minimum advance/start in hard rock tunnelling (Hurt and MacAndrew 1985). Also, the fast traverse speed is preferred, as the cutting results at fast speeds simulate more accurately the pick cutting in a real production tunnelling machine. However, except in the study of the effect of wear rate, all the cuts in Pennant Sandstone were carried out at slow traverse speed (0.27 m/s). This was because, at high traverse speed, wearflat generation is so rapid that the wear effect will dominate the tool force masking the effects of other parameters. Nevertheless, jet pressure is the most important parameter in the present study and appears in all experiments.

From the results of the primary experimental programme, it is clear with respect to water jet assistance that rocks can be divided into two groups; one group with significant jet penetration, and the other with no significant jet penetration. In order to study the effects of different parameters in both groups, it is desirable to cut the selected rock types from each group. Usually Grindleford Sandstone is chosen to represent the group with significant jet penetration, and Middleton Limestone and/or Pennant Sandstone to represent the group without significant jet penetration.

The experimental design to investigate the effects of different parameters is described in the following sections.

3.2.4.1 Effect of Nozzle Diameter

The effect of nozzle diameter was mainly investigated in Grindleford Sandstone. The study was carried out in the usual unrelieved cutting mode as well as relieved cutting mode. Table 3.3 gives details of variables employed during testing.

A limited study was also carried out in Pennant Sandstone in relieved cutting mode. Table 3.4 provides the details.

Variable	Level	Value
1. Jet Pressure	4	0, 18, 44, 70 MPa
2. Depth of Cut	1	10 mm
3. Traverse Speed	1	1.10 m/s
4. Nozzle Diameter	4	0.6, 0.9, 1.2 (1.5)*
5. Tool Bluntness	1	Sharp
6. Cutting Mode	2	Unrelieved/Relieved
7. Jet Position	1	Jet before tool

( )* for unrelieved cutting only.

Table 3.3 Experimental Design : Effect of Nozzle Diameter (Grindleford Sandstone).

Variable	Level	Value
1. Jet Pressure	4	0,18, 44, 70 MPa
2. Depth of Cut	1	10 mm
3. Traverse Speed	1	0.27 m/s
4. Nozzle Diameter	2	0.6, 0.9 mm
5. Tool Bluntness	1	Sharp
6. Cutting Mode	1	Relieved
7. Jet Position	1	Jet before tool

<u>Table 3.4</u> Experimental Design : Effect of Nozzle Diameter (Pennant Sandstone).

3.2.4.2 Effect of Tool Bluntness

The effect of tool bluntness on water jet assistance was mainly investigated in both Grindleford Sandstone and Middleton Limestone. The cuts were carried out in the unrelieved mode, with the jet positioned either before or behind the tool (Table 3.5).

A smaller programme was also undertaken to investigate the effect in the relieved cutting mode on Pennant Sandstone. Only the jet before the tool configuration was used. This is set out in Table 3.6.

3.2.4.3 Effect of Jet Position

The jet positions studied are either before the tool or behind the tool, with detailed configurations shown in Section 4.2.5. The effect of jet position was investigated in Grindleford Sandstone and Middleton Limestone, together with a study of the effect of tool bluntness (see Table 3.5).

3,2,4,4 Effect of Wear Rate

The effect of wear rate on water jet assisted cutting was studied in Pennant Sandstone at a fast traverse speed. The high strength and abrasivity of this rock provides an opportunity to investigate wear rate for a relatively short cutting distance. Around 16m was cut by a new tool in each combination of variables (Table 3.7).

Variable	Level	Value
1. Jet Pressure	4	0, 18, 44, 70 MPa
2. Depth of Cut	1	10 mm
3. Traverse Speed	2**	0.27, 1.10 m/s**
4. Nozzle Diameter	1	0.9 mm
5. Tool Bluntness	2	Sharp; Blunt
6. Cutting Mode	1	Unrelieved
7. Jet Position	2	Before/Behind tool

**Traverse speed was 1.10 m/s only for Middleton Limestone.

Table 3.5 Experimental Design : Effect of Tool Bluntness (Grindleford Sandstone and Middleton Limestone).

Variable	Level	Value
1. Jet Pressure	4	0, 18, 44, 70 MPa
2. Depth of Cut	1	10 mm
3. Traverse Speed	1	0.27 m/s
4. Nozzle Diameter	1	0.9 mm
5. Tool Bluntness	2	Sharp; Blunt
6. Cutting Mode	1	Relieved
7. Jet Position	1	Jet before tool

Table 3.6 Experimental Design : Effect of Tool Bluntness (Pennant Sandstone).

Variable	Level	Value
1. Jet Pressure	2	0, 70 MPa
2. Depth of Cut	1	10 mm
3. Traverse Speed	1	1.10 m/s
4. Nozzle Diameter	2	0.6, 0.9 mm
5. Tool Bluntness	1	Sharp (at the beginning)
6. Cutting Mode	1	Relieved
7. Jet Position	2	Before/Behind tool

Table 3.7 Experimental Design : Effect of Wear Rate (Pennant Sandstone).

3.2.4.5 Effect of Cutting Mode

The cutting modes used in this study were either unrelieved or a single relieved cutting. The unrelieved cutting is previously described (Section 3.2.3) and details of the relieved cutting can be found in Section 8.6. Other parameters investigated together include nozzle diameter and tool bluntness. The experimental designs for both Grindleford Sandstone and Pennant Sandstone are set out in Tables 3.8 and 3.9 respectively.

3.2.4.6 Effect of Slot Depth

The effect of slot depth to the drag tool cutting was studied in Grindleford Sandstone. A 0.9mm water jet of 70MPa at different traverse speeds was used to cut slots of various depth in trimmed rock surface. The tool was then positined carefully in the same line with the slot and cutting was taken without water jet assistance. The results are interpreted together with those for hybrid cutting (Table 3.10).

Variable	Level	Value
1. Jet Pressure	4	0, 18, 44, 70 MPa
2. Depth of Cut	1	10 mm
3. Traverse Speed	1	1.10 m/s
4. Nozzle Diameter	3	0.6, 0.9, 1.2 mm
5. Tool Bluntness	1	Sharp
6. Cutting Mode	2	Unrelieved; Relieved
7. Jet Position	1	Jet before tool

Table 3.8 Experimental Design : Effect of Cutting Mode (Grindleford Sandstone).

Variable	Level	Value
1. Jet Pressure	4	0, 18, 44, 70 MPa
2. Depth of Cut	1	10 mm
3. Traverse Speed	1	0.27 m/s
4. Nozzle Diameter	1	0.9 mm
5. Tool Bluntness	2	Sharp; Blunt
6. Cutting Mode	2	Unrelieved; Relieved
7. Jet Position	1	Jet before tool

Table 3.9 Experimental Design : Effect of Cutting Mode (Pennant Sandstone).

Variable	Level	Value
1. Depth of Cut	1	10mm
2. Traverse Speed	1	1.10 m/s
3. Tool Bluntness	1	Sharp
4. Cutting Mode	1	Unrelieved
5. Rock Type	1	Grindleford Sandstone
6. Slot depth	5	0, 3.7, 5.9, 7.4, 10.9 mm

Table 3.10 Experimental Design : Effect of Slot Depth (Grindleford Sandstone).

3.3 Parameters not Investigated

3.3.1 Stand-Off Distance

The stand-off distance, measured to the tool tip was either 64 mm for the jet before tool configuration, or 80 mm for the jet behind the tool configuration.

Shorter stand-off distance is always preferred as more efficient energy transfer is possible. However, if the stand-off distance is too short, the nozzle is vulnerable to damage by the debris during cutting. Hence the stand-off distance chosen represents a realistic compromise between nozzle safety and energy transfer efficiency. Leach and Walker (1966) showed that a good design nozzle can transfer 90% of the jet energy to target material when the stand-off distance is less than 100 times nozzle diameter. The nozzle mostly used during the present study was of 0.9 mm diameter. Hence the stand-off distance of 64 mm represents about 70 times nozzle diameter and a high energy transfer efficiency is expected.

Jet penetration is the dominant parameter in water jet assisted cutting. The effect of stand-off distance, if any, will be reflected in jet penetration obtained.

For the jet behind the tool configuration, a stand-off distance of 80 mm is required to provide clearance between rock and nozzle.

3.3.2 Additives

Polymer-type additives are always suggested to improve coherence and hence cutting ability of water jets. However, these are not inexpensive. Furthermore, the nature of rock tunnelling makes it impossible to collect and re-use the fluid, as is the practice in manufacturing industries.

The additive used in the present study was the general purpose soluble cutting oil with the sole purpose of protecting the water pump from rusting.

3.3.3 Nozzle Design

As jet penetration is the most important factor affecting water jet assistance (to be detailed later) the effect of nozzle design can be estimated by jet penetration, which was measured for each rock cut.

3.3.4 Jet Type

Only a continuous steady jet was used throughout the project.

Bresee *et al.* (1972) reviewed the comparative benefits of using continuous and pulsed jets for excavation. While a pulsed jet can produce very great pressure impact, the average delivery rate is slow. An example is as quoted. A continuous jet of 5.6 mm nozzle diameter at 70 MPa has an energy delivery rate of around 1875 kW. An Exoteds water cannon delivering 5 shots per second, with 16.4 ml water 'bullets' through a 5.6 mm nozzle at 490 MPa will have an average energy delivery rate of only 20 kW. In the light of the continuous nature of the tunnelling machine, a continuous jet is more desirable.

A cavitation jet can sometimes claim superiority over the continuous steady jet (Johnson *et al.* 1972), but its delicacy does not gain the approval of those who intend to use it in the hostile environment of underground tunnelling. Many cavitation jets have their applications in submerged operations.

3.3.5 Tool Type

A wedge-shaped, tipped tool is the most popular type of drag tool used in the mining industry of the United Kingdom. Fear of frictional sparking causing firedamp ignition means that point attack tools are not normally used except in the heavy and powerful roadheader. Throughout the present study, only the Wimet Swiftsure SS412 HW tool was used, which is a large, heavy-duty, radial tool. Details and specification can be found in Appendix A.

3.3.6 Lead-On Distance

The lead-on distance was 1-2mm, either before the tool tip for the jet-before-tool configuration or below the tool tip for the jet-behind-the-tool configuration.

For rocks that the jet cannot penetrate, the purpose of the jet is to aid debris clearance. As all the cracks are initiated by the tool tip, the jet should be as near to the tool tip in order to provide maximum efficiency.

For rocks that the jet can penetrate significantly, the jet can relieve the tool tip from inefficient crushing. Maximum efficiency is obtained when the jet can utilise the post-chip, curvilinear rock surface and penetrate and relieve the tool tip at minimal jet power. Positioning the jet as near as possible to the tool tip can provide optimal benefit. Section 8.7 provides more detail.

Experimental results evidencing the benefits of reduced lead-on distance have been reported elsewhere (Hood 1976; Dubugnon 1981; Plumpton and Tomlin 1982; Tecen 1982).

3.4 Replication and Randomisation of Experiments

3.4.1 Replication

Since every type of rock exhibits some heterogeneity to some extent, several replications of a test are required in order to provide a statistically significant value. The minimum number of tests required can be related to the coefficient of variance in the following fashion:

Coefficient of Variance (%)	Minimum Number of Tests
30	9
25	6
20	4
15	3

The previous cutting results for Bunter Sandstone obtained in the Department of Mining Engineering of this University (Roxborough et al. 1975) showed that the coefficient of variance for both cutting and normal forces was normally around 10% to 15%. Hence it was decided that four replications of each test should be carried out and presented as a mean value.

3.4.2 Randomisation

Most of the cutting experiments in this project were carried out in the unrelieved cutting mode on a trimmed surface. Trimming the rock surface is a tedious and time-consuming process. As a result it was decided to have cuts of the same depth of cut in one surface in order to reduce the trimming work. As the cutting characteristics of the rock may vary from surface to surface, the assignment of different depths of cut to different surfaces was randomised.

Within each repetition of the same depth of cut the sequence of cutting for different jet pressures and different traverse speeds were completely randomised.

Randomisation, together with repetition, is capable of evening up errors likely to exist in experimental results. These errors may be due to drift in the instrumentation system, gradually changing cutting characteristics within the rock and the wear rate of the tool.

*　　*　　*

CHAPTER FOUR

CHAPTER FOUR

EXPERIMENTAL EQUIPMENT AND MEASURING SYSTEMS

4.1 Introduction

This chapter is intended to provide a description and basic details of the equipment and measuring techniques used throughout this project. Further information and details may be obtained by reference to Appendix A.

4.2 Experimental Equipment

The experimental hardware, excluding the instrumentation, consisted of a 50-tonne linear cutting rig and a 75-kW high pressure pump. The diagrammetic representation of the cutting rig facilities is shown in Figure 4.1. Details of nozzles and the cutting tool used are also included in this section.

4.2.1 Linear Cutting Rig

The linear cutting rig used during this project was an existing 50-tonne rock planing machine previously used for roller disc cutting studies (Fauvel 1981; Hekimoglu 1984). The major modification involved the replacement of a large diameter, double-acting ram, with a small diameter double-acting ram to increase the traverse speed capability from 0.25 m/s to 1.0 m/s. As a smaller diameter ram was used the new force limit in the cutting direction was 5-tonne. An overall view of the rig is given in Plate 4.1.

A = Dynamometer/Tool/Water jet assembly
B = Ram
C = Structure
D = Hydraulic Accumulators
LPW = Low Pressure Water
HPW = High Pressure Water
LPHO = Low Pressure Hydraulic oil
HPHO = High Pressure Hydraulic oil

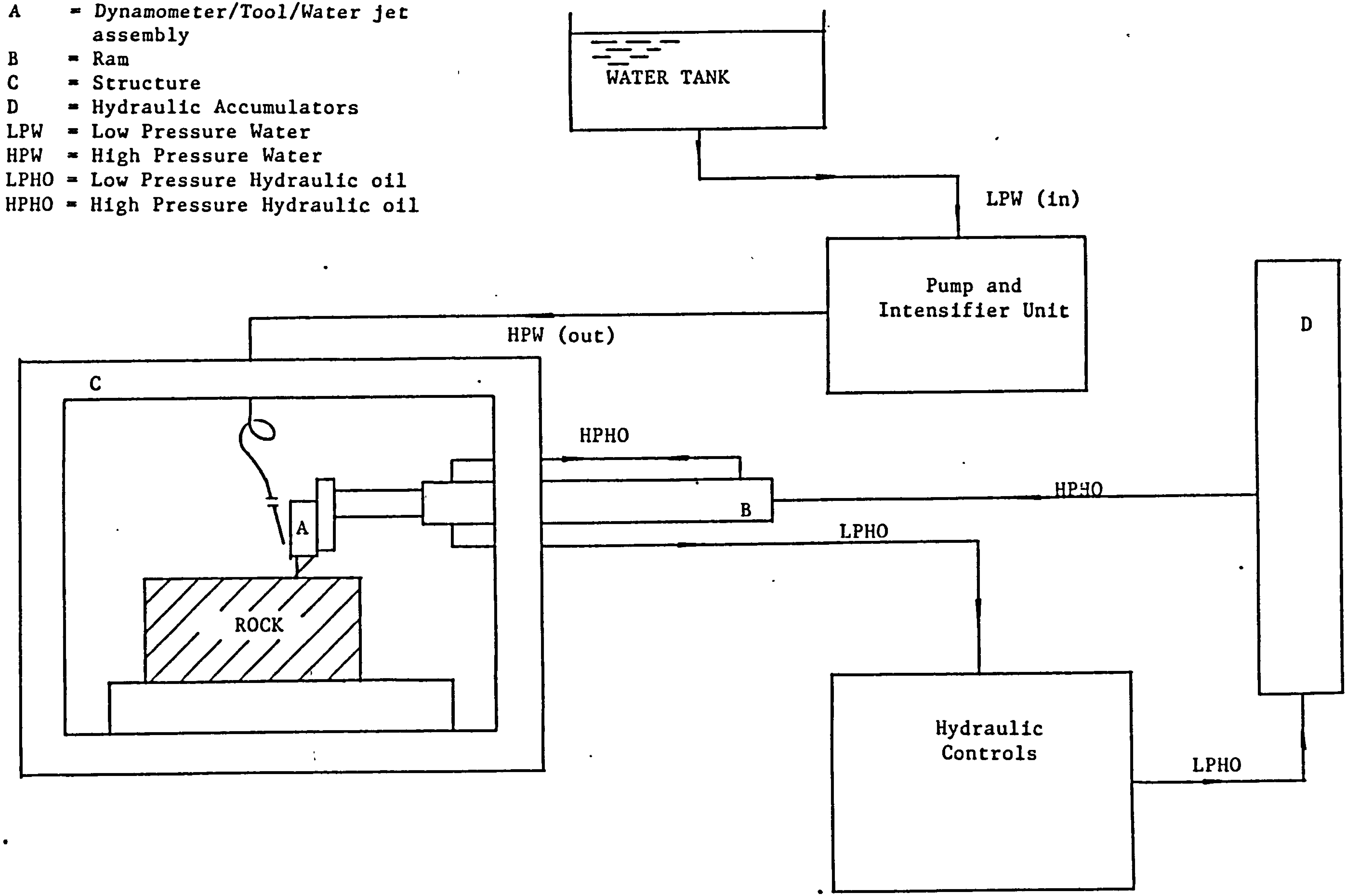

Figure 4.1 Diagrammatic representation of the cutting rig facility.

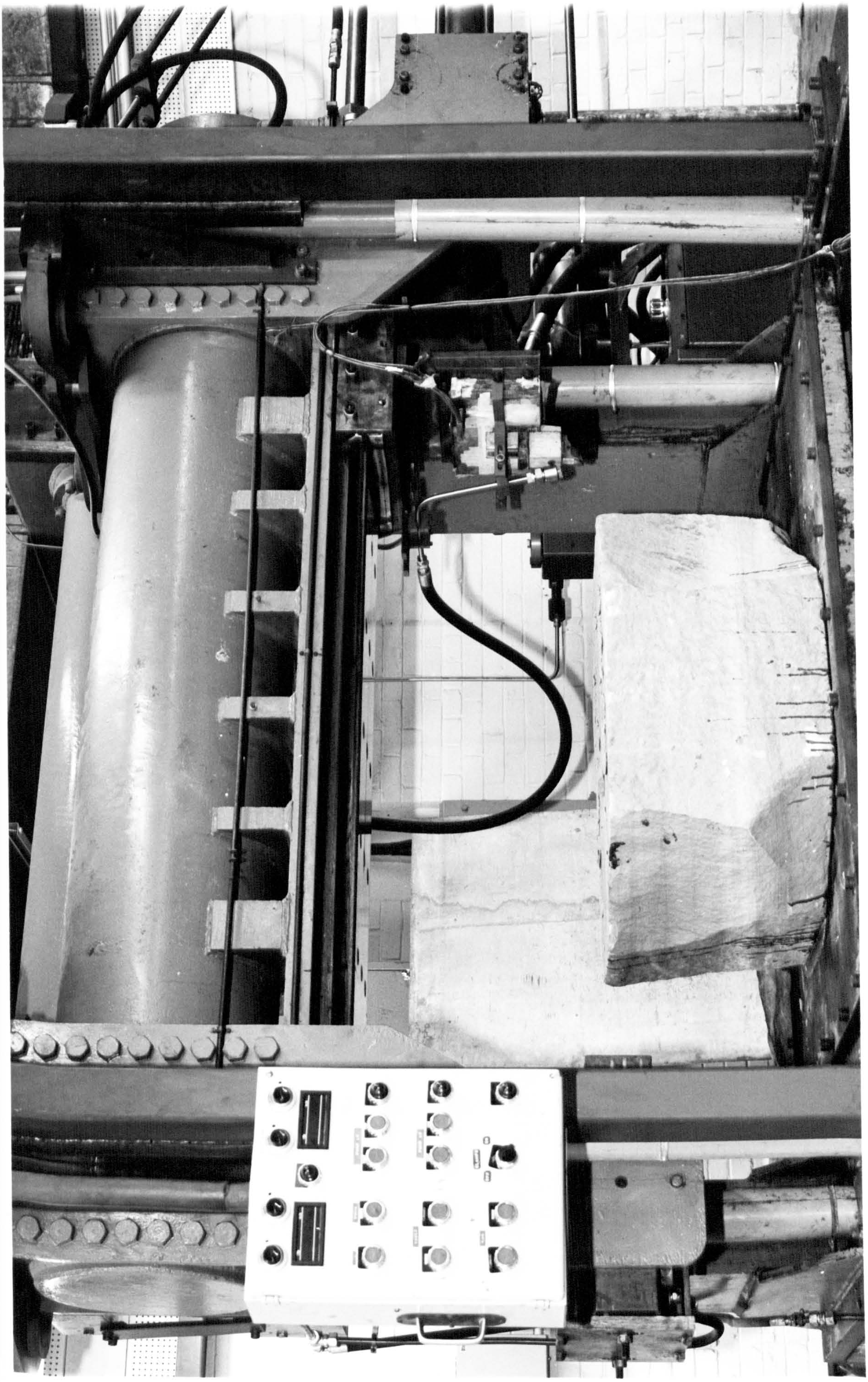

Plate 4.1

Only the essential features of the rig will be described here, as mechanical details are obtainable elsewhere (Fauvel 1981)

4.2.1.1 <u>Frame Structure</u>

The main structure of the rig consists of a rectangular base frame and four columns.

The base frame is constructed of four large, rectangular sections bolted together at the corners. The rear columns are rigidly fixed to the base frame and served as support and guides to the cutter slide assembly. The two columns are laterally restrained with a large circular beam fixed at the top. The front columns are bolted to the base frame mainly to improve vertical stiffness when used together with the clamps. Two guides are fixed on the base frame where a specimen table can slide over. The whole structure is freely supported at the four corners by the concrete floor, and self-stabilised by its own weight.

4.2.1.2 <u>Cutter Slide Assembly</u>

The main structure is a large-diameter tube which acts as a rigid beam. A thick metal plate is welded to it which is, in turn, bolted with the cutter slide. The cutter slide is of a trapezoidal section to enable the tool slider to hang on and slide along it.

The slide assembly is attached to the mainframe by four pairs of shoes which slide along vertical guide plates on the rear columns. The vertical positioning of the assembly is carried out by four screw jacks which are powered by an electric motor via drive shafts and gearboxes. A potentiometer is fixed so that the vertical position of the assembly is shown on a digital volt meter (DVM) on the control panel.

The four screw jacks, because of their long length and small diameter, provide insufficient vertical stiffness to the assembly. A clamping system was designed (Fauvel 1981) to improve this situation. Two large clamps with eight shoes are placed on the top of the cutter slide assembly. The clamps are hydraulically powered and are capable of providing a gripping force of approximately 25 tonne for each shoe. Cutter deflection was 0.6mm at a vertical thrust of 10 tonnes, after modification.

The slider is basically a large block of steel with the top side machined to provide a matching trapezoidal slot for the slides. A large clevis is bolted at the back of the slider which allows the attachment of the cutting ram. At the front end of the slider, a vertical plate is bolt-fixed at the top and supported by a short, but large, metal prop at the bottom. The other end of the short prop is connected to the clevis to provide the horizontal rigidity of the vertical plate. The vertical plate provides the base and the support or the jet/tool/dynamometer assembly.

Movement of the ram is controlled by limiting switches on the cutter slide assembly, for both foward and reverse motion. It is important to have these switches well located in suitable positions, particularly during the cutting at 1.10 m/s traverse speed, in order to prevent the jet/tool/dynamometer assembly from running into the stop and sustaining damage.

4.2.1.3 Hydraulic System

Two independent hydraulic systems are operated. The main system provides the power for the cutting tool and the clamping system serves to improve the stiffness of the rig.

(a) Main Hydraulic System : The main hydraulic system is illustrated schematically in Figure 4.1. The desired power output is provided by a battery of accumulators which are charged using a high pressure, low delivery volume pump. Another system utilising a low pressure, high volume pump is not used because of its slow speed. The traverse speed of the ram can be changed continuously up to 1.10 m/s by operating the flow control valve. The hydraulic panel, together with accumulators, is shown in Plate 4.2, while some details about the hydraulics of the ram can be found in Plate 4.3

(b) Clamping Hydraulic System : The clamping hydraulic system consists of a small motor and pump assembly mounted at the top of the left-hand rear column. When actuated, this system can provide a clamping pressure of 21 MPa.

The clamping hydraulic system is controlled by a switch on the control panel. When the clamps are

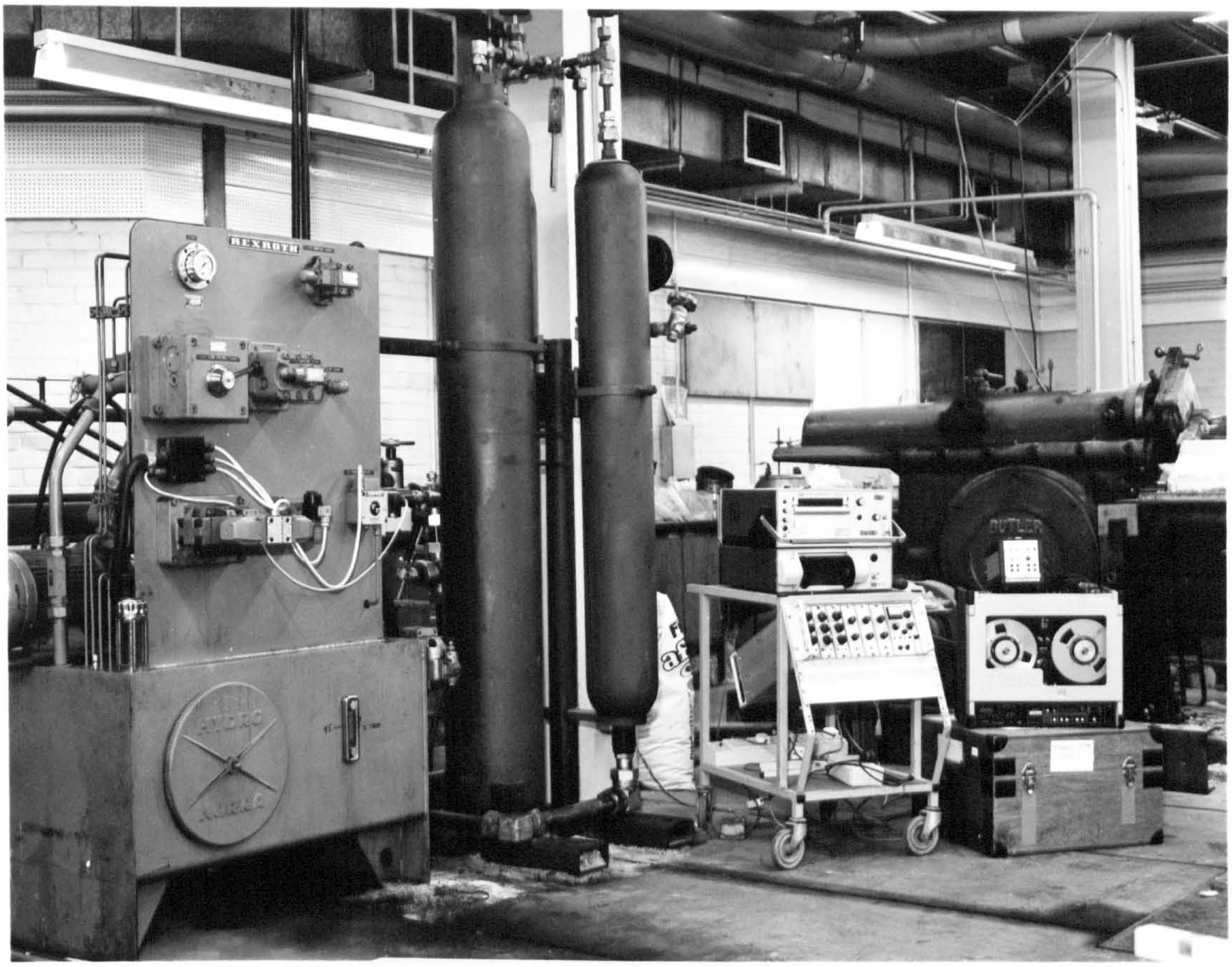

Plate 4.2

Plate 4.3

operating, the cutter positioning switches are automatically isolated in order to prevent damage to the vertical drive system.

4.2.1.4 Jet/Tool/Dynamometer Assembly

A steel dynamometer (Allington 1969) is fixed to a back plate which, in turn, is fixed to the vertical base plate. The attachment of the vertical base plate to the cutter slider and to the ram has been described earlier (Section 4.2.1.2).

The cutting tool is fixed to a matching tool holder which, in turn, is firmly held to the dynamometer. More details about the dynamometer can be found in Appendix A.

The water jet is fixed in position by attachment to the back plate and the cutter slider, which are independent of the tool/dynamometer arrangement. Accurate positioning of the jet is made possible by fine adjustment of the fastening screws when the pump is running at low pressure output.

Because of the adverse effect of moisture on electrical signals and rusting of the metal dynamometer, the dynamometer is protected from the jet water splashing. A perspex 'box' was made which covers most parts of the dynamometer. Where a gap is needed to allow deformation of the dynamometer during rock cutting, a spongy, draught-stopping tape is fixed. The importance of stopping any water ingress into the dynamometer was highlighted at an early stage in the project when the strain gauges peeled off because of the metal rusting separating the bond between strain gauges and dynamometer.

The jet/tool/dynamometer assembly is shown in close-up in Plate 4.4.

4.2.1.5 Specimen Table and Drive System

The specimen table is a large, thick steel plate with deep rib reinforcement underneath. The table is supported on two sides by the guides, which are part of the base frame, and is free to slide back and forth along the guides.

Positioning of the table is achieved by two screw jacks which are mounted on the front beam of the base. The jacks are powered by an electric motor and a 2:1 right-angle drive gearbox. Travel of the table is controlled by a pair of limiting switches fixed underneath one of the guides.

A potentiometer device is mounted under the table. When calibrated, this gives the horizontal position of the table, which is shown on a digital volt meter (DVM) on the control panel.

4.2.1.6 Mounting of Samples

The maximum size of sample which can be accommodated by the rig is limited to 1.5m x 1.0m x 1.0m. Usually the quarry is requested to supply the rock samples with one diamond sawn flat base surface. The rock is then bonded to a metal plate using high strength Araldite 2003 epoxy resin. After the bond has set, the plate is bolted to the table.

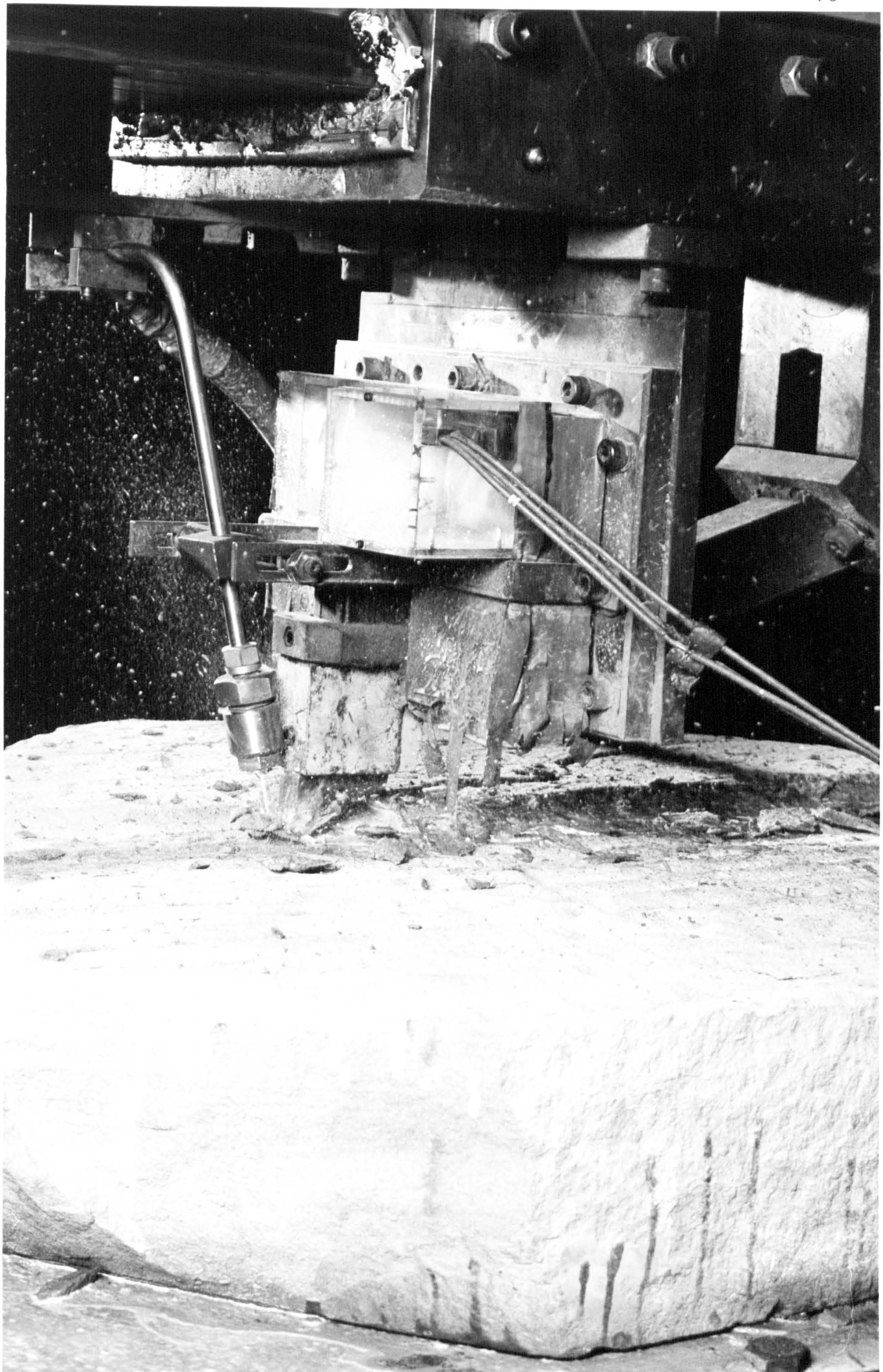

Plate 4.4

Sometimes an irregular block of rock is supplied. In this case, the rock is trimmed to provide a flat surface before adhesion to the plate is possible. Four metal channels are fixed on the table with the rock block positioned in the centre. Wood packing is placed between the rock and the channels to secure the rock in position. Then the rock is trimmed in small depth increments until a flat surface is obtained. The rock is subsequently mounted in the same way as that described earlier.

4.2.1.7 Protective Measures

Because of the potential danger of the high pressure water jet to operating personnel, a strict safety procedure is observed. Basically the whole linear cutting rig is enclosed. For the front, a 5mm transparent, shatter-proof Makrolon polycarbonate sheet is used. For the other sides 9mm plywood is used. Because of the frequent vertical movement of the cutter slide assembly, a thick plastic curtain is used to prevent water splashing on the right-hand side of the rig. This protective measure is considered adequate as ram and motors occupy most of this space.

This arrangement provided satisfactory protection during the three-year period of operation of the rig.

4.2.2 High Pressure Water Supply

The high pressure water supply was provided by a 75 kW Presswell Hydroflo intensifer type pump with a capacity of 45 litre/min at 70 MPa (Plate 4.5). The high pressure

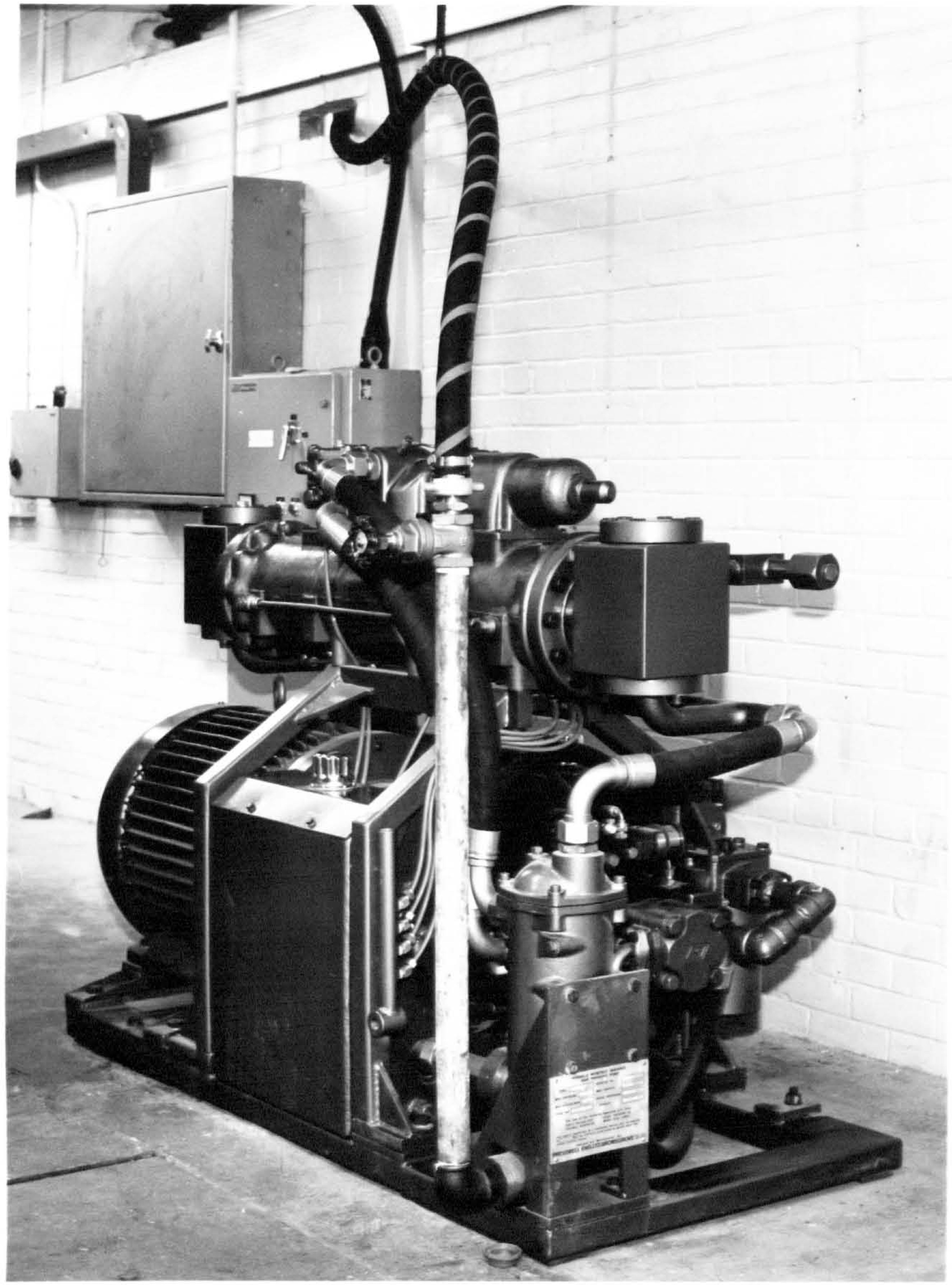

Plate 4.5

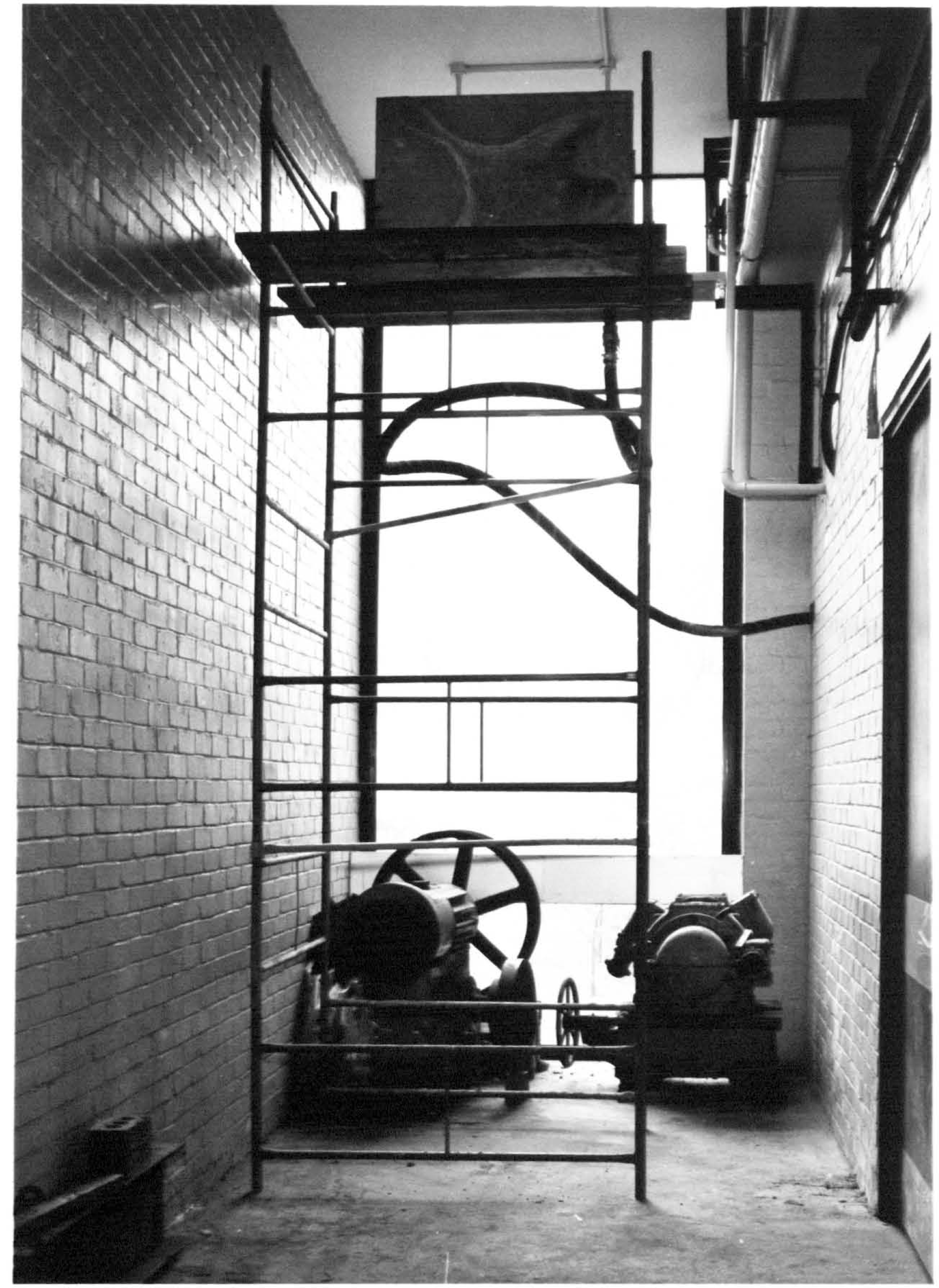

Plate 4.6

output from the pump is taken to the nozzle through a 12.7mm OD stainless steel tubing and braided flexible hose. The flexible hose allows the nozzle to move freely with the tool.

The water supply to the pump is from a 50-gallon water tank. The tank is mounted on a scaffolding tower which provides the necessary 2m head above the intensifier unit (Plate 4.6).

A problem with this pump was its inconsistent pressure output (an example is given in Figure 4.2) and normally the minimum pressure is only up to 50%-60% of the mean value. This phenomenon is due to the nature of the double acting intensifier and the compressibility of water. The water delivered from each stroke is approximately 0.10 litre and the pulse period can be obtained by dividing stroke volume by flow rate. Fluctuation of water pressure can be reduced by installation of an accumulator which, unfortunately, was not available from the pump manufacturer.

A conversion kit is available to convert the present 70 MPa to a 210 MPa system. It is expected that the pressure fluctuation problem will become even more acute at the higher pressure and some form of pressure damping is recommended.

Throughout this project the jet pressure quoted is the mean pressure measured during the course of rock cutting.

4.2.3 Nozzle

Two different types of nozzle have been used during this research. Plate 4.7 shows a general view and Figures 4.3 and 4.4 contain design details of the two nozzles.

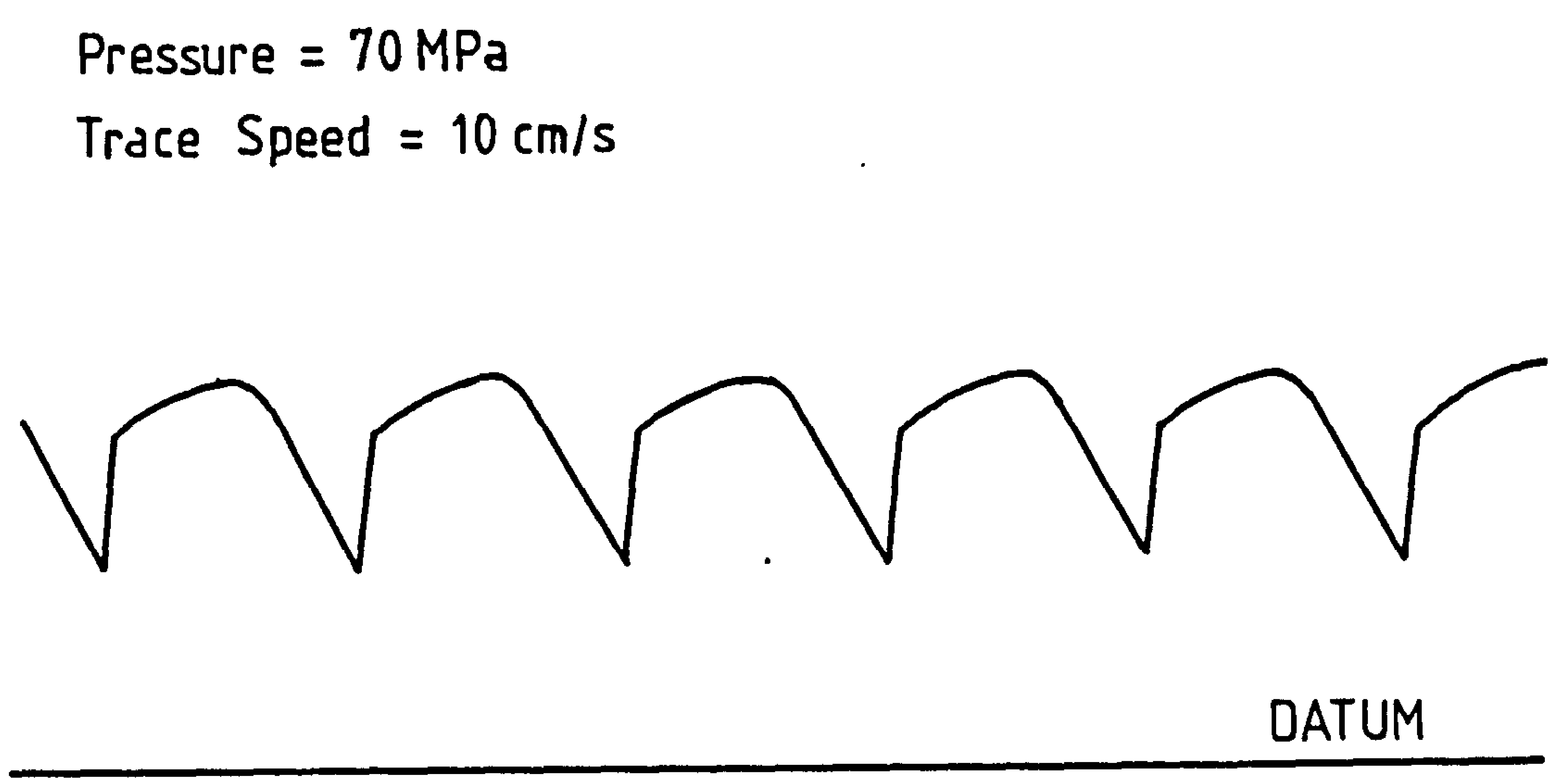

Figure 4.2 Fluctuation of Jet Pressure Output.

Plate 4.7

Plate 4.8

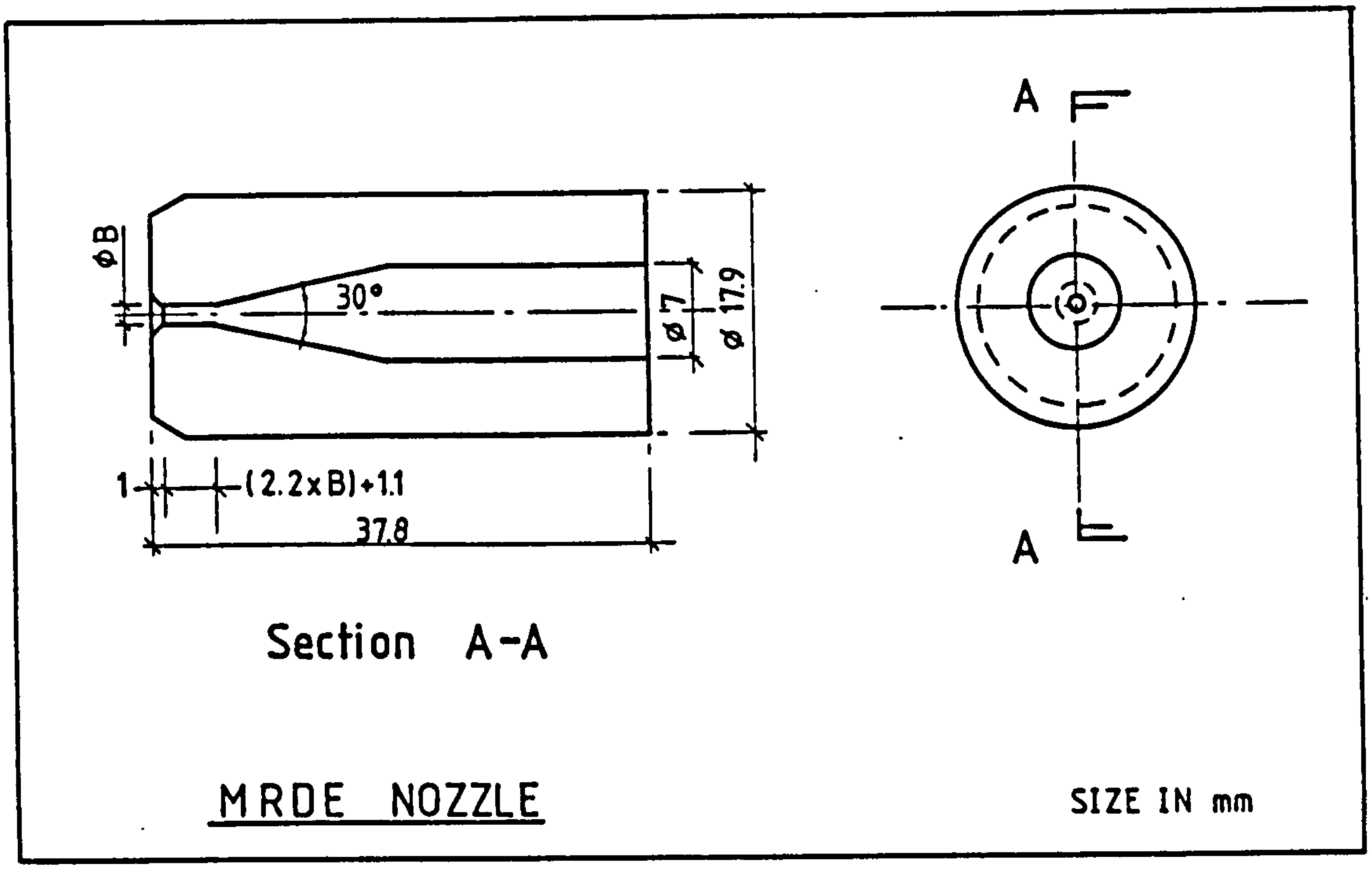

Figure 4.3 MRDE Nozzle Design Details.

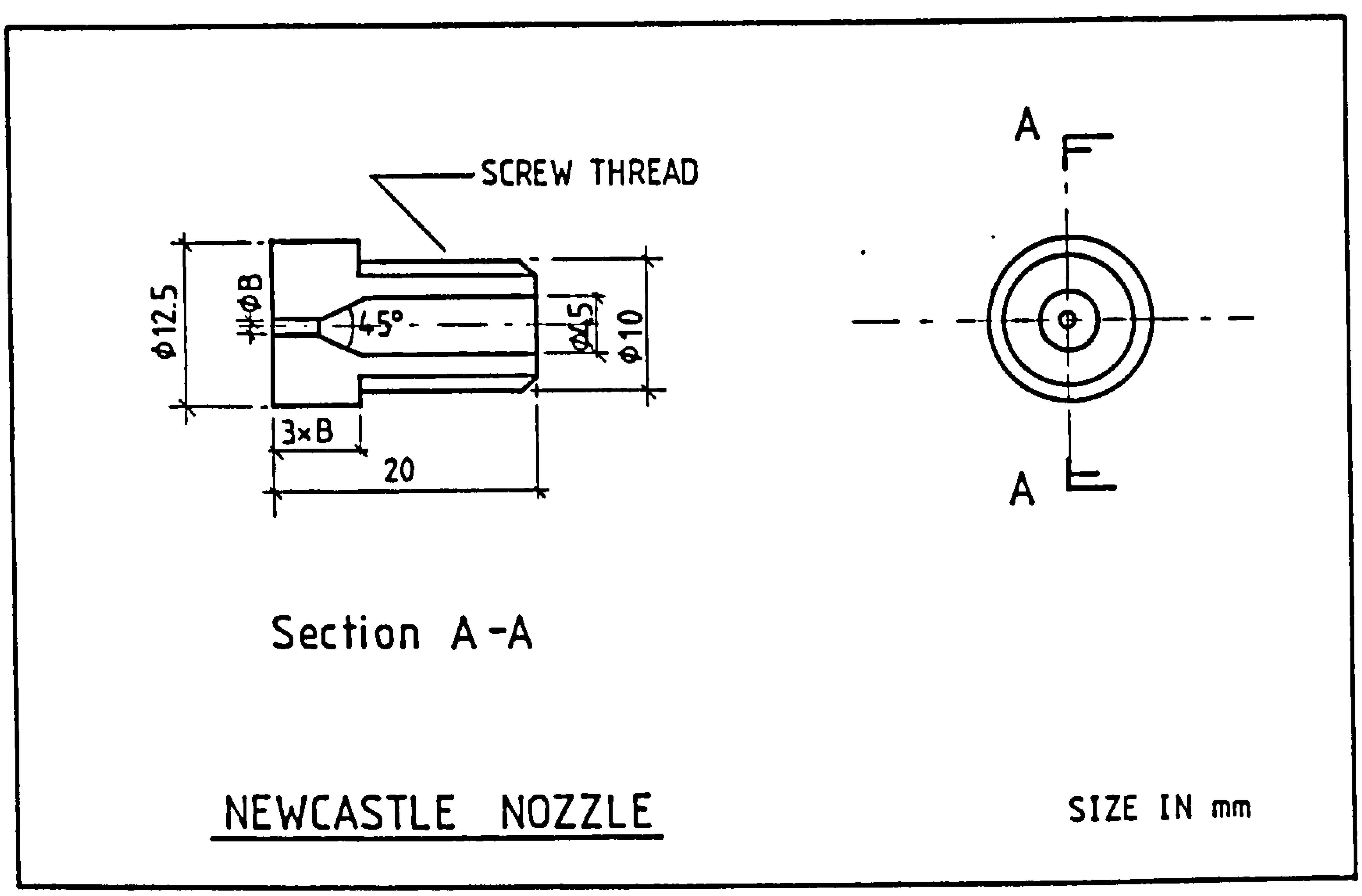

Figure 4.4 Newcastle Nozzle Design Details.

The larger nozzle is made of tungsten carbide and designed by MRDE/NCB. The nozzle has a 30° contraction angle and was used in the primary cutting experiments with Dumfries Sandstone and Penrith Sandstone. At a later stage, when the effect of jet position was investigated, the nozzle was regarded as being too large to be positioned behind the tool within reasonable stand-off distance. The nozzle holder has an outside diameter of 38mm.

Consequently, a brass nozzle was manufactured in the Department's workshop. The nozzle was fixed by screwing into the stainless steel pipe. A Dowty washer (a metal washer with a rubber ring inside) was placed between the nozzle and pipe to act as a seal, which gave satisfactory results. As a result of manufacturing difficulties the nozzle designed was altered and the new contraction angle was 45°. This nozzle was used in all cutting experiments with Grindleford Sandstone, Pennant Sandstone and Middleton Limestone.

A simple test was carried out to compare the performance of two nozzles by slotting Grindleford Sandstone and the results are presented in Figure 4.5. The two nozzles performed in very much the same way in respect of the effect of stand-off distance, with the Newcastle nozzle having a slightly deeper penetration.

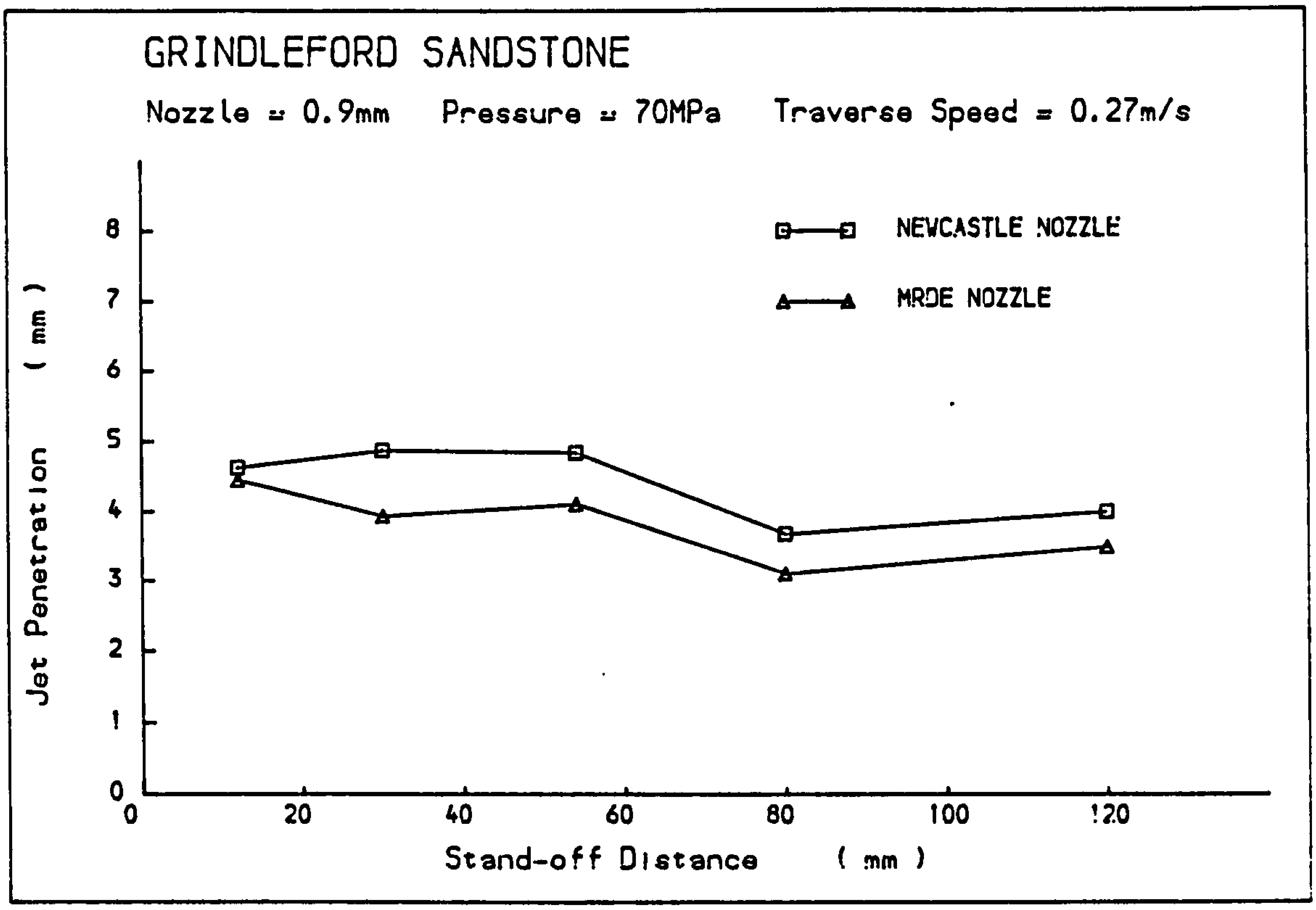

Figure 4.5 Performance comparison between MRDE and Newcastle nozzles.

4.2.4 Cutting Tool

The only tool used was a Wimet Swiftsure SS412 HW heavy duty radial tool.

When a blunt tool was required, an artificially induced blunt tool was used. The tool tip of a used tool was ground to give a wearflat of about $21mm^2$ and a wearflat angle of about $-4°$, which is common for a developed blunt tool (Kenny and Johnson 1976). After the grinding, the tool cut 30m of

Grindleford Sandstone to round off any sharp edges. This method of blunting is acceptable as Kenny and Johnson (1976) showed that the blunt tool forces are contributed mainly by the wearflat.

The blunt tool used represents a moderately blunt tool by mining standards.

Plate 4.8 shows both the sharp and the blunt tools.

4.2.5 Jet Mounting

Two jet positions were tested during the research study. One was the jet-before-tool configuration and the other was the jet-behind-tool configuration. These are shown in Figures 4.6 and 4.7 respectively.

In the jet-before-tool configuration, the nozzle was positioned so that the jet impinged about 1-2mm before the tool tip and at an angle of 77.5° toward the tool. The distance between jet and tool tip was 64mm.

In the jet-after-tool configuration, the nozzle was positioned immediately after the tool tip and the jet impinged about 1-2mm under the tip. The direction of the jet was parallel to the back clearance angle of the tool, which was about 11°. The distance between tool tip and jet, in this case, was 80mm.

4.3 Measuring Systems

Instrumentation systems were set up to measure the tool forces, jet pressure and traverse speed. The typical arrangement

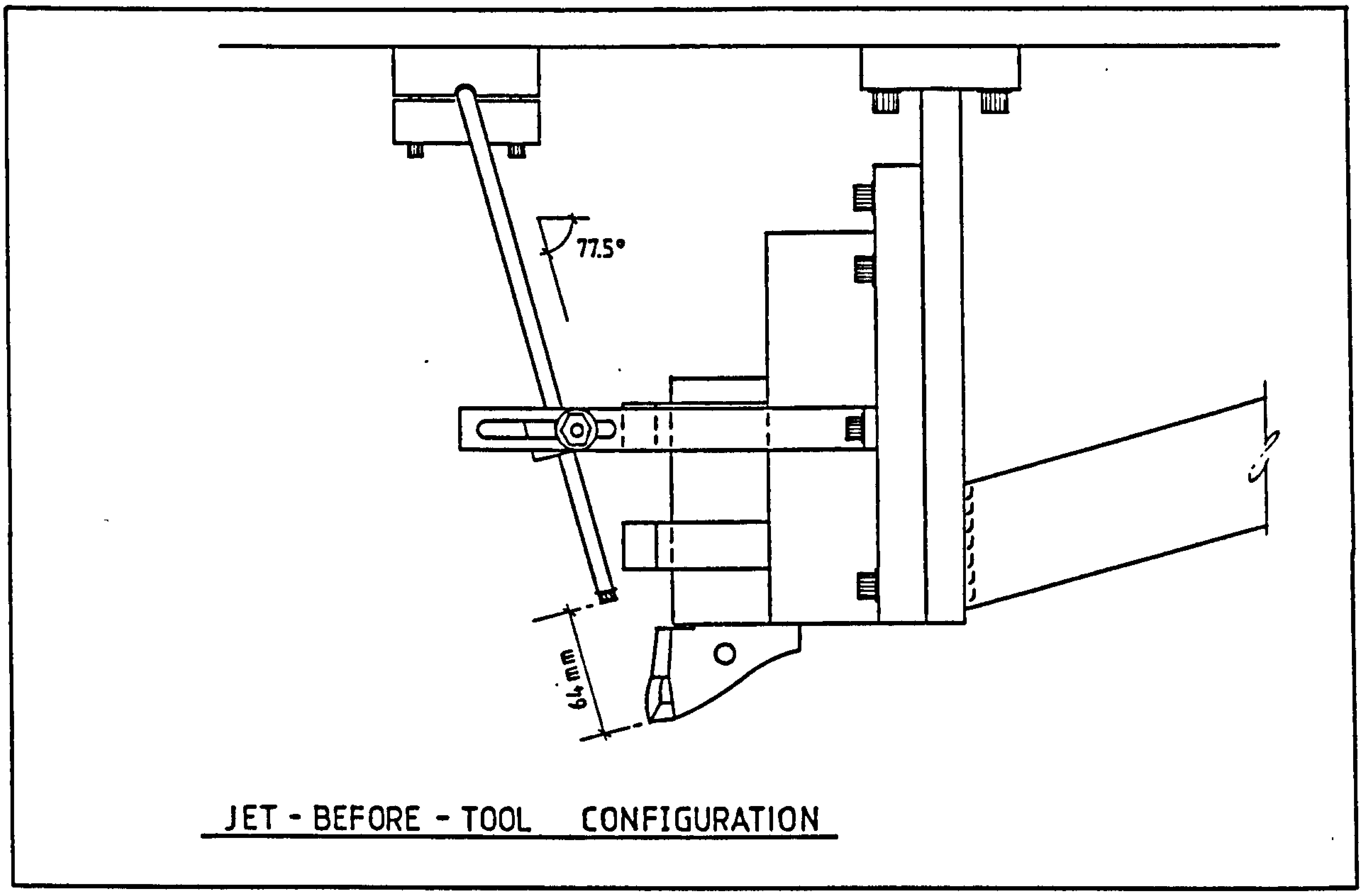

Figure 4.6 Jet-Before-Tool Configuration.

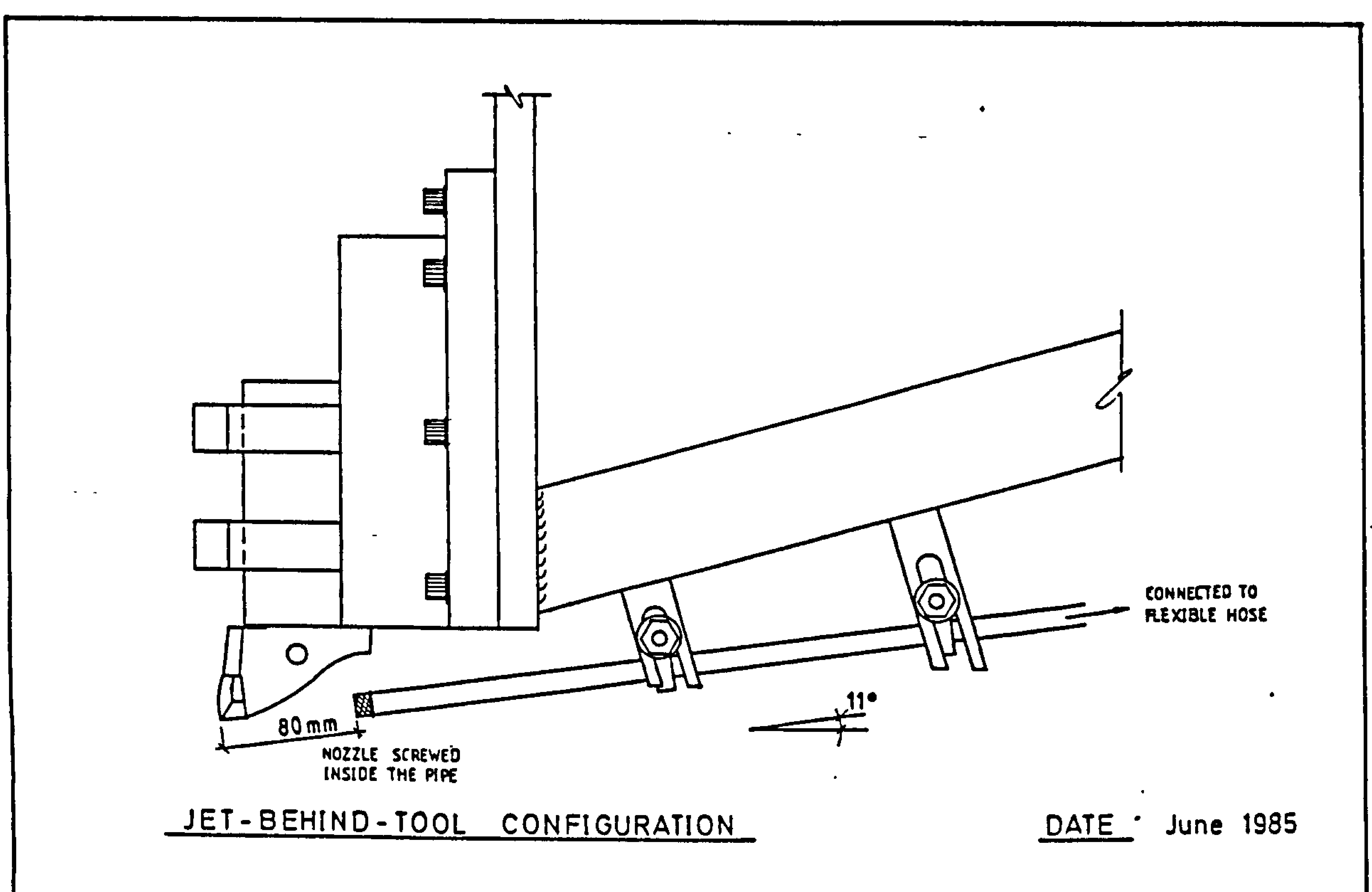

Figure 4.7 Jet-After-Tool Configuration.

of all instruments is illustrated in Plate 4.9. The control panel of the mechanical system was positioned near the measuring system so that both systems could be operated simultaneously during rock cutting.

4.3.1 Force Measuring System

4.3.1.1 Triaxial Dynamometer and Data Acquisition System

The tool force experienced by the tool during rock cutting is transmitted to a force transducer via the tool holder. The force transducer is a four-post steel triaxial dynamometer which is capable of resolving the tool force into three orthogonal directions. Full details can be found in Allington's (1969) thesis and the dynamometer was successfully used for rock cutting research afterwards (Hewitt 1975; Tecen 1982; Hekimoglu 1984).

Basically, three sets of strain gauges are attached in precise position on the surface of the four steel posts of the dynamometer; each set is designed to measure the three mutually perpendicular tool force components. The strain gauges form a Wheatstone Bridge, which is energised by a carrier amplifier SE4000 system. The strains, which are proportional to the tool force, distort the bridge balance and generate electrical signals.

Amplified signals of -2 to +2 volts are recorded on a SE3000 precision tape recorder. The data is processed and analysed digitally as detailed in Section 4.3.1.3. From time

Plate 4.9

to time it may be desirable to have a chart output for direct visual inspection and assessment. In this case the tape is played back and signals converted from voltage to current using the SE1050 signal conditioning system. The force traces are then shown on a photographic paper output on an SE3006 UV chart recorder.

Although three tool component forces could be measured, only cutting and normal force components were recorded. The sideway force was ignored because most of the cuts were unrelieved cuttings in a trimmed surface, and the sideway force tended to be very small.

4.3.1.2 Calibration Tests

Calibration tests have been carried out to provide a correlation between the tool force experienced and the electrical signal recorded. The general arrangements for cutting and normal force calibrations are shown in Plate 4.10.

A special calibration tool which simulates the cutting tool, with a steel ball mounted with its centre at the position of the tool tip was specially machined. An NCB/MRDE Type 405 load cell is placed between the calibration tool and a jack which is powered by an hydraulic hand pump. The load cell is connected to a Vishay strain indicator so that the strain can be obtained. The loading is applied and simultaneous readings are taken from the tape recorder and the strain indicator.

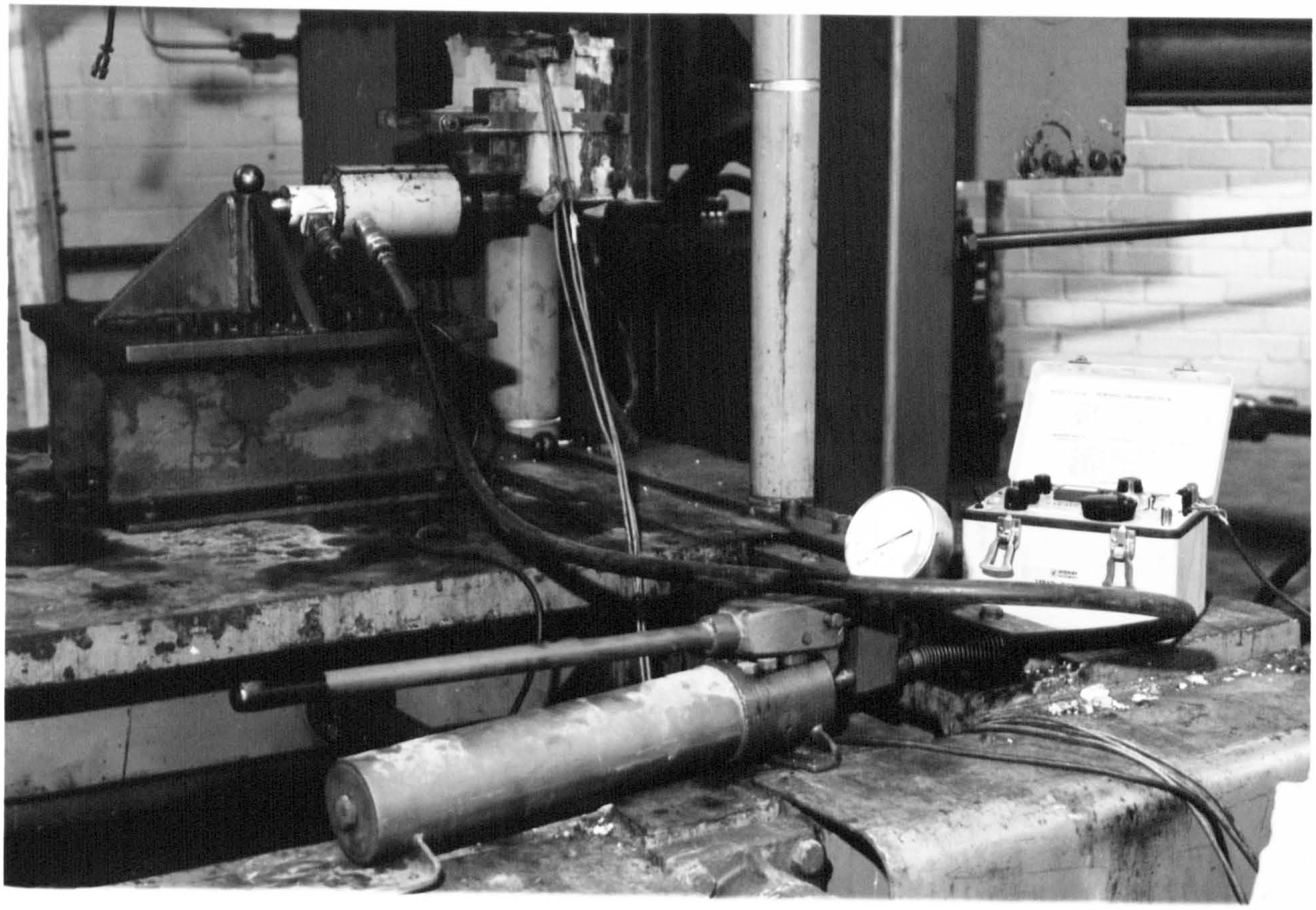

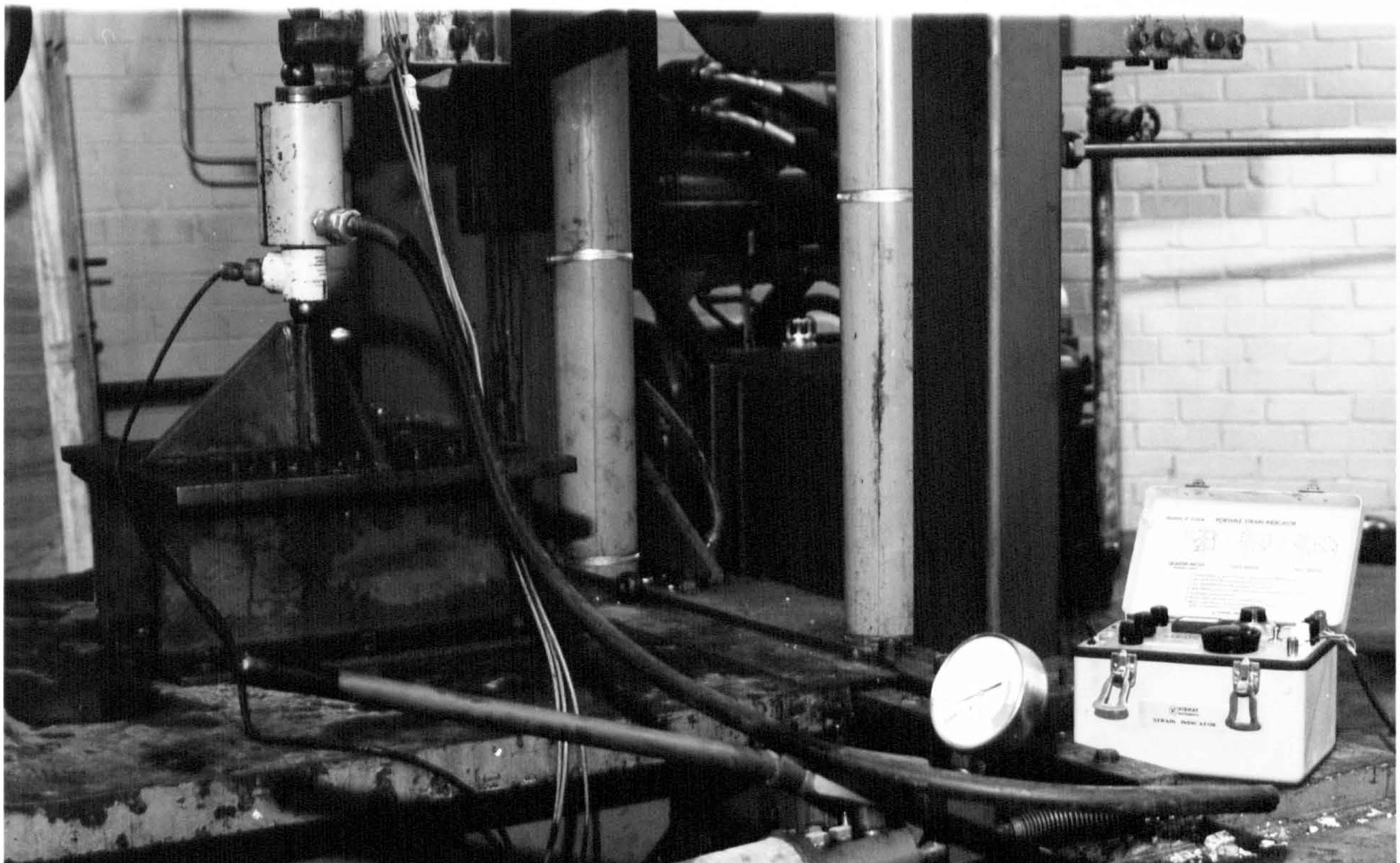

Plate 4.10

Calibration tests were carried out at least five times, depending on the consistency of both cutting and normal forces. The dynamometer was calibrated to the maximum tool forces likely to be experienced during the experiments. After the test, the load cell is calibrated using the Department's Avery 25t compression machine.

Typical calibration curves of cutting and normal forces are plotted in Figures 4.8 and 4.9 respectively. Generally the linearity of the curves was very good; however, there was some cross-talk between the normal force channel and the cutting force channel during normal force calibration. This interaction was due to the moment created by the normal force to the dynamometer as the tool tip was about 80mm before the dynamometer instead of directly underneath. However, this interaction was ignored for two reasons. Firstly, it magnitude was small for most of the normal forces encountered. Secondly, and most importantly, the moment provided by the cutting force tended to offset the moment provided by the normal force. Interaction from the cutting force to the normal force channel, on the other hand, was found to be very small.

As the dynamometer was situated in an extremely hostile environment where excessive moisture, dust, vibration, airborne noise, are common, at least one calibration test was carried out for each rock type. The calibration test was necessary to guarantee meaningful results were obtained over the life of the project. One of these exercises led to the discovery of a strain gauge failure and the dynamometer was subsequently cleaned and refitted with strain gauges.

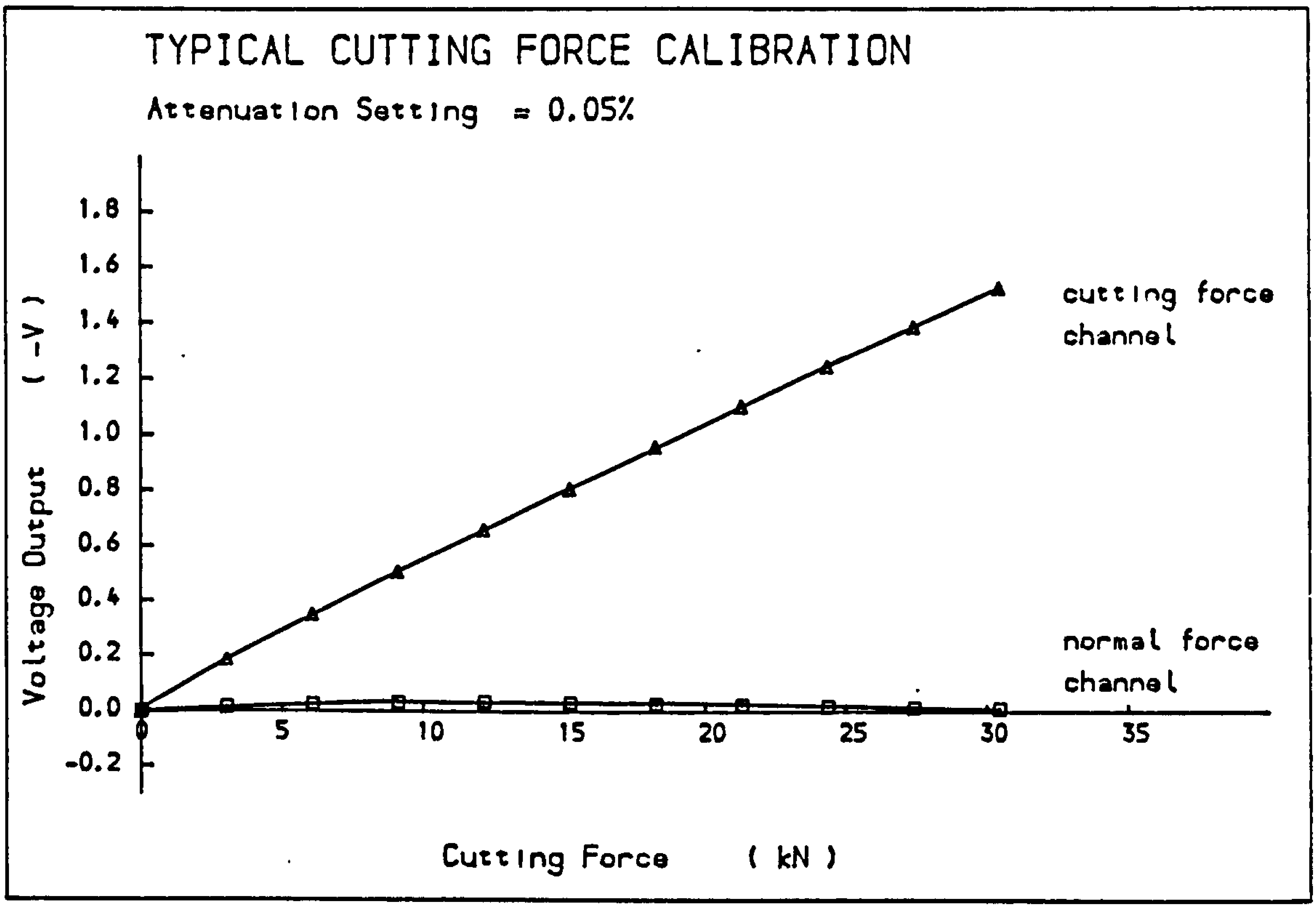

Figure 4.8 Typical Cutting Force Calibration.

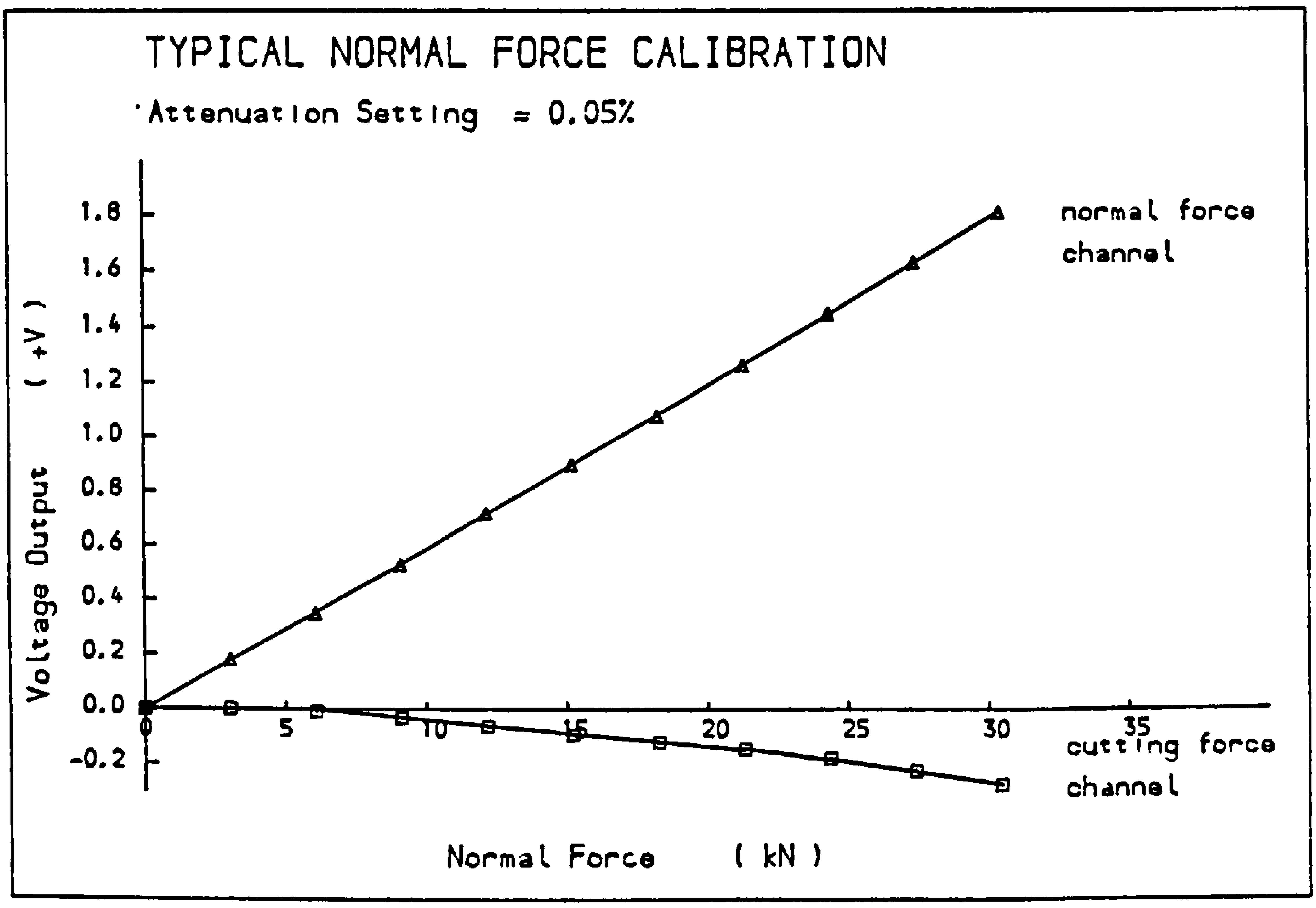

Figure 4.9 Typical Normal Force Calibration.

4.3.1.3 Digital Data Analysis

The general set-up for data analysis is shown in Plate 4.11 and a block diagram is set out in Figure 4.10.

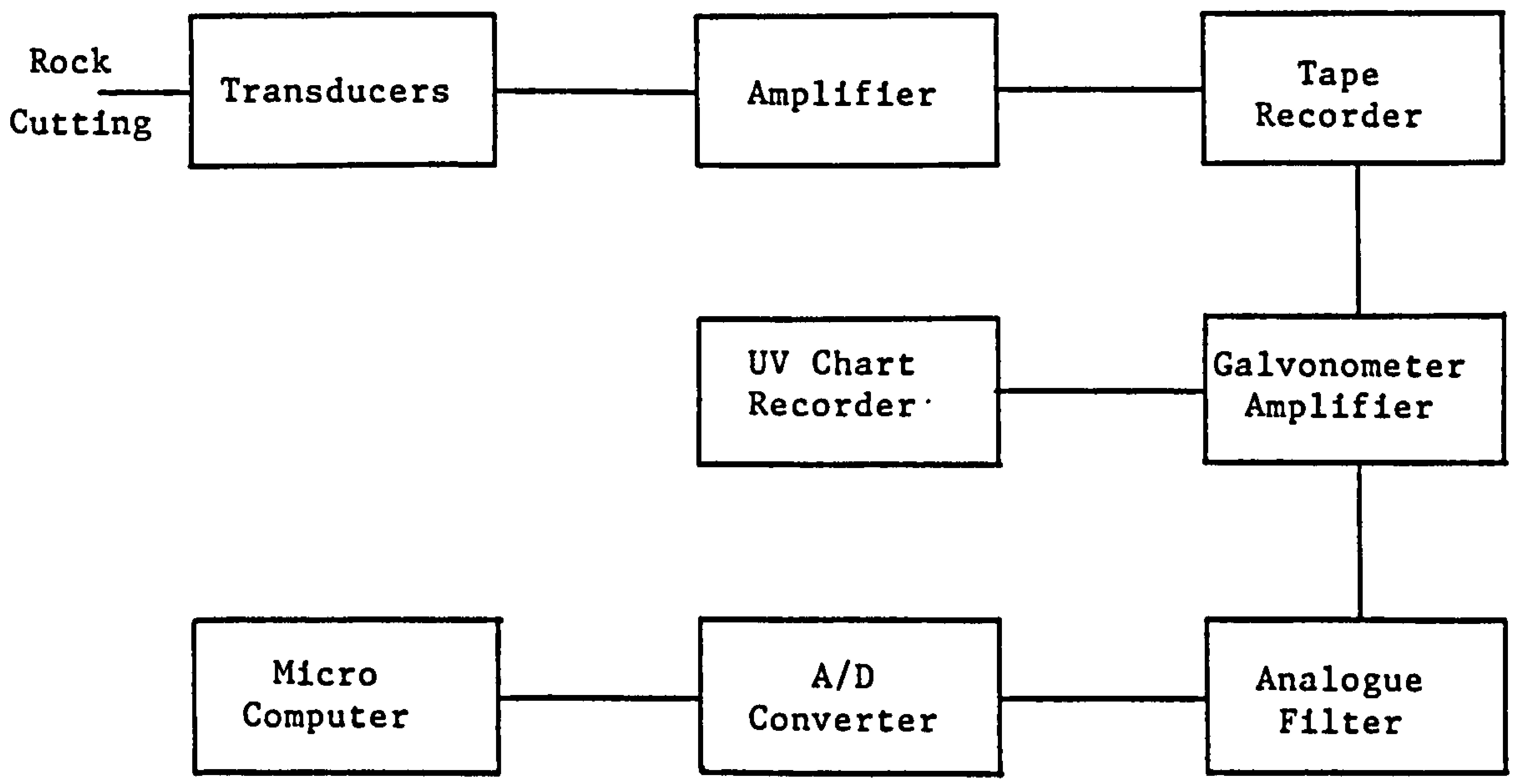

Figure 4.10 Analogue-Digital Data Acquisition System.

The signal from the tape recorder was first filtered using an analogue filter. The cut-off frequency is set at 500 Hz, which is less than half of the sampling rate, in order to avoid any aliasing errors. The signal was then amplified by means of the SE1052 signal conditioning system to ±5v before being fed into the 12-bit A/D converter. The A/D converter had a sample rate of 1.08 kHz for three channels and digitised signals were then output to a Sirus-1 computer.

Plate 4.11

Logging and analysis programs for the digital data have been developed during the project and have proved successful. The listings of two programs in PASCAL language can be found in Appendix F.

The logging program was automatically triggered to execute when the tool started to cut the rock. The first 50mm and last 100mm of cut were ignored to eliminate the non-representative cutting of the first and end chips. The force datum was established by taking the average of 100 readings after the cutting. Figure 4.11 illustrates the details. A subroutine was written within the program specially to check in case of signal overflow in order to avoid any gross error.

The length of cut and traverse time were required for the logging program.

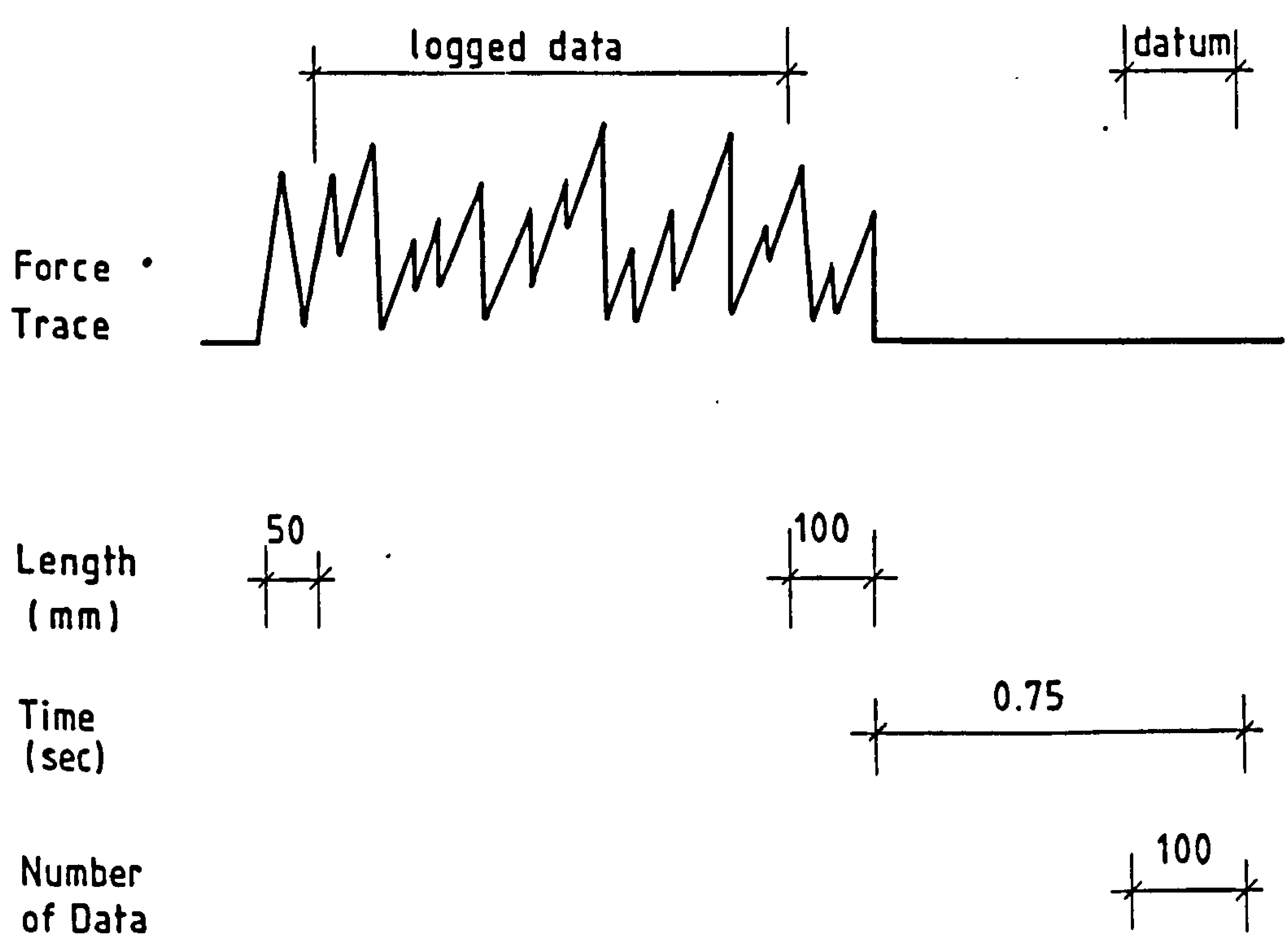

Figure 4.11 Digital data logging arrangement.

4.3.2 Jet Pressure Measuring Systems

4.3.2.1 Instrumentation

Jet pressure was monitored during all experiments. A diaphragm type pressure transducer of capacity 207 MPa was positioned just before the flexible hose. An Intersonde K3020 amplifier was used to energise the transducer circuit and amplify the signals. The electrical signals were then fed to the tape recorder, simultaneously with the signals from the triaxial dynamometer, and the analysis was carried out in the same way as that for the tool force.

4.3.2.2 Calibration

Although a calibration certificate was supplied by the manufacturer, the instrumentation was calibrated to ensure that accuracy of the calibration constant was maintained throughout the work. A Budenberg deadweight pressure gauge tester was used. Calibrated weights were placed on the apparatus to provide the known jet pressure and the signal output was noted. A calibration constant was obtained which compared favourably with the calibration certificate.

4.3.2.3 Flow Rate and Jet Power

In order to evaluate the jet power, the flow rate was first determined. Water was collected in a large bucket with the jet energy dissipated using metal pipings with several bends. The flow rate of the nozzle was determined by dividing the volume of water obtained by the running time of the jet. Flow rates for the Newcastle nozzles of various diameters are set out in Figure 4.12.

The coefficient of discharge, which measures the ratio of actual flow rate to theoretical flow rate, can be determined using the equation:

$$Cd = \frac{\text{actual flow rate}}{\left(\frac{\pi}{4}\right)\left(\frac{2}{\rho}\right)^{0.5} do^{2}\, p^{0.5}}$$

where: Cd = discharge coefficient

ρ = fluid density

d_o = nozzle diameter

p = jet pressure.

The discharge coefficients for various jet diameters are tabulated in Table 4.1.

Nozzle Diameter (mm)	Discharge Coefficient (Cd)
0.6	0.823 ± 0.002
0.9	0.831 ± 0.011
1.2	0.779 ± 0.004
1.5	0.842 ± 0.013

Table 4.1 Discharge Coefficients for various jet diameters (Newcastle Nozzles).

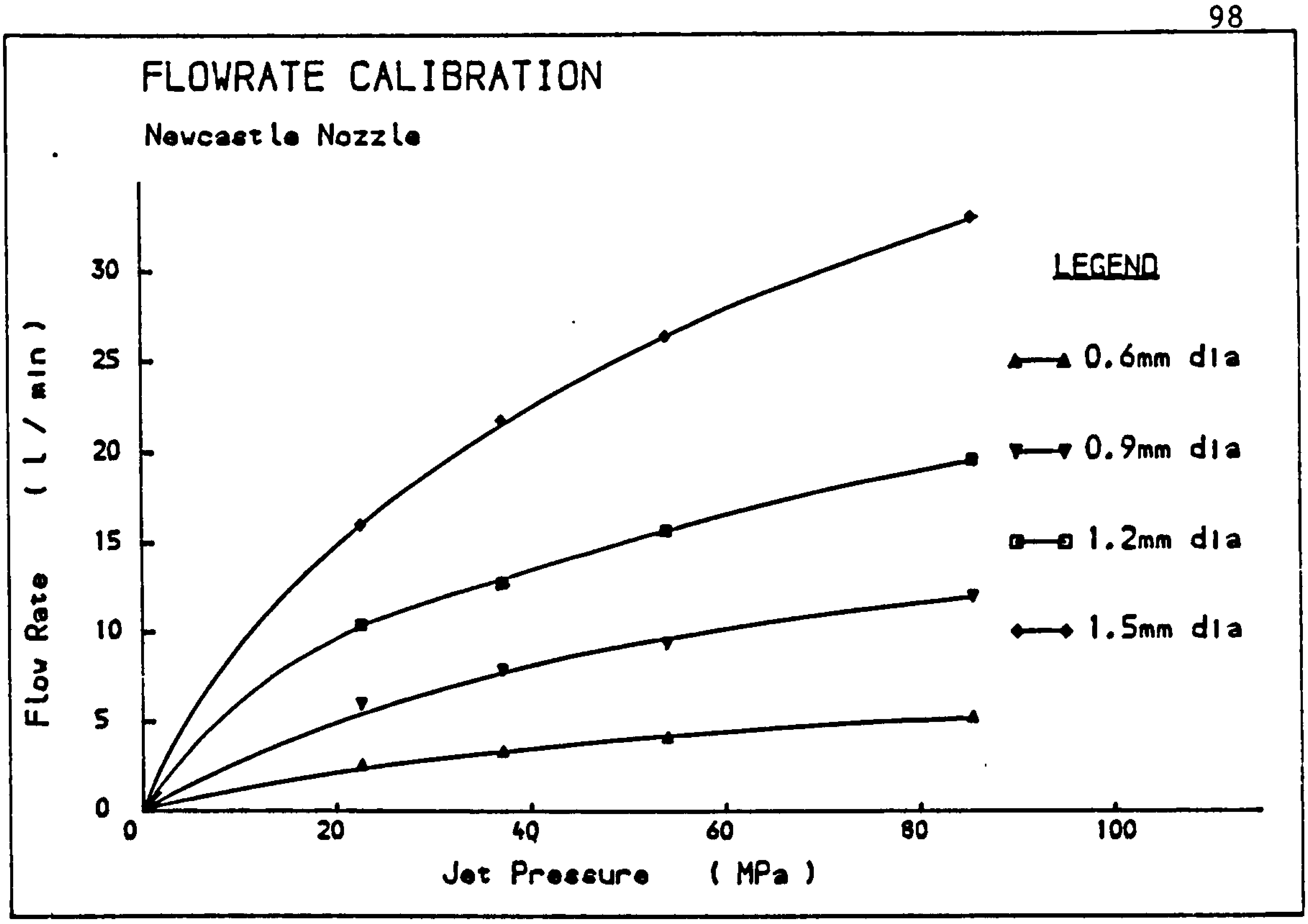

Figure 4.12 Flow Rate versus Jet Pressure for Various Nozzle Diameters.

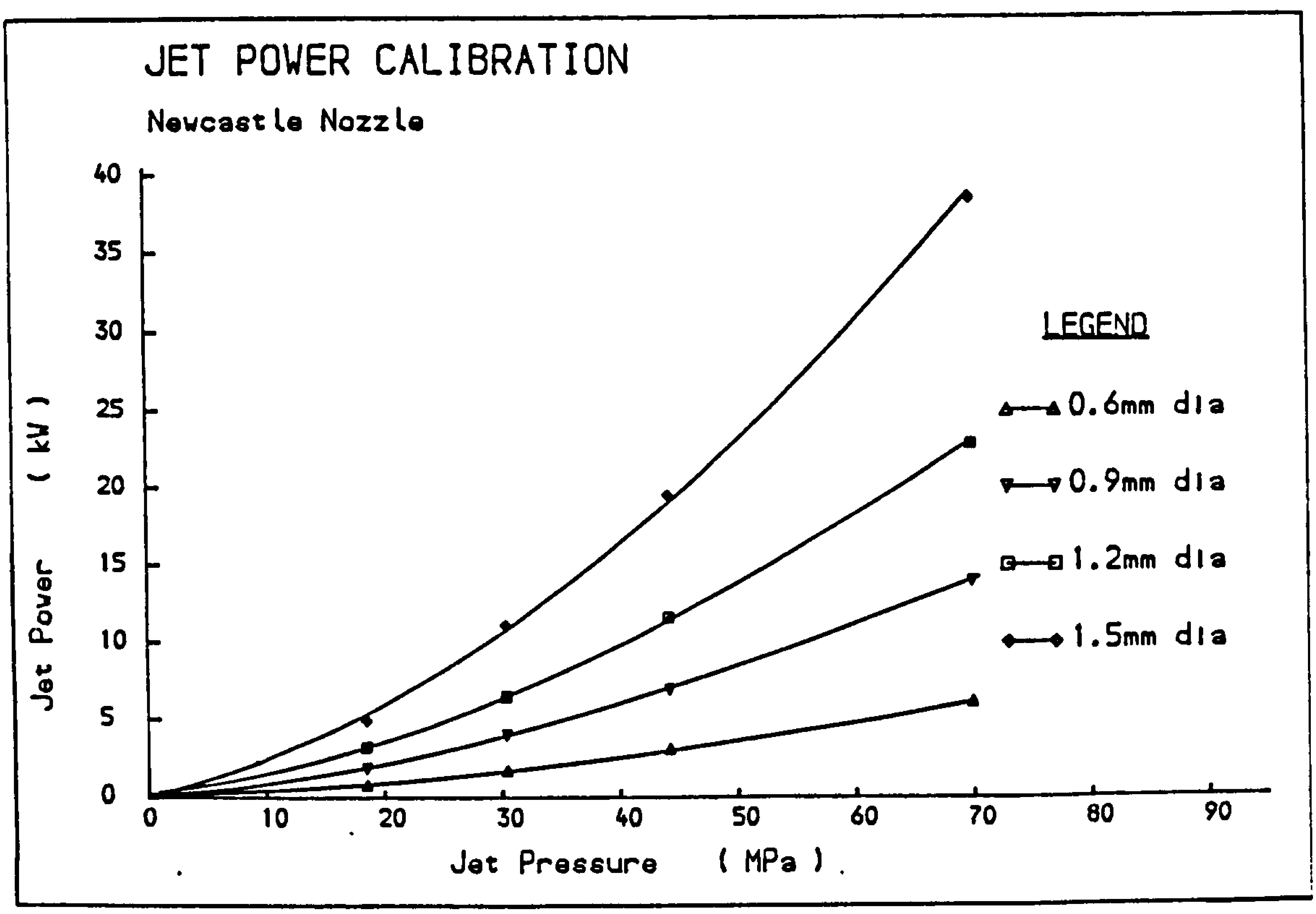

Figure 4.13 Jet Power Versus Jet Pressure for Various Nozzle Diameters.

The jet power, which is equal to jet pressure times flow rate, is plotted in Figure 4.13.

4.3.3 Traverse Speed Measuring System

Traverse speed was required not only for monitoring purposes but also for data logging.

Two microswitches 0.89m apart were fixed on the cutter slide assembly and triggered by the traversing cutter slider. The ON/OFF signals were picked up by an SE/SM200 time counter which was capable of reading up to 0.0001 second. The traverse speed calculated represents an average speed over 0.89m, where most of the rock cutting activity took place.

An exercise was carried out early in the project to examine speed fluctuation as there was concern regarding the time required by the ram to reach its full speed at fast cutting. Four metal markers were fixed on the cutter slide assembly covering a distance of 1.2m. An inductive proximity switch was attached to the cutter slider. When the proximity switch passed the metal marker during traversing, electrical signals were generated. The signals were recorded and replayed on the UV recorder. Traverse speed between successive metal markers was determined, based on paper output speed, and the results were compared with the traverse speed obtained using the microswitches. It was found that the ram reached its full speed in a very short time and then maintained a constant speed throughout the cutting process. Hence the rock was cut at a constant traverse speed and this speed was unaffected by the cutting force experienced. Small variations of speed did occur between cuts, but in a random way and these were not considered significant.

4.3.4 Discussion

Although the present data acquisition system was satisfactory, preference is placed on the on-line data acquisition and analysis system.

The main disadvantage of the present system is that the results are analysed only after the experiments are completed. Any anomaly will not be discovered until the tape recorder is brought up to the computer room and the data analysed. Time was spent in setting up the logging system, digitising and analysing the data.

The on-line system, on the other hand, provides instant data-logging and analysis. Any anomaly is spotted and remedial work is much easier. The digitised data can be plotted on the screen and this eliminates the expensive photographic paper used by the UV recorder. The tape is ideal to store high density data in multi-channel applications. However, the memory size of a normal microcomputer was sufficiently large for two force channels and one jet pressure channel when cutting a maximum of 1.2m as in the present work. The microcomputer is cheaper than the tape recorder which should be devoted to mass data recording when the capacity of a microcomputer is exceeded.

The on-line data acquisition system has been tried successfully and is recommended for future work. The block diagram of the tested system is shown in Figure 4.14.

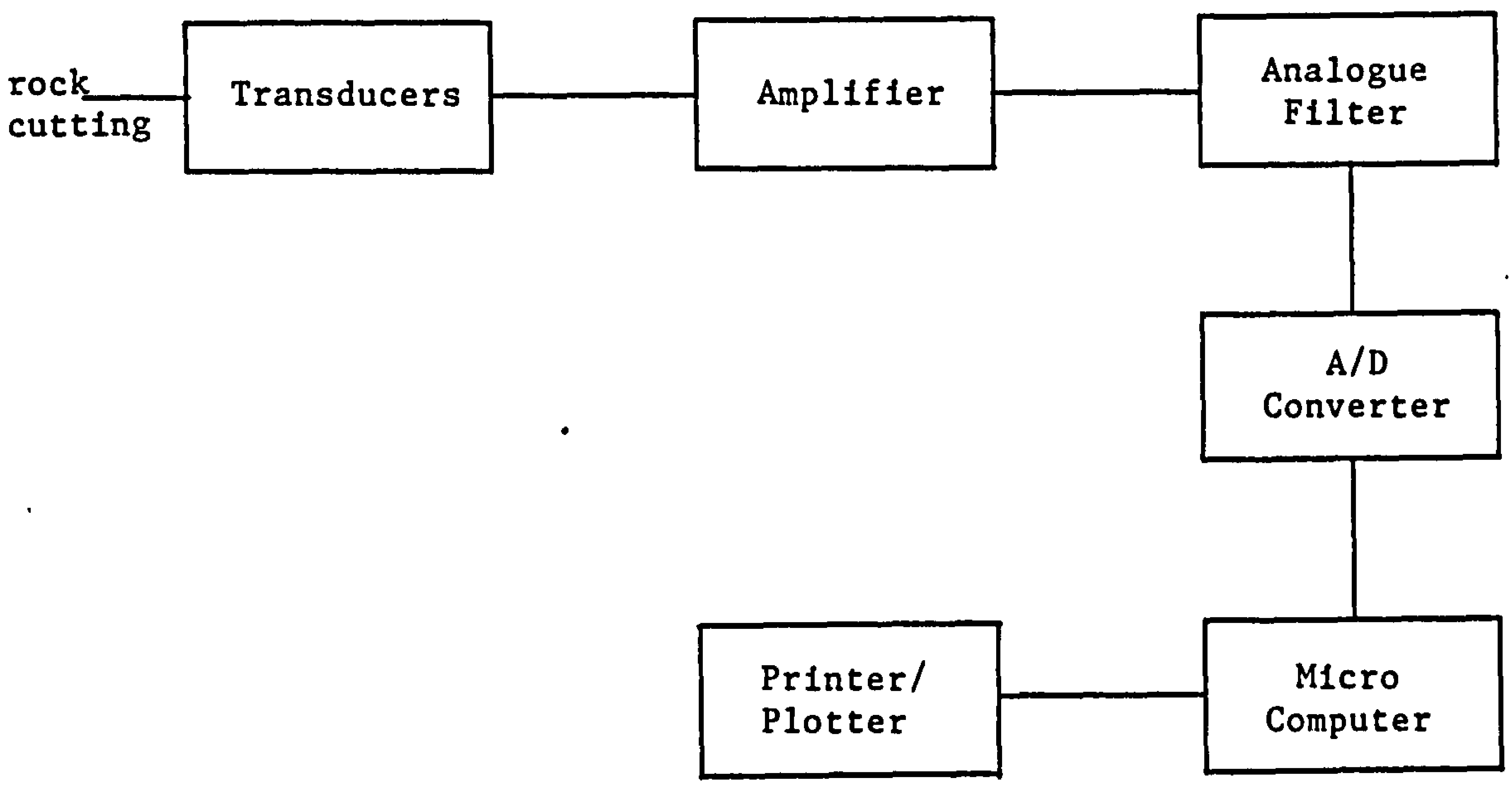

Figure 4.14 Suggested Digital Data Acquisition System.

* * *

CHAPTER FIVE

CHAPTER FIVE

MECHANICAL AND PHYSICAL PROPERTIES OF EXPERIMENTAL ROCKS

A range of tests were carried out to characterise the properties of rocks used in this project.

Where applicable the tests were carried out to the recommendation of the International Society for Rock Mechanics Commission on Testing Methods (Brown 1981) and no details will be given here. When no standard test procedure was available the well established or well known procedures were followed. The test procedures used are now described.

Usually tests were repeated in five specimens of each rock in the present study. All tabulated results are presented in Section 5.11.

5.1 Uniaxial Compressive Strength (ISRM suggested method)

A specimen 42mm in diameter and 84mm long, giving a length to diameter ratio of two, was tested.

5.2 Uniaxial Tensile Strength (ISRM suggested method)

The uniaxial tensile strength was measured indirectly by the Brazilian test. The 'Brazilian Disc' specimens of size 42mm diameter x 21mm thickness were used.

5.3 Porosity and Dry Density (ISRM suggested method)

The saturation and caliper techniques, as detailed by the ISRM suggested methods, were used.

5.4 Dynamic Young's Modulus

The dynamic Young's moduli of experimental rocks were measured using an instrument called a 'Pundit'. A pundit is capable of generating ultrasonic longitudinal pulses and measuring accurately the time of transmission across the specimen.

The dynamic Young's moduli of tested rocks were estimated using the following simplified formula:

$$Ed = \gamma \times Cp^2$$

where: Ed = dynamic Young's modulus

Cp = longitudinal pulse velocity

$= \dfrac{\text{specimen length}}{\text{transit time}}$

γ = bulk density of specimen.

5.5 Permeability

The rock sample was enclosed in a rubber jacket and placed in a Hoek triaxial cell. A confining pressure of at least twice the head pressure was applied in order to prevent any possible flow along the rock/plastic interface. A water pressure head of 10 MPa maximum was applied and readings taken after equilibrium was reached.

The coefficient of permeability k was determined from the following equation:

$$k = \frac{ql}{hA}$$

where: q = discharge rate

l = length of sample

h = pressure head

A = cross-sectional area of sample

The general set-up of the apparatus is shown in Plate 5.1.

5.6 Core Grooving Test

A core grooving test developed in the University of Newcastle upon Tyne (Department of Mining Engineering) is used extensively in the assessment of the machineability of rock for roadheader and other drag tool equipped machines (Plate 5.2).

The test may be carried out on either core samples or block samples of rock. Four cuts are normally made in the rock sample at a constant depth of 5mm with a tungsten carbide tool 12.7mm wide, chisel-edged, with a -5° front rake and +5° back clearance angle. The tungsten carbide used in the present study was CM grade, supplied by Hoybide. This tool, mounted on an instrumented shaping machine, cuts at a traverse speed of 150 m/s. The shaping machine was instrumented with a strain-gauged triaxial force dynamometer rigidly fixed to the machine's crosshead. For the standard instrumented cutting test, forces were only analysed in the cutting and normal directions, since sideways forces are balanced, due to the symmetrical design of the cutting

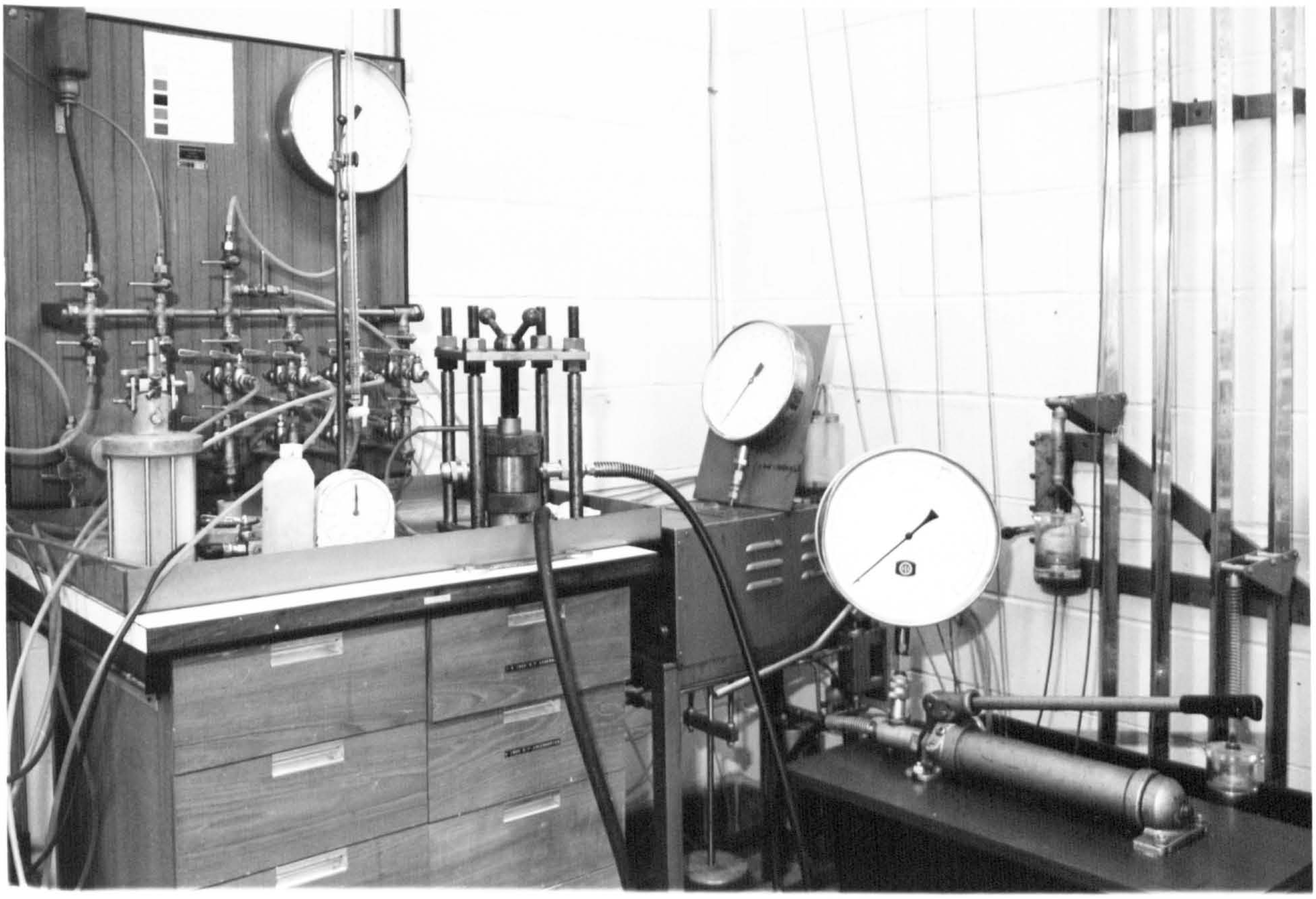

Plate 5.1

Plate 5.2

tool. The strain gauge output from the dynamometer was recorded as analogue traces on an ultraviolet chart recorder. Together with recorded information, the weight of debris and length of cut, the analysis provided the following cutting parameters :

(a) Cutting and normal, mean, mean peak and peak force components acting on the cutting tool (kN).

(b) Specific energy (MJ/m^3) : This is defined as the work done to excavate a unit volume of rock. It is obtained by dividing the mean cutting force component by the yield, the latter being expressed as the volume of material excavated per unit length cut.

(c) Cutting wear (mm/m) : This is the wear flat on the loading face of the tungsten carbide insert measured following the standard cutting procedure.

5.7 Abrasivity (Newcastle Abrasivity Test)

Based on the standard CERCHAR scratch abrasivity test, but utilising a softer silver steel stylus of 275 Vickers, compared with 661 Vickers of the standard CERCHAR tip. The test is very simple but effective and involves scratching the rock surface with a steel stylus having a sharp 90° cone angle for 1cm under a 7 kg normal load. The abrasivity is measured as the wear flat generated in 0.1mm units. A travelling microscope with an eyepiece micrometer is used to measure the wear flat in two orthogonal directions. The test provided reliable results for describing both the relative and absolute abrasivity of rock specimens. Four to six tests per rock type were carried out to ensure accuracy and reliability.

5.8 Cone Indenter

This pocket instrument was developed by the National Coal Board for the purpose of making rapid assessment of the rock indentation hardness. It has been shown that the cone indenter number can be used to estimate the uniaxial compressive strength within Coal Measures rocks in the UK (Szlavin 1971). McFeat-Smith (1977) furthered the application by correlating the standard cone indenter number with the performance of roadheaders. The test procedure is described in MRDE Handbook No.5 (1977).

5.9 Rebound Hardness and Plasticity

A Coates Sclerescope was used to measure the surface rebound hardness. At least 20 readings were taken and even more for coarse grained rocks. The results were influenced by rock mineralogy, elasticity and cementation, and McFeat-Smith (1977) found it a key factor in the prediction of the cutting wear of drag tools.

Since drag tool cutting involves much rock crushing (Section 6.1), a measure of change in rebound values after repeated tests at the same location may provide some information on the tool forces. A coefficient of plasticity is defined (McFeat-Smith 1977) as follows:

$$K = \frac{H_2 - H_1}{H_2} \times 100\%$$

where: K = coefficient of plasticity

H_1 = average rebound value

H_2 = final rebound value after approximately 20 tests.

5.10 Petrographic Description

A thin section of each rock was prepared from which a description of the micro-structural features, grain angularity, grain size, cementing materials and quartz content was obtained through a point count.

5.11 Results

Properties \ Rock	Dumfries Sandstone	Grindleford Sandstone	Penrith Sandstone	Pennant Sandstone	Middleton Limestone
1. Uniaxial Compressive Strength (MPa)	22.7±2.7	58.9±8.6	82.9±9.1	172.8 ±10.1	113.2 ± 6.7
2. Tensile Strength (MPa)	1.99± 0.50	8.65± 1.27	7.81± 0.59	23.39 ±0.46	12.58 ± 0.46
3. Dry Density (kg/m^3)	1947±6	2362±3	2390±2	2652±3	2562±13
4. Porosity (%)	23.47± 0.09	8.75± 0.30	8.59± 0.15	1.58± 0.03	3.79± 0.77
5. Standard NCB Cone Indenter Number	0.90± 0.21	2.83± 0.27	2.46± 0.33	4.30± 0.72	3.45± 0.44
6. Rebound Hardness	11.7± 1.2	36.2± 0.9	37.8± 0.9	53.1± 0.5	44.5± 1.4
7. Plasticity (%)	60	19	12	9	8
8. Permeability (m/s)	2.76×10^{-6}	2.38×10^{-8}	6.16×10^{-10}	**	2.26×10^{-11}
9. Dynamic Young's Modulus (GPa)	7.75± 0.24	16.53± 0.26	7.10± 0.45	38.93± 0.59	77.34± 2.39

** Impermeable

TABLE 5.1 Mechanical and Physical Properties of Rocks used.

		DUMFRIES SANDSTONE	GRINDLEFORD SANDSTONE	PENRITH SANDSTONE	PENNANT SANDSTONE	MIDDLETON LIMESTONE
MCF	(kN)	0.39±0.11	1.64±0.28	1.61±0.24	2.87±0.39	2.39±0.29
MPCF	(kN)	1.07±0.27	3.71±0.69	3.88±0.11	7.40±1.07	6.78±0.76
PCF	(kN)	1.35±0.35	4.59±1.06	4.51±0.33	9.30±1.12	8.76±1.01
MNF	(kN)	0.28±0.06	1.31±0.05	1.78±0.44	2.50±0.77	1.73±0.18
MPNF	(kN)	0.62±0.15	2.56±0.13	3.17±0.50	5.04±1.02	4.16±0.40
PNF	(kN)	0.77±0.12	2.97±0.14	3.75±0.43	5.87±0.79	5.47±0.58
Yield	(g/cm)	3.95±1.02	2.57±0.41	2.29±0.11	2.15±0.31	2.43±0.43
Specific Energy	(MJ/m^3)	1.94±0.28	15.06±1.22	16.70±1.85	35.48±1.29	25.64±3.81
Wear Rate	(mm/m)	0.27	0.34	0.60	0.32	0.06
Density	(g/cm^3)	1.98	2.37	2.39	2.66	2.57
Newcastle Abrasivity	($^1/10$ mm)	1.9	4.6	6.6	5.3	1.9

TABLE 5.2 Cutting Characteristics of Experimental Rocks

	DUMFRIES SANDSTONE	GRINDLEFORD SANDSTONE	PENRITH SANDSTONE	PENNANT SANDSTONE	MIDDLETON LIMESTONE
Count	680	701	693	615	-
Quartz (%)	66.4	72.2	78.0	45.6	microcrystalline
Cement (%)	16.4	12.7	13.8	39.1	calcite (miorite) with
Void (%)	15.5	5.5	3.4	5.3	more than 10% grains
Calcite (%)	0.9	0.7	0.4	1.0	(wackestone) slightly
Mica (%)	0.8	3.1	0.5	4.1	dolomitised, grains
Feldspar (%)	-	2.6	0.9	-	up to 0.5mm
Others (%)	-	3.2	1.1	6.8	
Grain size (mm)	0.05 - 0.30	0.1 - 0.5	Major 0.3-0.4 Minor 0.1-0.15	0.03 - 0.05	
Angularity	sub-rounded to rounded medium to high sphericity	sub-angular to sub-rounded medium sphericity	rounded, medium to high sphericity	angular to sub-rounded, medium sphericity	
Cement Material	mainly silica	silica with some clay	silica and clay, 60:40	clay cement with small grains of quartz < 0.05mm and some calcite	
Remarks	poorly cemented	low void space with interlocking grains			

Table 5.3 Petrographic Description of Experimental Rocks.

CHAPTER SIX

CHAPTER SIX

CUTTING MECHANISMS OF WATER JET ASSISTED DRAG TOOL ROCK CUTTING

Before the cutting mechanisms of water jet assisted rock cutting can be understood the mechanisms of drag tool rock cutting and water jet rock cutting must first be examined.

6.1 Mechanisms of Drag Tool Rock Cutting

6.1.1 Tool Actions

A drag tool cuts rock in a parallel motion along the surface. In a broad sense, the tool can be regarded as a traversing indenter. The cutting force is the force required to plough through the rock, while the normal force has to keep the tool on course.

The sequence of events observed during the cutting of all five rock types was very similar. A schematic representation can be seen in Figure 6.1.

Four stages have been highlighted to represent a typical single chipping cycle:

(1) Immediately after a major rock fracturing, a large, scallop-shaped fragment (chip) is formed by rock breaking to the sides and ahead of the tool at a shallow angle. A curvilinear surface remains. At this point, the tool is doing least work, and the force traces are momentarily at their lowest; near zero for a sharp tool. The effective depth of cut tends to zero at this instant.

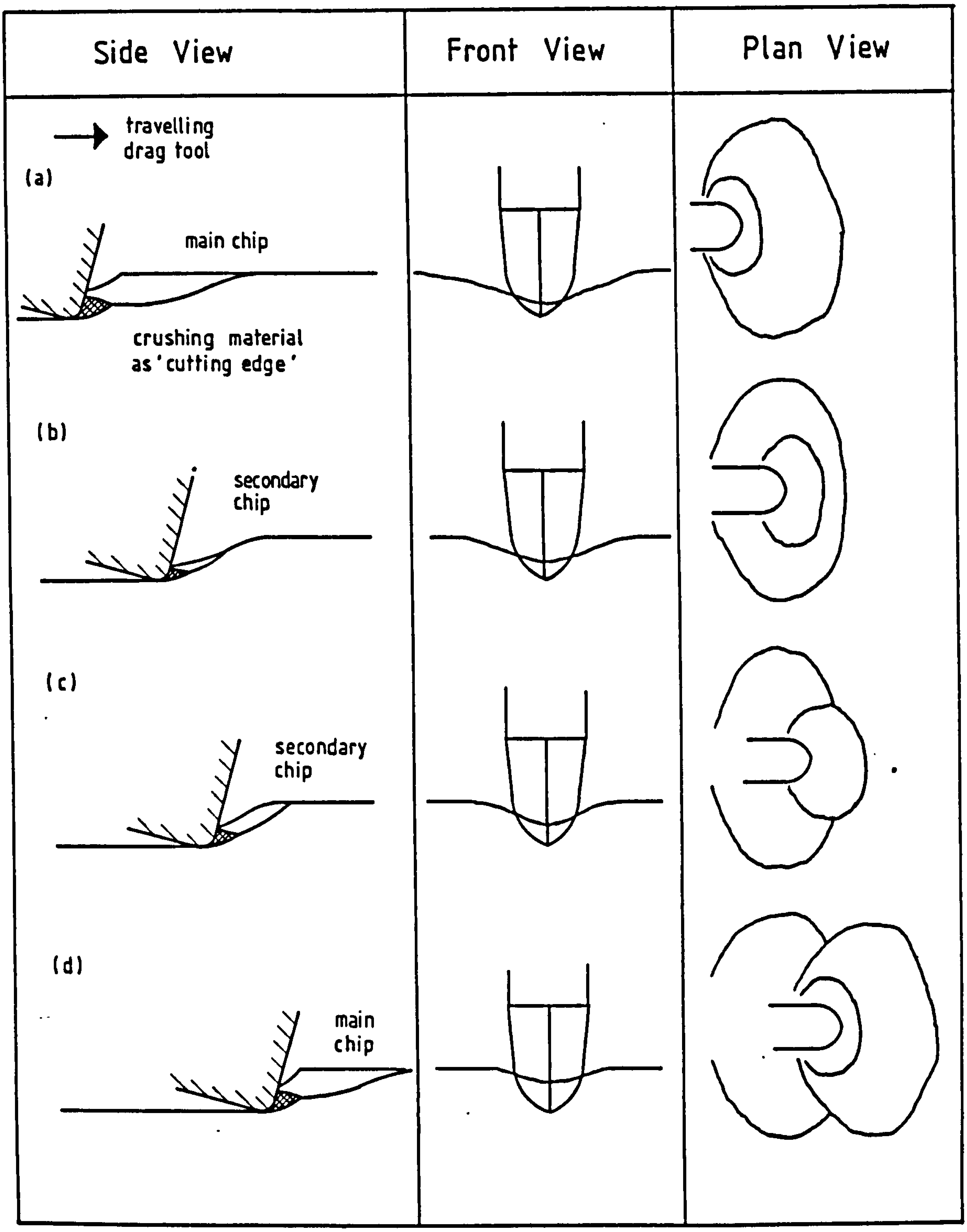

Figure 6.1 Schematic illustration of unassisted drag tool rock cutting process.

(2) As the tool moves forward, the effective depth of cut increases. Initially, much of the rock material in front of the tool is crushed. Due to tool/rock interface friction, crushed/ intact rock friction, and internal friction within the crushed material, the crushed material tends to adhere to the tool tip. The forward movement of the tool further compacts and consolidates the crushed material.

During and after consolidation, the crushed zone transmits the stress and acts virtually as a 'cutting edge' for the drag tool. As the tool traverses further, a microcrack system is developed and small, secondary chips are sometimes produced as a form of stress relief. Some crushed material may be lost altogether due to this secondary chipping event.

(3) The further the tool travels the bigger the size of the crushed zone as the crushed material cannot escape due to confinement by the tool and the surrounding intact rock. Secondary chipping is still the best way to relieve the high stress accumulated within the crushed zone. Additionally, the tool wedge assumes an increased task in clearing a way through the rock for the tool. This may be described as profiling.

(4) Secondary chipping generally produces a steeper rock surface. As the tool travels, more rock material is crushed and consolidated. The crushed zone, therefore, increases in size but stress relief in the way of secondary chipping is more difficult due to the steep rock surface. Eventually a stage is reached where the driving force provided by the tool through the crushed zone is greater than the critical force level for the rock and a dominant median crack is initiated (Swain and Lawn 1975; 1976). The crack initially propagates in a fashion predicted by the stress field produced by indentation on a semi-infinite space, but modified at a later stage due to the relieving effect of the surface.

Figure 6.2 illustrates the three different stages during crack propagation.

The rock cutting was considered as a discrete repetition of this cutting cycle.

Depending on the functions performed by the tool, four actions can be identified:

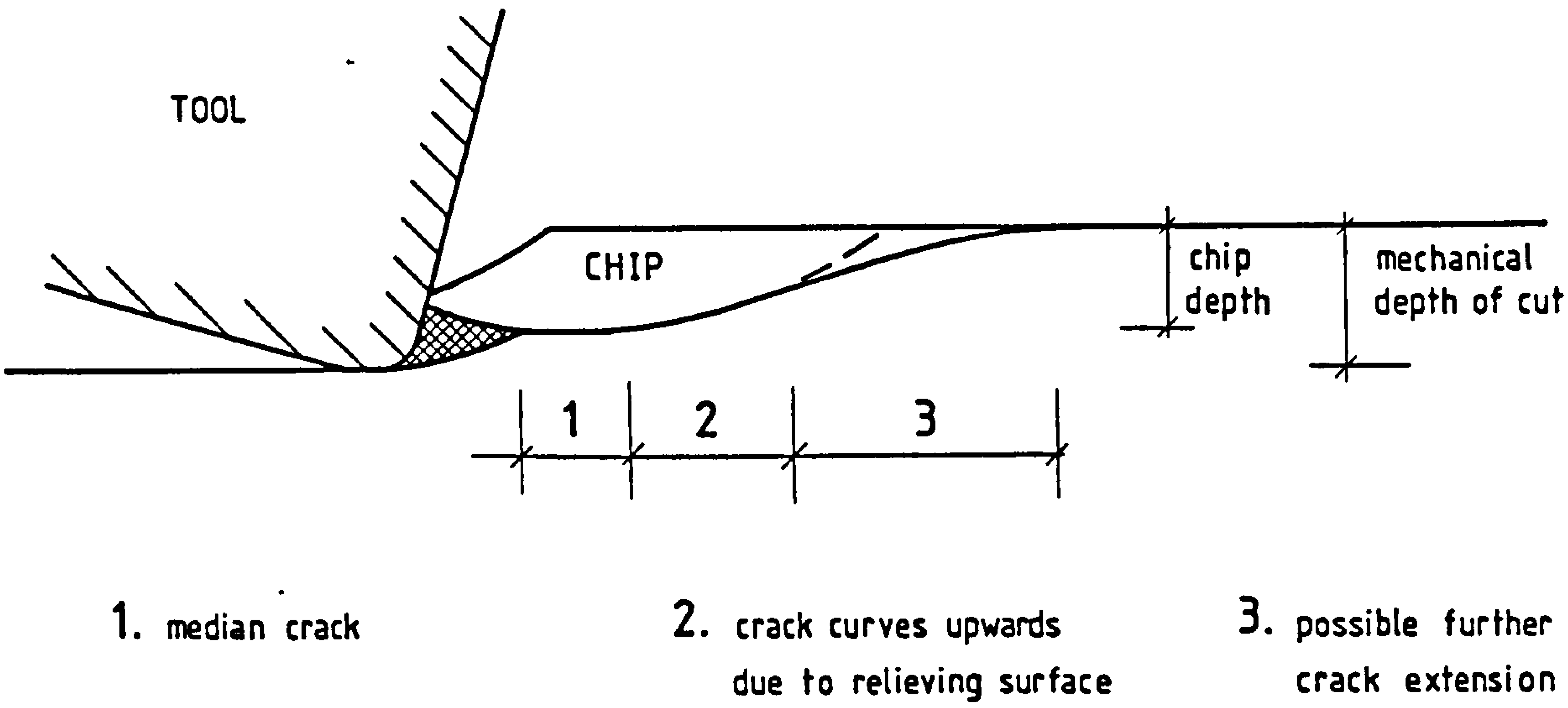

Figure 6.2 Typical Section of a Primary Chip.

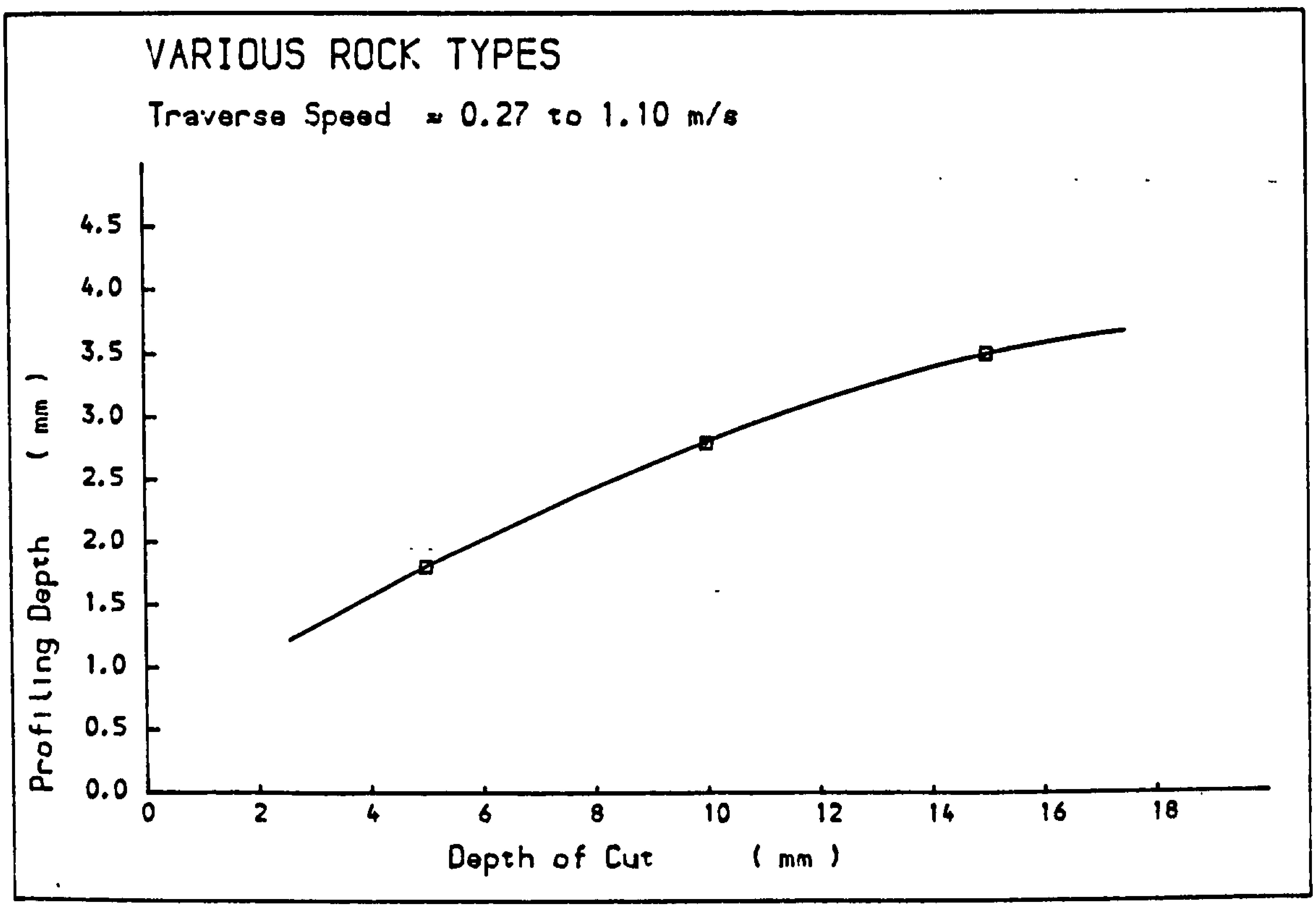

Figure 6.3 Profiling Depth versus Mechanical Depth of Cut (Cutting Speed = 0.27-1.10 m/s).

(1) Crushing : the rock material is trapped and crushed underneath the wearflat.

(2) Profiling : the tool wedge sweeps through the remaining material and clears its own profile.

(3) Primary Chipping : the tool tip, through the crushed zone, initiates a large rock chip ahead of the tool.

(4) Secondary Chipping : similar to the primary chipping process but the chips are of a smaller size.

Of these four actions, chipping is much preferable because the tool can make use of weaker tensile strength of most rocks and promote cracking. Although the chipping action causes a peak load on the tool, large pieces of rock surface are removed and the cutting efficiency is high. Profiling can be regarded as miniature chipping and is not as efficient as chipping because cracks are generated from cutting wedges (line load) rather than the tip (point load). Crushing is most undesirable as it involves mainly debris comminution which is wasteful of energy.

The actual proportion of forces contributed by each action is dependent on tool type, rock type, depth of cut and traverse speed. Further research is recommended to construct a constitutive model that can estimate the component tool forces based on known tool variables, rock types and operational variables as these are important for the evaluation of tool force reductions from water jet assistance.

6.1.2 Chip Shape Analysis

In order to understand the actual cutting mechanics of the drag tool during rock cutting, chips from the mechanical cutting of different rock types were collected and analysed.

Generally the chips were of a 'scallop'-shape, with size dependent on depth of cut. The region of the rock around the crushing zone was marked by a light colour due to the formation and spread of many tiny cracks through grains or along boundaries (Brace 1960). Occasionally, usually at a slow traverse speed, a rock chip may come out with the crushed material still adhering to it. Plate 6.1 illustrates this. The crushed zone resembles a distorted cone and is burst into the rock by the pushing drag tool. Half of the crushed zone of the big chip shown in Plate 6.1 is removed to provide a better illustration of the size of the crushed zone. Typical chips are cut along the direction of the traversing tool and the sections are shown in Plate 6.2. The crushed zone is responsible for truncated corners in the left-hand side of the chip sections.

About 15 to 20 typical chips from differing depths of cut for various rock types were collected and the chip depth determined. For a 5mm depth of cut, only the Pennant Sandstone chips were of an identifiable shape to allow chip depth determination. Chips from both cutting speeds had a similar chip depth in each rock and the results are pooled together. The

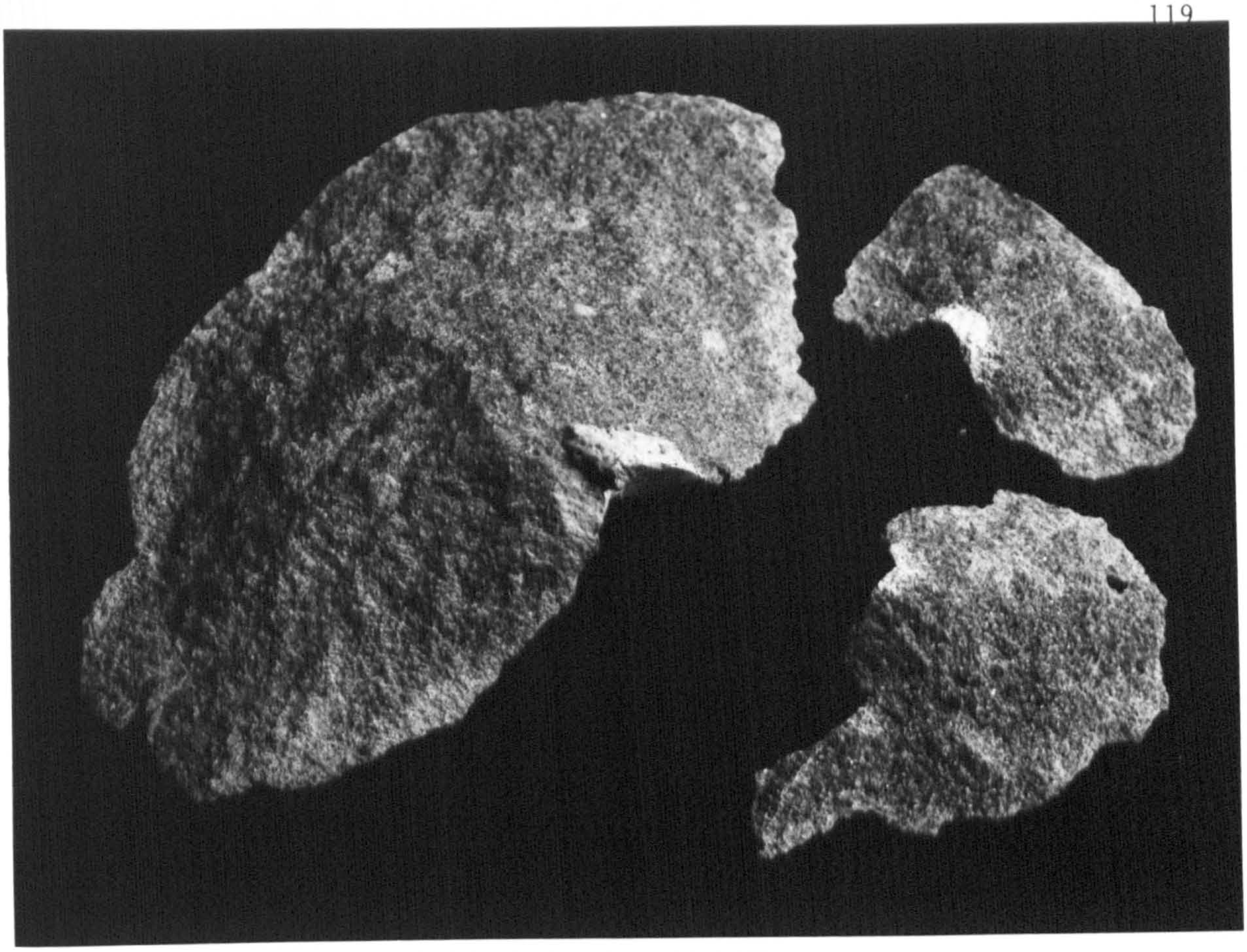

Plate 6.1

Plate 6.2

results are summarised in Table 6.1, showing that chip depth was very similar for different rocks. The reproducible chip depth for different rocks at different depths of cut would suggest that chip depth depends only on tool tip geometry. One of the factors likely to affect chip depth is the rake angle of the tool; the larger the positive angle, the deeper the chip depth should be.

The most interesting finding was that chip depth was less than mechanical depth of cut for the drag tool used. This is because the median crack was initiated at the end of the cone-shaped crushed zone which had a finite size depending on depth of cut. A typical chip section is drawn in Figure 6.2.

If profiling depth is defined as:

mechanical depth of cut = chip depth + profiling depth,

the profiling depth can be accurately estimated (correlation coefficient = 1.00) using the following equation:

$$\text{Profiling depth} = 1.455 \times \ln(\text{depth of cut}) - 0.544.$$

The results are plotted in Figure 6.3, showing the profiling depth increase with depth of cut in a convex manner, and this is expected to approach a constant value when the cut is deep enough.

6.1.3 Discussion

For the type of drag tool used in this project, the transmission of mechanical energy from the tool to the rock is

Mechanical Depth of Cut	Chip Depth (mm)			Mean (mm)
	Dumfries Sandstone	Grindleford Sandstone	Pennant Sandstone	
5	-	-	3.2	3.2 (64%)
10	7.2	7.1	7.3	7.2 (72%)
15	11.1	11.8	11.9	11.6 (77%)

Table 6.1 Chip depth in unassisted cutting.

not direct but via the crushed zone. This indirect tool/rock energy transmission is not efficient. However, the situation is regarded as inevitable when the rock to be cut is strong. Energy transmission can be improved by using a drag tool of large positive rake angle which, unfortunately, tends to suffer due to tip shattering when high impact forces are experienced during hard rock cutting.

6.2 Mechanisms of Water Jet Rock Cutting

The mechanism of material failure due to water jet impingement is usually explained as a fracture phenomenon of an elastic brittle material. Bowden and Brunton (1961) showed that, at high impact velocity (500 m/s), the characteristics of water jet impact are similar to those of a solid projectile. The water behaves in a compressible manner and a short, intense compression pulse moves into the solid from the region of impact. The general types of deformation and damage were found to be:

(1) circumferential surface fracture;
(2) subsurface flow and fracture;
(3) large-scale plastic deformation leading to a permanent depression of the surface;
(4) shear deformation around the periphery of the impact zone; and
(5) failure due to the reflection and interference of stress waves.

The predominant form of deformation will depend mainly on the mechanical properties of the solid and on the velocity of impact. Brunton (1966) and Field (1966) furthered the research in a similar direction.

The mechanism of water jet rock cutting is different due to the fact that most rocks are permeable and it is possible that the water penetrates the voids between grains and spalls them off. In one experiment, Forman and Secor (1974) placed a very thin copper sheet between a continuous jet and the surface of a limestone block. This permits transmission of the jet pressure to the rock without allowing water ingress to the pore structure. No rock damage was observed, even when jet pressure substantially higher than the threshold pressure was applied. It was concluded that pore pressure distribution, coupled with the mechanical stress field due to jet loading, was responsible for the rock failure due to water jet impingement.

Porosity and permeability, which govern the ease with which a fluid can flow through the pore space, are identified as two of five rock properties governing jet penetration. The other relevant rock properties are Young's modulus, Poisson's ratio and tensile strength.

It was observed during the jet slotting experiments with jet pressures up to 70 MPa carried out in the present study, that the water jet left a clean and tidy straight cut in the Dumfries, Grindleford and Penrith sandstones. This would suggest that the travelling jet penetrates in an erosive manner rather than by gross internal fracture. This was proved by Rehbinder (1980) when he collected all debris spalled during water jet cutting and found that the debris consisted of single grains which have a size distribution similar to the rock block itself. Occasionally some spalling occurs along the slot edge and some kinds of existing flaws such as cracks and joints are accountable to this phenomenon.

When much higher jet pressure is used, reflected tensile stresses can be induced at boundary faces creating fracture on a reasonable scale. Farmer (1967) estimated that a jet velocity in the region of 2000 m/s is necessary for the intermediate sandstones with compressive strengths of 50 to 100 MPa. The maximum jet velocity used during the present project was just over 300 m/s and no fracturing of this kind was observed.

6.3 Mechanisms of Water Jet Assisted Drag Tool Rock Cutting

Based on the detailed observations of a single representative cutting cycle by the drag tool, together with the effect of a high pressure water jet impinging 1-2mm ahead of the tool tip, a hybrid cutting model is proposed. Depending on the magnitude of jet penetration, three stages are identified. The model describes the different roles played by the water jet in each stage. The model predicts the existence of an optimal jet penetration, with which maximum tool force reductions can be obtained.

The functions performed by the water jet in different jet penetrations are described as follows:

6.3.1 Insignificant Jet Penetration

In this case, the water jet cannot reach the tool tip due to its inability to penetrate the rock except immediately after a chip is formed. The only function of the jet is to flush out the debris and assist in chip removal once formed, hence reducing secondary debris comminution.

As the jet is incapable of penetrating and relieving the tool tip, the energy wasting crushing activities underneath the tool tip are essentially unaffected. Force reduction is mostly marginal.

The rock cutting process is similar to that for unassisted cutting, as shown in Figure 6.1.

6.3.2 Optimum Jet Penetration

When the water jet starts to penetrate the rock, the slot produced can reduce crushing activities underneath the tool tip. The more the jet penetrates, the less force is wasted in the crushing events.

However, when the jet penetrates deeper, the penetration may disturb the crushed zone, which acts as the substitute cutting edge of the tool; this results in reduced chipping events. Secondary chipping events are firstly reduced and are then followed by primary chipping events.

At optimum penetration the water jet is able to reduce the energy wasting crushing events whilst still retaining the energy efficient chipping events. The key is to have the right jet penetration sufficiently deep to relieve the tool tip immediately after a primary chip, but not so deep as to remove the crushed zone necessary to induce major crack initiation at a later stage. In this sense, the optimum jet penetration is related to profilig depth (Section 6.1.2). This situation represents the best compromise between reduction in crushing and chipping events with respect to minimising tool force. The optimum situation is shown schematically in Figure 6.4.

The existence of optimum jet penetration highlights the dual purpose of the water jet in drag tool rock cutting. On one hand, the water jet can beneficially reduce crushing events and, on the other, can detrimentally reduce chipping events. This optimum jet penetration represents a situation where force reduction, due to reduced crushing events, is equal to force increase due to reduced chipping events. The force increase from reduced chipping events is due to increased profiling action which is not as efficient as chipping.

6.3.3 Excessive Jet Penetration

When jet penetration is deeper than the optimal value, the crushed zone for the chipping events is disturbed. The tool tip is further relieved from the crushing events underneath the wearflat; however, the water jet also flushes away the 'cutting edge' formed by the crushed zone before the tool tip. Depending on the jet penetration, chipping events are either reduced or can even be eliminated completely. The tool then operates through a mainly profiling action.

The chipping event is efficient because the tool tip makes use of the much lower tensile strength of the rock to remove a large piece of the rock surface ahead of the tool. Hence the force required for the profiling action is much reduced. If chipping events are suppressed, the tool is cutting through the rock mainly by profiling action. Although the tool tip is completely relieved, the benefits of reduced crushing events are more than offset by the increase in profiling activities. The net gain is reduced from the optimum condition.

Unless there is a change of cutting mechanism, further assistance of water jet to tool force reductions is not expected when the jet penetration is deeper than mechanical depth of cut.

A schematic diagram showing the typical cutting situation is given in Figure 6.4.

6.3.4 Discussion

Based on the effect of jet penetration on the tool actions, a hybrid cutting model is proposed to depict the effect of water jet to tool forces at various jet penetrations. The model is summarised in Figure 6.5, which shows the effect of jet penetration on tool functions such as crushing, chipping and profiling. The proportion of tool forces contributed by these tool functions is hypthetical. Due to the different effects of jet penetration on the magnitude of the force reductions

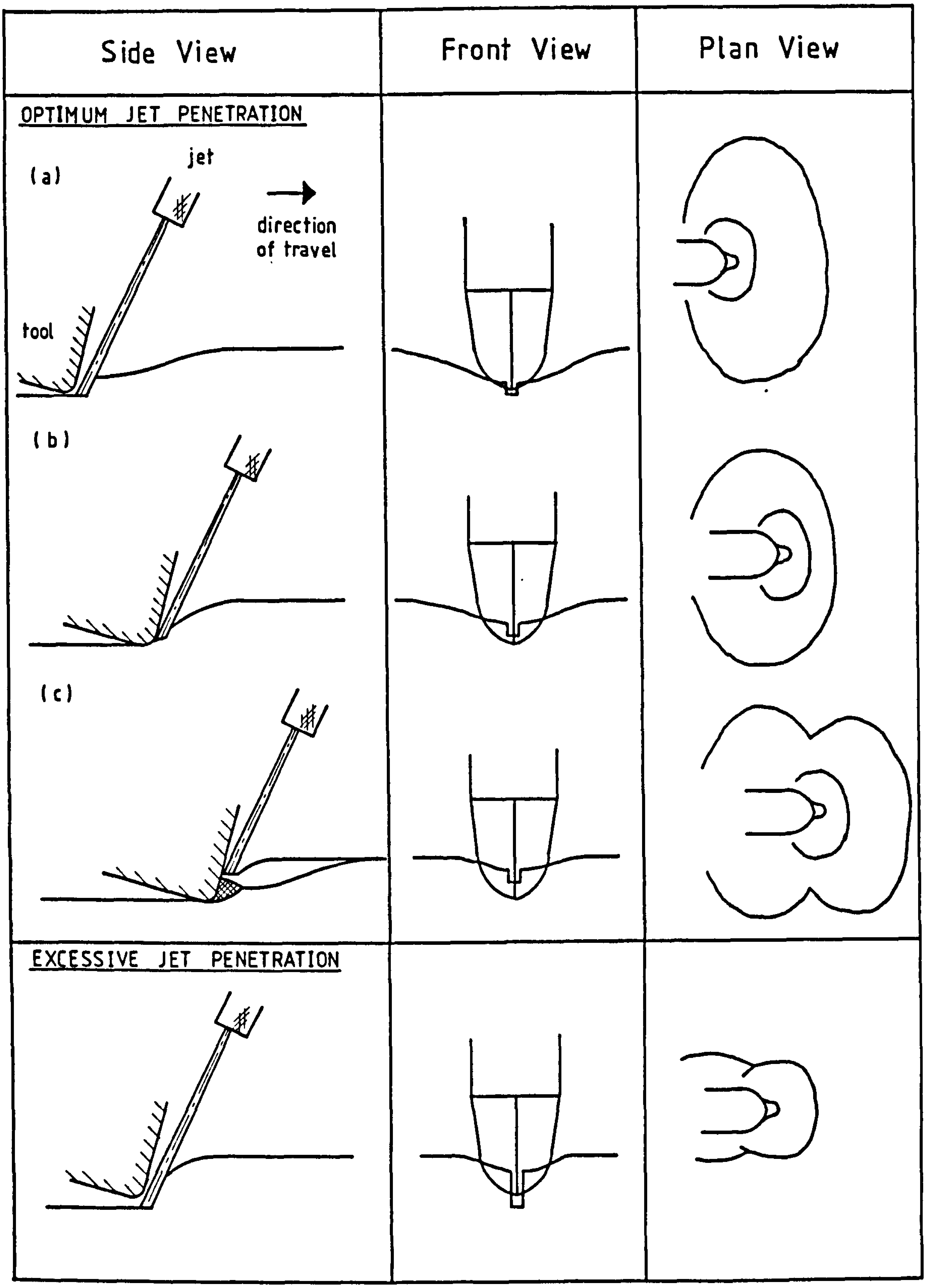

Figure 6.4 Schematic illustration of Water Jet Assisted Rock Cutting.

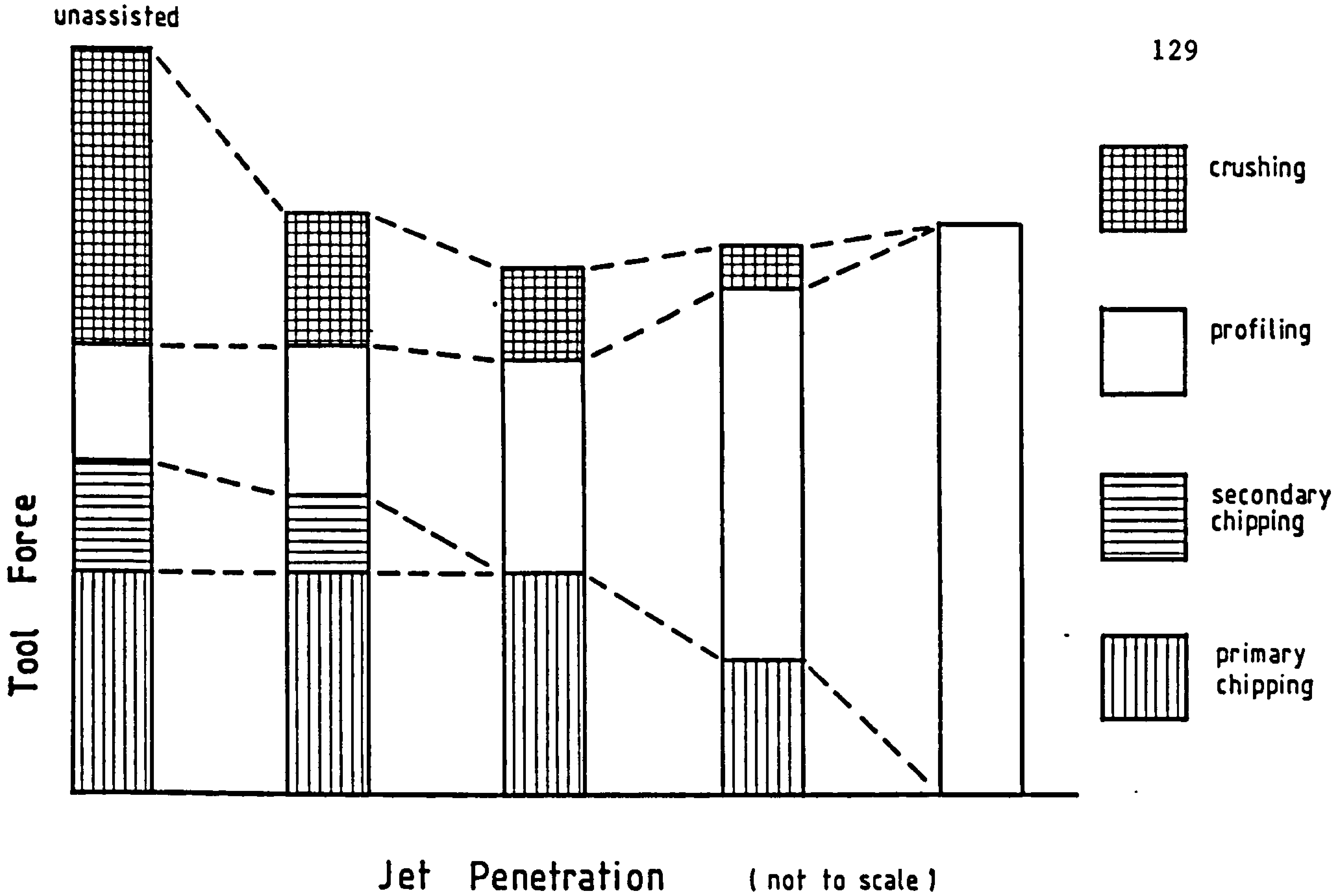

Figure 6.5 Summary of the application of the model and the effect of water jet on different tool actions.

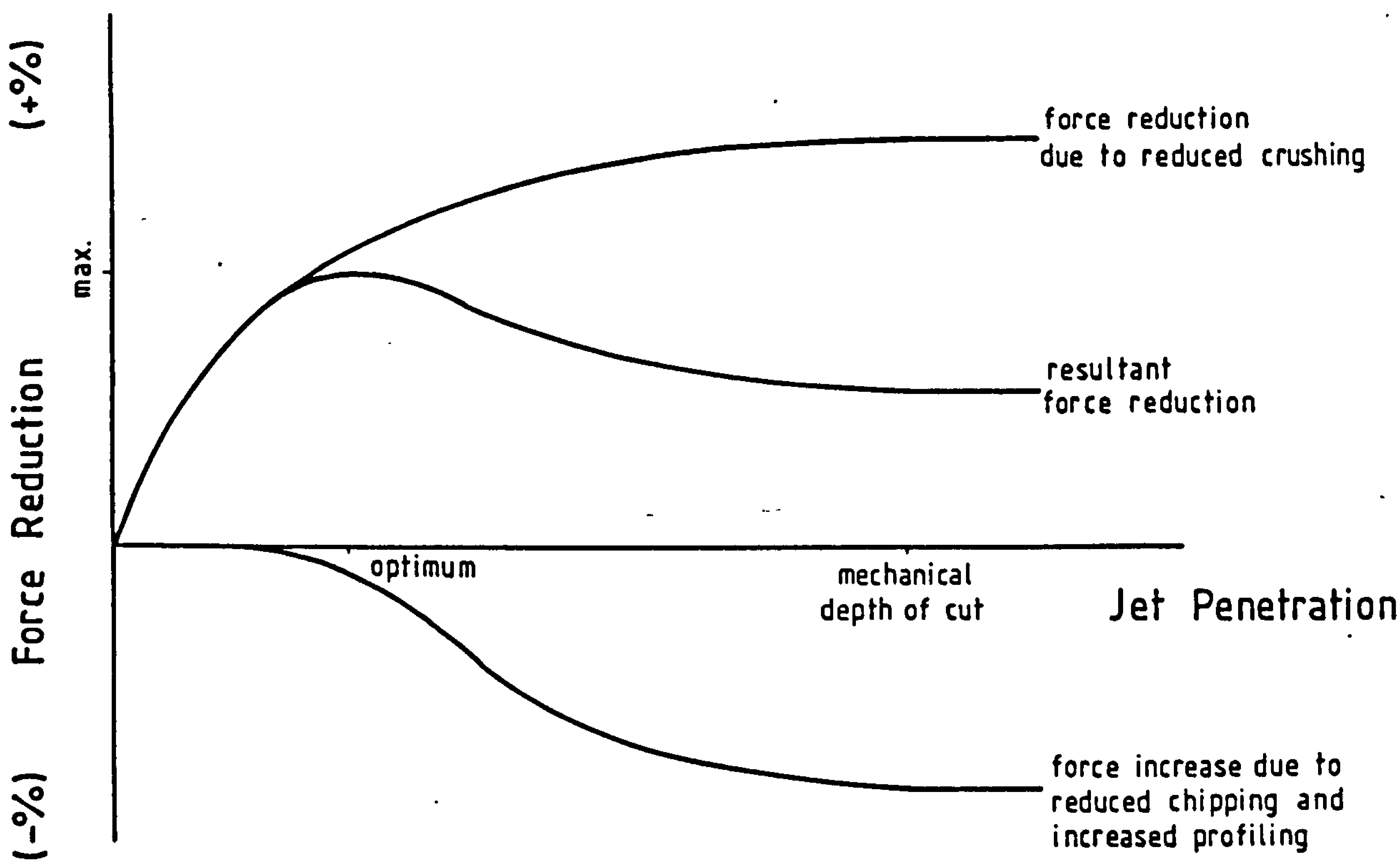

Figure 6.6 Generalised relationship between tool force reduction and jet penetration.

experienced, there exists an optimum jet penetration which maximises the tool force reduction produced. When the jet penetration is deeper than mechanical depth of cut, the resultant force reduction is expected to have a constant residual value.

In Figure 6.6. the force reduction due to reduced crushing, and force increase due to increased profiling, are plotted against the jet penetration, together with the resultant force reduction.

6.4 Summary

For the drag tool rock cutting, the cutting mechanism suggested is based on careful observation of the sequence of a typical cutting cycle by a drag tool used in the present study. Four tool actions are identified, including crushing, profiling, primary chipping and secondary chipping. These observations are supplemented by the examination of rock chips. For water jet rock cutting, rock removal is carried out by erosion rather than internal fracturing,.

Depending on jet penetration, the water jet has different effects in terms of tool force reductions. A model is proposed to describe the effects of the water jet at different jet penetrations. An optimum jet penetration is predicted to exist at which maximum force reductions are obtained. Unless there is a change of cutting mechanism, no improved assistance is expected from the water jet when jet penetration is deeper than mechanical depth of cut.

* * *

CHAPTER SEVEN

CHAPTER SEVEN

PRIMARY EXPERIMENTAL RESULTS

7.1 Introduction

Five rock types of different strengths and abrasivities were cut in a standard experimental programme. The programme was designed such that each rock was cut with the same operational conditions, allowing the results to be compared. The main parameters investigated were jet pressure, depth of cut and traverse speed.

Before the water jet was introduced, the results for the drag tool alone tests were first analysed. In addition, water jet penetration tests were undertaken at selected traverse speeds and jet pressures to allow jet penetration characteristics for each rock to be determined.

Depending on the jet penetration characteristics, the rocks can be divided into two distinct groups. Dumfries Sandstone, Grindleford Sandstone and Penrith Sandstone belong to the group where jet penetration is significant under the present system. Pennant Sandstone and Middleton Limestone, however, are in the second group where jet penetration was not observed even at the slowest traverse speed and highest jet pressure.

The validity of the proposed model of water jet assisted cutting is assessed by examination of the experimental results. Alternative water jet assistance mechanisms are also assessed with particular reference to the effect of moisture on the cuttability of rocks.

In order to evaluate water jet assistance, most results are interpreted in terms of tool force reductions with respect to corresponding unassisted cutting. The other results, including mean and mean peak tool forces can be found in Appendix C.

7.2 Drag Tool Rock Cutting

Drag tool rock cutting is not the main theme of the present work. However, it is useful to examine the unassisted rock cutting first so that the effects of water jets can be identified in assisted rock cutting.

The excavation of rock using wedge tools has been the subject of extensive research for some considerable time (Whittaker 1962; Pomeroy 1963; Barker 1964; Roxborough and Rispin 1973; Roxborough and Phillips 1975). No fundamental study of wedge tool cutting was carried out in the current research as full details are available elsewhere. Because only one tool type was used during the whole of the project, only the operational parameters, including depth of cut and traverse speed, will be dealt with here.

7.2.1 Effect of Depth of Cut

When a chisel type drag tool is used, the tool forces increase linearly with depth of cut. However, the tool used in this project had a complex tip geometry with ridged front and pointed bottom. The results are plotted in Figures 7.1 to 7.4 for cutting speeds of 0.27 m/s and 1.10 m/s.

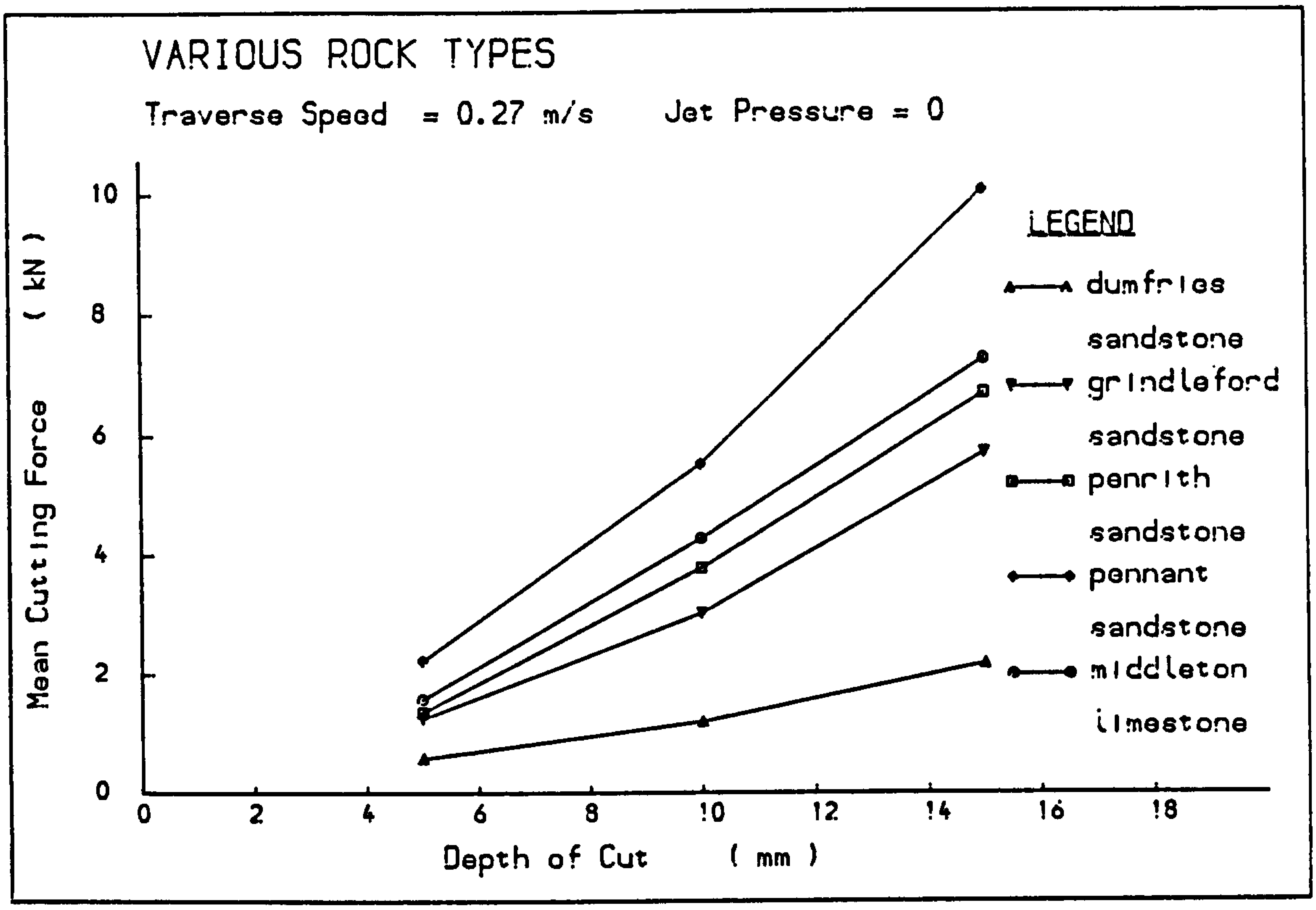

Figure 7.1 Mean Cutting Force versus Depth of Cut Unassisted cutting at 0.27 m/s traverse speed.

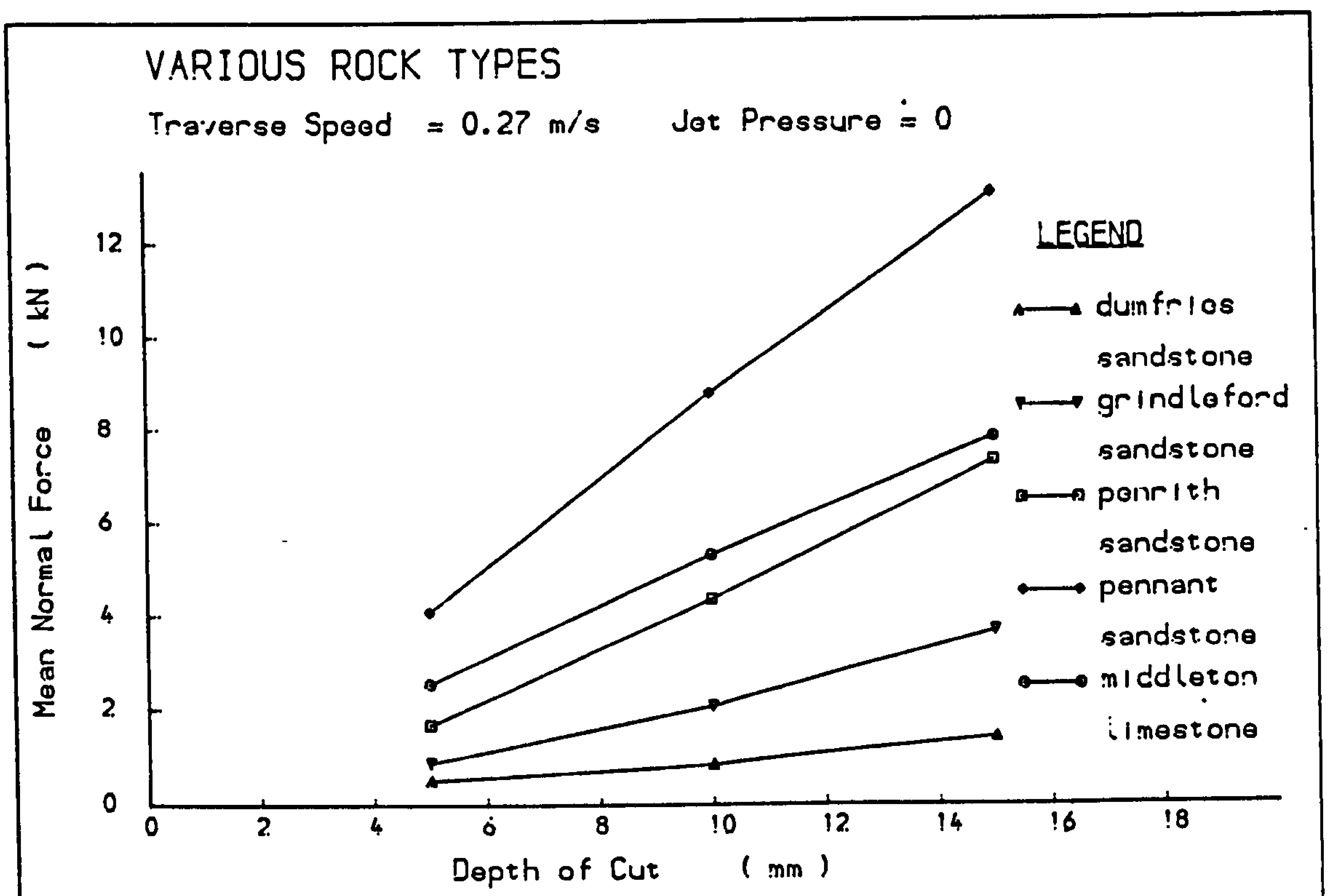

Figure 7.2 Mean Normal Force versus Depth of Cut Unassisted cutting at 0.27 m/s traverse speed.

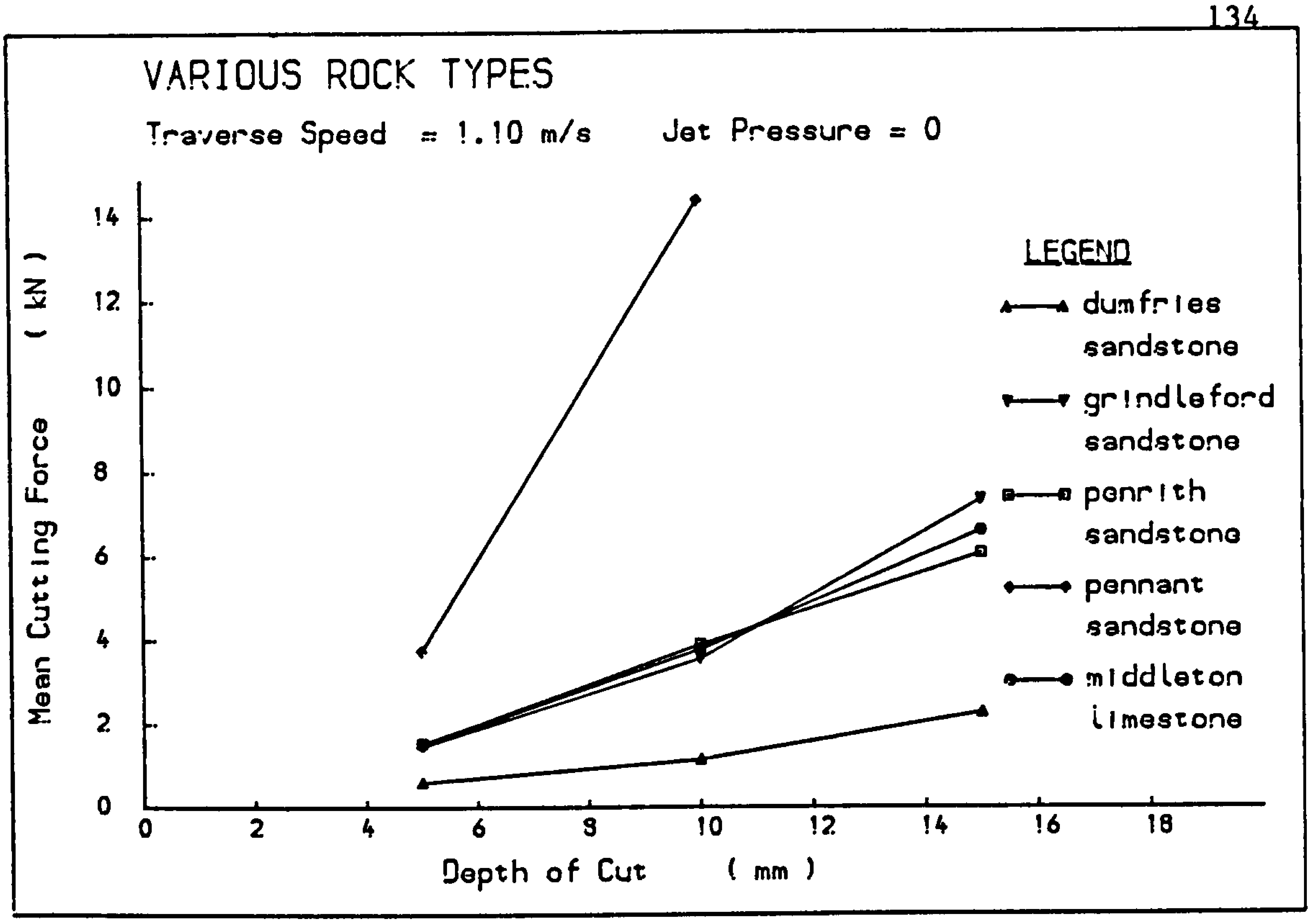

Figure 7.3 Mean Cutting Force versus Depth of Cut : Unassisted Cutting at 1.10 m/s traverse speed.

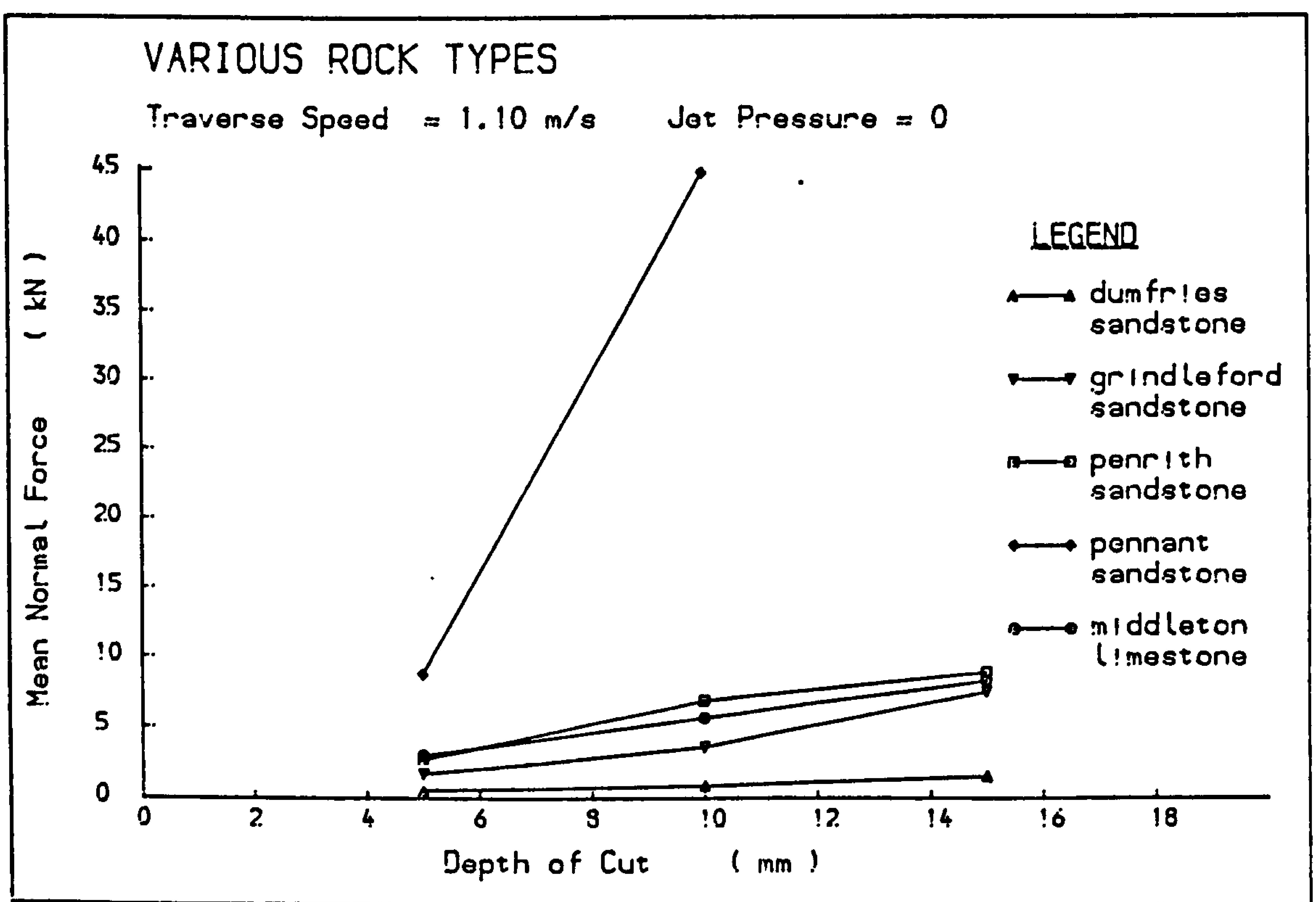

Figure 7.4 Mean Normal Force versus Depth of Cut : Unassisted Cutting at 1.10 m/s traverse speed.

At the slow cutting speed, the mean normal force increases linearly with depth of cut, mostly with the intercept at zero force. For the cutting force, however, the force increases non-linearly with depth of cut. This difference is due to the fact that the area of the tool in contact with the rock increases linearly with depth of cut in the normal direction but linearly with the square of depth of cut in the cutting direction. This non-linear relationship for the cutting force is expected to cease for high depths of cut. Tool forces for all five rock types, both cutting and normal components, have the magnitude in the same hierarchical order as the compressive strength, although a linear proportionality is unjustified.

At the fast speed, the much higher forces for Pennant Sandstone are very noticeable. The rapid wear of the tool made the 15mm depth of cut impossible for this rock due to the possibility of damaging the dynamometer. For the other rocks, the trend was generally similar to that at low speed. However, there was a marked difference in that the force magnitude no longer followed the uniaxial compressive strength hierarchy. Grindleford Sandstone and Penrith Sandstone, with a compressive strength lower than that of Middleton Limestone, have the higher cutting force and normal force respectively. As the tool component forces in cutting Middleton Limestone were relatively unchanged at both speeds it would seem the traverse speed effect exists in these two sandstones.

7.2.2 Effect of Traverse Speed

7.2.2.1 Literature Review

The effect of cutting speed on tool force has not been the subject of much research, which is surprising, considering its importance relevant to the understanding of fundamental rock cutting at high speeds.

O'Dogherty (1963) showed that variations in cutting speed over the range 1-3 m/s did not affect mean cutting force in cutting coal. This has been attributed to the much faster propagation speed of tensile cracks during chip formation. In another coal cutting test, with cutting speeds up to 10 m/s, however, Gregor (1968), claimed that cutting force increases linearly with tool velocity. The increase of fracture stress with increase of strain rate is suggested as an explanation.

Roxborough (1973) cut the non-abrasive anhydrite at traverse speeds of 0.15 to 0.57 m/s and found that cutting speed has no significant effect on the tool forces. The indifference of cutting force to cutting speed has been further proved in cutting Bunter Sandstone (porosity 23%) in a similar speed range (Roxborough and Phillips 1975). Nishimatsu (1979), based on the theoretical review on the effect of crack propagation speed and strain rate, concluded that cutting force is independent of tool speed. No cutting tests were carried out.

The much faster crack propagation speed compared with the tool speed and small increase of fracture stress with strain rate are always quoted to support the claim that traverse speed has no effect on the tool forces (Nishimatsu 1979). It is generally agreed that the much faster crack propagation speed has no effect on cutting force. Hood (1976) measured the crack propagation speed of norite, using a high speed camera (1,000 frames per second),and estimated crack propagation speed as about 80 m/s. However, it is doubtful to apply laboratory uniaxial compression test results and to conclude that strain rate has no effect on tool forces. The uniaxial compression test measures rock performance on a macroscopic scale, while activities around the tool tip are on a microscopic scale.

Another surprising fact is that the normal force component of the tool force has in the past been ignored in most research.

7.2.2.2 Results

One tool was used for each rock type with the exception of Pennant Sandstone for both traverse speeds of 0.27 m/s and 1.10 m/s. Although a wearflat was generated during the course of the cutting experiments, the randomised cutting sequence enabled tool forces to be compared for a similar amount of wear. The results of tool force increase due to the fast speed are presented in tabular form in Table 7.1. Abrasivity and quartz content are shown in Table 7.2.

Although it is debatable that cutting force is independent of cutting speed, it is obvious that fast speeds cause a greater increase in the normal force for Grindleford and Penrith sandstones,

Rock	Depth of Cut (mm)	MCF (%)	MNF (%)	MPCF (%)	MPNF (%)
Dumfries Sandstone	5 10 15	3.4 -4.1 4.1	1.9 3.5 7.8	3.9 1.9 11.7	0.0 -1.1 6.4
Grindleford Sandstone	5 10 15	17.3 17.8 28.3	93.3 72.9 104.9	21.7 13.7 16.9	79.4 57.0 72.0
Penrith Sandstone	5 10 15	13.1 3.2 -9.7	64.3 57.7 21.3	10.9 -13.0 -13.9	48.8 27.1 8.2
Middleton Limestone	5 10 15	-4.4 -11.7 -9.2	18.4 6.2 5.6	-5.9 -15.8 -12.0	16.6 -0.7 1.0

TABLE 7.1 Tool Force Increase (%) for Cutting Speed from 0.27 m/s to 1.10 m/s.

Rock	Newcastle Abrasivity ($^1/10$ mm)	Quartz Content (%)
Dumfries Sandstone	1.9	66.4
Grindleford Sandstone	4.6	72.2
Penrith Sandstone	6.6	78.0
Pennant Sandstone	5.3	45.6
Middleton Limestone	1.9	0.0

Table 7.2 Abrasivity and Quartz Content for Various Rocks

but has no effect in the case of Dumfries Sandstone or Middleton Limestone. As each rock was cut with a similar degree of wear at both speeds it may be that certain rock properties account for the difference. The high correlation between normal force increase and abrasivity suggests that it may be that the same rock properties are responsible for the high values. It is believed that one of these may be the hard mineral content.

The quartz was of a grain size less than 0.5mm in all the sandstones tested and could easily be trapped underneath the wearflat. The quartz was then subjected to compulsory grinding and crushing. Powdered rock was observed in the track left by the tool. Hence the rate of crushing of the quartz may have contributed to the high increase in normal force in the Grindleford and Penrith sandstones. The insensitivity of the normal force increase to quartz content in the Dumfries Sandstone is quite possibly due to its high porosity and softness and the fact that the quartz was compressed rather than ground and crushed.

Kenny and Johnson (1976) found that the tool wear per cut did not increase until a critical speed was reached. Once the critical speed was reached, wear increased rapidly with speed. This increase was attributed to temperature effects. It is most likely that the higher force and temperature may stem from the same cutting mechanisms at high tool speeds. The critical speed may be a function of hard mineral content and hardness of rock.

7.2.3 Mean and Mean Peak Forces

Mean forces are always quoted as this directly affects the cutting performance of a roadheader. Mean peak forces, which measure the average chipping forces, are important only when the tool tip strength and pick box design are considered. When the tool bluntness was constant, the mean peak force was found to have a constant ratio to the mean force.

During this primary experimental programme, pristine tools were used to cut all rocks. Except for the Pennant Sandstone, the mean peak force to mean force ratio was found to be very similar for all rocks. The pooled ratio is 2.33 ± 0.18 and 2.00 ± 0.17 for the cutting and normal force components respectively. The consistence of the ratio is reflected by the small standard deviations. The ratio was higher for cutting force than for normal force. This proves that the cutting force depends more on chipping force, while normal force depends more on crushing force.

The constant mean peak to mean force ratio had been utilised in some simplified rock machineability studies (Nishimatsu et al. 1979).

7.3 Water Jet Rock Cutting

Before each rock type was cut, jet penetration characteristics of the rock were determined by traversing the jet over a trimmed flat rock surface. Jet penetration was measured using a depth gauge with a probe width of 5mm. Ten measurements for each cut were taken and averaged.

Jet penetration was possible only for Dumfries Sandstone, Grindleford Sandstone and Penrith Sandstone. The results are set out in Figures 7.5 to 7.7. All results were obtained using a 0.9 diameter nozzle at a stand-off distance of 54mm. The stand-off distance, representing the jet to rock surface distance, assumed a mechanical depth of cut of 10mm. No jet penetration was observed in either the Pennant Sandstone or the Middleton Limestone, even at 70 MPa jet pressure and 0.27 m/s traverse speed.

For the reasons detailed in Section 8.2 there was no advantage in having a wide cut. The efficiency of jet cutting was compared by using hydraulic specific energy, which is defined as the jet energy per longitudinal area predicted (J/mm^2).

Hydraulic Specific Energy (J/mm^2)

$$= \frac{\text{Jet Power (W) x Traverse Time (s)}}{\text{Jet Penetration (mm) x length of cut (mm)}}$$

$$= \frac{\text{Jet Power (kW)}}{\text{Jet Peneteration (mm) x Traverse Speed (m/s)}}$$

7.3.1 Threshold Pressure

The threshold pressures, depending on the traverse speed, were observed for all three rocks. Normally, the higher the traverse speed, the higher the threshold pressure. Threshold pressure was approximately 4 MPa for Dumfries Sandstone and 9 to 14 MPa for Grindleford Sandstone. Threshold pressure for Penrith Sandstone was not clear, but was estimated to be in the range

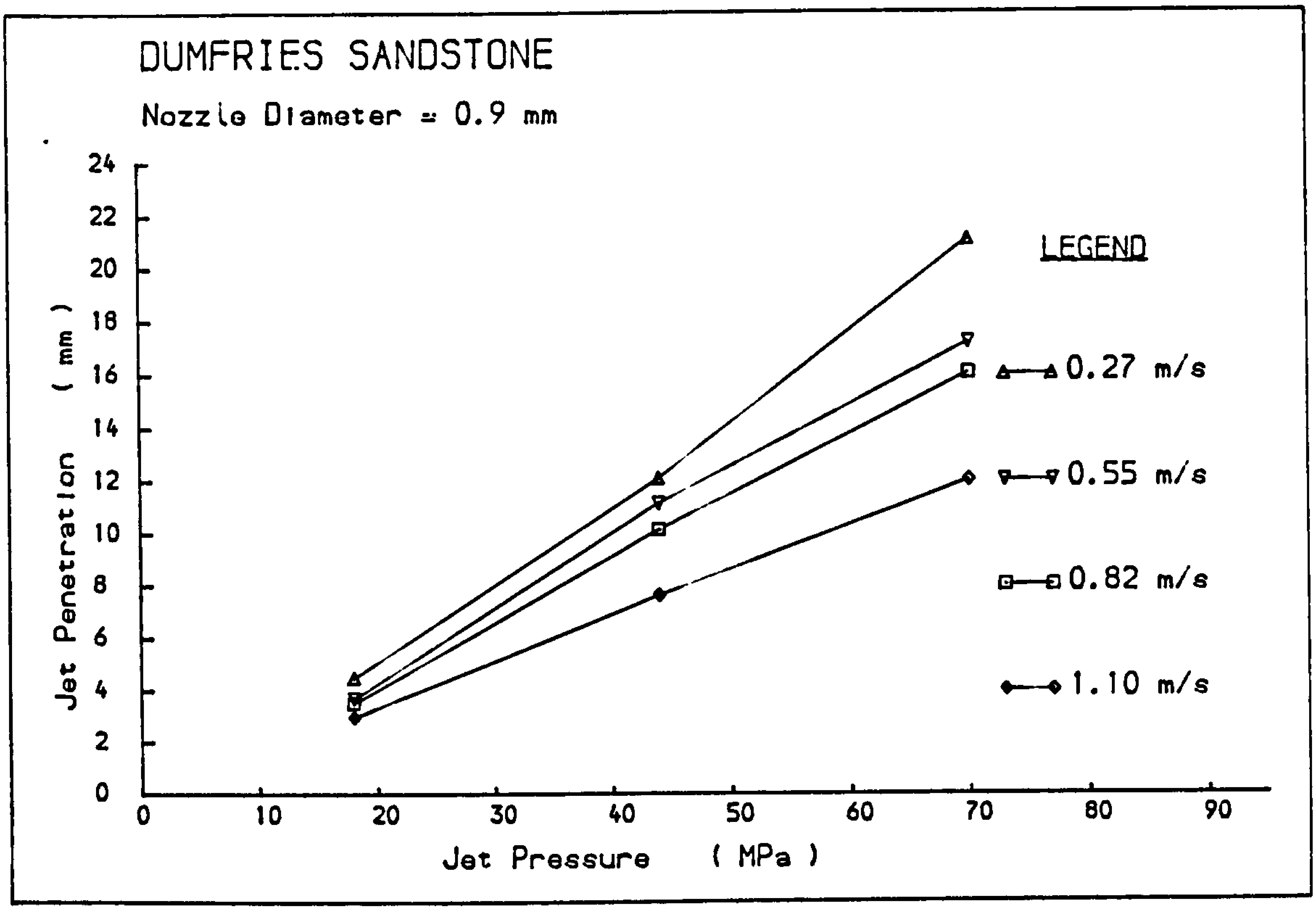

<u>Figure 7.5</u> Jet Penetration versus Jet Pressure : Dumfries Sandstone

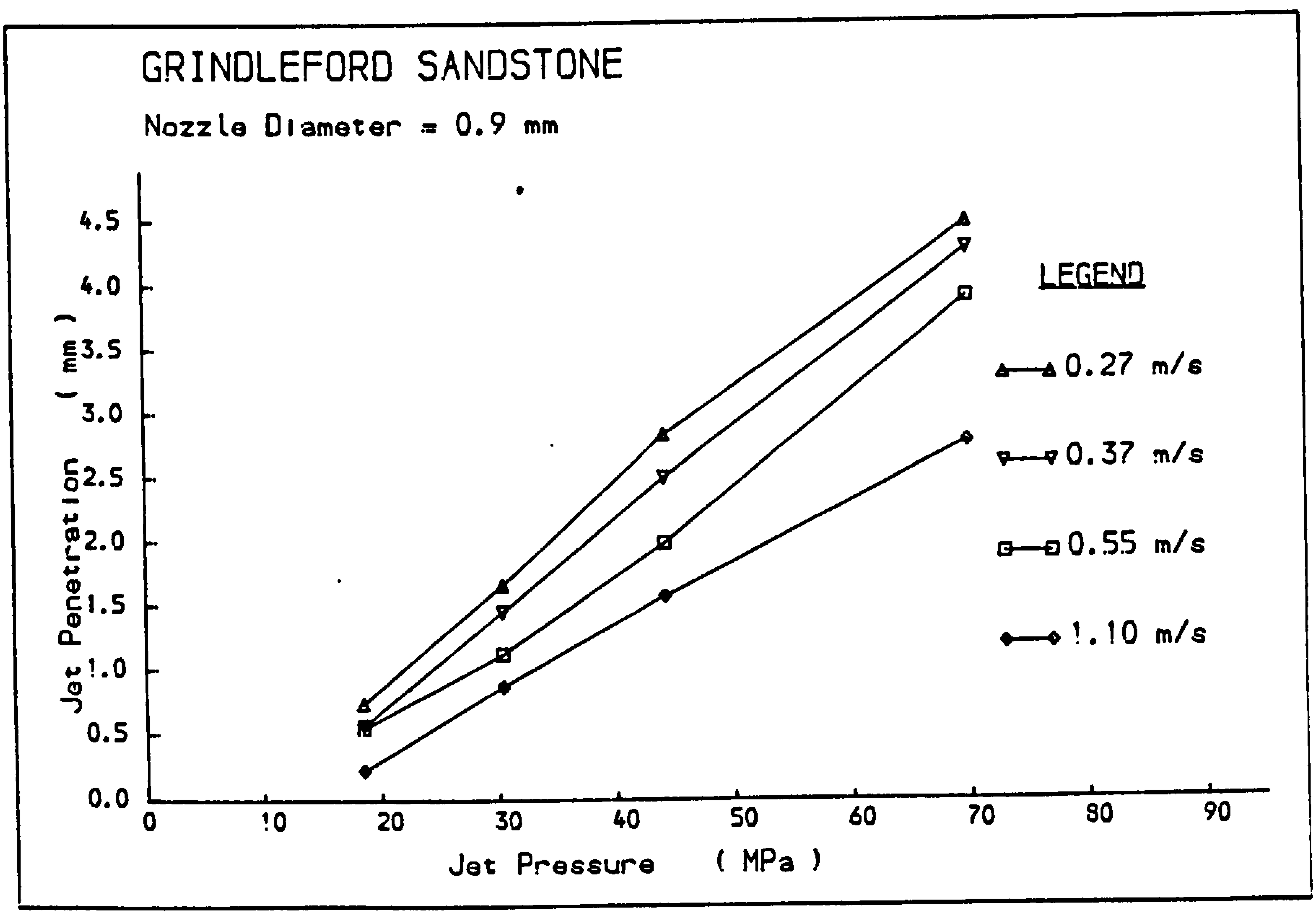

<u>Figure 7.6</u> Jet Penetration versus Jet Pressure : Grindleford Sandstone.

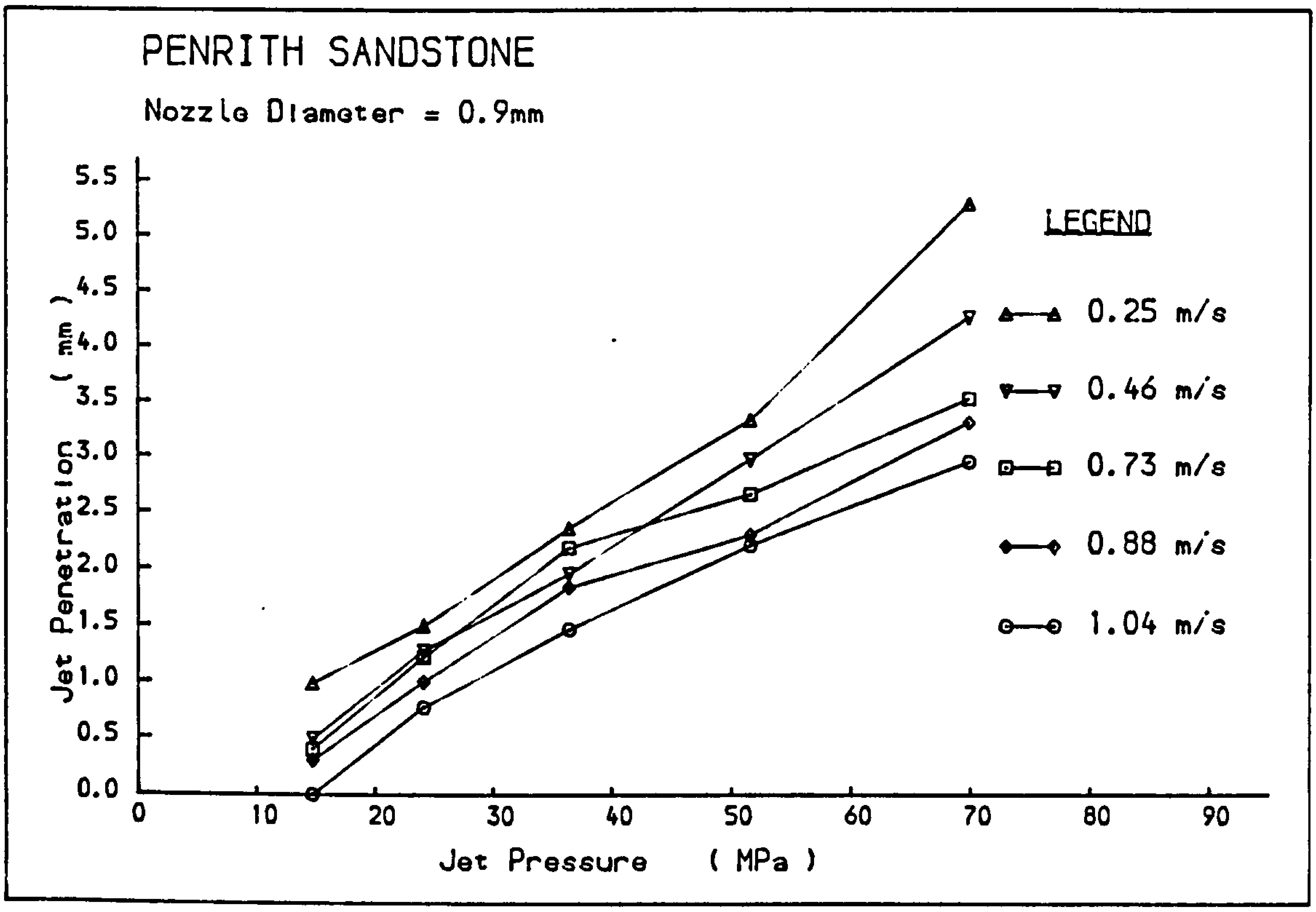

Figure 7.7 Jet Penetration versus Jet Pressure : Penrith Sandstone.

2 to 10 MPa. Threshold pressure can be used to define the erodability of the rock. Below the threshold pressure the jet can only remove grains of rock by a surface erosion process. Insignificant jet penetration is obtained. When jet pressure exceeds the threshold pressure the hydraulic force exerted on the rock grains is higher than the cohesive force holding the grain and significant jet penetration is possible. Only when threshold jet pressure is exceeded is jet penetration proportional to jet pressure and inversely proportional to traverse speed.

The importance of the threshold pressure is recognised by Rehbinder (1976) in his water jet cutting theory. Hashish and du Plessis(1978) estimated from their jet cutting theory that threshold pressure can be expressed as:

$$\text{Threshold Pressure, Pth} = 0.5\,\sigma_c$$

where σ_c = compressive (fracture) strength

Nozzle discharge coefficient is measured to be 0.832 for the 0.9mm nozzle. The estimated and actual threshold pressures are given in Table 7.3.

Hashish's model appears to over-estimate the threshold pressure for Dumfries, Grindleford and Penrith Sandstones. The grainless structure of Middleton Limestone violates the assumptions of all jet cutting theories that grain size must be smaller than jet size. Pennant Sandstone was too strong for the 70 MPa system to test for the threshold pressure.

Rock	Threshold Pressure (MPa)	
	Predicted	Actual
Dumfries Sandstone	11.4	4
Grindleford Sandstone	29.5	9-14
Penrith Sandstone	41.5	2-10
Pennant Sandstone	86.4	N/A
Middleton Limestone	56.6	N/A

Table 7.3 Predicted and Actual Threshold Pressure.

7.3.2 Effect of Traverse Speed

The slower the traverse speed the more jet energy per unit length of cut, and the deeper the jet penetration. However, when jet penetration is compared in terms of jet energy input, the results are completely changed.

All the jet slotting results showed that the higher the traverse speed the lower the hydraulic specific energy (Figures 7.8 to 7.10). This indicates that deeper jet penetration is achieved at fast traverse speed for equal jet energy input.

There appears to exist a critical traverse speed beyond which there is no improvement in specific energy. The critical traverse speed was estimated to be between 0.55 m/s and 0.73 m/s for the three rocks tested.

7.3.3 Effect of Nozzle Diameter

The effect of nozzle diameter in rock erodability was investigated in Grindleford Sandstone. Basically the bigger the nozzle diameter the higher the jet power and hence the deeper the jet penetration. The results plotting jet penetration and hydraulic specific energy are shown in Figures7.11 and 7.12 respectively. An anomaly was observed in that the 1.5mm diameter nozzle did not produce a jet penetration compatible to the high jet power output. This may have been due to the small size of the Newcastle nozzle and the hydrodynamic efficiency being adversely affected when nozzle diameter is too big when compared with inlet diameter.

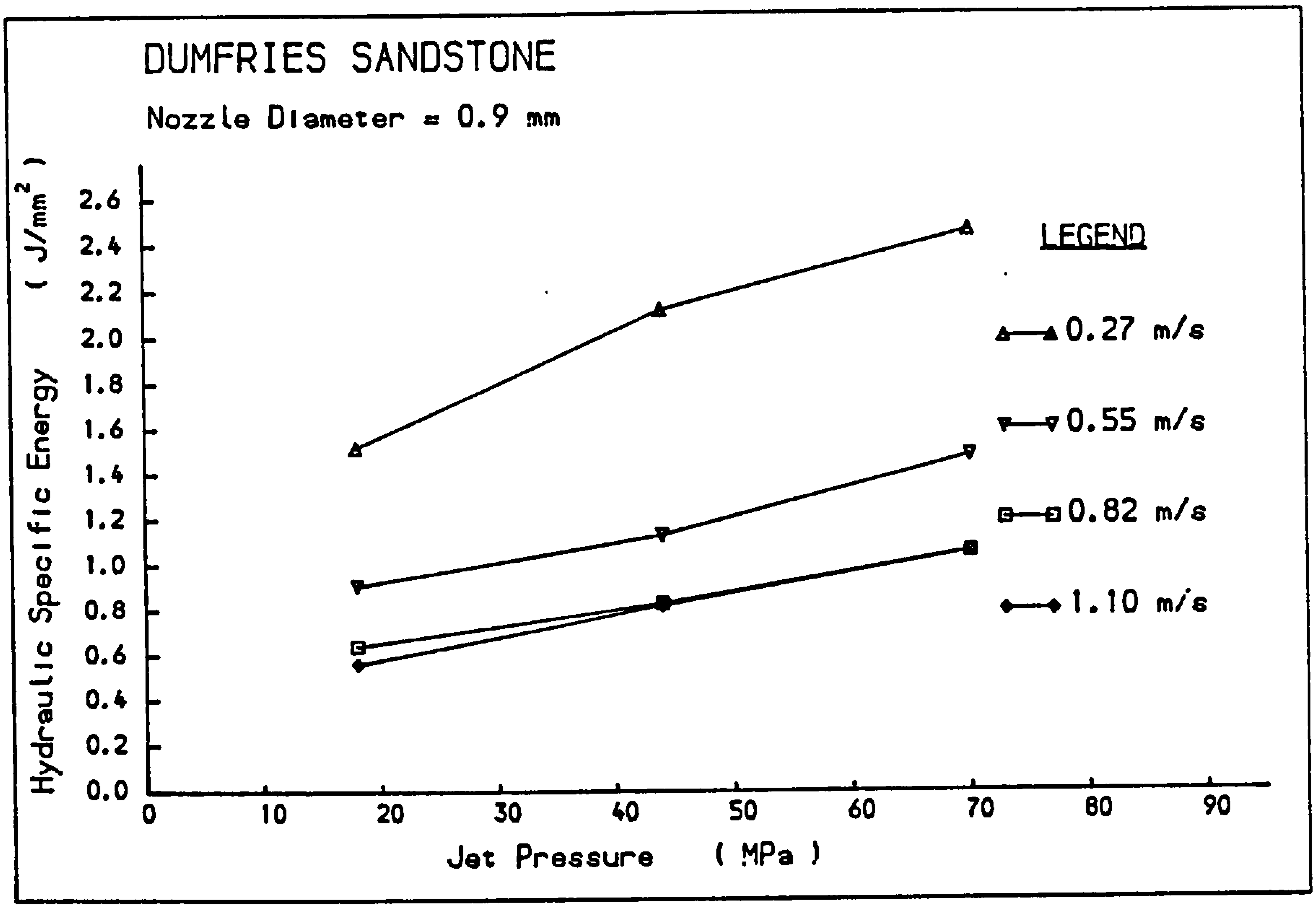

Figure 7.8 Hydraulic Specific Energy versus Jet Pressure : Dumfries Sandstone.

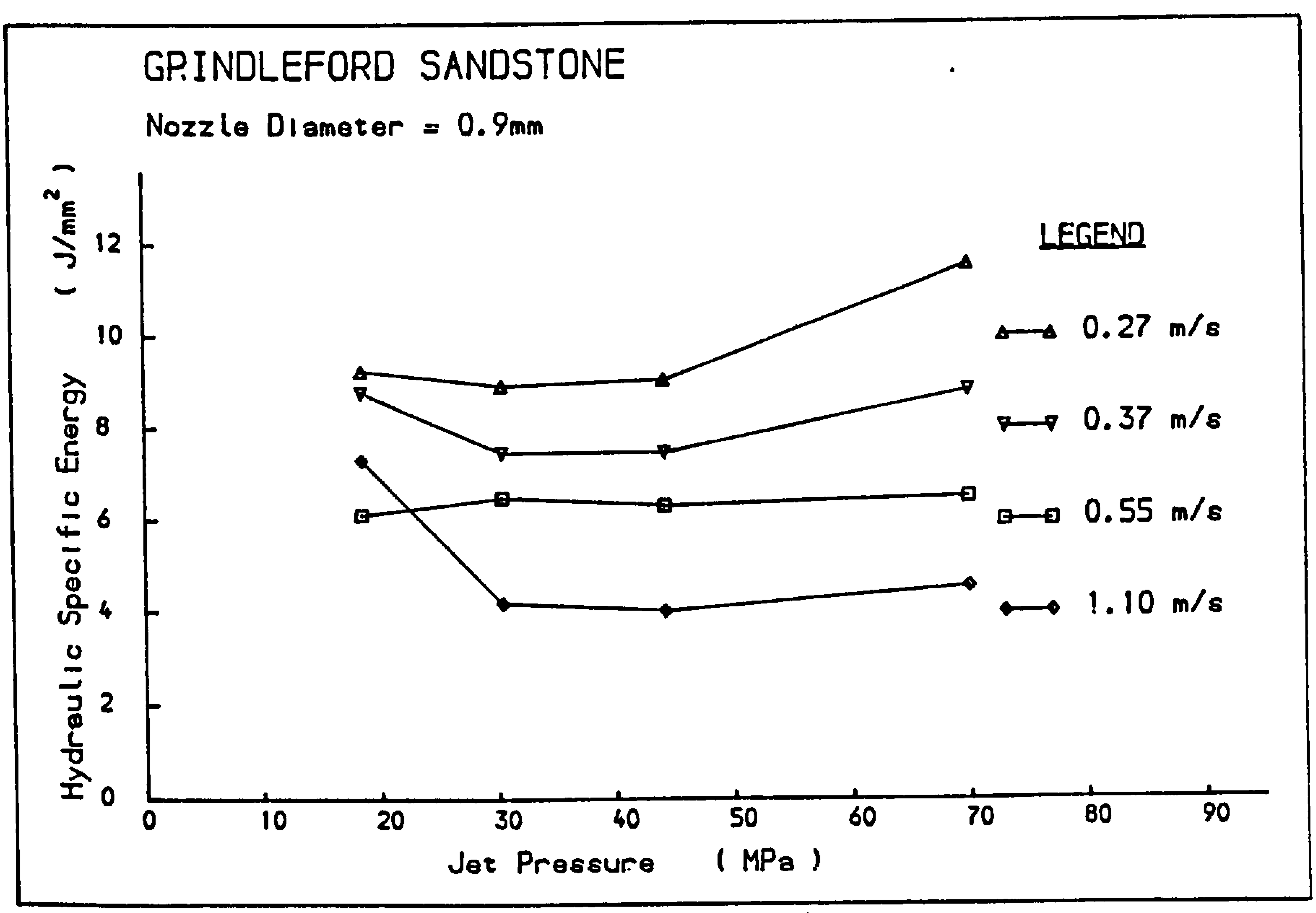

Figure 7.9 Hydraulic Specific Energy versus Jet Pressure : Grindleford Sandstone.

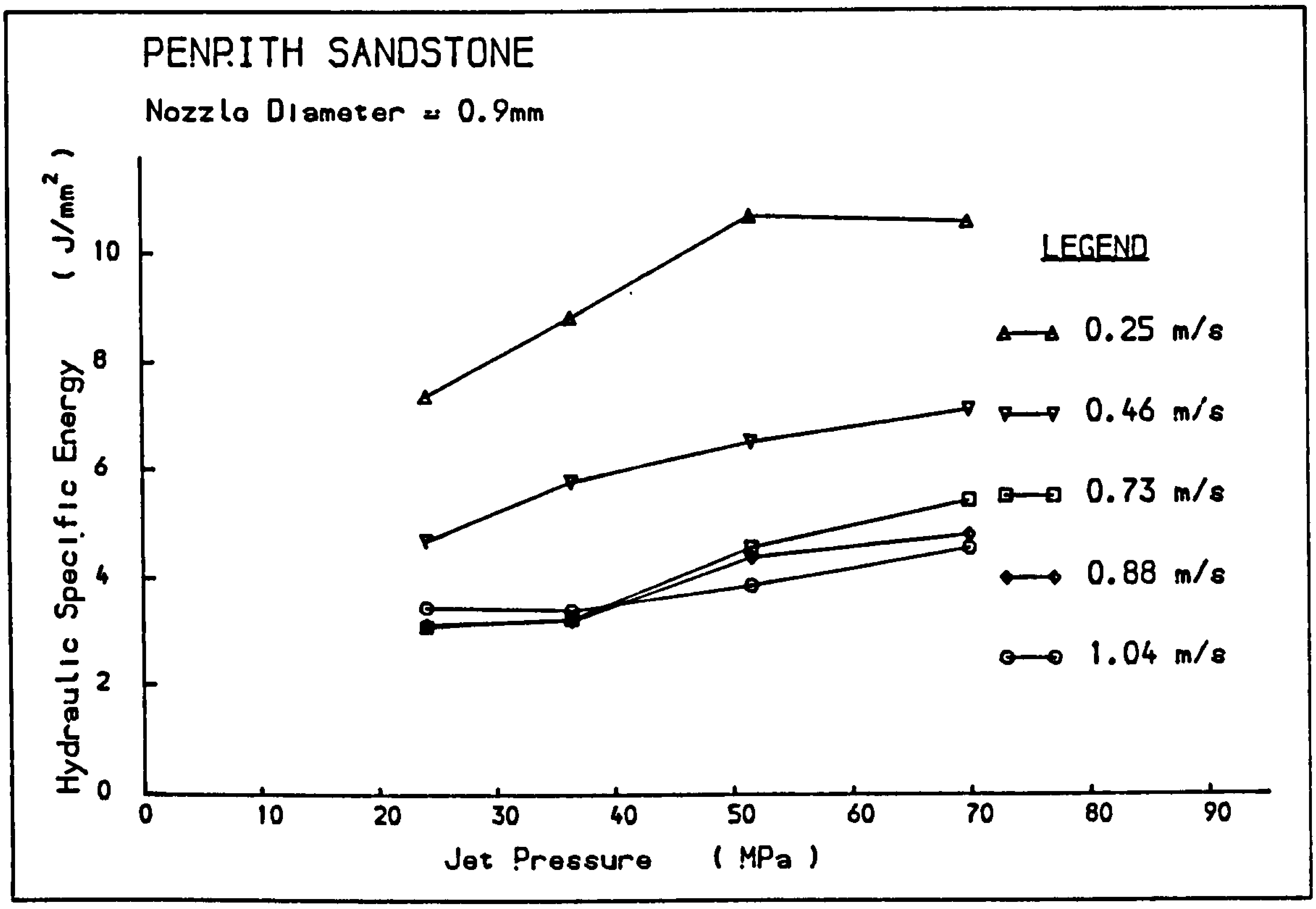

Figure 7.10 Hydraulic Specific Energy versus Jet Pressure : Penrith.Sandstone.

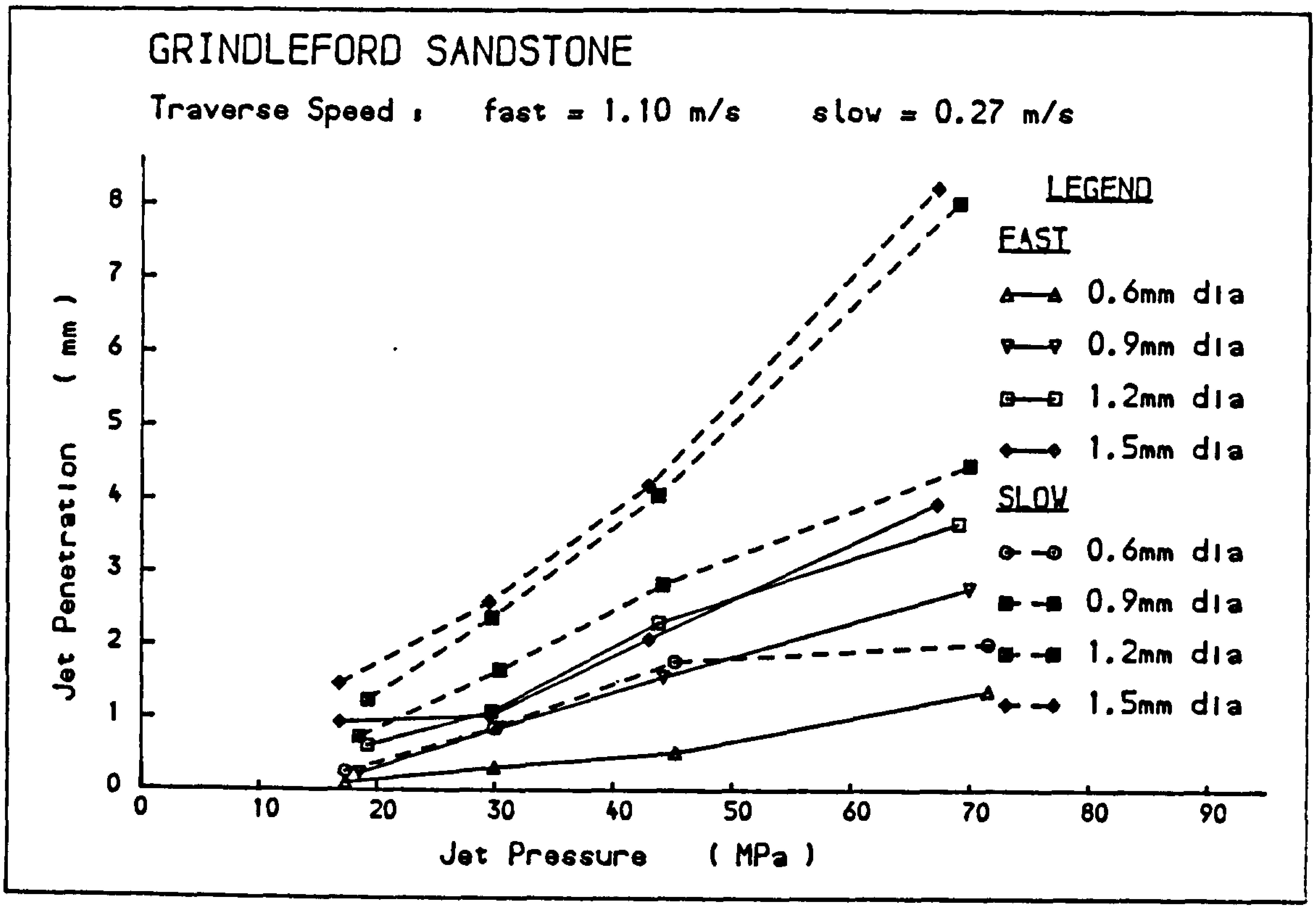

<u>Figure 7.11</u> Jet Penetration versus Jet Pressure for Various Nozzle Diameters : Grindleford Sandstone.

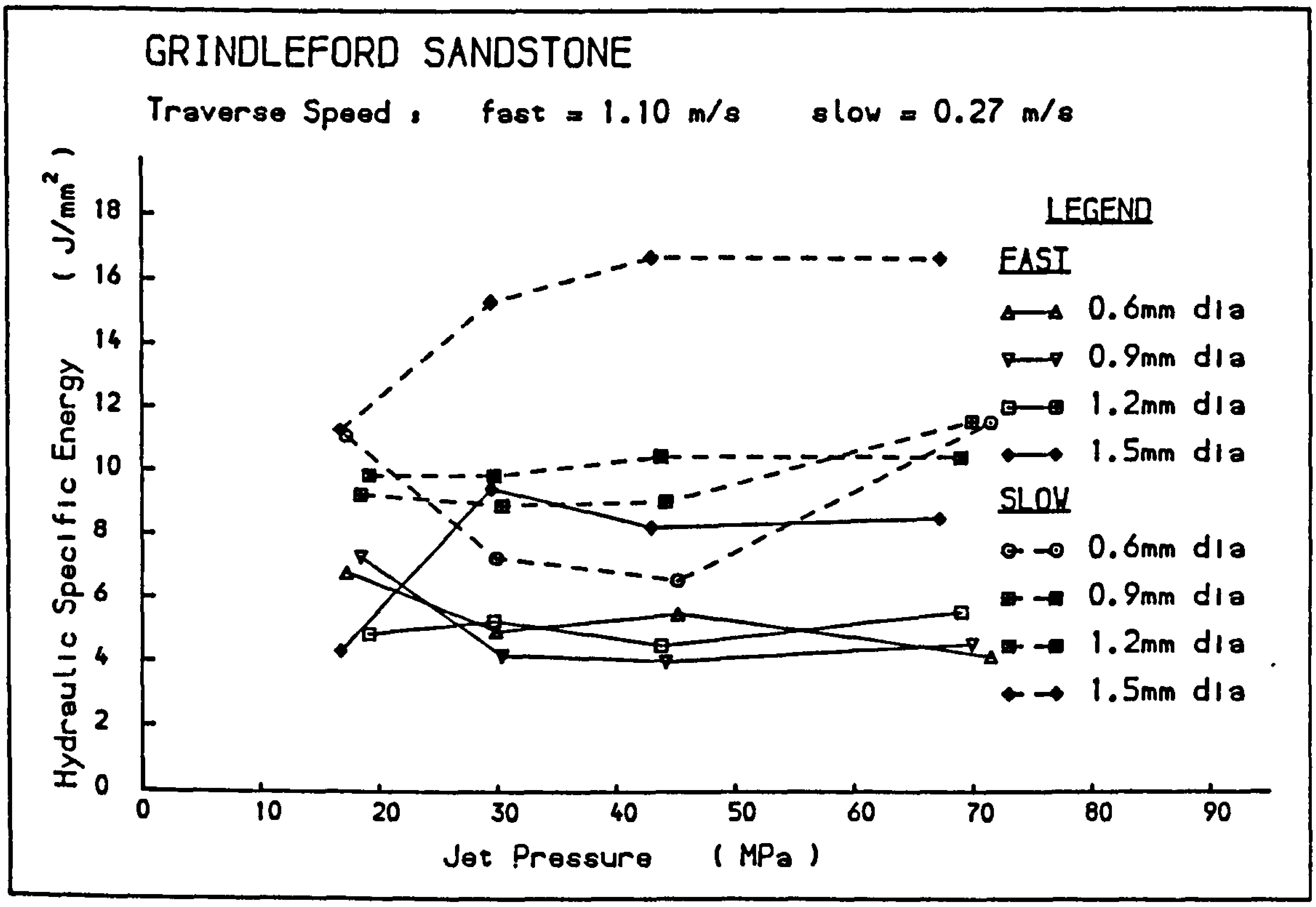

<u>Figure 7.12</u> Hydraulic Specific Energy versus Jet Pressure for various Nozzle Diameters : Grindleford Sandstone.

If pressure and the diameter of the jet are given, the power is uniquely determined by:

$$\text{Jet Power} = Cd \left(\frac{\pi}{4}\right) \left(\frac{2}{\rho}\right)^{\frac{1}{2}} d_o^{\,2} P^{3/2}$$

where: Cd = nozzle discharge coefficient

ρ = fluid density

d_o = nozzle diameter

P = jet pressure.

Jet power is more dependent on nozzle diameter than jet pressure. Hence it is preferable to have higher jet pressure than a larger nozzle diameter for the same jet power if the slot width is unimportant, as in this case. It was expected that hydraulic specific energy would decrease with nozzle diameter. This was generally the case in jet slotting of Grindleford Sandstone at the slow traverse speed, although it was not clear at the fast traverse speed due to difficulty in measuring the shallow jet penetrations.

All the nozzles had a higher specific energy for the slow traverse speed and this was supported by experiments with the other rock types.

7.4 Water Jet Assisted Drag Tool Rock Cutting : Rocks with Significant Jet Penetration

When interpretation of results was being carried out care was exercised with regard to the cutting results for Dumfries Sandstone. The block of Dumfries Sandstone tested had a high degree of heterogeneity. Alternative layers of strong and weak bands were found covering the whole thickness of the block. In terms of tool forces measured the following problems were noted:

(1) The tool forces were dependent on whether the hard band or the soft band of rock was cut;

(2) Rock 'slabbing' was possible when cutting the soft band of rock. Much lower tool forces were obtained when rock 'slabbing' occurred (which was unpredictable); and

(3) The steel dynamometer was too insensitive to provide decent signal outputs in cutting this weak rock at shallow depths of cut.

Hence the tool forces measured tended to fluctuate considerably, although randomisation and replication of experimental tests tended to reduce the extent of fluctuation. Consequently, the test results should be interpreted with care and only the general trend considered. Most of the analysis and interpretation was carried out based on Grindleford and Penrith sandstone results. The Grindleford Sandstone results are particularly emphasised due to its homogeneity and stable cutting characteristics. Grindleford Sandstone was used extensively during the secondary experimental programme to represent the rock group with significant jet penetration.

7.4.1 Optimum Jet Penetration

The cutting results of the rocks in this group are plotted in Figures 7.13 to 7.18 with respect to jet penetration/ depth of cut ratio. A much clearer picture is given as all the effects of jet presence, traverse speed and depth of cut are represented by a single parameter of jet penetration/depth of cut ratio.

By examining the curves at depths of cut of 10mm and 15mm the existence of an optimum jet penetration is obvious. The optimum jet penetration is approximately 20% for cutting force and 30% for normal force respectively.

The difference between cutting and normal force reductions was found for both the optimum jet penetration and the magnitude of force reductions. This can be attributed to the greater influence of crushing below the tool on the normal force than on the cutting force. When the jet penetration was significant, as in this case, the major water jet assistance was to slot the rock and relieve the tool tip from crushing and confinement. Hence the force reduction was always higher for the normal force component than for the cutting force component at the same jet penetration. Higher jet penetration is preferred so far as normal force reductions are concerned. Cutting force, however, depends more on chipping force than on crushing force, and tends to have a smaller optimum jet penetration. The difference between cutting and normal force reduction is generalised in Figure 7.19.

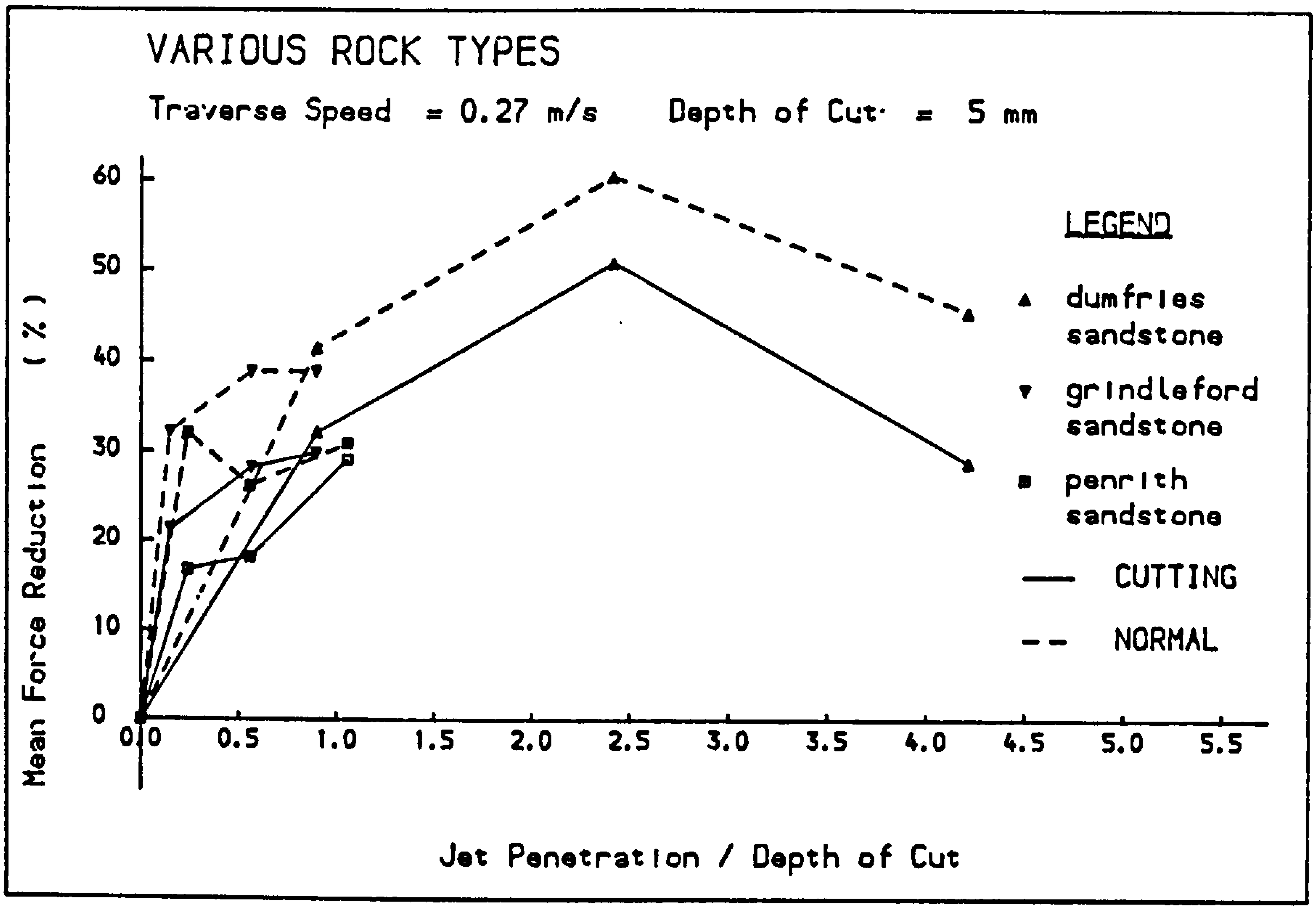

Figure 7.13 Mean Force Reduction versus Jet Penetration : Depth of Cut = 5mm ; Traverse Speed = 0.27 m/s.

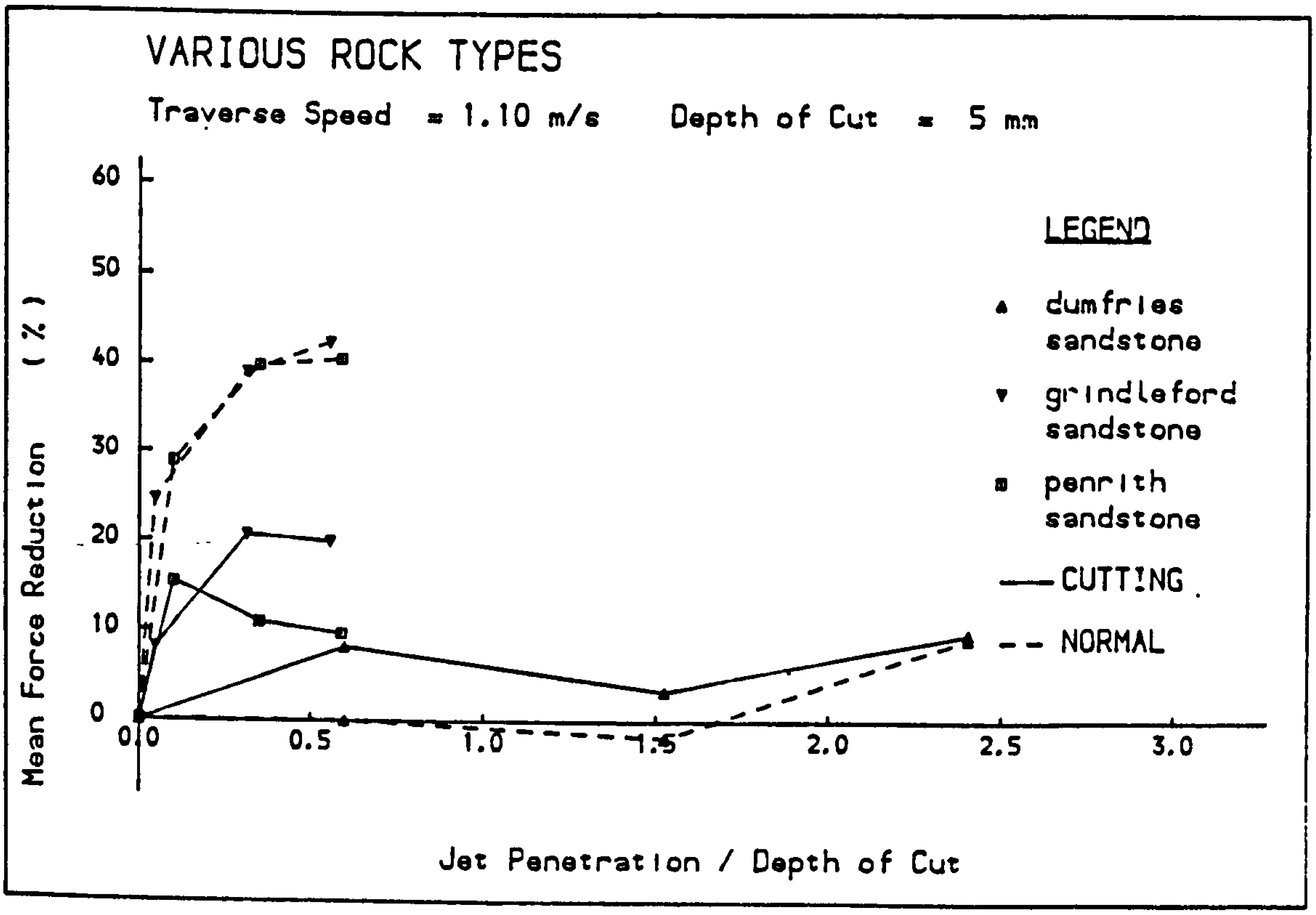

Figure 7.14 Mean Force Reduction versus Jet Penetration : Depth of Cut = 5mm ; Traverse Speed = 1.10 m/s.

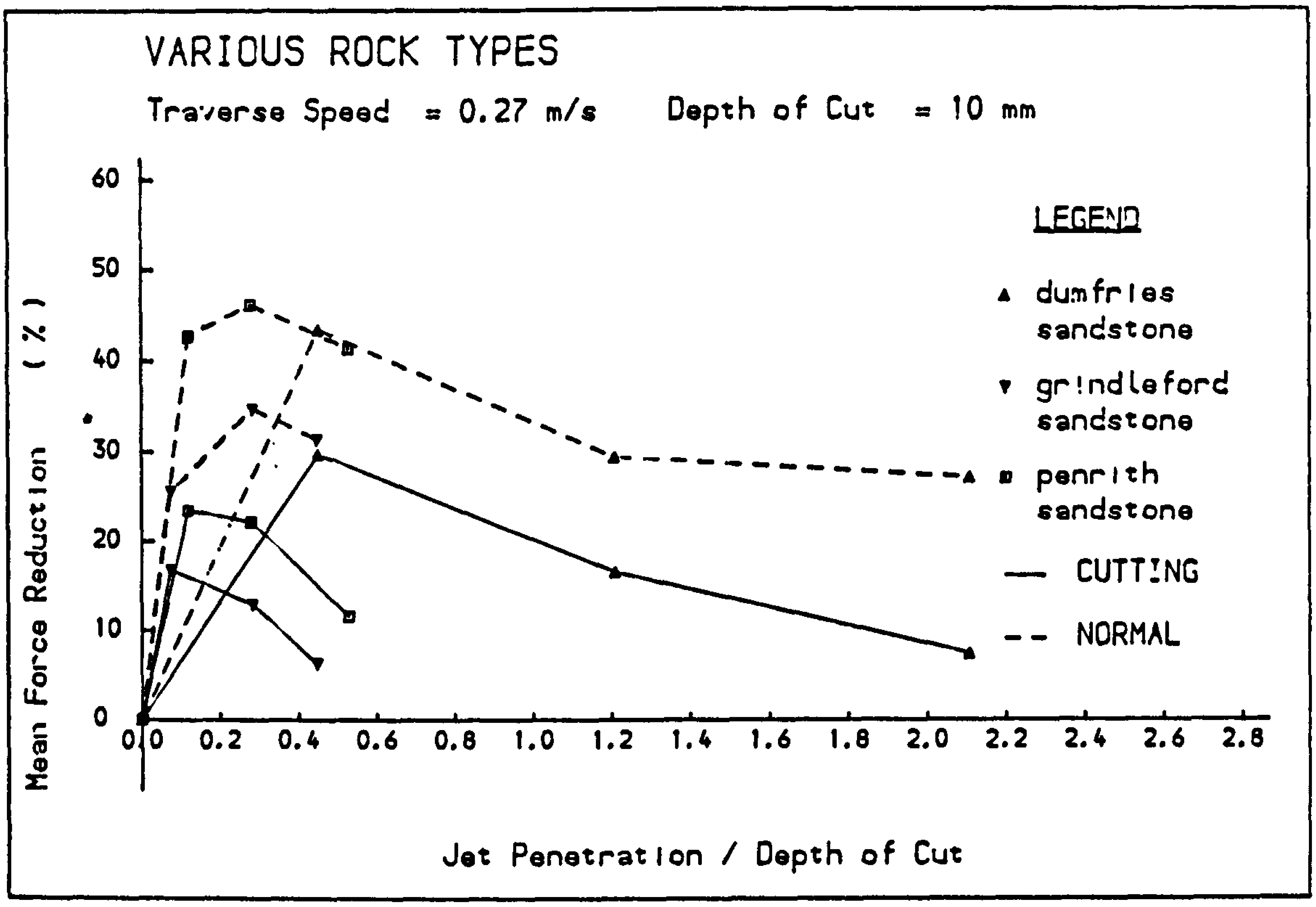

Figure 7.15 Mean Force Reduction versus Jet Penetration : Depth of Cut = 10mm ; Traverse Speed = 0.27 m/s.

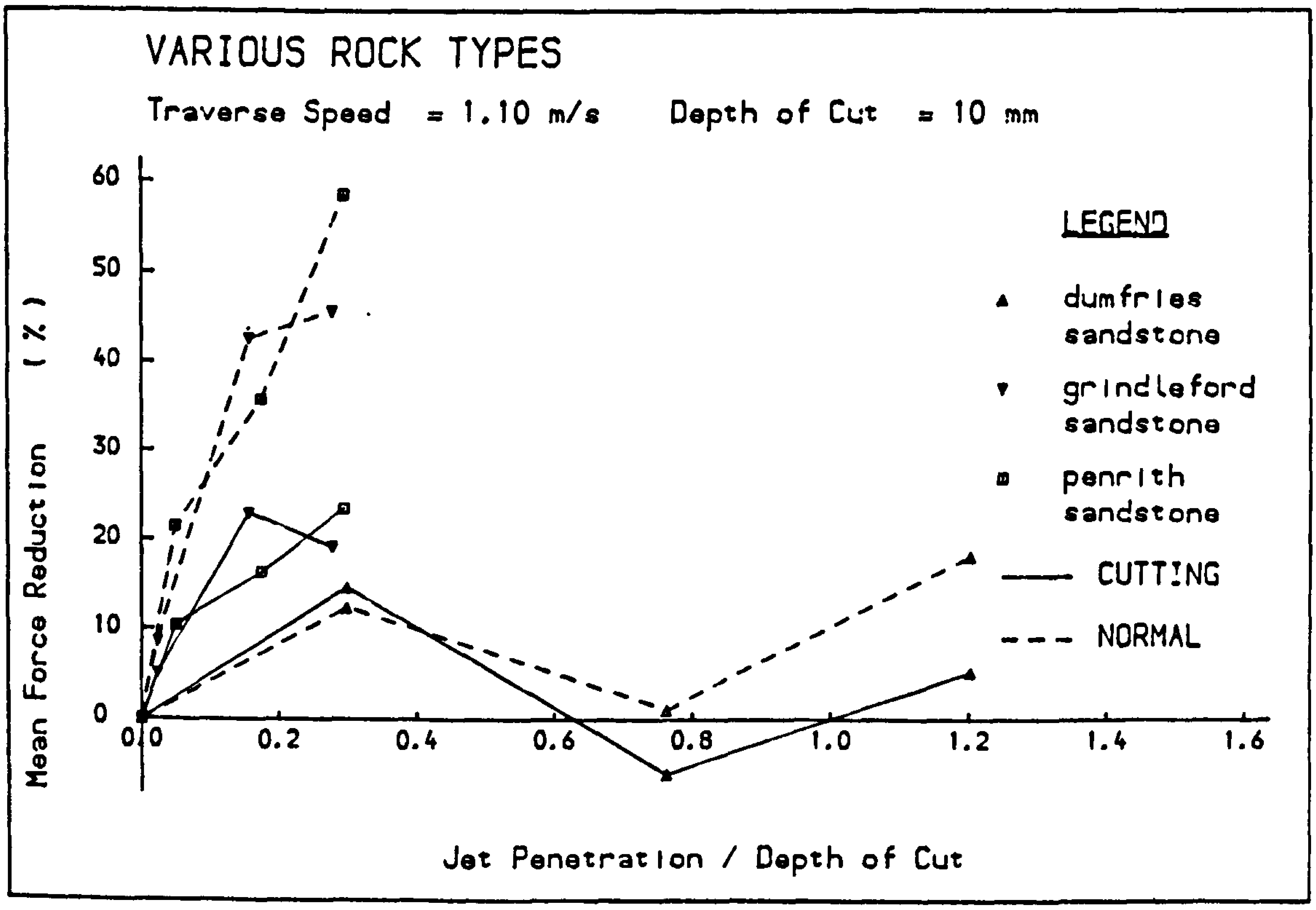

Figure 7.16 Mean Force Reduction versus Jet Penetration : Depth of Cut = 10mm ; Traverse Speed = 1.10 m/s.

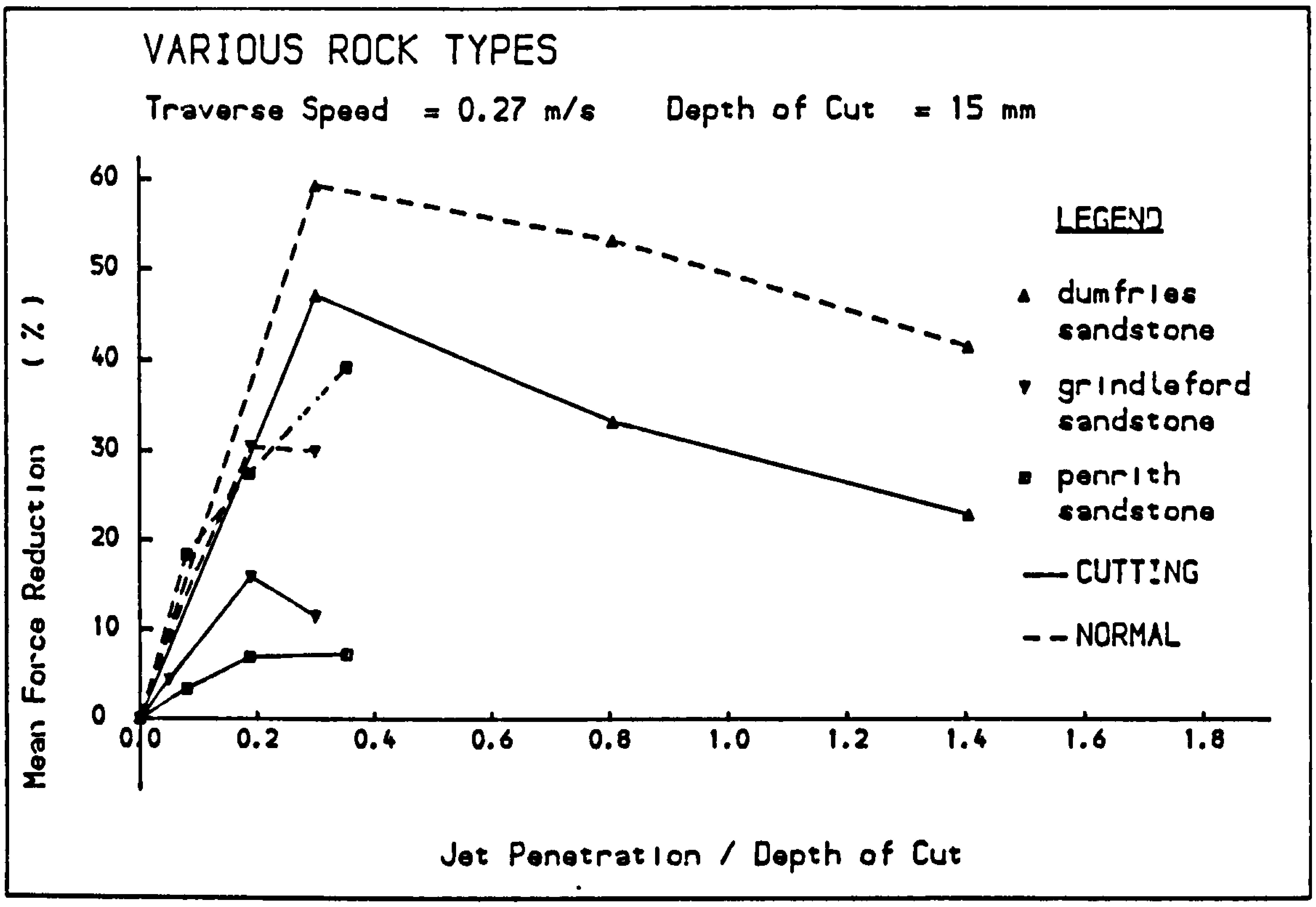

Figure 7.17 Mean Force Reduction versus Jet Penetration : Depth of Cut = 15mm ; Traverse Speed = 0.27 m/s.

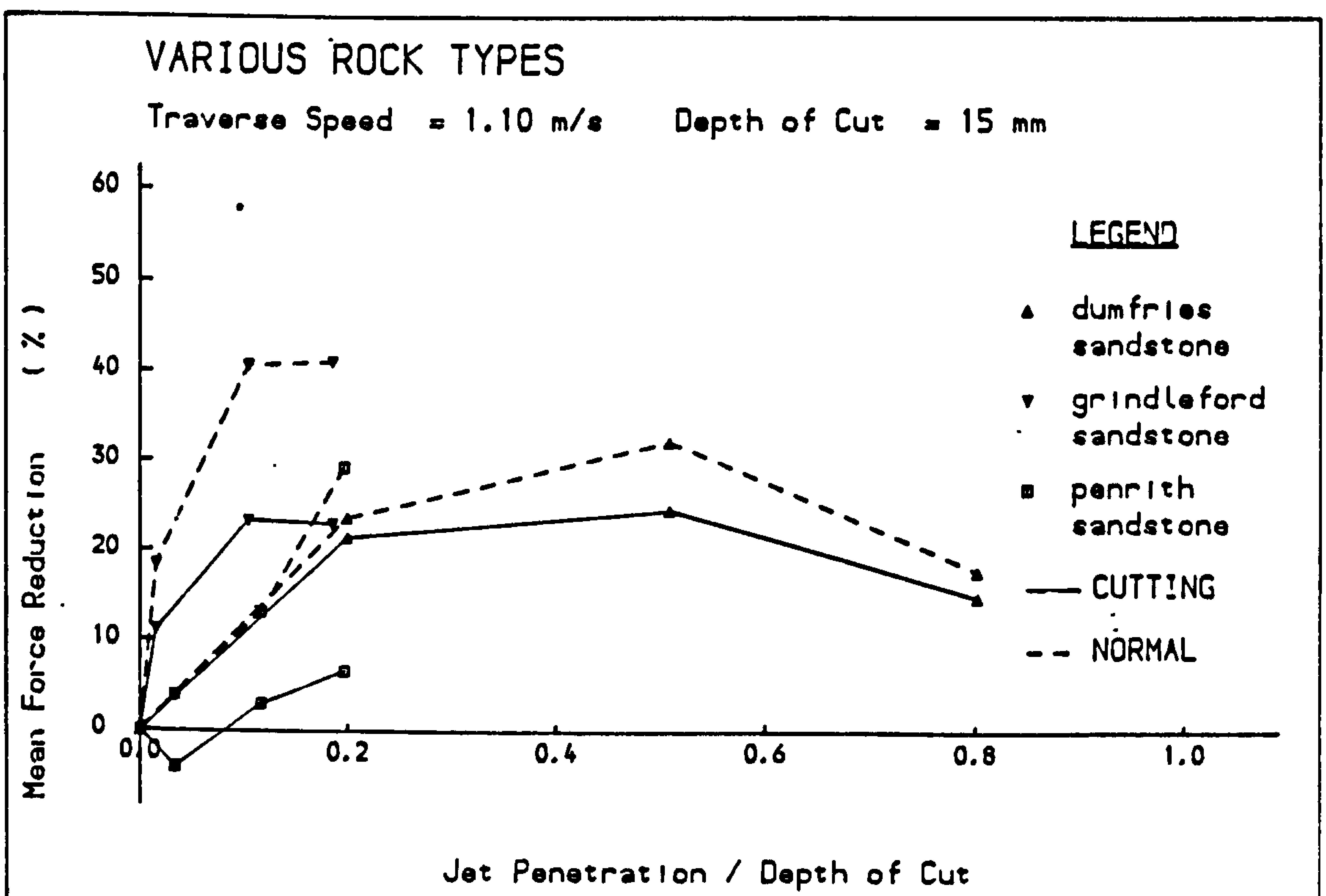

Figure 7.18 Mean Force Reduction versus Jet Penetration : Depth of Cut = 15mm ; Traverse Speed = 1.10 m/s.

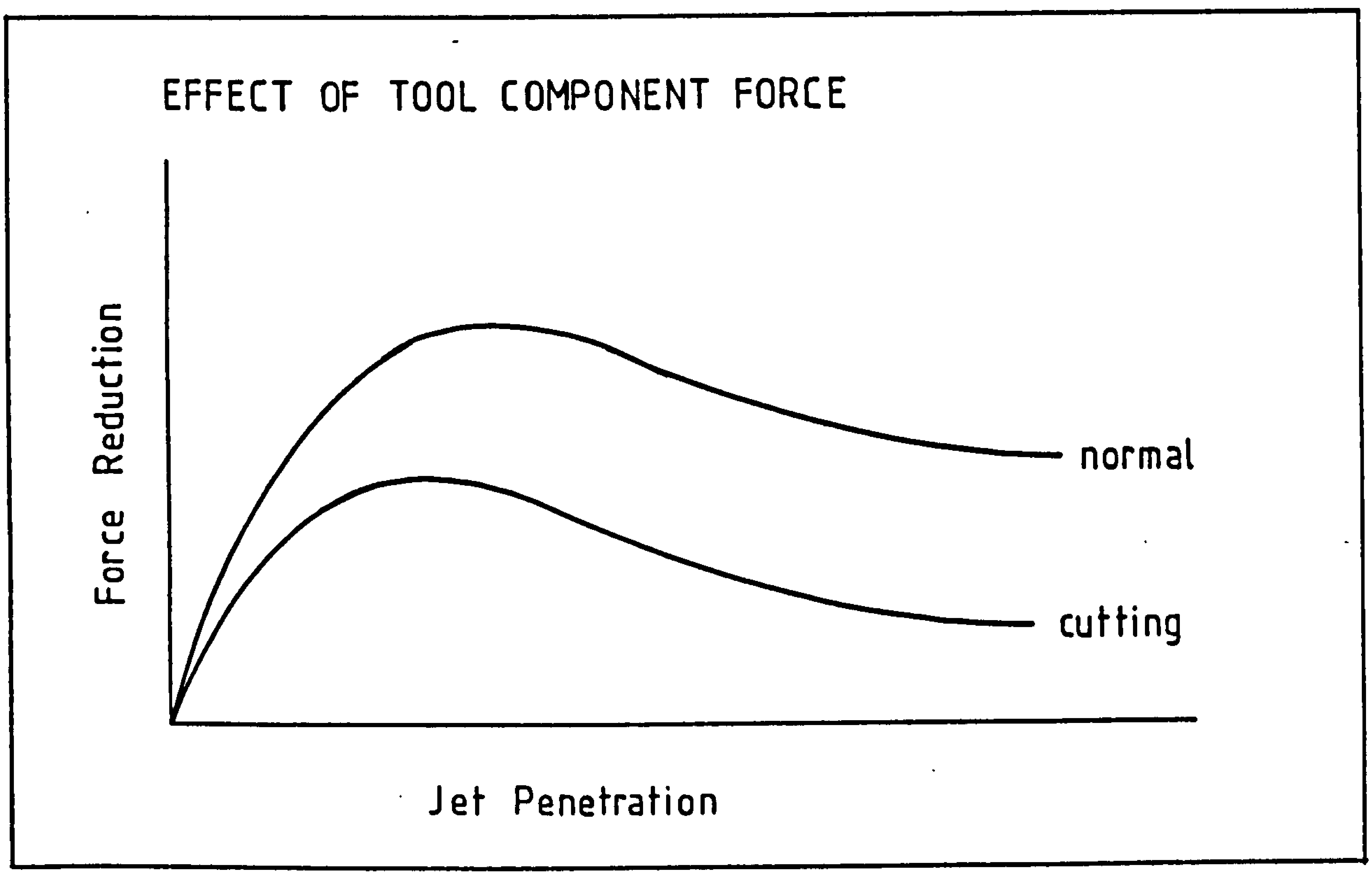

Figure 7.19 Generalised relationship between Cutting and Normal Force Reduction and Jet Penetration.

After the optimum jet penetration is exceeded, chipping events are suppressed and profiling activities dominate the cutting action of the tool. Hence the benefits of reduced amounts of crushed materials are offset by increased profiling. The net gain is reduced from the optimum condition. A good example can be seen in Figure 7.15 where the rocks were cut at slow speed with a depth of cut of 10mm. Since the cutting force is composed of more chipping force and less crushing force when compared with normal force, the force reductions decreased rapidly after optimum jet penetration was exceeded. Normal force reductions, however, were only slightly decreased after optimum jet penetration was exceeded.

The proposed hybrid cutting model has applied particularly well in the Grindleford Sandstone for both speeds and Penrith Sandstone for the slow speed. The lack of optimum jet penetration for Penrith Sandstone at fast speed was attributed to the high abrasivity of this rock (Newcastle abrasivity = 6.6). The tool was blunter for the Penrith Sandstone than for the Grindleford Sandstone. Blunt tools tend to have a higher optimum jet penetration and higher force reduction when compared with sharp tools (Section 8.3) and the optimum was not reached in these cutting tests for Penrith Sandstone at high speed.

7.4.2 Effect of Depth of Cut

While the optimum jet penetration was observed around 20% to 30% of the mechanical depth of cut for the 10mm and 15mm cuts, it was much higher for the 5mm depth of cut.

It has been shown that the tool performs four actions during the course of rock cutting (Section 6.2):

(1) Crushing;

(2) Profiling;

(3) Chipping (primary); and

(4) Chipping (secondary).

Although all four actions can be found in any practical range of depth of cut, the proportions contributed by each action are different. At 5mm depth of cut, the chips are very small and provide little assistance in the surface removal process. The principal actions of the tool are crushing and profiling. Hence force increase due to increase in profiling is negligible and the tool force reduction is essentially the force reduction due to reduced crushing events (Figure 6.6). Optimum jet penetration is estimated to be similar to the mechanical depth of cut.

The effect of depth of cut on the force reduction can be generalised in Figure 7.20.

7.4.3 Effect of Traverse Speed

Generally, for all depths of cut, force reductions were higher for the Grindleford and Penrith sandstones, and lower for the Dumfries Sandstone at 1.10 m/s than at 0.27 m/s traverse speed. Water jets are most effective in reducing tool forces by slotting and relieving the tool tip from crushing. Since more forces were required to cut the Grindleford Sandstone and Penrith Sandstone at fast speed in unassisted cutting mode (Section 7.2.2), higher force reductions were obtained at the same jet penetration.

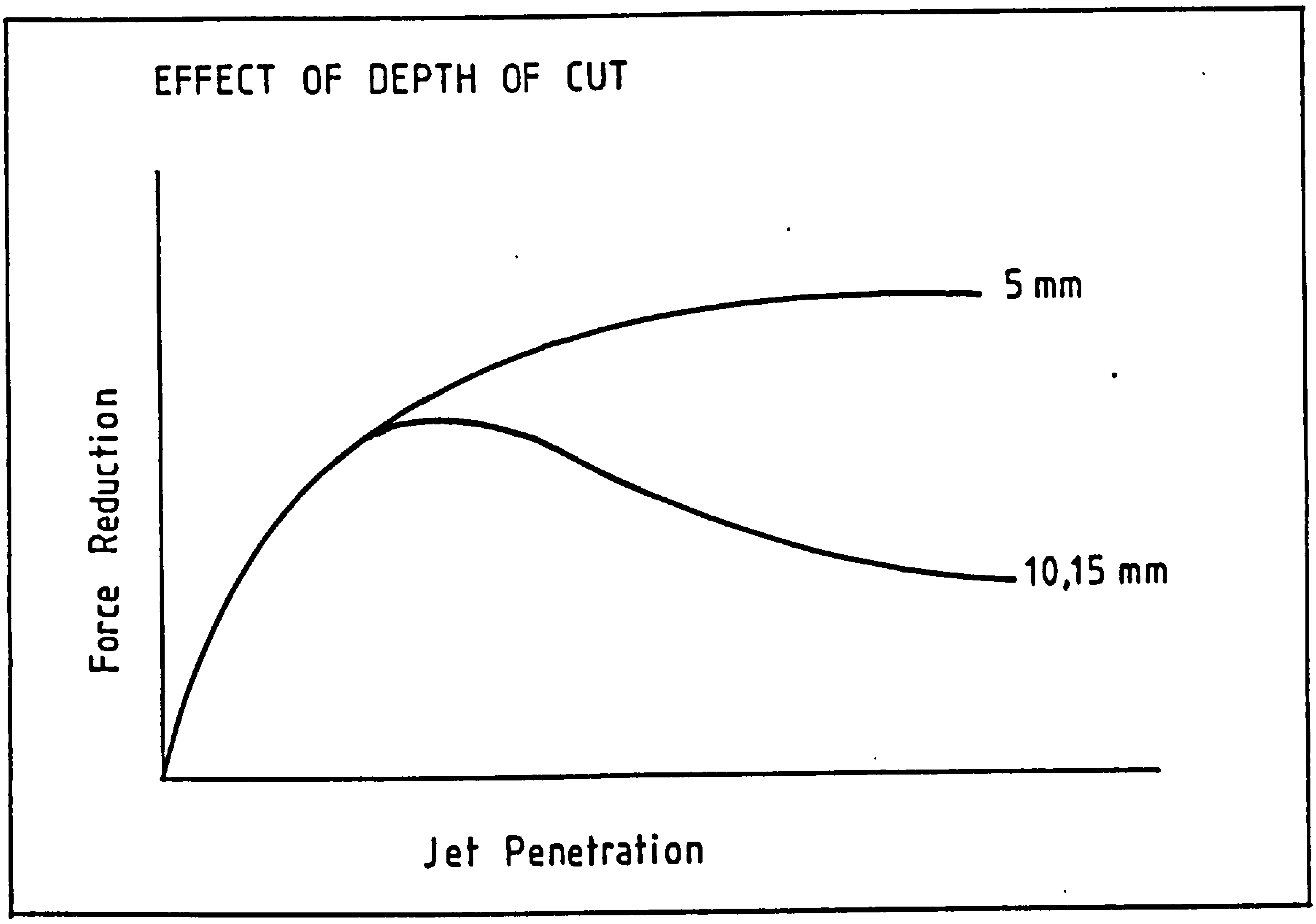

Figure 7.20 Generalised effect of Depth of Cut on Force Reduction.

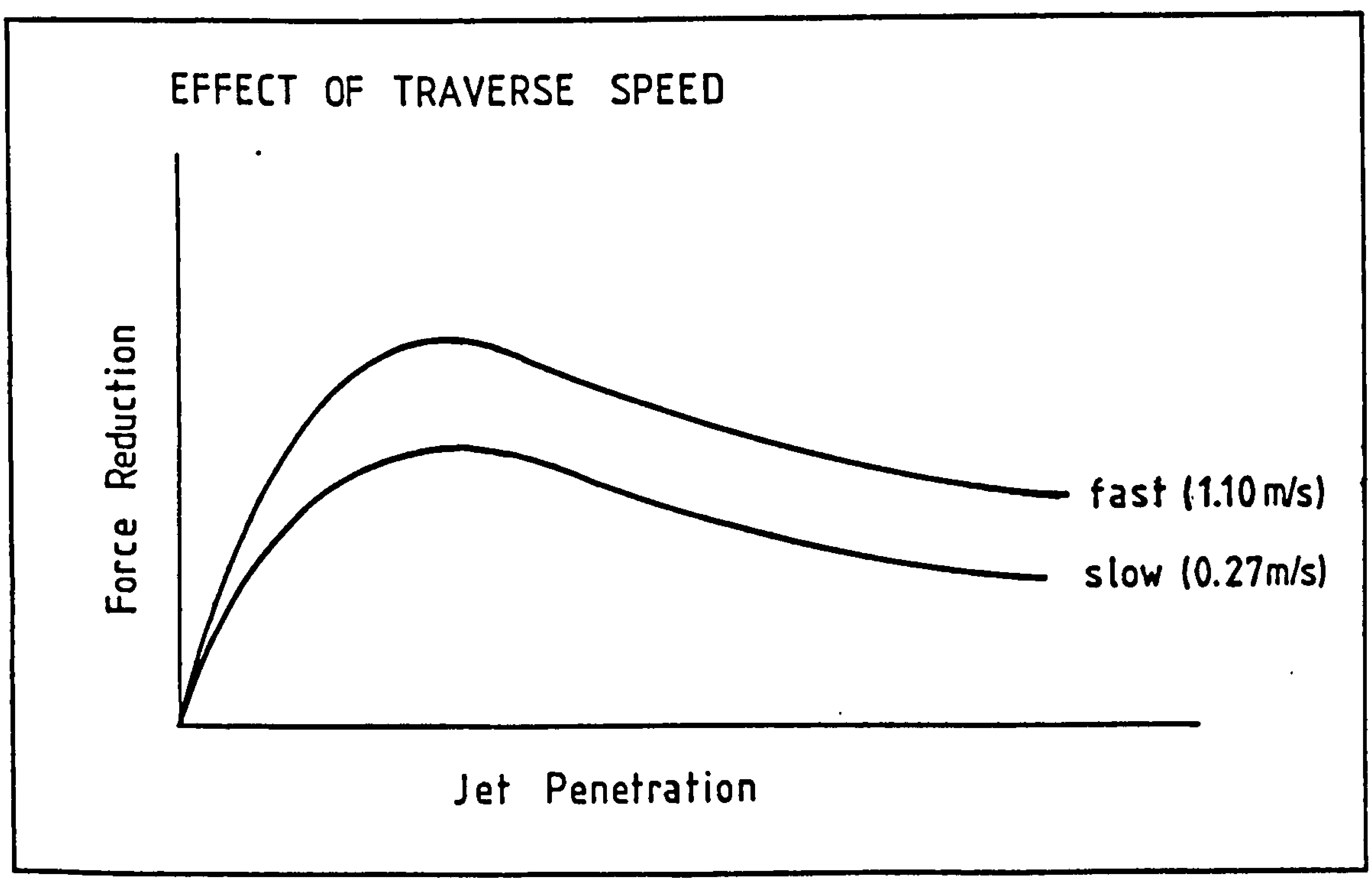

Figure 7.21 Generalised effect of Traverse Speed on Force Reduction for Grindleford and Penrith sandstones.

For these strong sandstones, the effect of traverse speed can be generalised in Figure 7.21.

For the Dumfries Sandstone, however, there was no increase in tool forces due to the speed effect. As more jet energy is available at slow traverse speed, higher force reductions were expected. The most impressive results are the comparable magnitude and similar trends of force reductions between cutting and normal forces. The significant force reduction in the cutting direction is attributed to the poor cementation of the rock. The binding mineral is so weak that grains can be rubbed out by hand. When jet impingement level is similar to the tool tip, the radial outward flow of the water can be highly erosive and remove rock ahead of the tool. Hence the tool tip is relieved by the water jet in both cutting and normal directions in a similar manner.

7.4.4 Hydraulic Fracturing

A number of alternative and additional cutting mechanisms to the proposed model have been attributed to high pressure water jets. Perhaps the most commonly quoted water jet assisted cutting mechanism involves the concept of hydrofracturing. The idea is that the jet is able to flow into the major crack system prior to unstable fracture propagation and pressurise the cracks. The water jet will then aid crack propagation and thus reduce the tool force. This mechanism, if operating, would significantly reduce mean peak cutting force.

For rocks with significant jet penetration, like Grindleford Sandstone and Penrith Sandstone, significant reduction in mean peak cutting force is not observed for jet pressures up to 70 MPa. The reduction is typically less than 14% (Figures 7.22 to 7.27). An examination of the analogue chart output confirmed the insensitivity of mean peak cutting force reduction to the water jet assistance. A significant reduction in mean peak cutting force does occur at 5mm depths of cut at 0.27 m/s cutting speed, which is attributed to the total suppression of chipping rather than hydraulic fracturing, as breakout is much reduced.

The mean peak normal force reductions generally follow the trends of mean normal force reductions, but with a smaller magnitude. This reiterates the major purpose of the water jet is to penetrate and relieve the tool tip from crushing events from which mean normal force reductions have most of the benefits.

7.5 Water Jet Assisted Drag Tool Rock Cutting : Rocks with Insignificant Jet Penetration

Both Middleton Limestone and Pennant Sandstone are classified within this category. No jet penetration was observed during slotting tests, even at the highest jet pressure (70 MPa) and slowest traverse speed (0.27 m/s).

A pristine tool was normally used to cut each rock during this primary experimental programme. The effect of wear rate was smooth out by means of replication and randomisation of tests. However, the high strength, together with the high abrasivity of

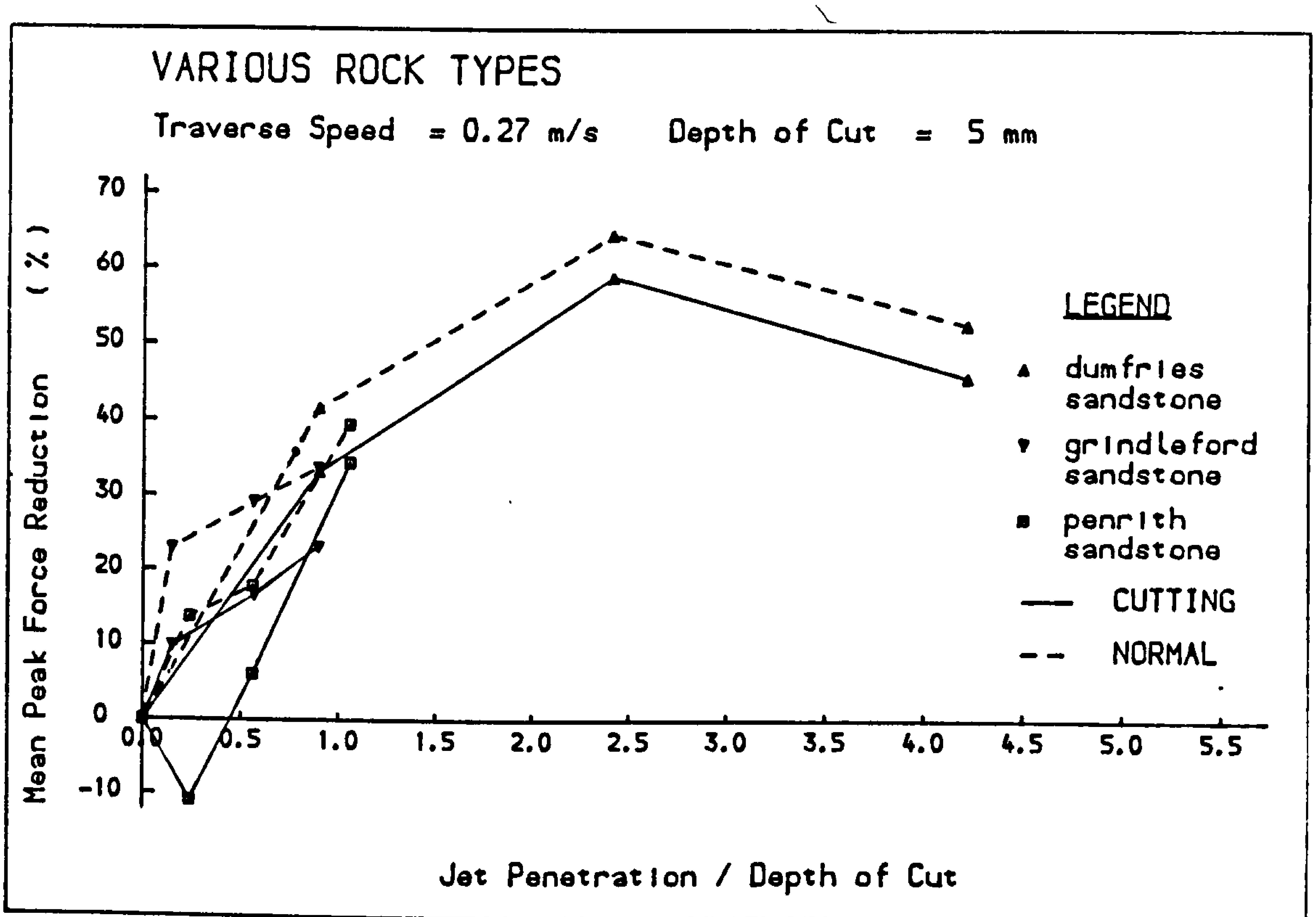

Figure 7.22 Mean Peak Force Reduction versus Jet Penetration: Depth of Cut = 5mm ; Traverse Speed = 0.27 m/s.

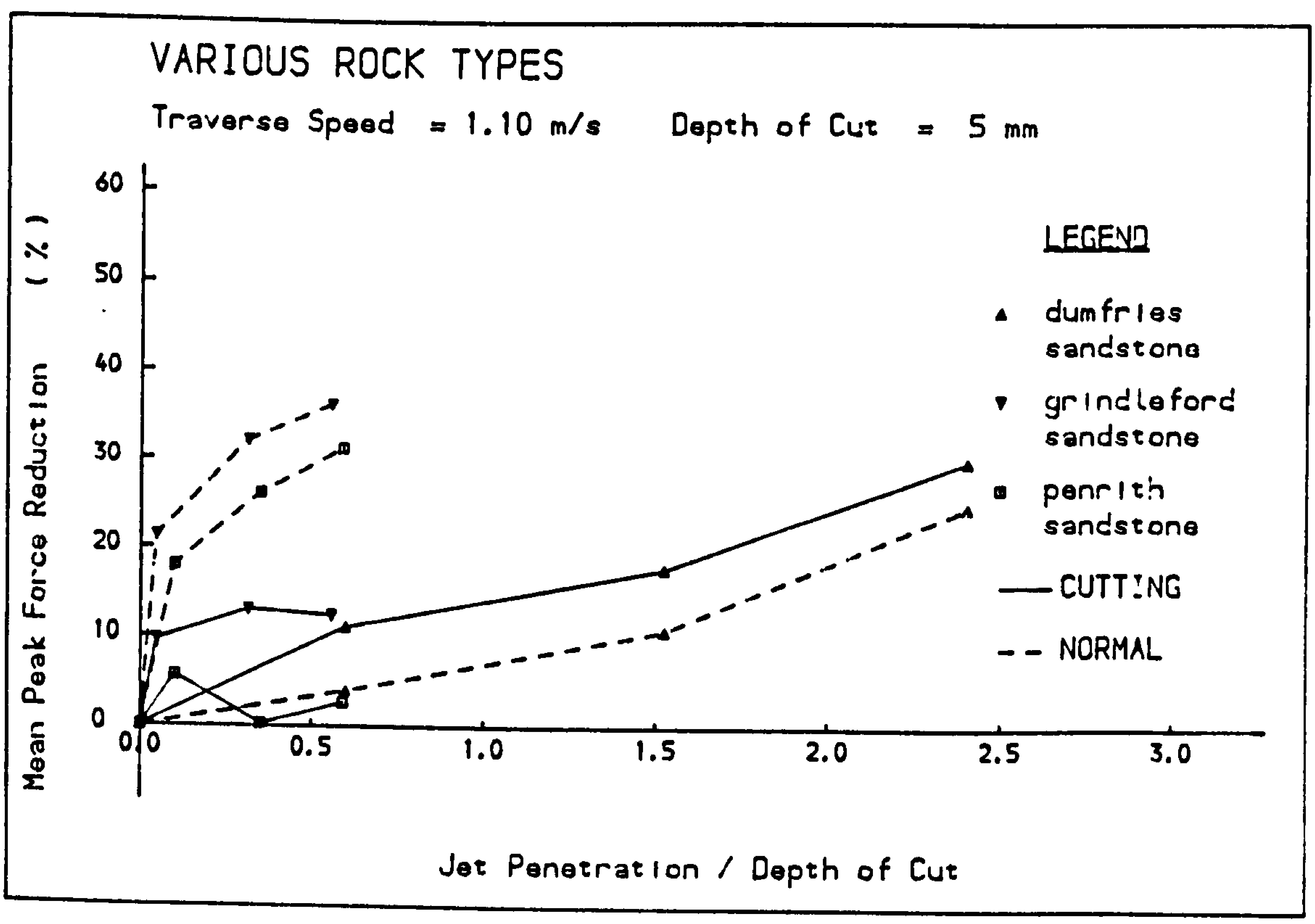

Figure 7.23 Mean Peak Force Reduction versus Jet Penetration : Depth of Cut = 5mm ; Traverse Speed = 1.10 m/s.

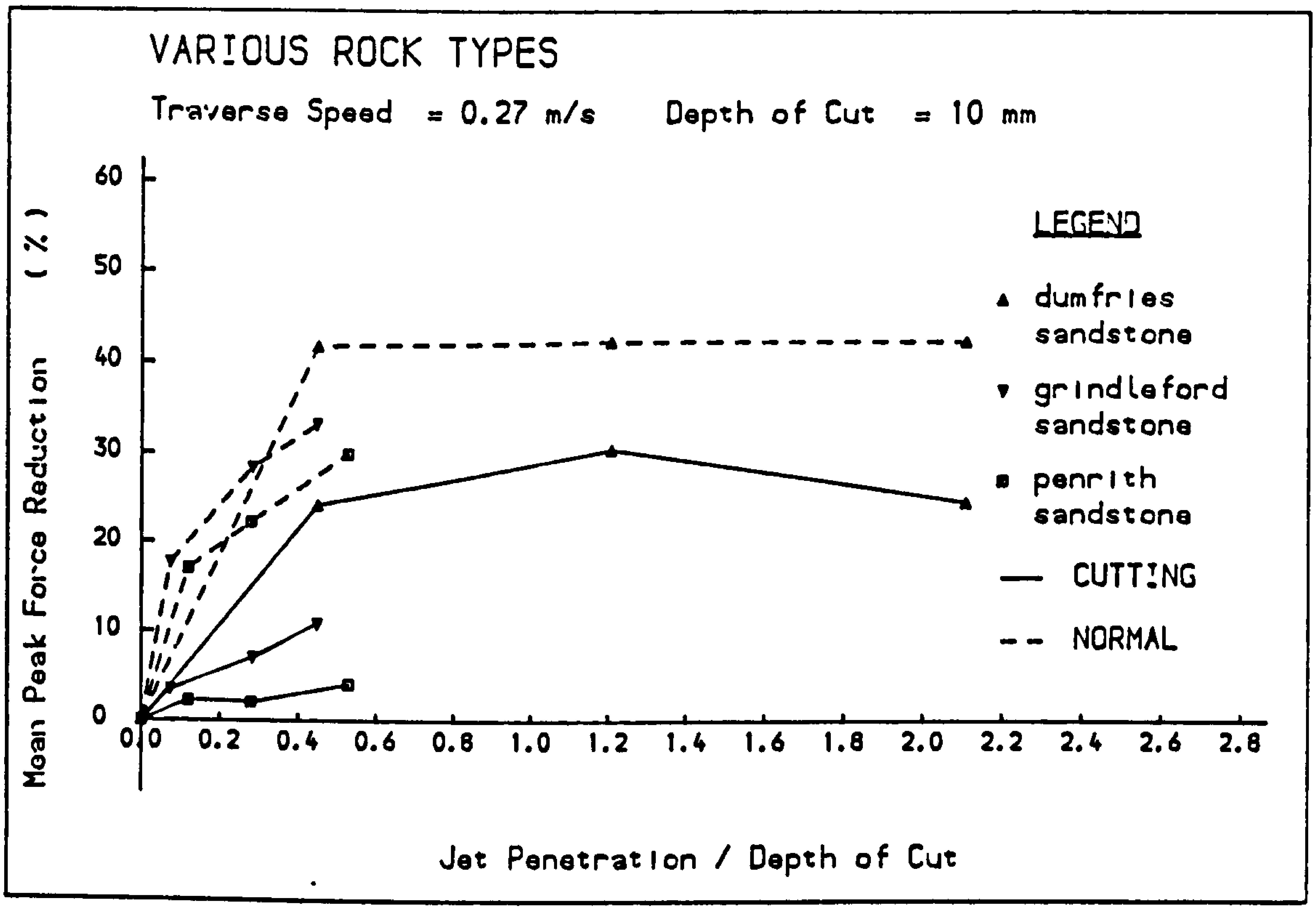

Figure 7.24 Mean Peak Force Reduction versus Jet Penetration : Depth of Cut = 10mm ; Traverse Speed = 0.27 m/s.

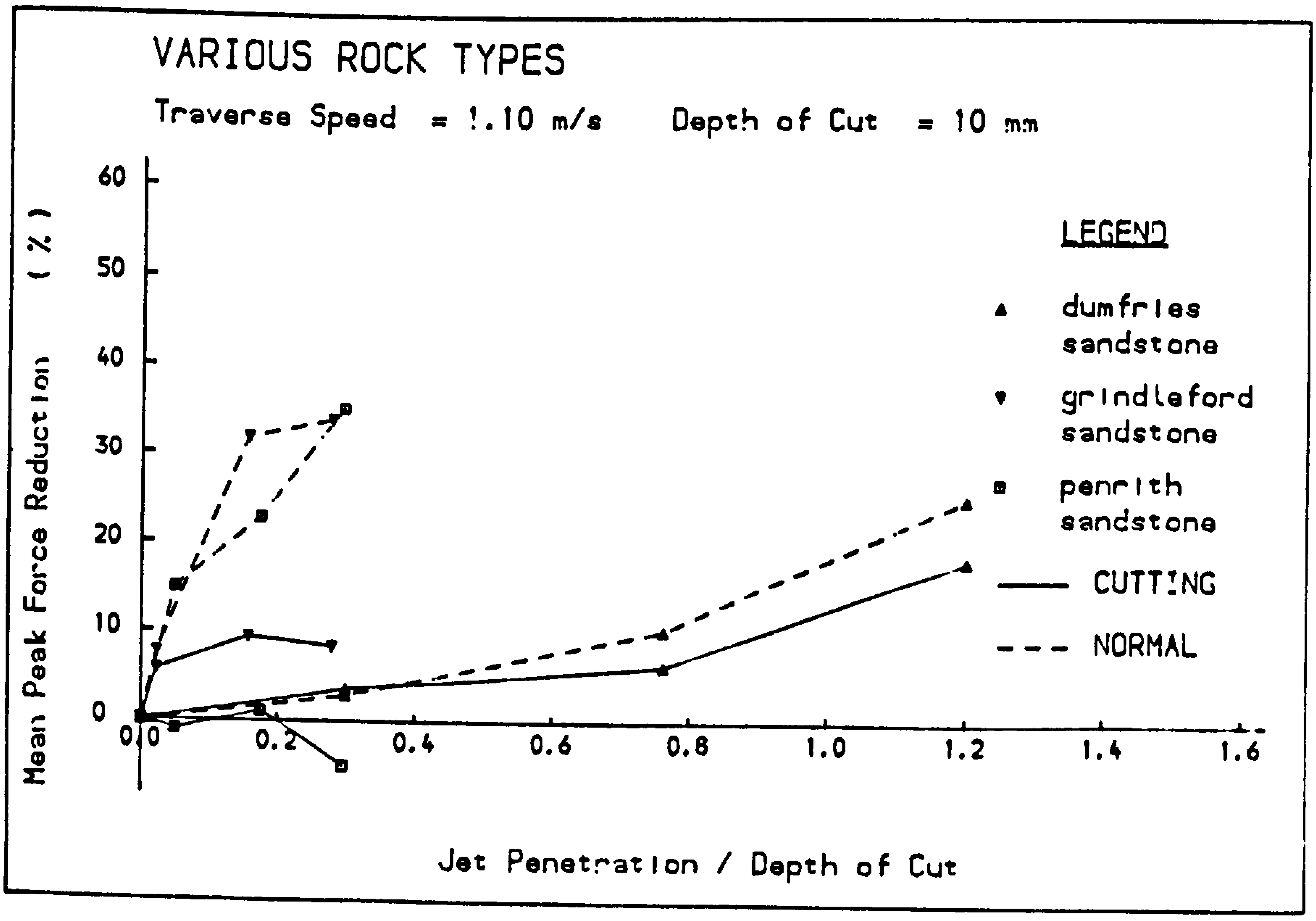

Figure 7.25 Mean Peak Force Reduction versus Jet Penetration : Depth of Cut = 10mm ; Traverse Speed = 1.10 m/s.

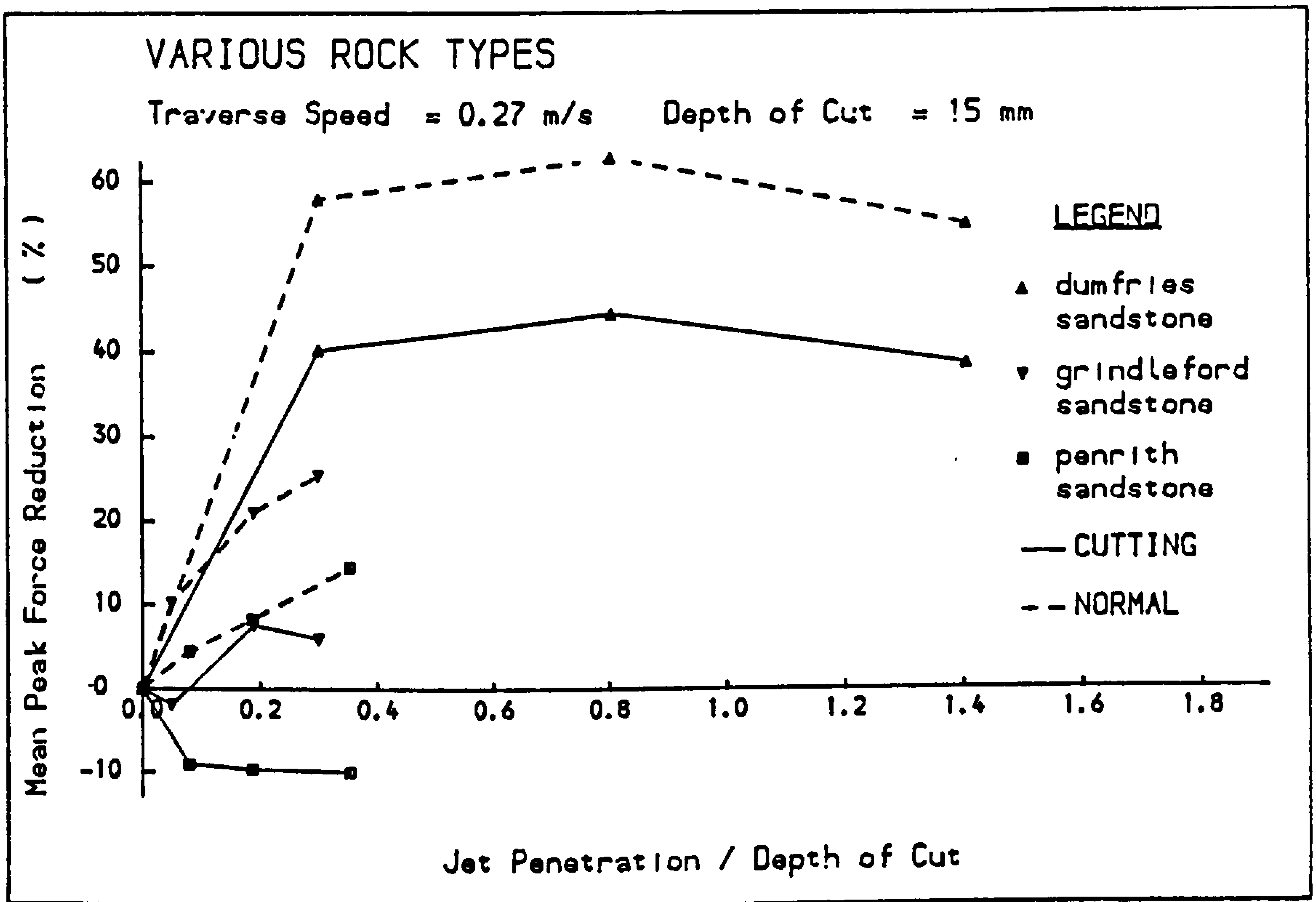

Figure 7.26 Mean Peak Force Reduction versus Jet Penetration : Depth of Cut = 15mm ; Traverse Speed 0.27 m/s.

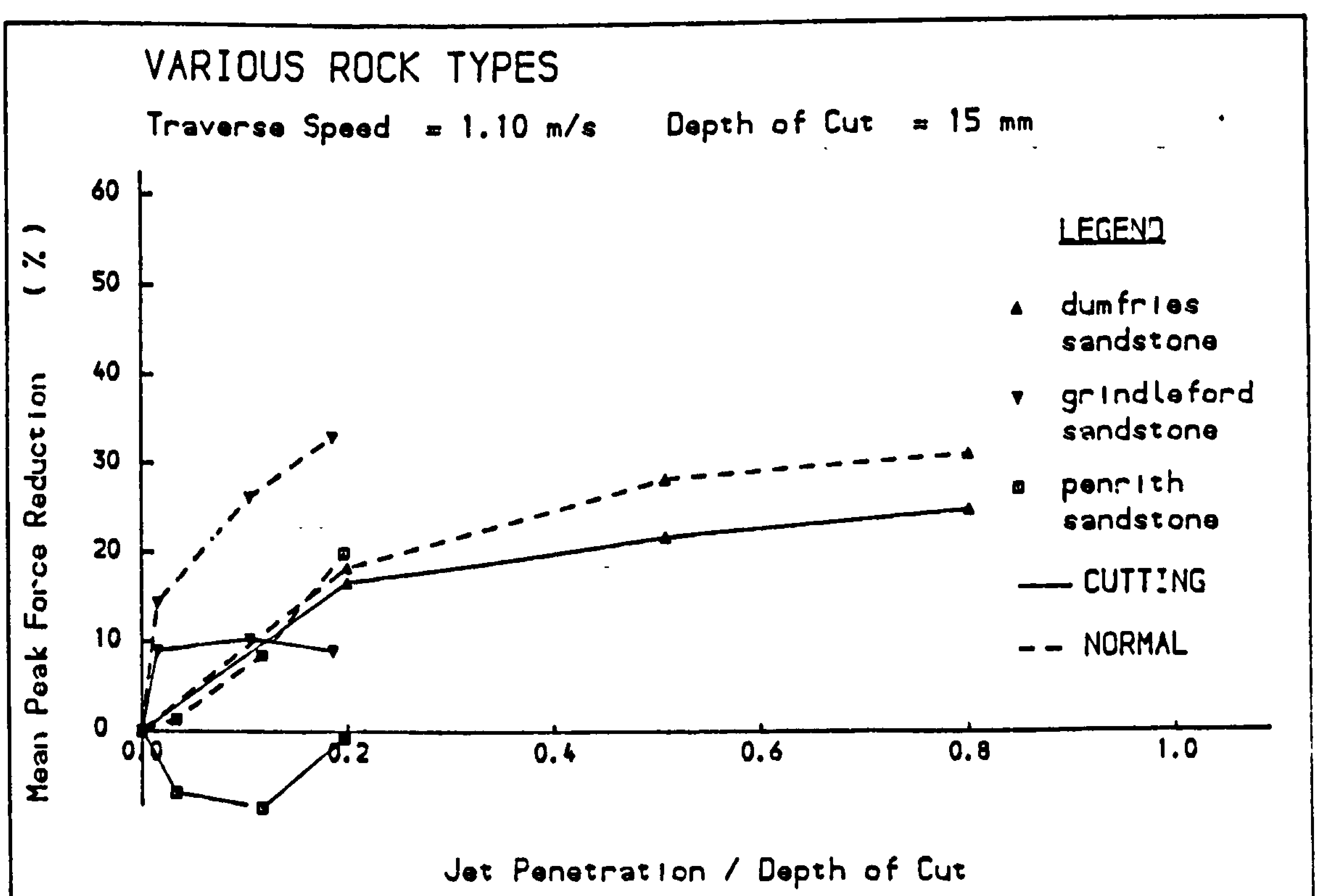

Figure 7.27 Mean Peak Force Reduction versus Jet Penetration : Depth of Cut = 15mm ; Traverse Speed 1.10 m/s.

the Pennant Sandstone, make the wear rate exceptionally high at fast speed and this cannot be rectified using the technique of repetition and randomisation. Therefore a new tool was used for 5mm and 10mm cutting at fast speed. Fast speed cutting at 15mm was omitted due to excessive tool force. When the wear rate was much reduced at slow speed a new tool was used for all depths of cut.

7.5.1 Pennant Sandstone

At high traverse speed, the rapid generation of wearflat dominates the tool forces measured. All the force reductions in both cutting and normal directions are less than 5% (Figures 7.28 and 7.29). The beneficial effects of the water jet, if any, are largely masked.

When the rock was cut at slow traverse speed, the most striking impressions were that cutting force increased with jet pressure at 10mm and 15mm depths of cut and the large force reduction observed during cutting at 5mm depth of cut. Before an explanation is attempted the basic cutting mechanisms of drag tool cutting will be reviewed.

After one chip, the tool is pushed into the post-chip curvilinear surface. Crushed material is accumulated before the tool and acts as a 'substitute' cutting edge of the tool. Eventually a large chip is formed when the stress within the crushed zone is sufficiently high to promote a tensile median crack. Before primary chipping, smaller secondary chipping is possible as a minor stress relief.

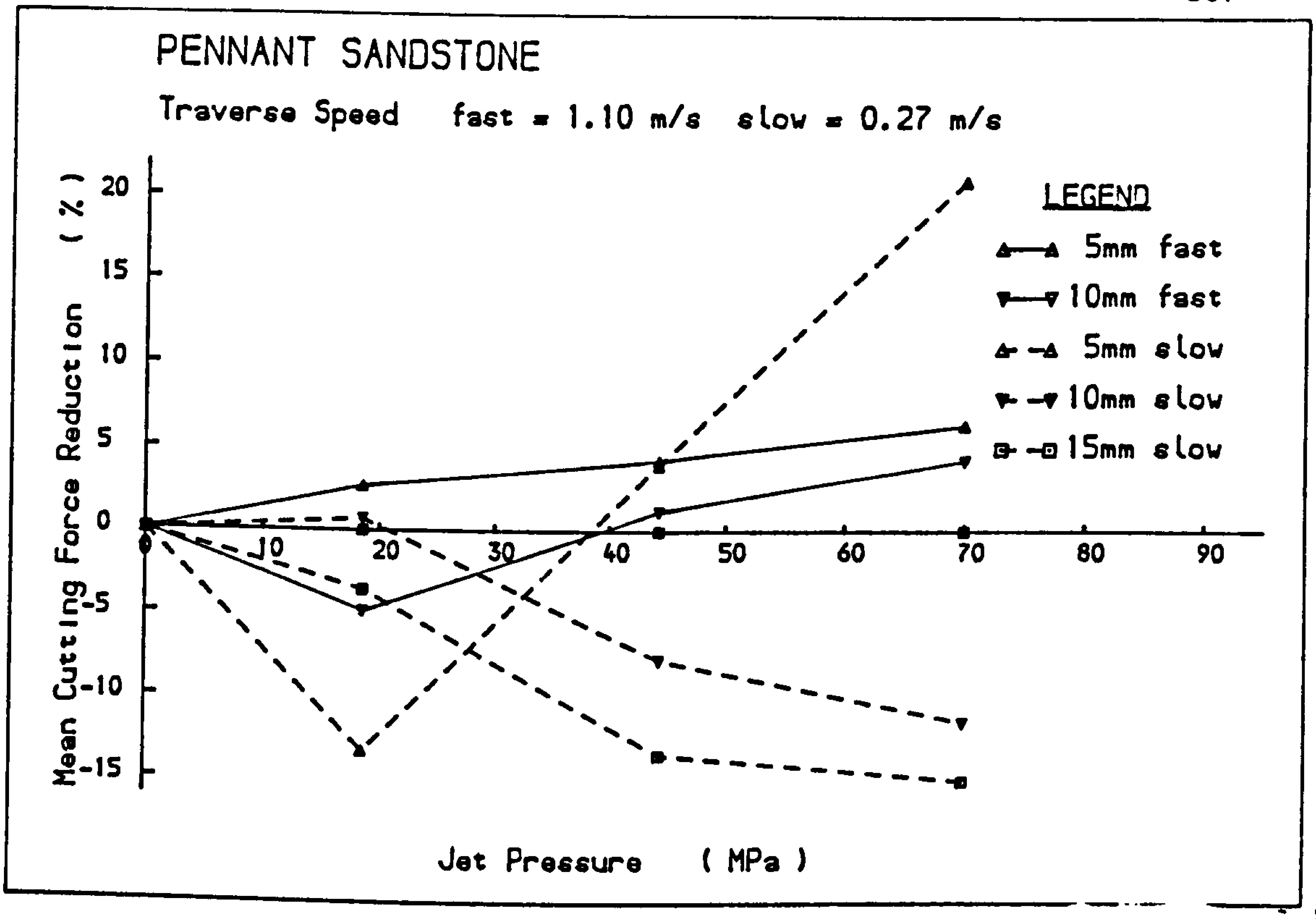

Figure 7.28 Mean Cutting Force Reduction versus Jet Pressure : Pennant Sandstone.

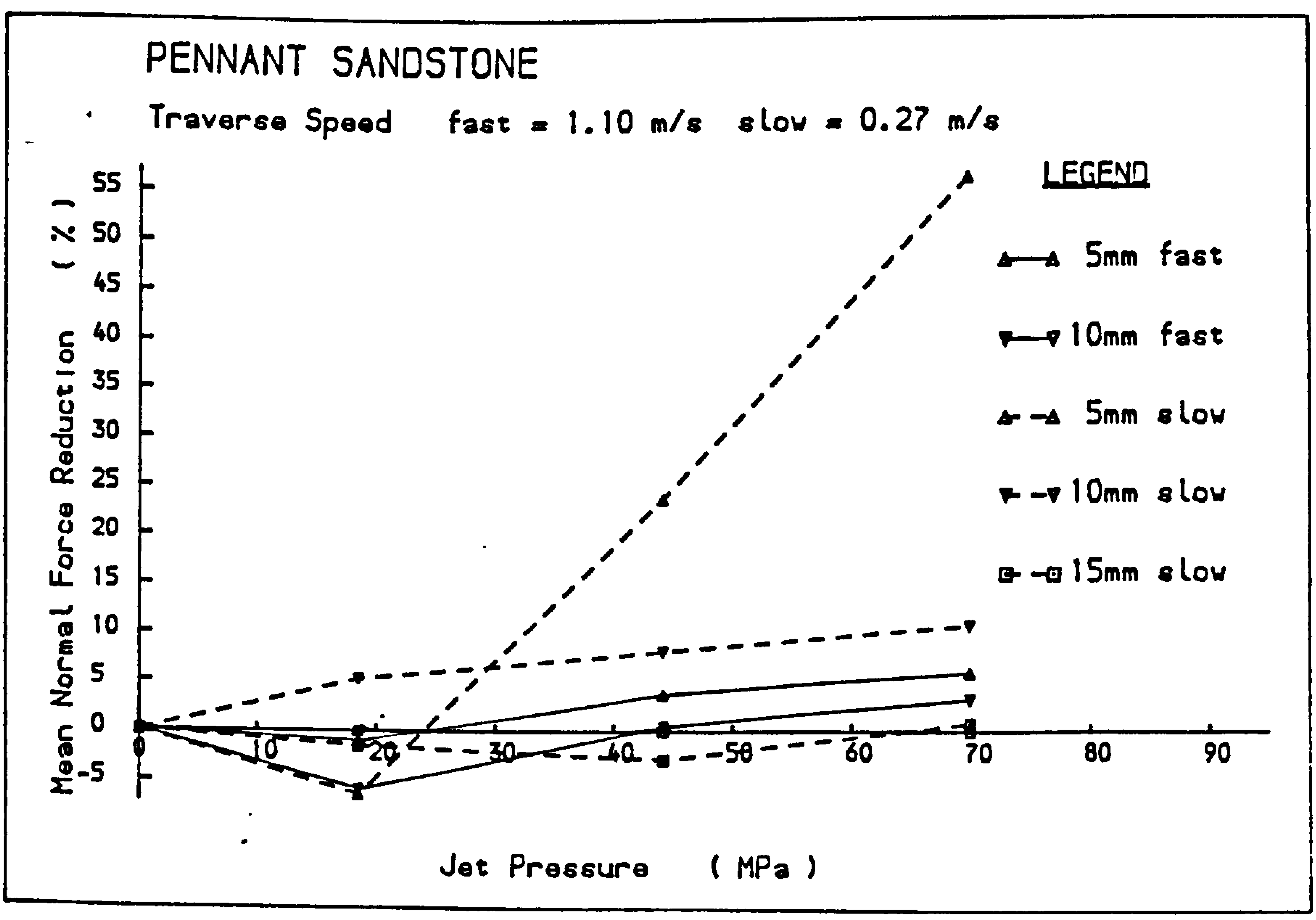

Figure 7.29 Mean Normal Force Reduction versus Jet Pressure : Pennant Sandstone.

When a water jet of 70 MPa was used to cut this strong Pennant Sandstone (173 MPa), the water jet could not penetrate the rock. Hence no erosion or rock removal was possible and the jet was merely transmitting jet pressure to the rock in a mechanical way. The consequence was that the jet held down the rock against the prizing effects of the crushed zone. Hence higher cutting force was required to initiate the crack. Figure 7.30 illustrates this.

However, when depth of cut is shallow, i.e. 5mm, the rock thickness between the crushed zone and the rock surface is finite. In this case, if the jet power is sufficiently high, the jet may be capable of breaking this thin rock layer and promoting chipping events. If this is possible the result would be significant force reductions. This kind of hydraulic fracturing was observed during the 5mm slow cutting of this rock. Figure 7.31 shows the force trace for a 5mm cut at slow speed, with a 70 MPa jet and without water jet asistance. The pulsing effect of the jet pressure is clearly shown, and the hydraulic fracturing is possible only at the high pressure part of the pressure pulse. When the jet pressure is at the lower end of the pulse, which is about 63% of the mean pressure, tool forces are as high as in the unassisted cutting mode.

Although the pulsating jet pressure output of the pump has been criticised during the project, on this occasion it provides excellent proof of the existence of a critical jet power. If the jet power is higher than critical jet power, the water jet can

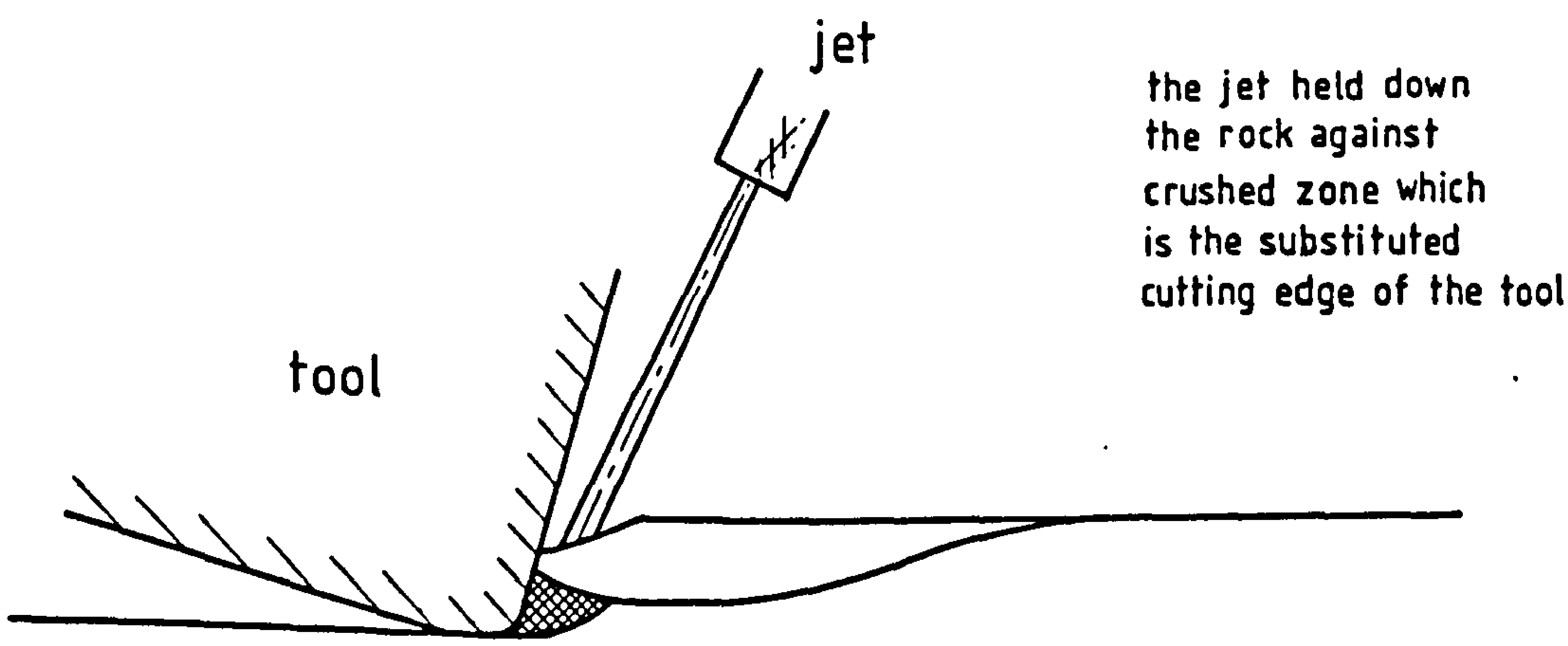

Figure 7.30 The Schematic Illustration of the Jet Action on Rocks without Jet Penetration.

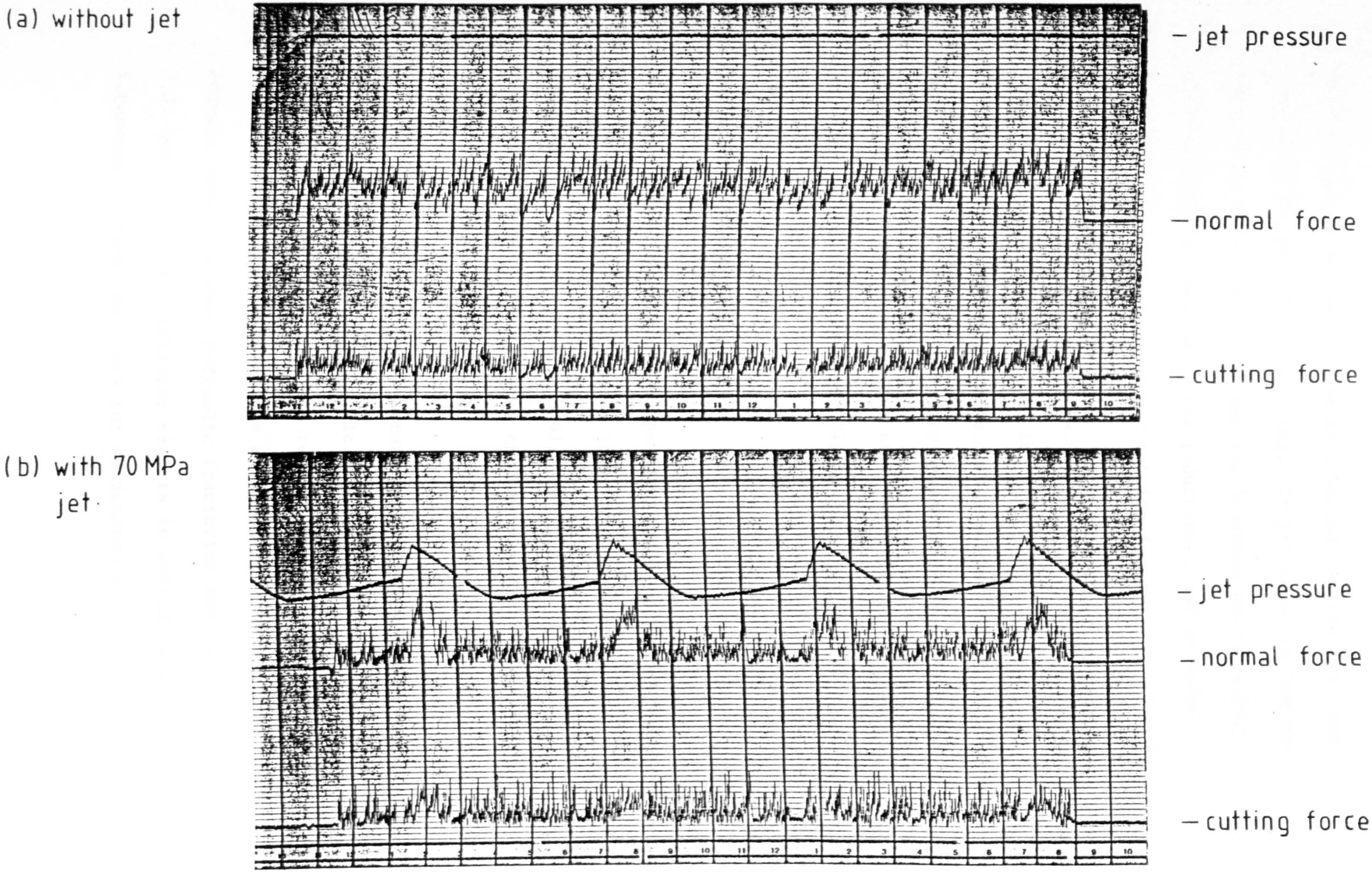

Figure 7.31 Analogue Tool Force Trace for 5mm Cutting at o.27 m/s, with and without 70 MPa Jet Assistance; Pennant Sandstone.

gain access to subsurface cracks produced by the tool and thus promote hydraulic fracturing. If jet power is low the water jet can at best flush out the loosened debris which contributes only marginal force reductions, and at worst hold the chips and cause higher cutting forces.

It was noted that encouraging results were obtainable only at 5mm hybrid cutting at the slow speed (0.27 m/s). Disappointing results were obtained when fast cutting (1.10 m/s) and/or higher depths of cut were attempted. The critical jet power is thus dependent on traverse speed as well as depth of cut, and is expected to be higher for higher traverse speed and/or depth of cut.

7.5.2 Middleton Limestone

Equally impossible to penetrate with a 70 MPa water jet was the Middleton Limestone of lower strength (UCS = 113 MPa) than Pennant Sandstone (173 MPa). The ability to resist jet penetration is due possibly to the grainless microcrystalline calcite structure of the rock.

As the Middleton Limestone was of lower strength it was more vulnerable to hydraulic fracturing than Pennant Sandstone. However, the force reductions obtained were small. Maximum normal force reductions were only 30% compared with 56% in Pennant Sandstone when hydraulic fracturing was possible (Figures 7.32 and 7.33). The inferior results in hybrid cutting of limestone compared to those for sandstones are reported elsewhere

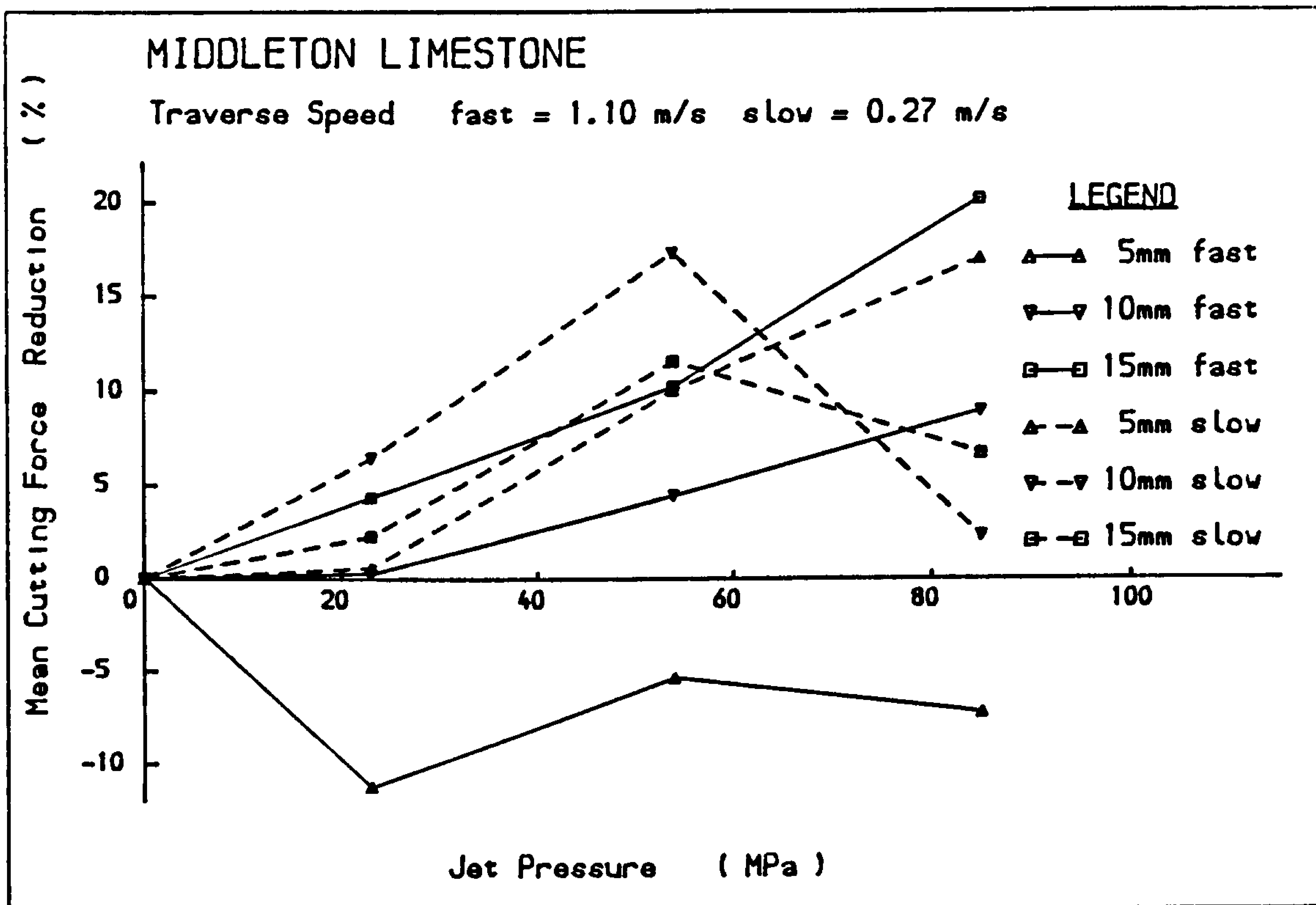

Figure 7.32 Mean Cutting Force Reduction versus Jet Pressure : Middleton Limestone.

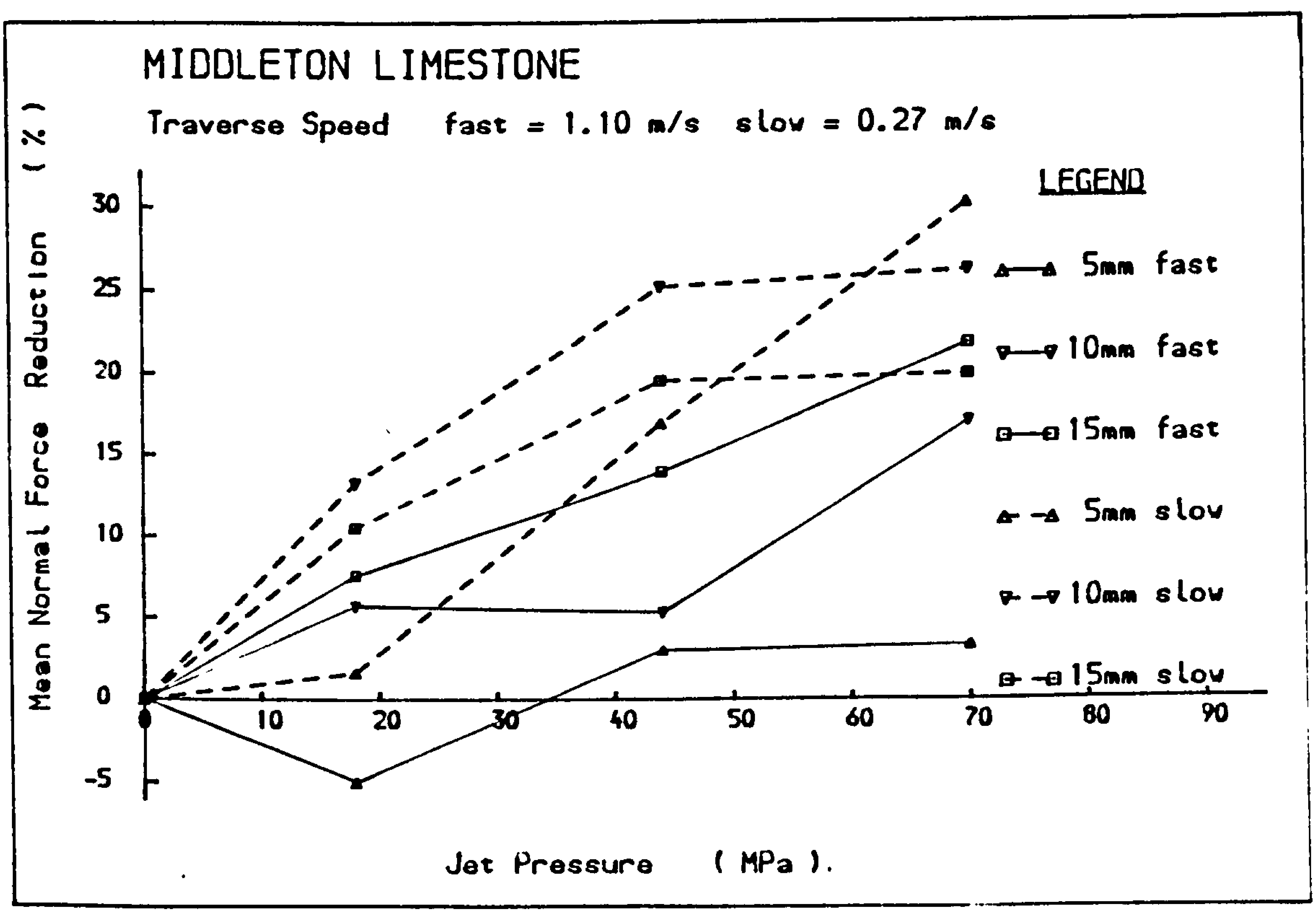

Figure 7.33 Mean Normal Force Reduction versus Jet Pressure : Middleton Limestone.

(Ropchan et al. 1980; Dubugnon 1981; Ozdemir and Evans 1983). The absence of dilatency under high confining pressure at the vicinity of the tool tip, as proposed by Dubugnon (1981) could be an explanation for the lower force reductions. When the dilatency disappears, the rock fails in a purely ductile fashion, implying that the crushed zone is plastic and free from pores and microcracks. This results in the disappearance of a boundary which is supposed to exist between the thin intact rock surface layer and the crushed zone just before the tool tip (Figure 7.30). The crushed zone and the thin layer of intact rock material are then of similar strength mechanically and the water jet cannot make use of the boundary to fracture this thin layer and gain access to the crack system to promote hydraulic fracturing. The tool force reduction is attributed mainly to debris removal rather than the much needed hydraulic fracturing.

Although rock chip formation is primarily a result of the growth of median cracks other cracking systems also operate concurrently. Lawn et al. (1975) investigated the mechanics of indentation fracture by sharp and blunt indenters. Depending on tool bluntness, cone cracks and lateral cracks are also generated. The cracks may not fully grow to intersect the surface and form chips, but the rock surrounding the indenter is weakened. Immediately following chipping, the weakened rock is exposed to the water jet. If the water jet is powerful enough to take advantage of the cracks and blast out the rock ahead of the tool, the tool force will be reduced due to the reduction of profiling events. Friedman and Ford (1983) described rock deformation and fractures induced by rock cutting tools.

In this case, how well a water jet performs depends on jet energy and rock strength. The slower the traverse speed, the higher the jet energy/unit length and the better the water jet performs. Running the water jet after the mechanical cutting illustrated this beneficial role of the water jet (Ozdemir and Evans 1983). Since the fractures produced by the tool within the rock mass are not fully developed, jet power must be high enough to overcome the residual rock strength before the fractured rocks can be removed. As Middleton Limestone is of a lower strength, it is more vulnerable to this type of chip removal than Pennant Sandstone, and higher force reductions are obtained, when hydraulic fracturing is impossible.

7.5.3 Discussion : Rock Dilatency

Many rocks exhibit brittle failure in compression and the rock breaks into subregions of intact material. These subregions must separate before complete unloading (failure) can take place. Under dynamic loading, rocks can increase their load-carrying ability in the short term as the unloading operation has a finite and limited velocity (Janach 1976). The unloading process involves frictional sliding and the formation of internal voids between these subregions, resulting in a non-elastic bulking of the failing material.

Generally crack initiation and hence dilatency or bulking can begin to occur at loads of about half the ultimate failure load (Cook et al.1984). If the water jet can penetrate the microcracks which define the intact subregions and aid the unloading process, the resistance of the rock to failure will tend towards a static value rather than a higher dynamic value.

However, small tool force reductions obtained in Pennant Sandstone suggested that this kind of water jet assistance is insignificant. The microcracks may be too small to be pressurised by the water jet. Furthermore, some microcracks may initiate in the interior of the rock (Linqvist et al. 1984) where the water jet can find no access. Unless the jet power is greater than the critical jet power for hydraulic fracturing, the water jet can take advantage of the rock dilatency only at the later stage of crack propagation, i.e. chipping. In this case, the jet assists in chip removal once formed and improves tool/rock force transmission. Force reduction is usually marginal. However, if debris clearance is a problem, then this force reduction could be substantial as demonstrated by experiments where the effects of chip confinement were exaggerated (Hood 1985).

7.5.4 Summary

For rocks that are strong, jet penetration may be insignificant. In this case the water can help to flush off the loosened debris, resulting in marginal force reduction. The force reduction is small because the jet cannot penetrate and reach the tool tip where most of the tool action takes place.

However, before jet power is high enough to slot the rock there exists a critical jet power at which hydraulic fracturing can significantly reduce the tool force. The normal force reduction in 5mm hybrid cutting of Pennent Sandstone at 0.27 m/s cutting speed is as high as 56%, while it is generally less than 10% in cases of higher depth of cut and/or faster traverse speeds (Figure 7.29). The mechanical loading of the jet to the rock surface is responsible for the onset of hydraulic fracturing as well as the cutting force increase before critical jet power is reached. This critical jet power is expected to depend on traverse speed, depth of cut and rock strength.

Although Middleton Limestone has a lower strength than that of Pennant Sandstone, hydraulic fracturing was not observed. The inferior force reductions in hybrid cutting of limestones are reported elsewhere and the lack of dilatency under high confining pressure is proposed as the reason for this reduced performance.

7.6 The effect of Moisture Content on the Cuttability of Rocks

7.6.1 Introduction

The influence of moisture content on rock strength is well known. Mann and Fatt (1960) studied the effect of pore fluids on the elastic properties of sandstone. Bulk compressibility and Young' modulus of the wet sandstone were found to be 10-30% greater and 8-20% less than for dry respectively. The influence of moisture content on the compressive strength of rocks was investigated by Colback and Wiid (1965). In general the compressive strength decreases with increase in moisture content. Compressive strength can be reduced up to 50% from that of the oven-dried samples to saturated samples. Other research studies also support the findings that rock is weaker if tested 'wet' ratehr than 'dry' (Obert et al. 1946; Price 1960; Parate 1973). There is no generally accepted explanation for the influence of moisture on rock strength, although several mechanisms have been proposed:

(1) fracture energy reduction;
(2) capillary tension decrease;
(3) pore pressure increase;
(4) frictional reduction; and
(5) chemical and corrosive deterioration.

In order to examine the possibility of using the moisture content effect as an explanation of tool force reduction in water jet assisted rock cutting, the moisture content effect on the cuttability of rocks was first tested.

7.6.2 Mechanical Effect

Very often the addition of water between the surfaces acts as a lubricant and reduces the effective friction coefficient. Evans and Pomeroy (1966) noted that the coefficient of friction between coal and steel in wet conditions is approximately 30% less than in dry conditions.

However, the drag tool during rock cutting is not sliding on the rock surface but grinding and crushing the rock grains trapped underneath the wearflat. Because of the small negative angle of the wearflat, most of the crushing force is provided by normal force components. If the water jet can penetrate the rock or flush out the debris, hence reducing crushing events under the wearflat, a higher reduction is obtained in the normal force component than cutting force component. This was observed in the present work for all five rock types. The reduced friction in the presence of water during rock cutting, if any, is of only secondary importance when compared with relief of the tool wearflat from crushing activities.

7.6.3 Chemical Effect

Water can affect crack propagation in rocks chemically by reacting with material at the crack tip (stress corrosion cracking). Fracture toughness in the presence of water has been reported lower than that measured in air and Barton (1982) provided a summary of the reductions in different rock materials.

According to Barton (1982), there exists a limiting crack velocity beyond which stress corrosion plays no part in the fracture process. This limiting velocity is of the order of 10^{-4} m/s to 10^{-1} m/s for most brittle materials. However, crack propagation speed during the rock cutting is measured as about 80 m/s (Tutluoglu *et al*. 1983). Hence the hypothesis attributing tool force reduction to stress corrosion cracking is rejected on the basis of a much faster crack propagation speed.

7.6.4 Laboratory Investigation

As a collaborative research, Rambanda (1984) carried out cutting tests in both the 'dry' and 'wet' states using nine rocks, including four sandstones, gypsum, marble, concrete, chalk and anhydrite. The 'dry' and 'wet' conditions are defined as:

Dry Condition : the specimens are air-dried for over two months before cutting; and

Wet Condition : the specimens are immersed in water for two weeks immediately before cutting.

The cutting results are summarised in Appendix G. Basically, the rocks can be separated into two groups, with the gypsum, grey sandstone and anhydrite in one group and the other rocks in another group. In the first group, both tool forces and specific energy decrease on wetting. In the second group, moisture tends to increase the mean cutting force, mean normal force and specific energy and to reduce mean peak forces and the yield. The improved cuttability in the first group, especially gypsum and anhydrite, is attributed to their vulnerability to structural changes under the effects of moisture. In group two, the moisture effect is regarded as mechanical rather than structural change.

The possible effect of moisture content on the cuttability of rock is also addressed by Roxborough and Phillips (1975) in the cutting of Bunter Sandstone. On average, all forces are about 20% higher when cutting in the wet condition, although the yield is relatively unaffected. Hence there seems a genuine force increase due to increase in moisture content, which is contrary to the results expected from the rock strength test results, as tabulated in Appendix G.

One possible explanation for this phenomenon is pore pressurisation. Before chipping is possible, the rock is subjected to compression by the tool. The pore water is pressurised, if all the pores are saturated, as water is relatively incompressible. If the strain rate is sufficiently high, which is usually the case in rock cutting, dissipation of pore pressure is negligible. Hence pore pressure tends to resist the travelling tool, and higher tool force is required if the effective stress concept is valid.

Rambanda's results tend to support the above explanation. Critical traverse speed (strain rate) is clearly dependent on the permeability and porosity of the rock, as well as the viscosity of the fluid and the distance between the point of stress from the rock surface. Obviously the deeper the depth of cut, the more difficult will be pore pressure dissipation to the surface and hence the greater the pore pressurisation effect. Further experiment may provide supporting evidence to this conceptual model.

7.6.5 Discussion

The effect of moisture content is regarded as being of secondary importance in water jet assisted cutting. The permeability of rocks is so low that the rate of water saturation by a water jet is never comparable to the tool speed in a practical tunnelling machine, which is usually over 1 m/s. Tool force increase in wet rock samples, however, rejects the hypothesis which attributes tool force reduction in water jet assisted cutting to the reduced rock strength due to higher moisture content.

7.7 Summary

Depending on jet slotting resistance, the rocks tested can be separated into two groups. One group are those with significant jet penetration and the other those with insignificant jet penetration.

For the rocks with significant jet penetration, the proposed model on water jet assisted drag tool rock cutting is generally applied. The optimum jet penetration with which force reduction is maximised, is found to exist. Optimum jet penetration is generally within the range 20-35% mechanical depth of cut, with the lower end for cutting force component and the upper end for normal force component.

An effect of traverse speed was found in Grindleford and Penrith Sandstone which tended to increase tool forces at higher speeds, especially normal force, even when tool bluntness was the same. The reason for this is not yet clear but this phenomenon accounted for the higher force reductions when cutting at high speeds with water jet assistance.

For the rocks without significant jet penetration, force reductions were generally small. However, the hydraulic fracturing mechanism was observed to operate and force reductions were substantial when the Pennant Sandstone was cut at 5mm depth of cut and 70 MPa jet pressure. In this case, the critical jet power to allow hydraulic fracturing to occur was lower than the threshold power to slot the rock. This critical jet power is dependent on traverse speed as well as mechanical depth of cut, and is beyond the capacity of the present 70 MPa jet system when higher depth of cut and/or faster traverse speed are attempted. Hydraulic fracturing was not observed to operate in the Middleton Limestone and the plasticity and lack of dilatency of the rock under high confining pressure around the tool tip are thought to be the explanation.

Traverse speed is clearly a dominant factor in the application of drag tools to strong and abrasive rocks such as Pennant Sandstone, as reflected by the rapid wear rate at a cutting speed of 1.10 m/s.

When water jet rock cutting is considered, a threshold jet pressure is found to exist, but is poorly predicted by published equations. The hydraulic specific energy,which measures the efficiency of the jet to penetrate the rock, is low at high traverse speeds.

* * *

CHAPTER EIGHT

CHAPTER EIGHT

SECONDARY EXPERIMENTAL RESULTS

8.1 Introduction

Though the major parameters of interest were reported in the previous chapter, there are many other parameters that influence hybrid cutting. These parameters are very important in their practical implications, as well as for the understanding of water jet assistance. The soundness of the proposed model can also be assessed by examining its applicability to other parameters.

As there were a lot of parameters to be investigated and the time available was limited, the scale of the research was reduced. Typically a depth of cut of 10mm and a traverse speed of 1.10 m/s were adopted, although occasionally the slower speed was also included. For the rock group with significant jet penetration, Grindleford Sanstone was chosen as the representative rock due to its homogeneity and consistent cutting characteristics. Middleton Limestone and/or Pennant Sandstone are representing the rock group without jet penetration. Parameters included for investigation were chosen to reflect practical interests and also to solve some doubts arisen from the primary experimental results. These include nozzle diameter, tool bluntness, jet position, wear rate and cutting mode. The effect of a slot in both the hybrid cutting and the tool-after-slot cutting was also studied. Although the parameters investigated are not exhaustive, they represent the most sought after interests in the field of water jet assisted rock cutting.

The results are mostly examined in terms of force reductions with respect to the corresponding unassisted mechanical cuts. Both absolute mean and mean peak tool forces are given in Appendix D.

8.2 Effect of Nozzle Diameter

8.2.1 Jet Penetration Significant (Grindleford Sandstone)

The effect of nozzle diameter is primarily shown by the jet penetration. The jet power is given by the expression:

$$\text{Jet Power} = Cd \left(\frac{\pi}{4}\right) \left(\frac{2}{\rho}\right)^{\frac{1}{2}} d_o^{\,2}\, p^{\,3/2}$$

where: d_o = nozzle diameter

p = jet pressure

Cd = discharge coefficient

ρ = fluid density.

Hence the jet power is proportional to the square of the nozzle diameter. The jet slot width is about 3 times the nozzle diameter, thus the jet power available to deepen the slot is linearly proportional to the nozzle diameter. Four different diameter nozzles have been tested during the jet slotting tests in Grindleford Sandstone and the results are shown in Figure 7.11. The general impression is that the jet penetration increases with jet pressure and nozzle diameter. The only exception is the 1.5mm nozzle, which has a jet penetration characteristic very similar to that of the 1.2mm nozzle. It is suspected that the 1.5mm diameter is too large for the miniature Newcastle nozzles which must be small enough to be positioned behind the tool. The hydrodynamic efficiency may be impaired and produce a smaller than expected jet penetration. Nevertheless, they did provide an excellent opportunity to study the influence of nozzle diameter, jet power and jet penetration on hybrid cutting efficiency.

All four nozzles have been used in cutting the Grindleford Sandstone with the jet-before-tool configuration. The mechanical depth of cut was set at 10mm and the traverse speed was 1.10 m/s. The result with mean tool component forces plotted against jet pressure are shown in Figure 8.1. The particularly poor force reduction using a 0.6mm nozzle was noted. Jet pressure alone, therefore, should not be used as the sole jet parameter without taking into consideration nozzle diameter. However, the jet power was found not to be the best parameter to summarise the effect of water jet assistance, as shown in Figure 8.2. Instead, the tool force reductions are plotted against jet penetration in Figure 8.3. It was noted that the parameter, jet penetration, is successful in grouping the results together with similar trends. It highlights the importance of the effect of jet penetration on hybrid cutting, as described in the hybrid cutting model (Section 6.3). The slot width, however, has little effect on cutting results.

8.2.2 Jet Penetration Insignificant (Pennant Sandstone)

When the jet pressure is not high enough to penetrate the rock, the main function of the jet is to flush out all loose debris

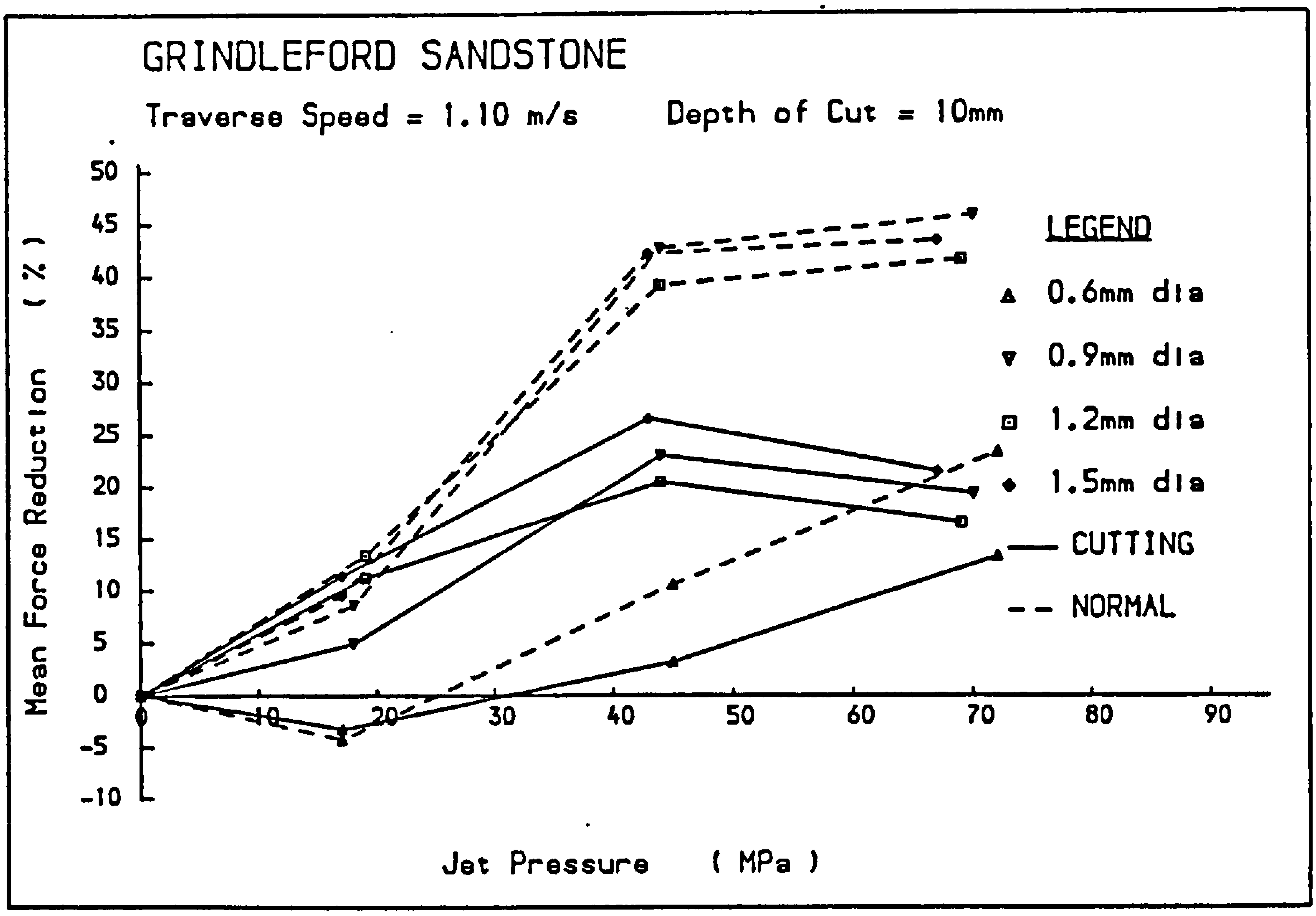

<u>Figure 8.1</u> Mean Force Reduction versus Jet Pressure for Various Nozzle Diameters : Grindleford Sandstone.

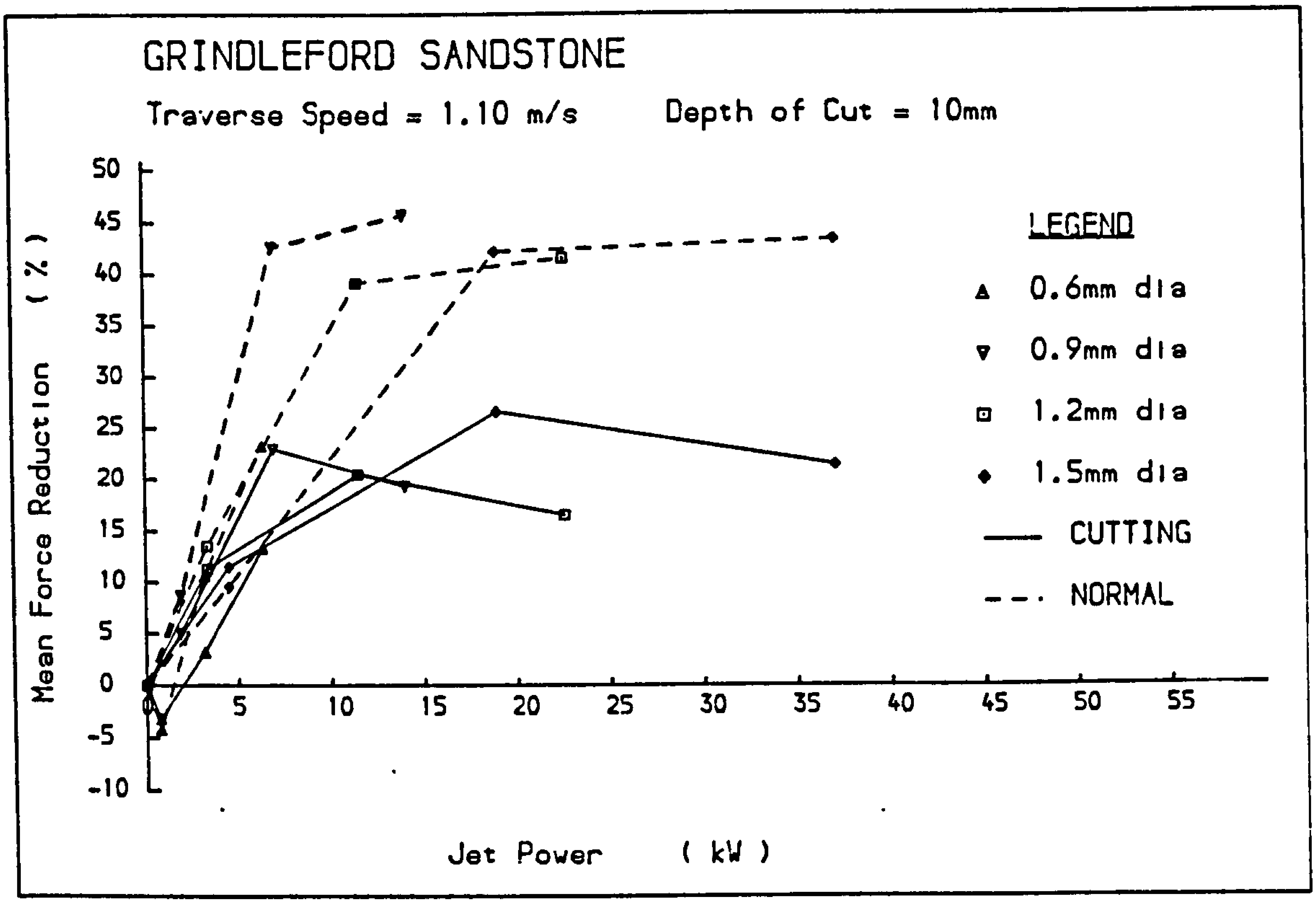

<u>Figure 8.2</u> Mean Force Reduction versus Jet Power for Various Nozzle Diameters : Grindleford Sandstone.

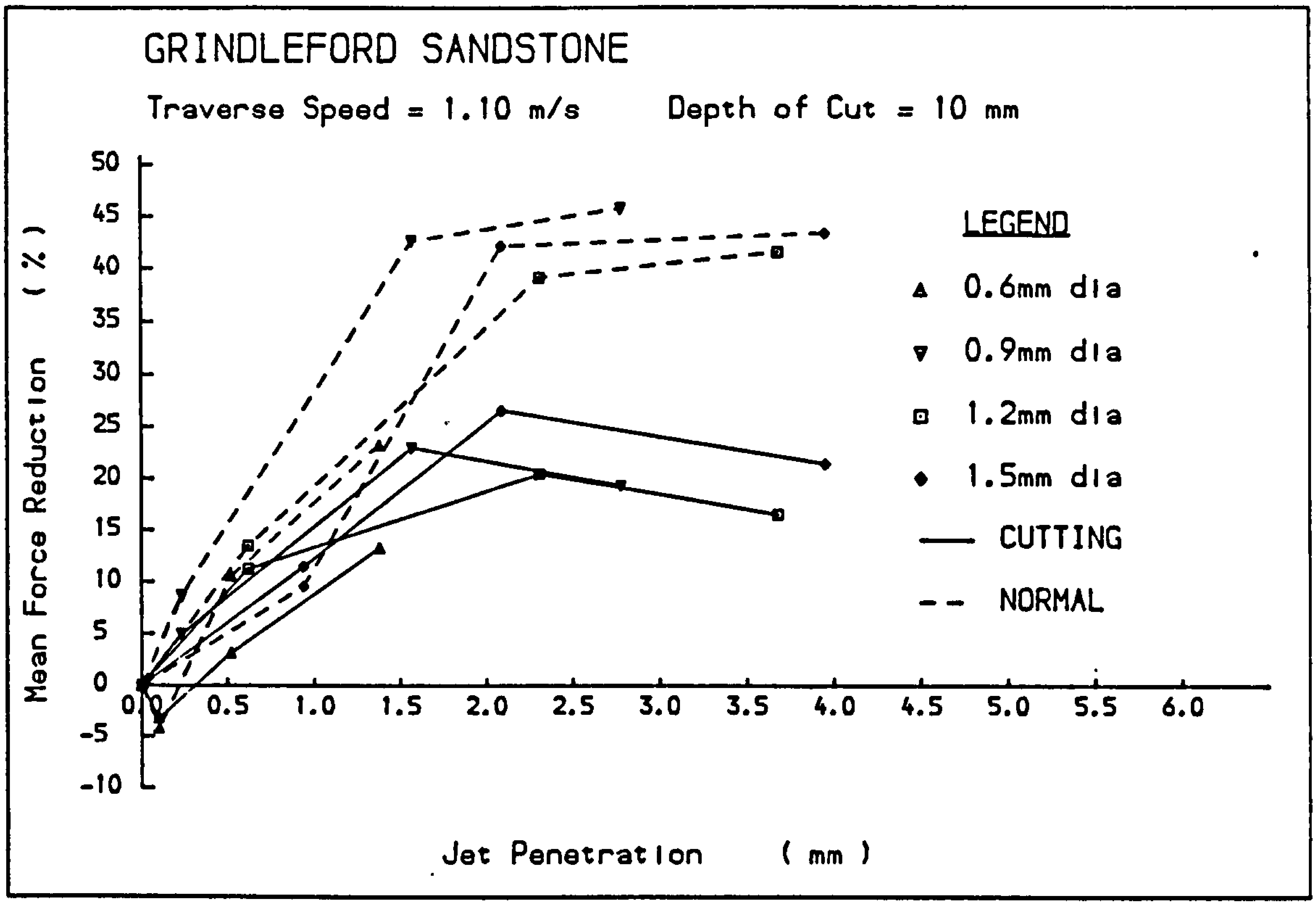

Figure 8.3 Mean Force Reduction versus Jet Penetration for Various Nozzle Diameters : Grindleford Sandstone

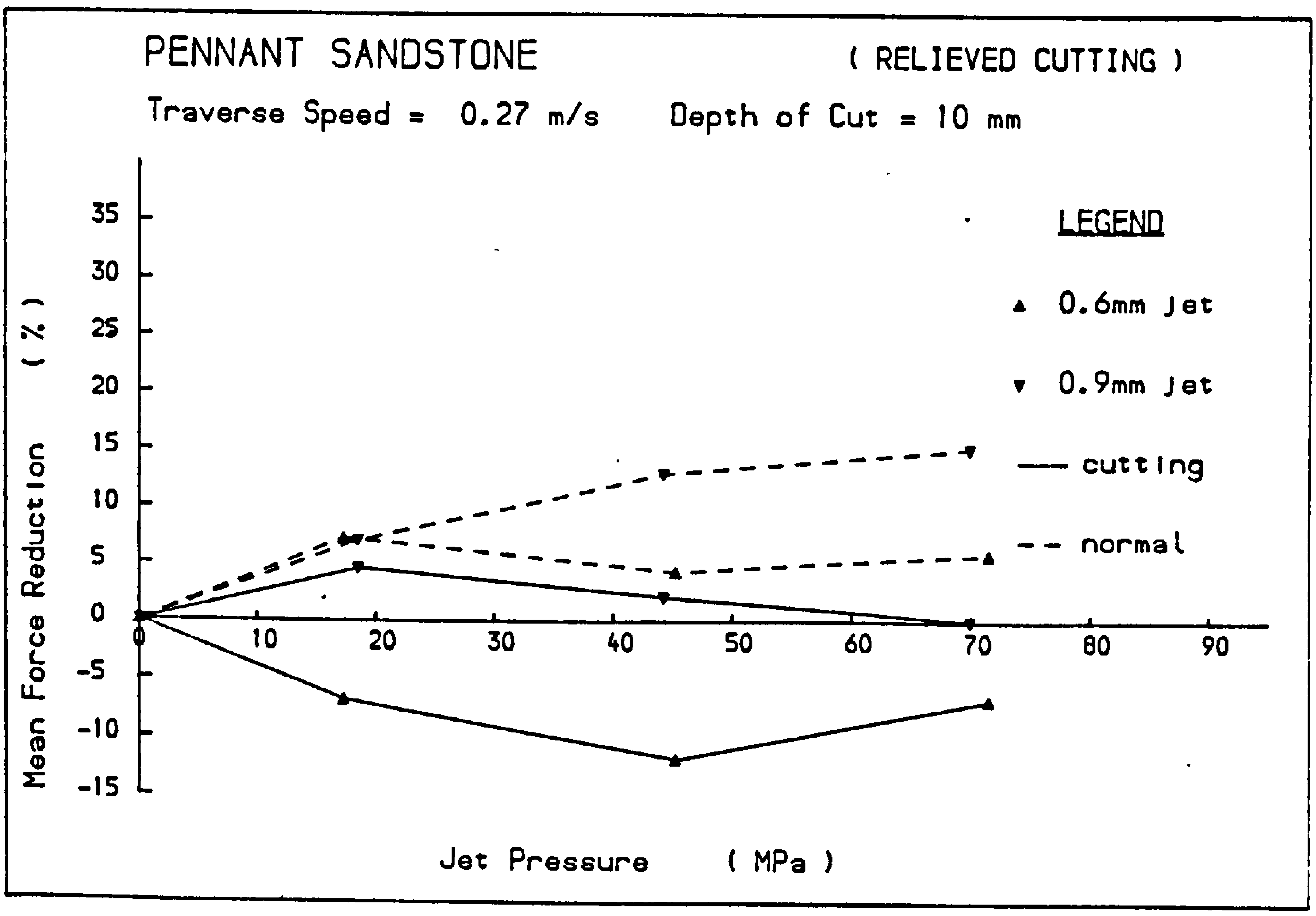

Figure 8.4 Mean Force Reduction versus Jet Pressure for Various Nozzle Diameters : Pennant Sandstone.

and improve tool/rock force transmission efficiency. From this point of view, the higher the jet power, the better the flushing ability of the jet. From Figure 8.4 it can be seen that greater force reductions are obtained when the 0.9mm nozzle is used instead of the 0.6mm nozzle. As tool tip relief by jet penetration is impossible, the maximum normal force reduction was only 15% compared with over 40% in Grindleford Sandstone.

8.2.3 Discussion

Hood (1985) proposed to use the jet energy as the key parameter to characterise the jet in hybrid cutting (Figure 8.5). Theoretically it is possible if the hydrodynamic performance of the nozzle remains the same for different nozzle diameters, nozzle design and nozzle materials, so that the jet penetration is linearly proportional to the nozzle diameter. Obviously this is impossible in reality. A good example is the 1.5mm diameter nozzle used in cutting Grindleford Sandstone during the present study. While there is an increase of 64% in jet power, the jet penetration of the 1.5mm diameter nozzle is only marginally better than that of the 1.2mm diameter nozzle. Furthermore, the jet slotting efficiency changes with different traverse speeds (see Section 7.3.2). Misleading results will be obtained if the jet energy is used as a predictor.

In addition to the theoretical soundness, as mentioned in the hybrid cutting model, there is practical significance in

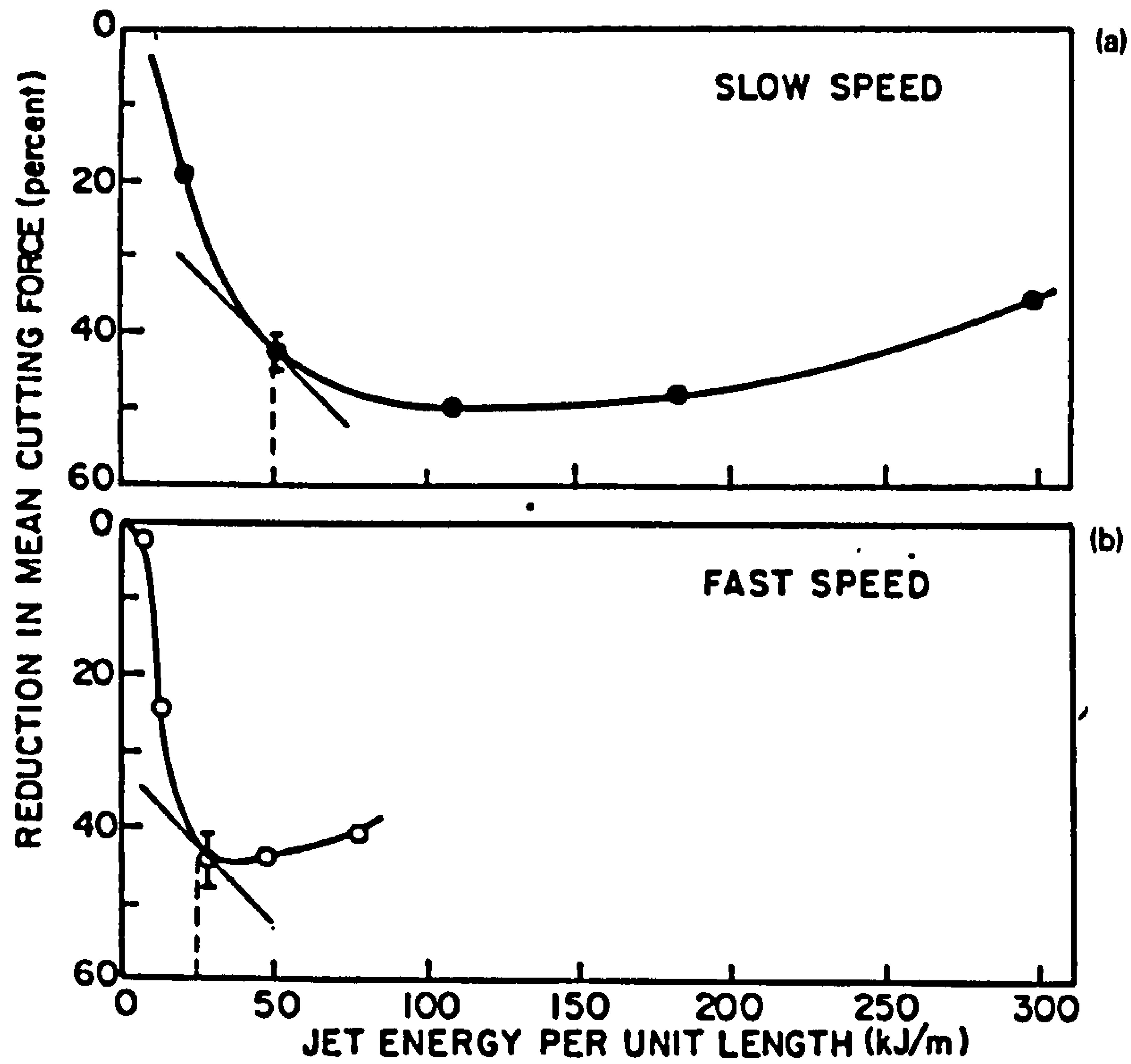

Figure 8.5 Mean Cutting Force Reduction as a Function of the Normalised Jet Power for Different Cutting Speeds (after Hood 1985).

establishing the jet penetration as a jet characterising parameter. It is a unique parameter to combine the effects of jet pressure, nozzle diameter, nozzle design, stand-off distance, traverse speed and their interactions, and provides a single factor to evaluate the effectiveness of water jet assistance when cutting a particular rock material.

8.3 The Effect of Tool Bluntness

Before the water jet was applied the effect of tool bluntness to unassisted rock cutting was first studied.

8.3.1 Unassisted Rock Cutting

The effect of tool bluntness on the tool forces is to increase the proportion of cutting and normal forces required to crush the rock underneath the wearflat. The results of cutting Grindleford Sandstone, Pennant Sandstone and Middleton Limestone with sharp and blunt tools at both slow and fast traverse speeds are plotted in Figures 8.6 and 8.7.

The introduction of this moderate wearflat caused drastic increase in tool forces. Since the wearflat angle is small, most of the crushing force is provided by the normal force. The increase in the normal force component is slightly less than threefold at a cutting speed of 0.27 m/s and is more than fourfold when the cutting speed is 1.10 m/s. The increase in cutting force is about 75-100%, and is similar for both speeds.

The effect of traverse speed which causes increase of tool forces with traverse speed in Grindleford Sandstone was

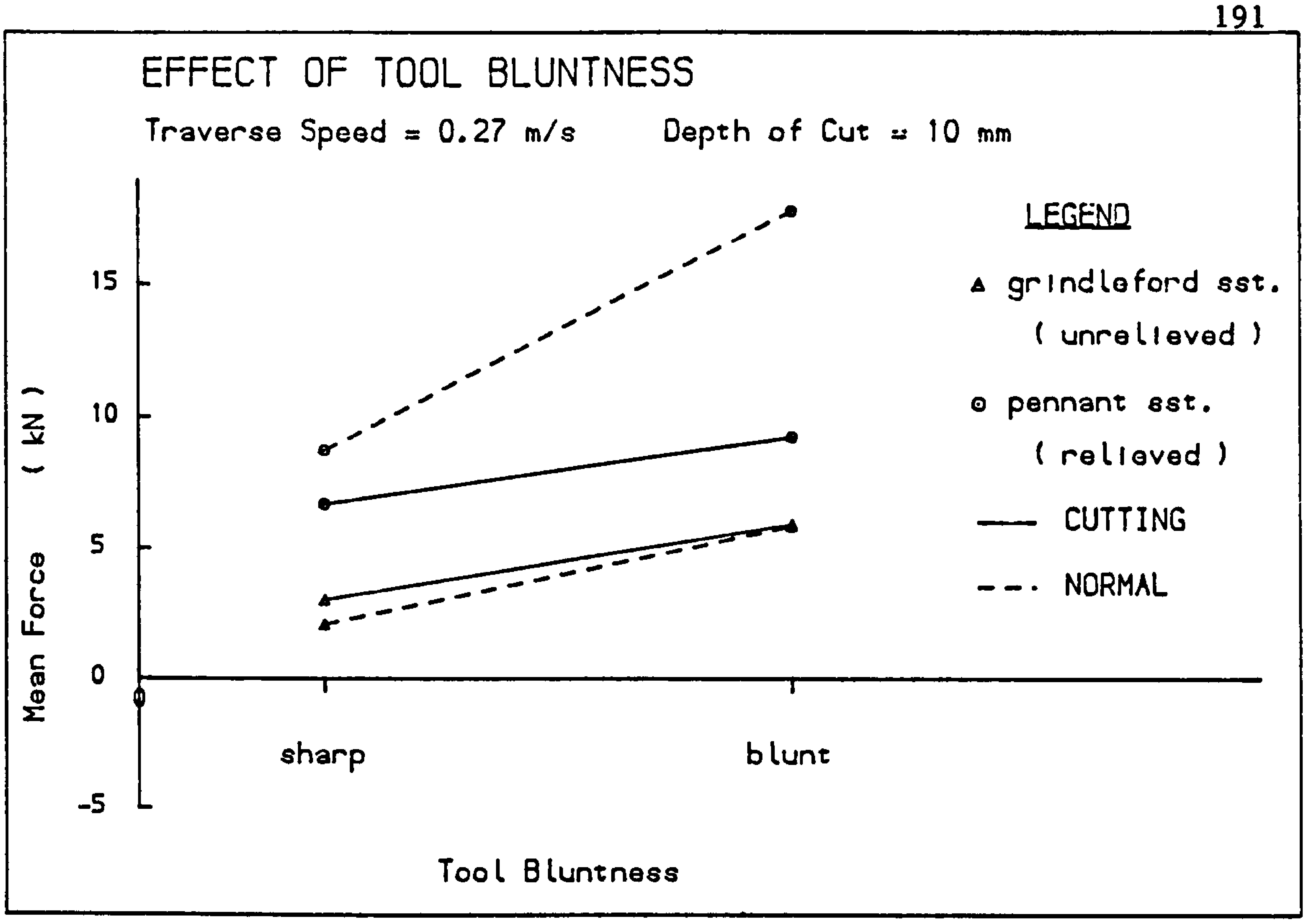

Figure 8.6 Mean Force versus Tool bluntness for various Rocks; Traverse speed = 0.27 m/s.

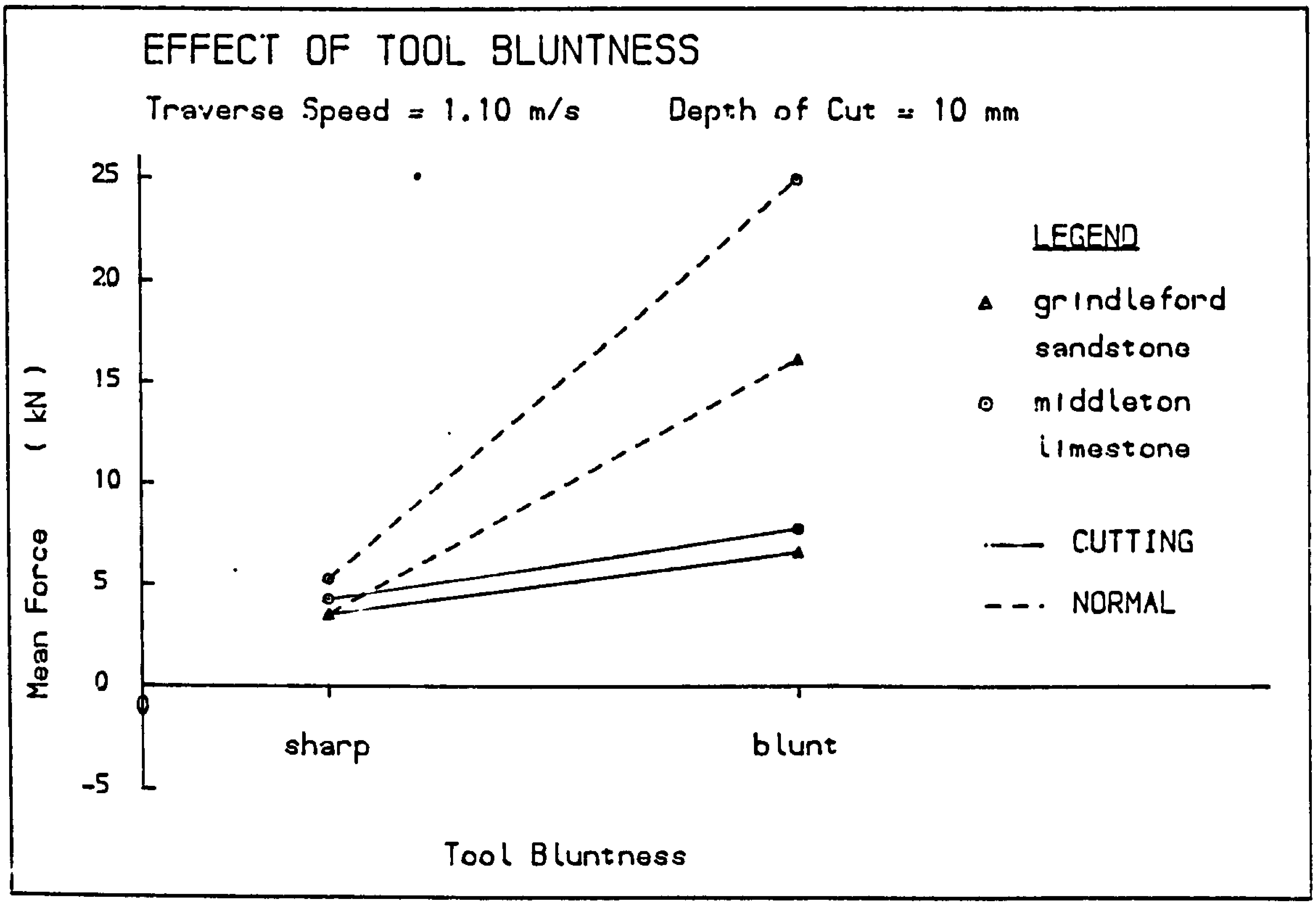

Figure 8.7 Mean Force versus Tool bluntness for various Rock; Traverse speed = 1.10 m/s.

observed for the blunt tool as well as the sharp tool. The higher percentage force increase for a blunt tool compared with that for the sharp tool would seem to support the suspected correlation between the effect of traverse speed and the crushing events underneath the wearflat which has a greater area for a blunt tool.

8.3.2 Jet Penetration Significant (Grindleford Sandstone)

As water jets are extremely effective in reducing crushing force components, when jet penetration is significant, hybrid cutting using a blunt tool produces a higher force reduction than when using a sharp tool (Figures 8.8 and 8.9). At a jet pressure of 70 MPa, the mean normal force reductions were 70% for a blunt tool and 45% for a sharp tool for the jet-before-tool configuration cutting at 1.10 m/s. The higher force reduction for the blunt tool is attributed to the higher force contribution from the crushing force component. The higher force reduction, together with the higher tool force for a blunt tool meant that the absolute force reduction was even more substantial (Figures 8.10 and 8.11). The results have significant practical implication as most tools used on a roadheader are essentially blunt and the tool speeds employed are high. The machine is usually arcing force limited. When the water jet is applied and the rock can be penetrated by the jet, a much improved machine performance is expected.

Typical force-time traces showing the difference between drag tool cutting and water jet assisted cutting for sharp and blunt tools are given in Figure 8.12.

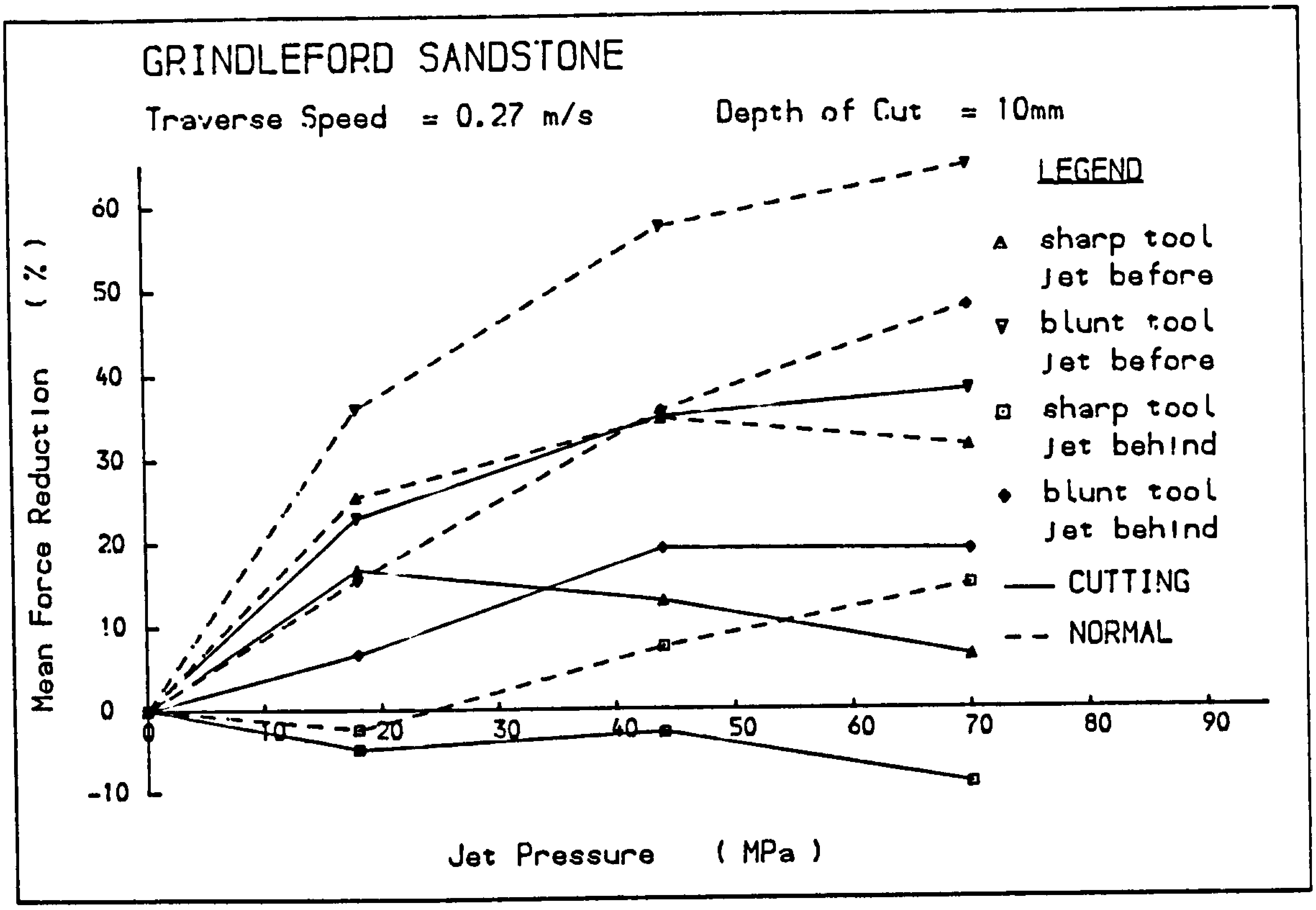

Figure 8.8 Mean Force Reduction versus Jet Pressure for sharp and blunt Tool in different positions; Grindleford Sandstone· Traverse speed = 0.27 m/s.

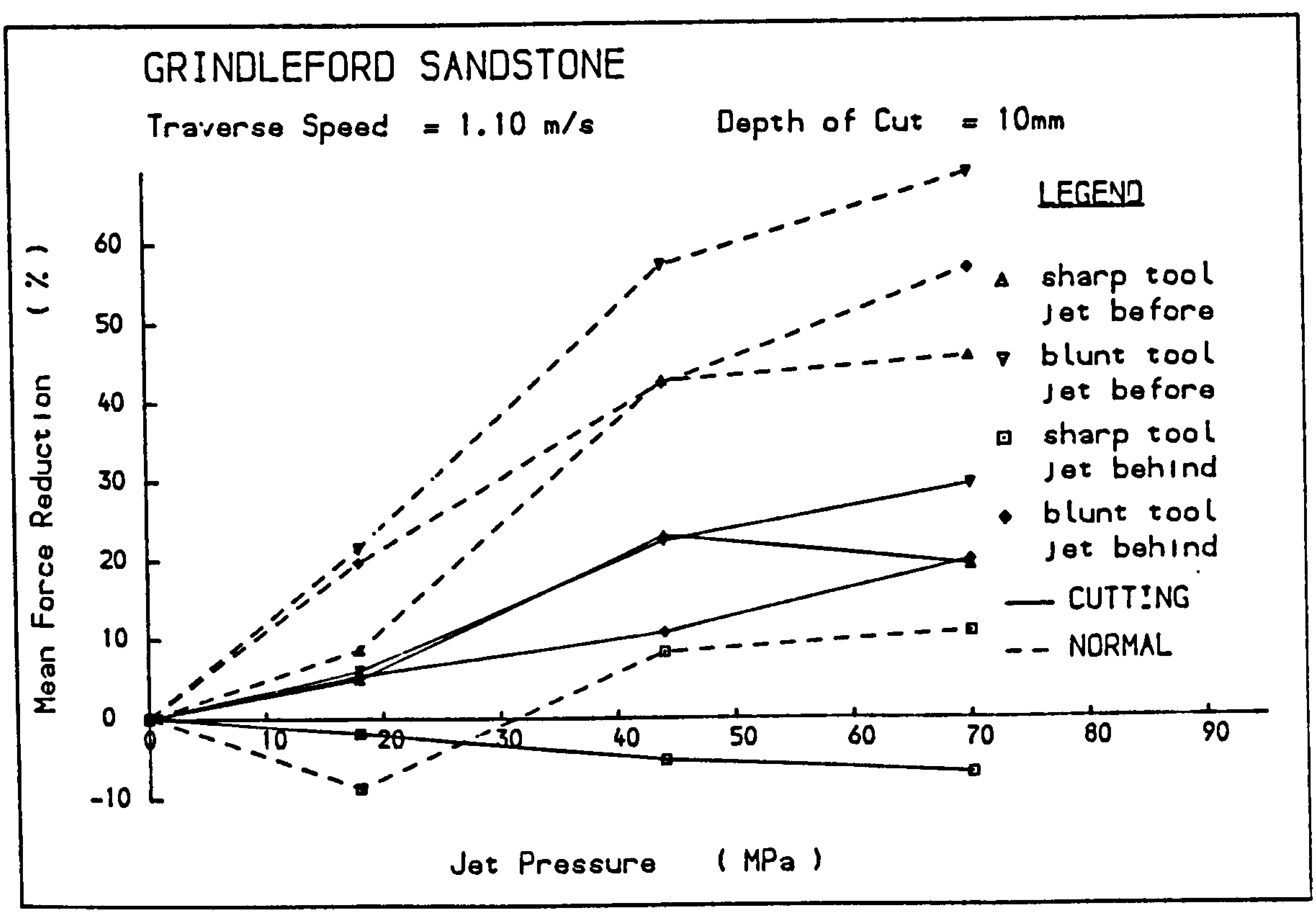

Figure 8.9 Mean Force Reduction versus Jet Pressure for sharp and blunt Tool with different positions: Grindleford Sandstone; Traverse speed = 1.10 m/s.

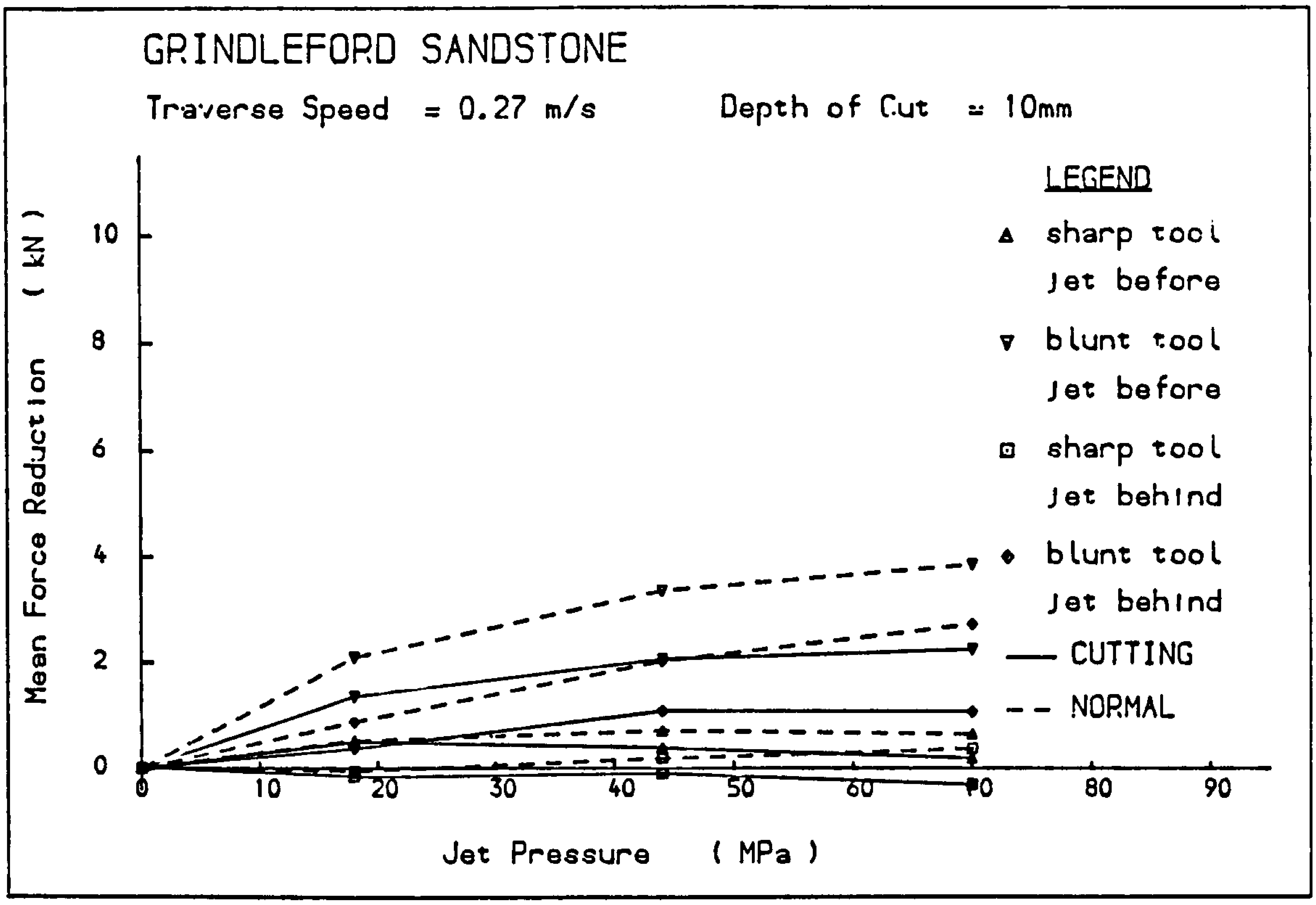

Figure 8.10 Absolute Mean Force Reduction versus Jet Pressure for sharp and blunt Tool with different jet configurations· Grindleford Sandstone; Traverse speed = 0,27 m/s,

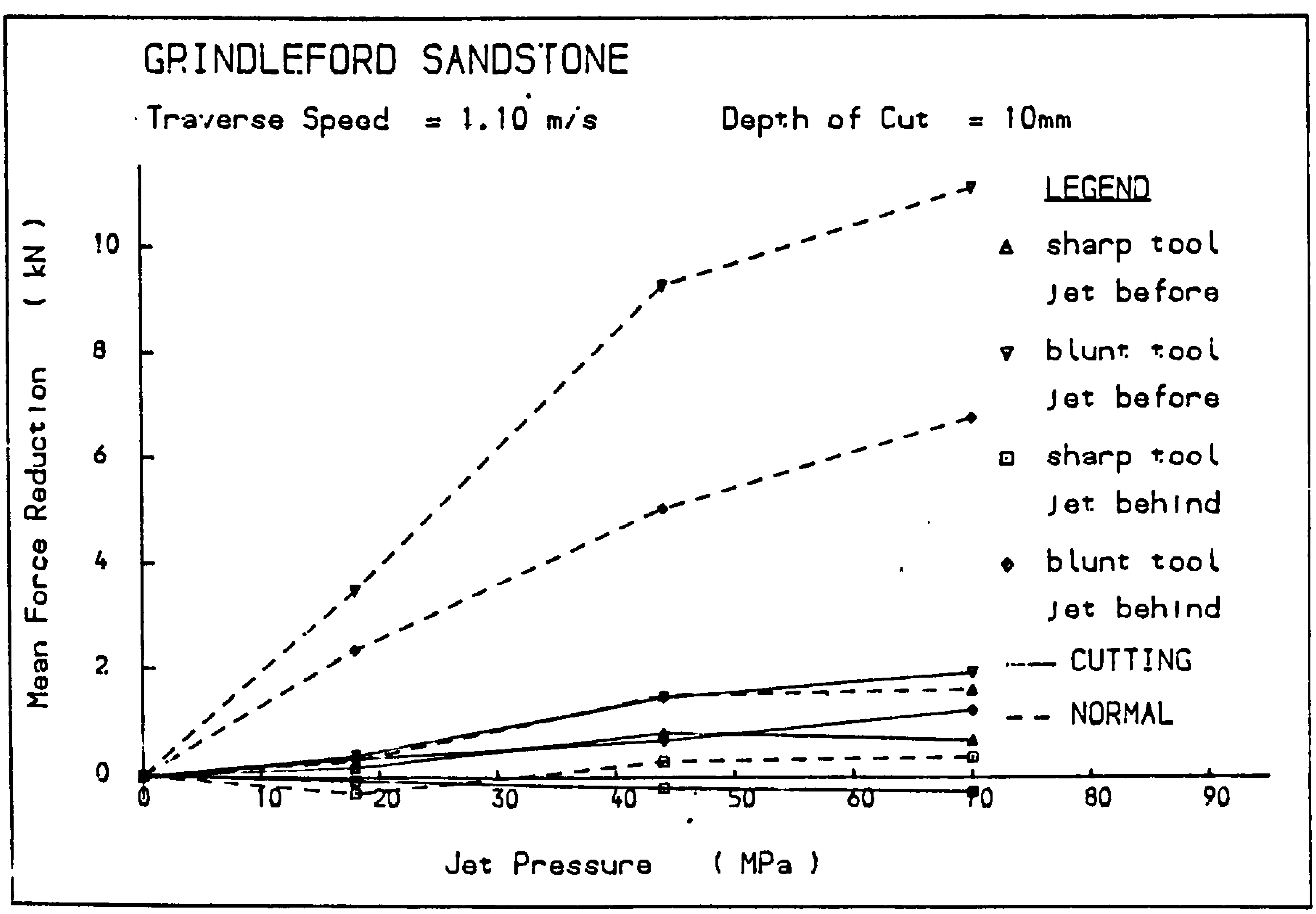

Figure 8.11 Absolute Mean Force Reduction versus Jet Pressure for sharp and blunt Tool with different jet configurations; Grindleford Sandstone· Traverse speed = 1.10 m/s.

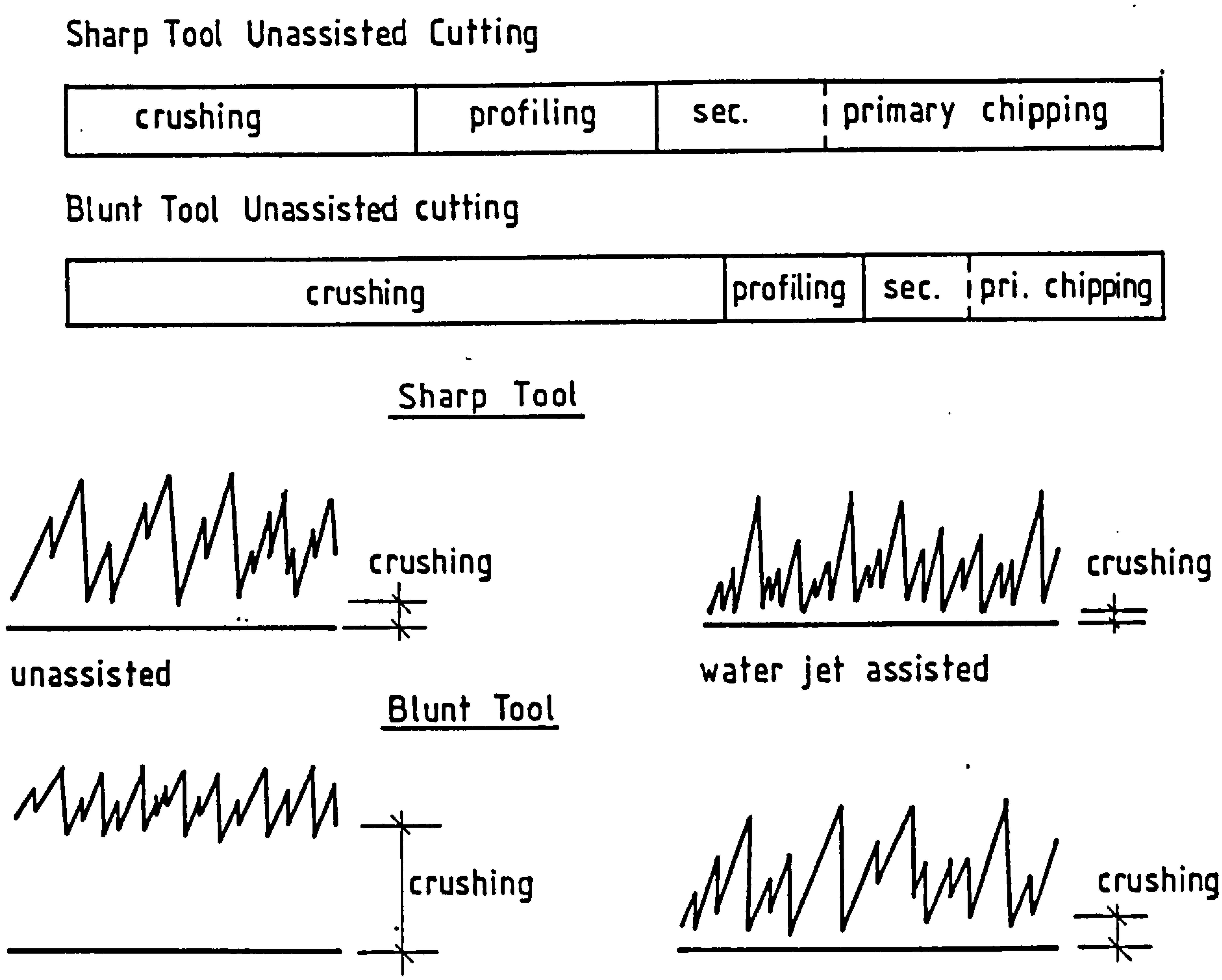

Figure 8.12 Comparison of sharp and blunt tool rock cutting and the effect of water jet assistance.

Not only is blunt tool hybrid cutting producing a large force reduction, but the optimum pressure is higher when compared with that obtained for sharp tool hyrid cutting. This highlights the important concept that the force acting on a tool should be considered to be composed of crushing and chipping components.

The water jet is useful in reducing the rock crushing under the wearflat but, if excessive jet penetration occurs, this tends to reduce the efficient chipping events as well. The optimum jet penetration, and thus optimum jet pressure, is a compromise between the relative magnitude between chipping and crushing force components. The greater the crushing events, the higher the optimum jet penetration. Optimum jet penetration hence depends on the degree of tool bluntness, and may approach the mechanical depth of cut in the case of very blunt tools.

A generalised figure showing the effect of bluntness is given in Figure 8.13.

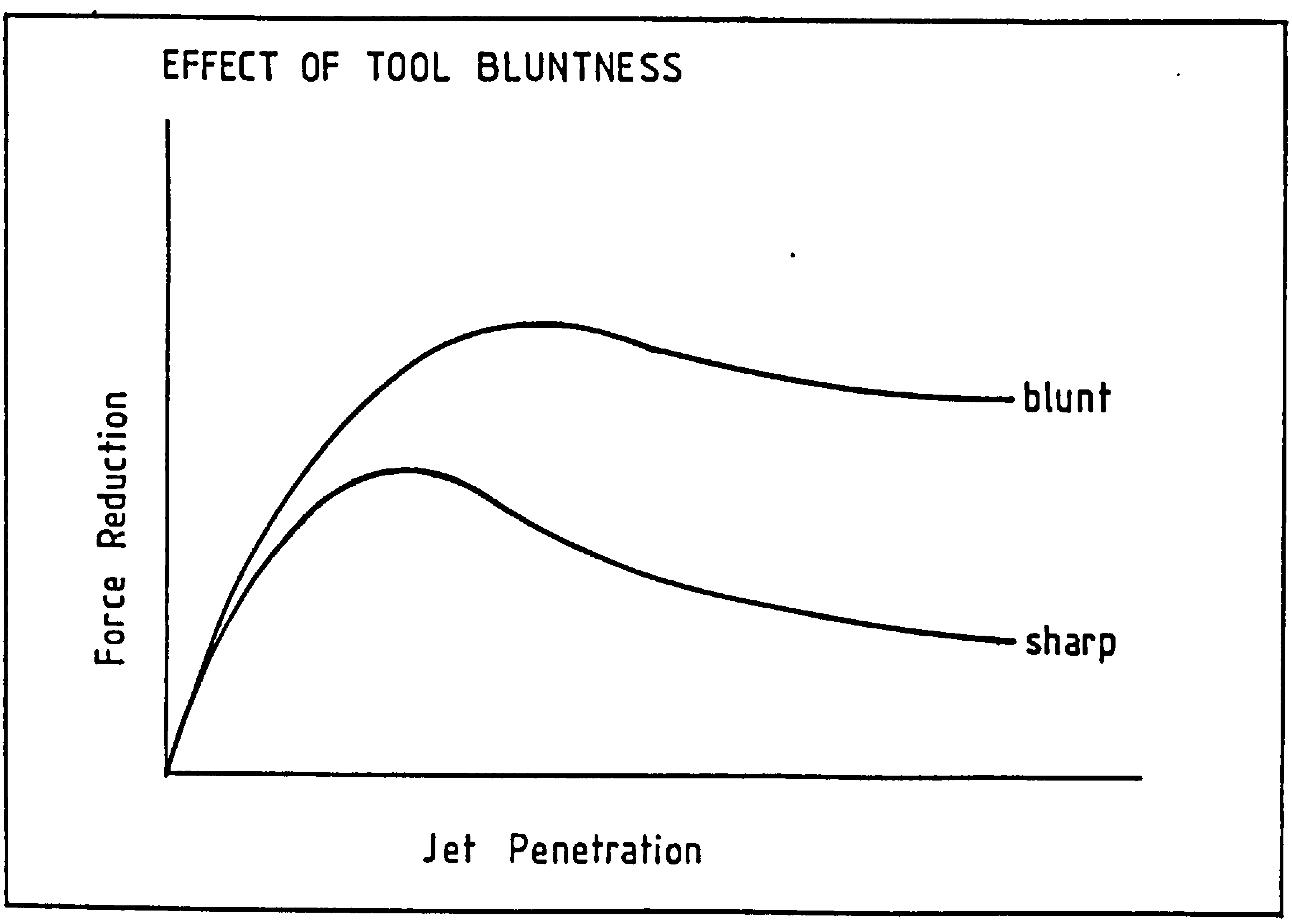

Figure 8.13 Generalised effect of tool bluntness on force reduction.

8.3.3 Jet Penetration Insignificant (Middleton Limestone and Pennant Sandstone)

In general the force reduction is small compared with that of Grindleford Sandstone where jet penetration is significant. For the jet-before-tool configuration, the normal force reduction is around 25% for sharp tool and less than 15% for the blunt tool (Figure 8.14). The most interesting finding is the lower force reduction in blunt tool cutting than that for sharp tool cutting which is contradictory to the findings for the rocks with significant jet penetration. The inferior performance of water jets with blunt tool cutting can be explained by the inability of the jet to penetrate and relieve the tool tip. The main purpose of the jet is debris clearance and aiding the chip removal once formed, which contributes much less in blunt tool cutting than in sharp tool cutting.

Similar findings are observed in cutting the Pennant Sandstone in relieved mode (Figure 8.15), although even lower force reductions were obtained.

8.3.4 Discussion

The much higher benefits of water jet assistance when jet penetration is significant was proved during this study of tool bluntness effect. When the rock can be penetrated, much higher force reductions are obtained for the blunt tool. In contrast, decreased force reductions are observed for the blunt tool when cutting the Middleton Limestone and Pennant Sandstone in which jet penetration is insignificant. The unclear difference

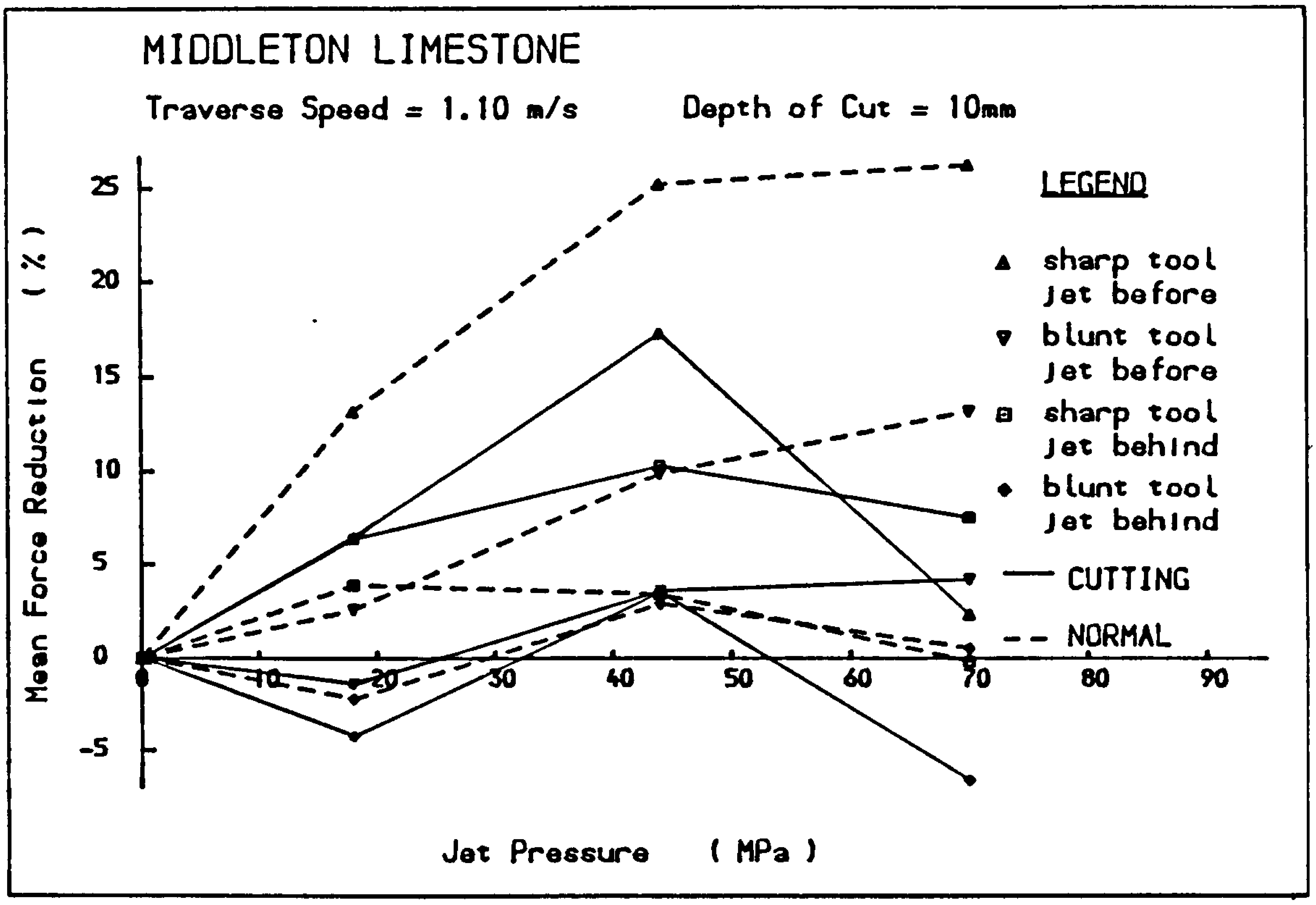

<u>Figure 8.14</u> Mean Force Reduction versus Jet Pressure for Sharp and Blunt Tools in Different Positions : Middleton Limestone : Traverse Speed = 1.10 m/s.

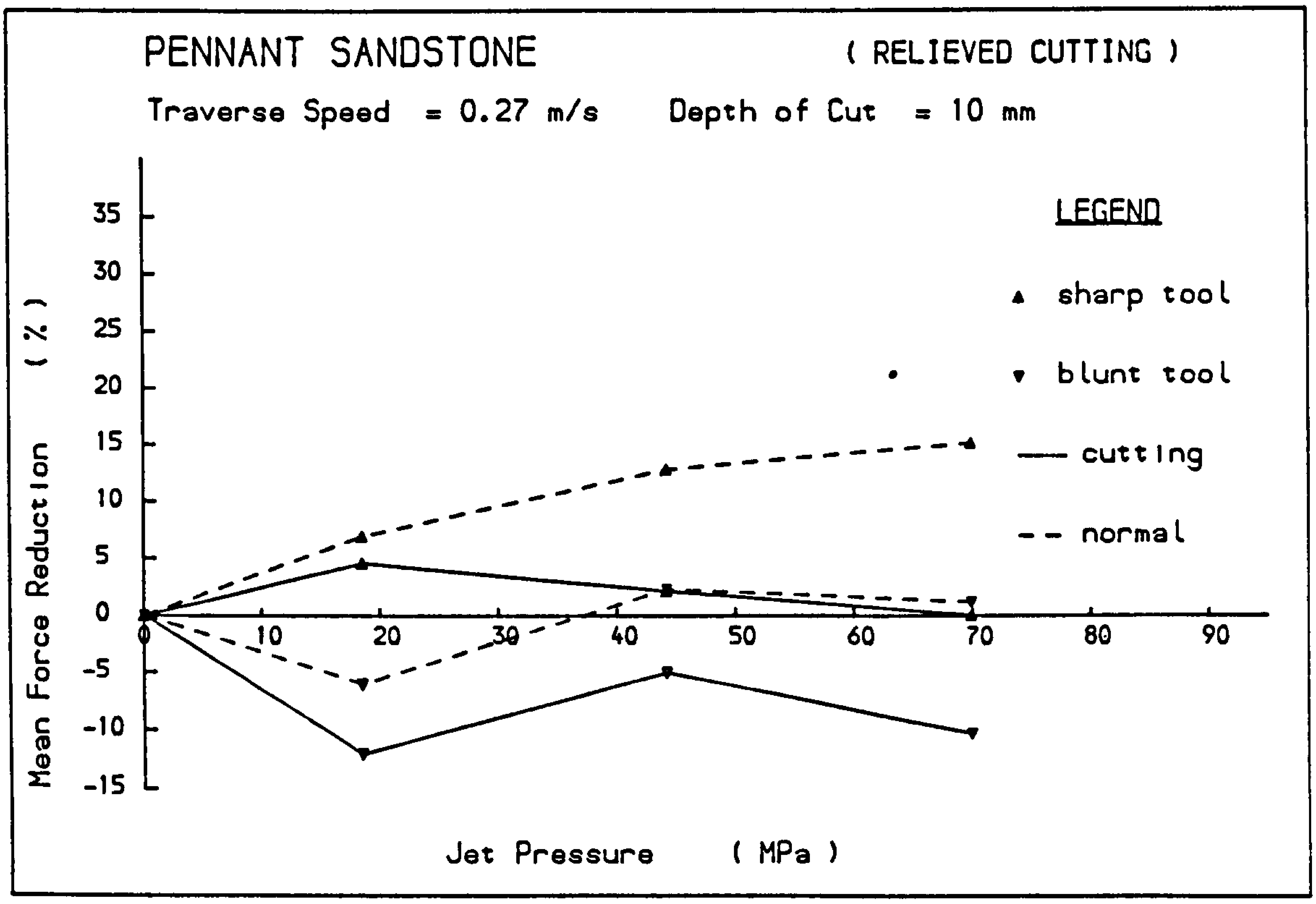

<u>Figure 8.15</u> Mean Force Reduction versus Jet Pressure : Pennant Sandstone : Relieved Cutting : Traverse Speed = 0.27 m/s.

between the two rock groups during cutting with a sharp tool is due to the small proportion of the force used in crushing the rock underneath the wearflat for the sharp tool. When the wearflat is generated, the crushing forces increase rapidly with the normal force several times higher than that for the sharp tool. In this case, the ability of the jet to penetrate and relieve the tool tip is very important in reducing the tool force. Hence much improved force reductions are obtained for the rock with significant jet penetration than for the rock without significant jet penetration when a blunt tool is used.

Hurt and Laidlaw (1979) investigated the cutting efficiency of three rock cutting tools and found that the V-bottomed radial tool generated considerably less force than that for a point attack tool when sharp. The effects of bluntness, however, reduced or completely eliminated these differences. Hence it seems that the point attack tool behaves in a similar fashion to a blunt radial tool with regard to tool force, with much of the tool force wasted in crushing the rock. The findings during this project suggest that optimum jet penetration is higher for the blunt tool. This could be the reason for Tecen (1982), in a smaller scale hybrid cutting research programme using point attack tools, concluding that the most efficient cutting was obtained when jet penetration approached the mechanical depth of cut. Further work is required to confirm these results.

8.4 Effect of Jet Position

The jet-behind-tool configuration was thought to have the advantage of having access to the tool tip at all times. The tip is cooled continuously during the course of cutting. In some cases, the jet-behind-tool configuration was found to be superior in terms of tool force reductions (Ropchan et al. 1980). In this section, the effect of jet position is studied.

8.4.1. Jet Penetration Significant (Grindleford Sandstone)

The general conclusion is that inferior performance is obtained from the jet-behind-tool configuration for both the sharp and the blunt tool cutting conditions at 0.27 m/s and 1.10 m/s (Figures 8.8 and 8.9). The results are particularly disappointing when the sharp tool is used, which shows less than 15% normal force reduction at both speeds, even when 70 MPa jet pressure is used.

In the jet-behind-tool configuration, the jet impinging angle is the same as the back clearance angle of the tool which is about 11°. The wearflat angle of the blunt tool in this case is -4°. Hence the wearflat is not completely relieved from crushing events even when jet penetration is significant and the degree of confinement is much reduced. The normal force reduction is about 50-55% at a jet pressure of 70 MPa, while it is almost 70% for a jet-before-tool configuration. The effects of different jet positions are illustrated in Figure 8.16.

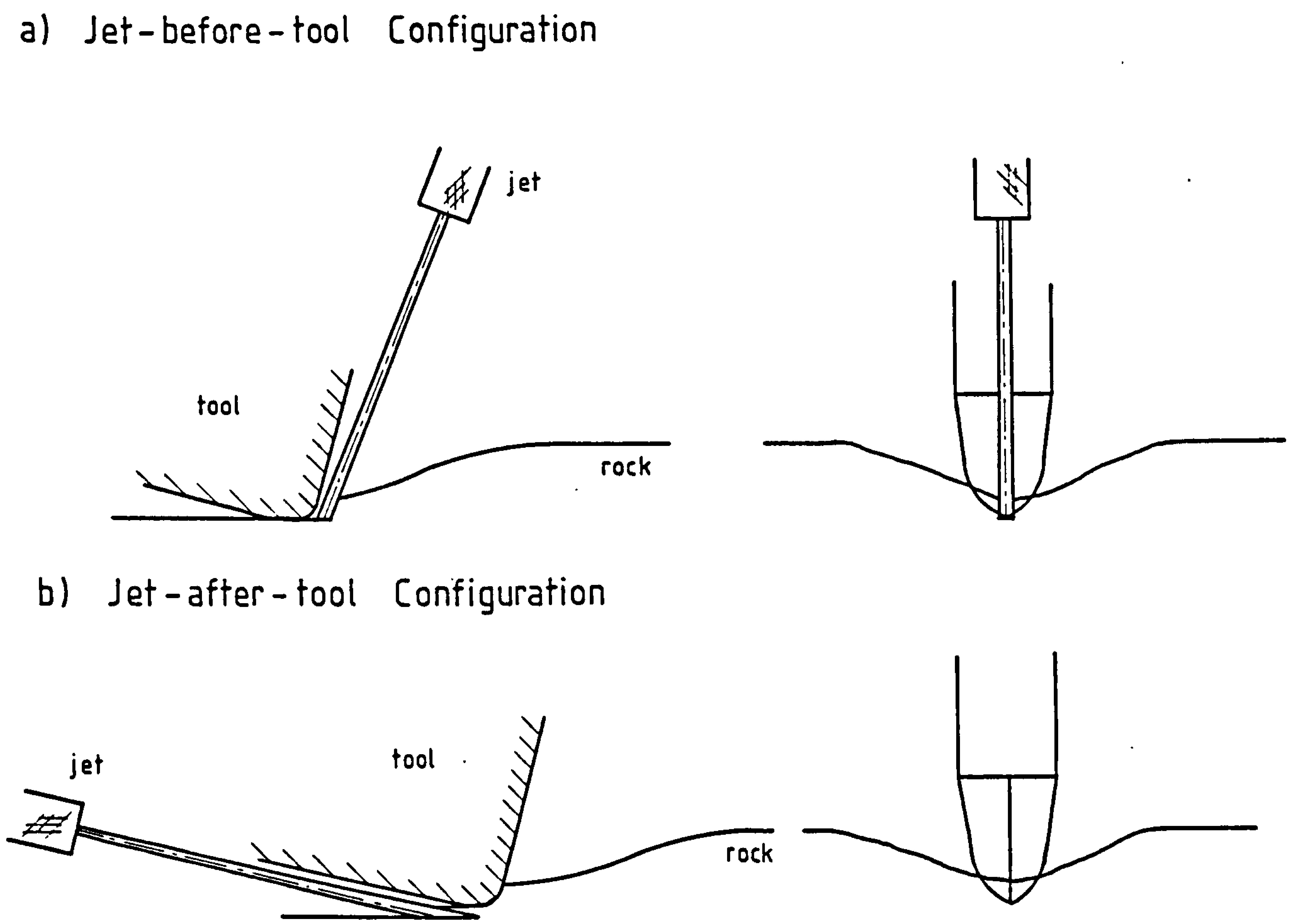

Figure 8.16 Schematic illustration of the effects of the water jet from different positions.

By positioning the jet behind the tool, the jet also loses its ability to flush out debris and improve the tool-rock force transmission, although this is not so important as the reduced crushing events to the tool force reductions. Provided the jet penetration is not excessive such as to disturb the crushed zone essential for primary chipping, the jet-before-tool configuration offers the extra benefit of being able to slot the rock ahead of the tool and aid profiling immediately after the chipping events. Without a slot, the profiling is similar to groove deepening. With a slot, the tool tip is relieved and the profiling is essentially a double relieved wedge cutting in which a lower tool force is expected (Figure 8.16).

The extra benefits provided by the jet-before-tool configuration are responsible for the improved tool force reductions in both cutting and normal force components.

8.4.2 Jet Penetration Insignificant (Middleton Limestone)

Most of the tool component forces with water jet assistance have produced fluctuations of around ±5% of the dry cutting values for the jet-behind-tool configuration (Figure 8.14). Taking into consideration the experimental errors, it is obvious that no benefit is derived from the water jet in this position. It reiterates the functions of the water jet in the hybrid cutting in this category of rocks which are debris clearance and helping with chip removal, which is only possible with the jet before the tool.

8.5 Effect of Wear Rate

Along with the blunt tool trials, the effects of water jet assistance on the wear rates experienced by drag tools and the changes in tool component forces was also undertaken. Pennant Sandstone, a very strong and abrasive rock, was chosen to provide high wear rates for short cutting distances.

Two jet diameters and two positions for the jet, in front and behind the tool, were used in this study. A pristine tool was used for each condition. The jet pressure was 70 MPa and the cutting speed was 1.10 m/s. The cutting and normal tool force components are presented in Figures 8.17 and 8.18 for the first 16 metres of cutting, together with results for unassisted cutting.

Generally all four jet configurations have similar force levels, demonstrating that the main purpose of the jet is to cool the tungsten carbide-rock interface, maintaining the carbide's hardness and hence resistance to abrasion, which drops rapidly with rise in temperature.

The component forces rise several fold from the sharp condition with the water jet assisted normal force components being generally 40% lower than for the unassisted mode of cutting. Little difference was observed in the cutting force component.

In cutting this rock, very low component force reductions were obtained with the 70 MPa jet with similar tool wear condition (Section 7.5.1). Hence the major benefits from water jet assistance are prolonged tool life and reduced tool forces due to less wear in the long run.

The wear of each tool after 16m of cutting is shown in Plate 8.1. The top tool was used for unassisted cutting. The tools on the right-hand side are those with the jet-before, while the tools on the left-hand side are those with the jet-behind;

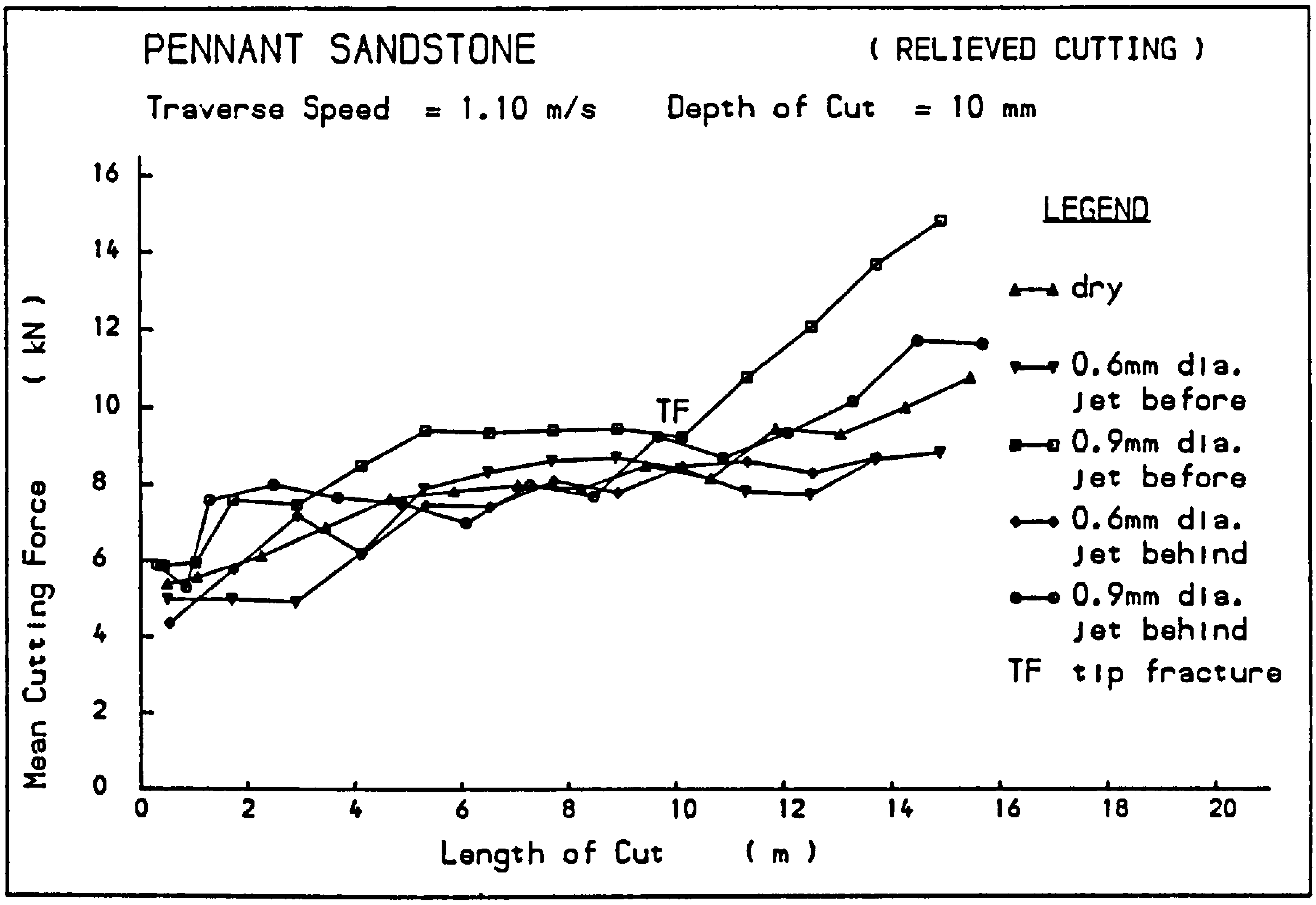

Figure 8.17 Mean Cutting Force versus Length of Cut with or withuot 0.6mm and 0.9mm water jets in different positions : Pennant Sandstone.

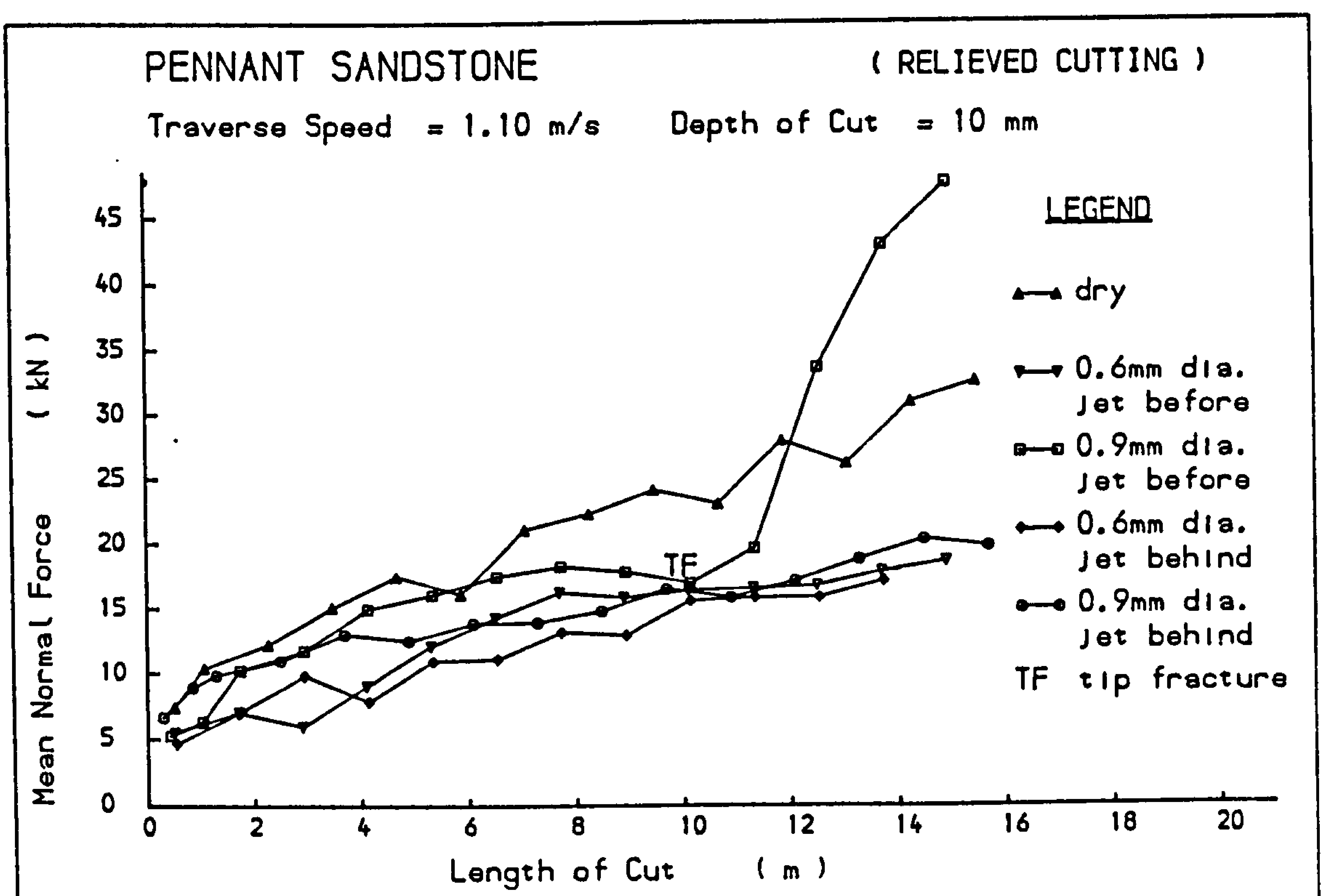

Figure 8.18 Mean Normal Force versus Length of Cut with or without 0.6mm and 0.9mm water jets in different positions : Pennant Sandstone.

Plate 8.1

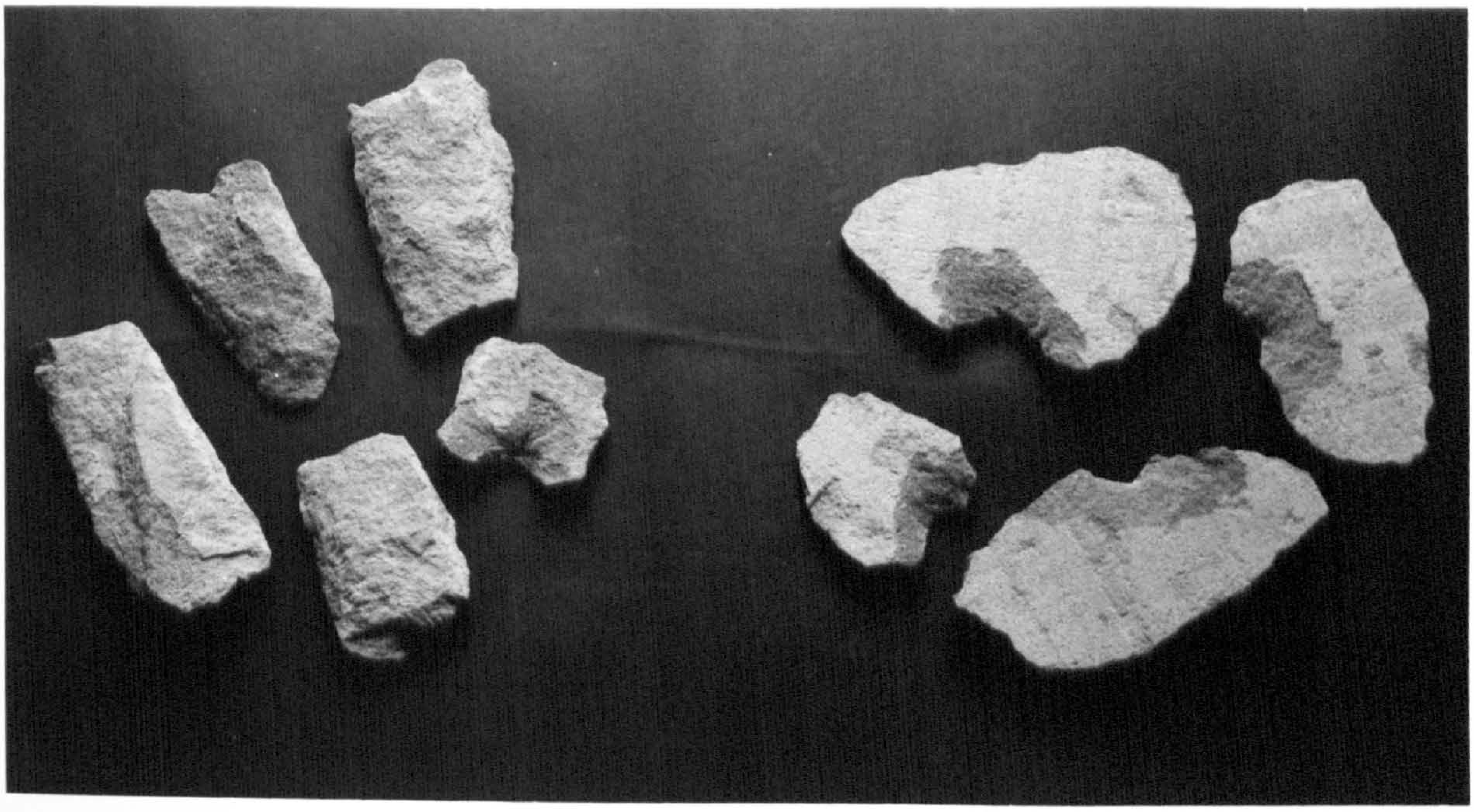

Plate 8.2

the upper ones were used with a 0.6mm jet diameter and the lower ones with a 0.9mm jet diameter. The similarity of wear between tools with different jet positions suggests no advantage is gained from positioning the jet behind the tool in cutting. It highlights the limited capacity of a drag tool in cutting this hard and abrasive rock as a sizeable wearflat was generated in only 16m of cutting. All the tools, with or without water jet assistance, have a wear mechanism which is a combination of tip removal and abrasion. The tool tip is sheared off after the first 1 or 2m of cutting, reflecting the tip geometry was not strong enough. Afterwards, the tool was subjected to abrasive wear. The wear rate is higher for the tool without water jet assistance, as reflected by the larger wearflat.

It should be noted that the cutting tool tip must be tough enough to resist impact shattering of the carbide insert before the benefits of water jet assitance can be gained in extending the range of application of drag tools to very strong rock materials. This is demonstrated by the failure of one of the tools during the test programme.

8.6 Effect of Cutting Mode

Though unrelieved, independent cuts on a trimmed surface are a convenient way to study the mechanisms of hybrid cutting, almost all tunnelling machines cut with a rotary motion, where the cuts are made adjacent to a preceding cut at a predetermined spacing, small enough to provide force relief. A study was carried out to investigate the effect of relieved cutting on water jet assisted rock cutting.

The cutting pattern adopted for this study simulated a roadheader cutting head with two tool spirals and one tool per line. The advance rate was assumed to be 20mm per revolution and the spacing between adjacent tool lines was 20mm (Figure 8.19). Although the depth of cut is changing on a production rotary machine, this study nevertheless provides a comparison between the results of unrelieved cutting and the relieved cutting which is typical of the many cutting head designs used in the UK.

The rocks used were Grindleford Sandstone and Pennant Sandstone, which represent the two categories of rock types in which the jet penetration is significant and insignificant respectively.

8.6.1 Jet Penetration Significant (Grindleford Sandstone)

In this study, three nozzles of different diameter were used and the traverse speed was 1.10 m/s to simulate the tool speed for a real tunnelling machine cutting hard rock. The tool component force reductions are plotted in Figure 8.20 and Figure 8.21, together with results obtained previously in unrelieved cutting, using the same nozzles.

The results show that the force reduction trends are very similar between the unrelieved and relieved cuts. The 0.6mm nozzle still maintains its inferior performance compared with the other nozzles, showing the importance of jet penetration for force reduction. For the 0.9 and 1.2mm jets, the force

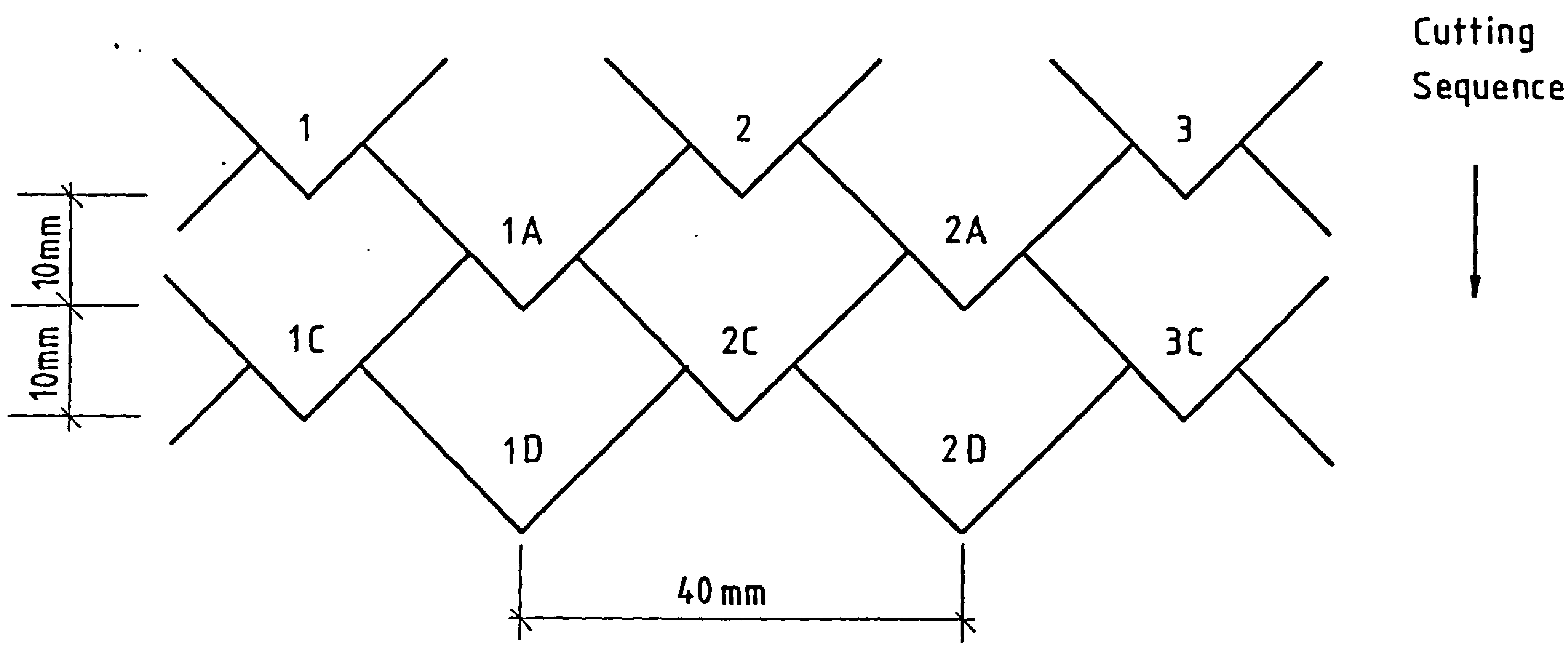

Figure 8.19 The Cutting Pattern for relieved cutting Mode.

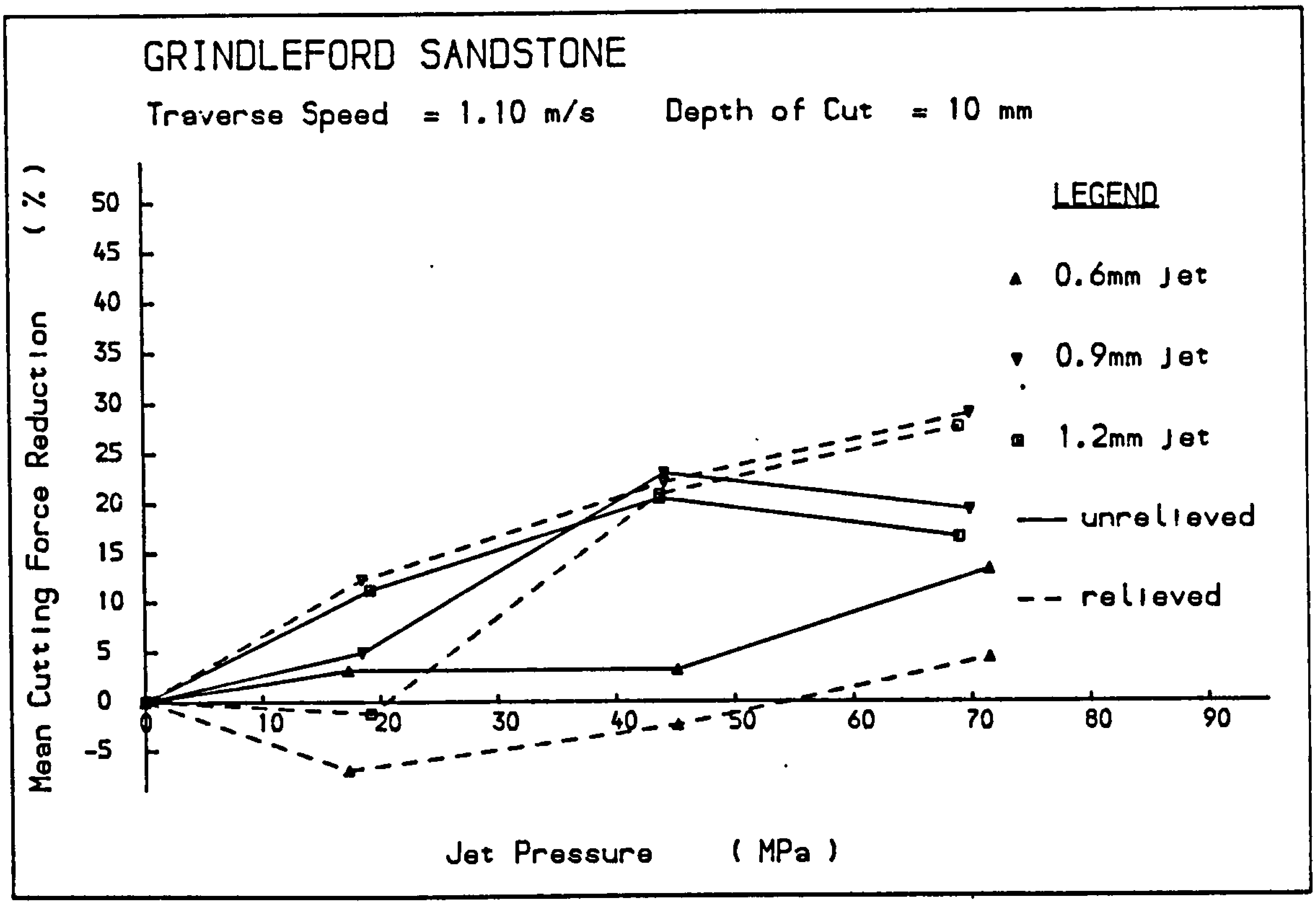

Figure 8.20 Mean Cutting Force Reduction versus Jet Pressure for Various Nozzle Diameters in Relieved or Unrelieved cutting mode : Grindleford Sandstone.

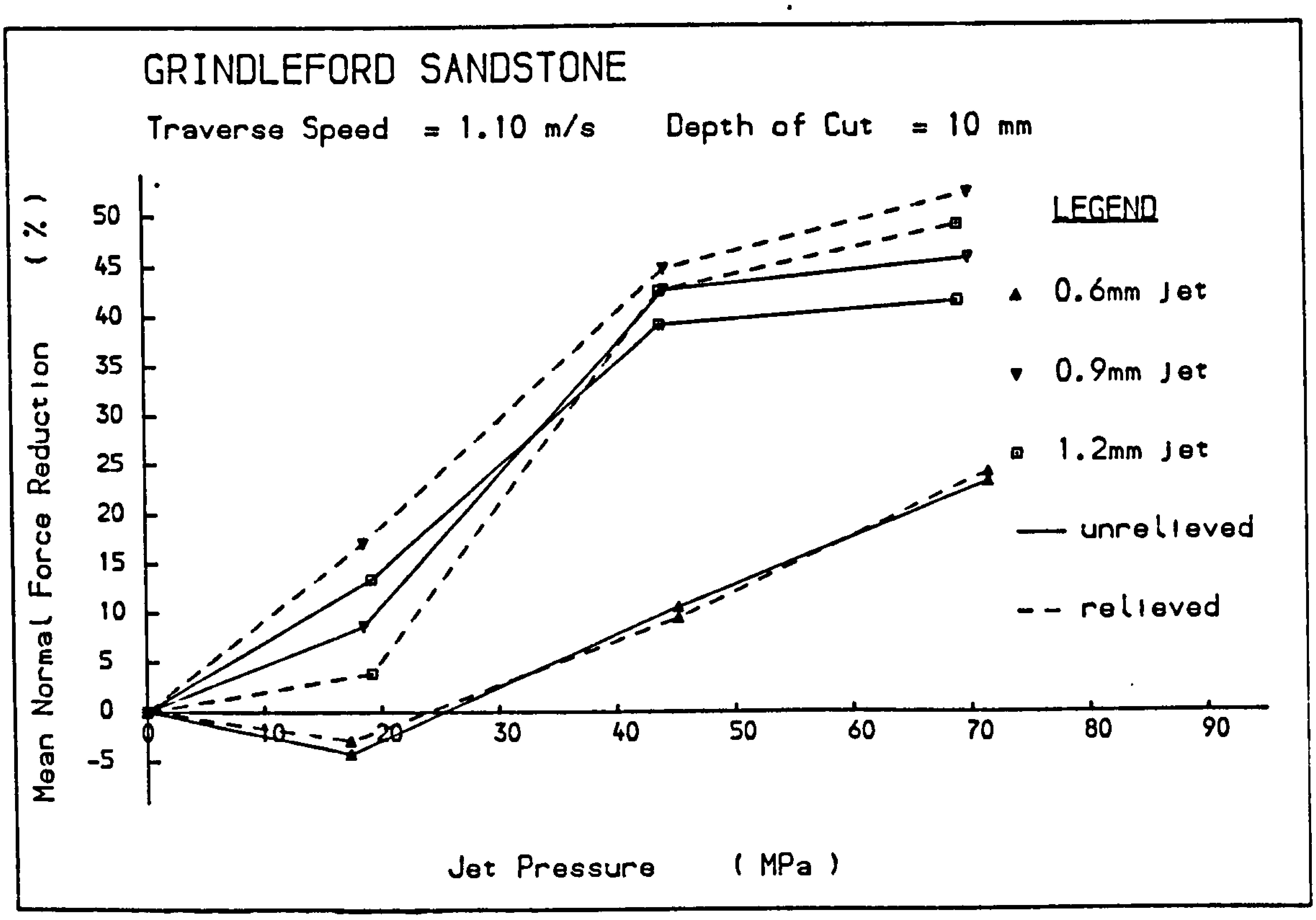

Figure 8.21 Mean Normal Force Reductions versus Jet Pressure for Various Nozzle Diameters in Relieved or Unrelieved cutting mode : Grindleford Sandstone.

reductions for the relieved cuts seem to be higher than those for the unrelieved cuts, especially as the jet pressure approaches 70 MPa. The reason could well be the fact that there were longer chips found for the relieved cuts (Plate 8.2). Hence the tool forces are composed of higher crushing force components and, therefore, more benefit was derived from the tip relief provided by the water jet. The optimum jet penetration, which is also dependent on the proportion of crushing, is expected to be higher (Section 8.3.2). This seems the case as estimated from the trends shown in the force reduction curves.

8.6.2 Jet Penetration Insignificant (Pennant Sandstone)

Although both force reductions were insignificant, as expected in this category of rocks, there was greater force reduction for relieved cutting compared with unrelieved cutting (Figure 8.22). The results are attributed, again, to the longer chips for relieved cuts. Longer chips resulted in less chipping events and more crushing events and hence the more work the water jet can do in the debris clearance to minimise grinding underneath the wearflat.

8.7 Effect of Slot Depth

In order to prove the proposed cutting mechanism of the hybrid cutting, a limited study was made to investigate the effect of slot depth on drag tool cutting. The rock used was Grindleford Sandstone.

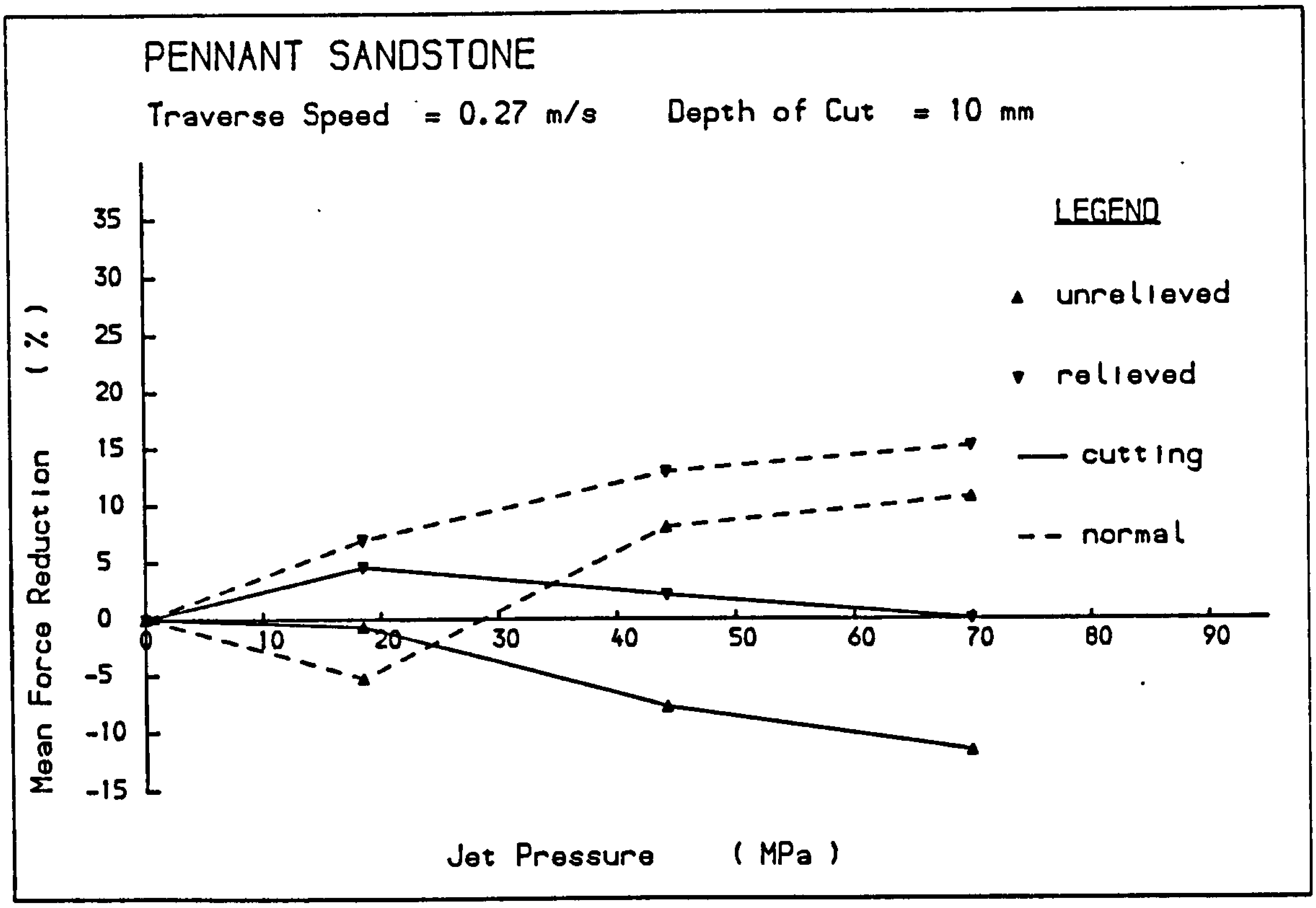

Figure 8.22 Mean Force Reduction versus Jet Pressure for Relieved or Unrelieved cutting mode : Pennant Sandstone.

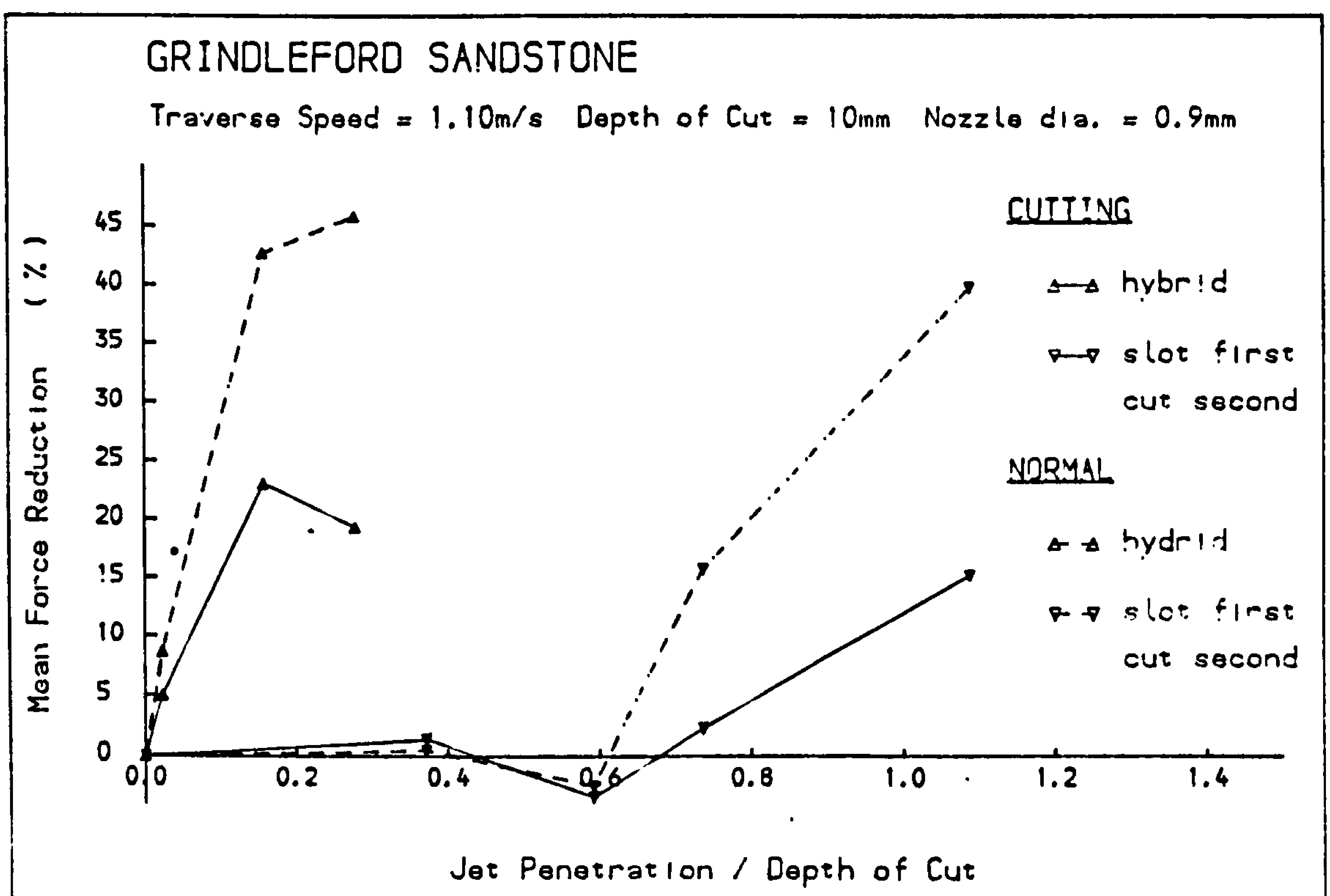

Figure 8.23 Mean Force Reduction versus Slot Depth for the jet acting together or separately with the tool : Grindleford Sandstone.

Slots of various depths were cut in a flat rock surface using a water jet of 70 MPa at different traverse speeds. A 0.9mm diameter nozzle was used and the depths of jet penetration were measured. The sharp tool was then positioned in line with the slot and the unrelieved independent cuts were then taken. The traverse speed was 1.10 m/s and the mechanical depth of cut was set to 10mm. The results are plotted in Figure 8.23 together with the results when the tool and jet acted together.

It is obvious from the figure that the jet must be superimposed onto the tool with the jet as near to the tool tip as possible in order to obtain maximum benefit with the same jet power. In the hybrid cutting the water jet makes use of the post-chipping curvilinear surface to relieve the tool tip. The nearer the jet impingement to the tool tip (lead-on distance) the less jet penetration required for the same relieving effect. If the lead-on distance is larger than the chip length, hybrid cutting will lose most of its advantage of dynamic penetration and the cutting becomes one of cutting rock with a preformed slot in the tool path. Findings showing the benefits of reduced lead-on distance were reported elsewhere (Ozdemir and Evans 1983; Tecen 1982; Plumpton and Tomlin 1982; Dubugnon 1981; Hood 1976) although no explanation was given. Figure 8.24 illustrates the difference schematically.

From the figure, it can be seen that the beneficial effect of the slot in the tool-after-slot cuts is possible only when the slot is over 7mm, i.e 70% mechanical depth of cut. It clearly shows that all the tool actions are concentrated at the

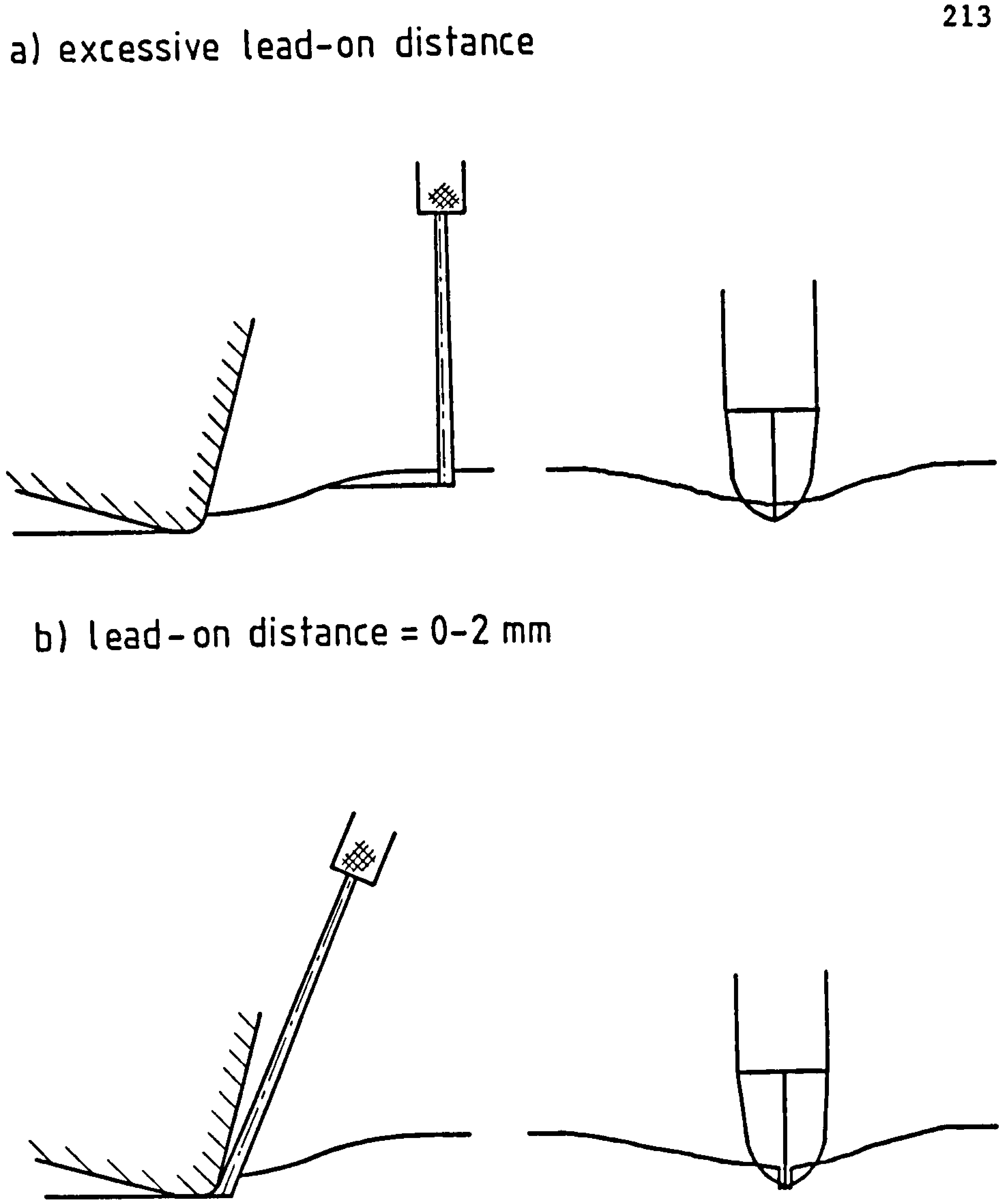

Figure 8.24 Schematic illustration of the effect of lead-on distance.

bottom few millimetres of cut where the centre of the crack system is situated. The value of 70% corresponds to the chip depth which is also around 70% of the 10mm mechanical depth of cut. Hence any slot depth less than the chip depth has no relieving effect for the tool tip. Obviously the above statement is only applicable to the tool-after-slot configuration, and the slot depth requirement for the hybrid cutting is much reduced. However, the results do show the importance of the bottom few millimetres of cut and the slot must be deep enough to provide any beneficial relief effect to reduce the tool force.

8.8 Summary

Through the smaller, but dedicated, experiment design, various variables likely to influence the water jet assistance have been studied.

The most important finding in this secondary phase experiment is to recognise the importance of jet penetration in tool force reduction. The difference between the rocks with significant jet penetration and those without significant jet penetration, which is not very clear when a pristine tool is used, becomes obvious when a blunt tool is used. As all tunnelling machines cut rocks with 'blunt' tools, the practical implication is significant. It shows that unless the water jet is powerful enough to penetrate the rock, marginal force reductions are obtained.

The importance of jet penetration is further recognised when water jets of different diameters are used. The slot width is proved to be of secondary importance compared with jet penetration.

When the rocks are too strong to be penetrated, the benefits derived from the water jet are the cooling of the tool tip and hence increased resistance to wear. The reduced wear rate leads to a longer efficient cutting form for the tool tip and longer tool life.

When the water jet is positioned behind the tool the non-matching of the jet impingement angle and the wearflat angle render the tool tip incompletely relieved. In addition, the jet loses some functions such as debris removal, and benefit from jet-behind-tool configuration is reduced.

Most of the cuts taken during this research programme were unrelieved and carried out on a trimmed rock surface. The relieved cutting results demonstrated that the trends established for unrelieved cutting are applicable to the practical rock cutting situation though there may be further minor improvements to be gained with relieved cutting.

The proposed model of water jet assisted drag tool rock cutting was found to be successful in predicting the trends for the effect of nozzle diameter, tool bluntness and cutting mode. The optimum jet penetrations and corresponding maximum force reductions were found to depend on the tool bluntness and cutting mode as well as traverse speed, depth of cut and rock type.

*   *   *

CHAPTER NINE

CHAPTER NINE

THE PREDICTION OF FORCE REDUCTIONS IN WATER JET ASSISTED ROCK CUTTING

9.1 Introduction

Knowing the results in advance is always advantageous. This is particularly true for the tunnelling profession. It is very desirable to know the excavation characteristics of rocks at the site investigation stage. Not only can the appropriate tunnelling machine be chosen, but the advance rate can also be predicted. Knowing the machineability of rocks also helps with planning the schedule and smooth running of the tunnelling project, which can result in enormous economic returns. Furthermore, the tender can be more accurate and the risk to a tunnelling firm reduced. Legal disputes between the client and the tunnelling consultant and/or contractor on the issue of unforeseeable geological situations, which is the most common one, is also reduced. The desire to estimate the rock machineability using small samples has led to extensive research in this University to investigate the correlation of rock properties and tunnelling machine performance (McFeat-Smith 1975; Fowell and Pyecroft 1980; Johnson 1985).

As the water jet assisted roadheader is expected to be fully commercialised in the very near future, the desire to estimate assistance from water jets is growing. Because so many variables and unknowns are involved in water jet assisted cutting, which include rock variables, tool variables, jet variables and operational variables, it is virtually impossible to approach the solution in a theoretical way. Basically an empirical approach is adopted, whilst knowledge of basic principles is still applied.

In this chapter, the unassisted tool forces are firstly predicted using the simple physical and mechanical properties of rocks. Due to the importance of jet penetration for predicting the force reductions with water jet assisted cutting, the theories of water jet rock cutting are first critically assessed using the experimental data obtained from this project. Based on the experimental results, a function is proposed to generalise the tool force reduction characteristics with the jet penetration. For the rocks without jet penetration, the critical jet power which signified the dominance of hydraulic fracturing is predicted by a suggested equation.

9.2 Prediction of Tool Forces in Drag Tool Rock Cutting

9.2.1 Suggested Empirical Equation

A simple empirical approach is adopted to predict the mechanical tool forces in the unassisted, unrelieved cutting mode on the five rocks. An elaborate or theoretical approach is deemed unnecessary and inappropriate for the following reasons:

(1) The published rock cutting theories, including Evan's Theory and Nashimatsu's Theory, are only applicable to the simple chisel-type drag tool. The tool used in this project has a tip geometry which is too complex to be modelled.

(2) There is no point in having an elaborate prediction equation which can only be used with one type of drag tool.

(3) The tool forces are measured from the unrelieved cuts which are uncommon in a tunnelling machine.

(4) During a tunnelling project, a tunnelling machine has to cut different types of rock with various degrees of cuttability. It is essential to make rapid assessment of the cuttability of a wide range of rocks rather than a detailed study of only one type of rock.

For the dual purpose of predicting the tool force and to study the sensitivity of the cuttability to certain mechanical and physical properties of the rocks, the tool forces are predicted using the equation:

$$\text{Tool force} = K\,(\,RI\,)^{m}\,(d)^{n}$$

where RI = rock property index

d = depth of cut

K, m and n = constants.

The effects of tool tip geometry, in this case, will be implied in the values of K, m, n as determined. The values of the constants K, m and n are determined by means of least square optimisation using the public NAG computer program available from the Computing Laboratory in this University. The goodness of fit is judged by the sum of squares of the residuals. The rock index having the least sum of squares of the residuals is the most indicative property on the cuttability of rock.

In total, nine physical and mechanical properties are included in this exercise, and the methods of determining the rock properties are set out in Chapter Five.

In this exercise, all the unassisted and unrelieved cutting results from various depths of cut for all five rock types at slow traverse speed are included.

9.2.2 Results

The physical and mechanical properties tested, together with the corresponding sum of squares of the residuals, are presented in tabular form in Appendix E .

At the slow traverse speed (0.27 m/s), the uniaxial compressive strength gives the best correlation in both the cutting and the normal force. Good linear correlation coefficients of 0.994 and 0.991 were obtained between the actual forces and predicted forces for the mean cutting and mean normal components respectively. This highlights the reason why the uniaxial compressive strength is sometimes the only rock parameter used in rock cuttability assessment. The better prediction obtained using the uniaxial compressive strength than the uniaxial tensile strength may well be due to the importance of confining compression and crushing actions with this drag tool.

The constants K, m and n, of the equation are estimated and tabulated in Table 9.1, together with the sum of squares of residuals and the correlation coefficient, when the uniaxial compressive strength is used as the rock cuttability index.

	MCF	MNF	MPCF	MPNF
K	0.008777	0.002815	0.024422	0.014585
m	0.629900	0.075500	0.570200	0.820500
n	1.402700	1.075200	1.448300	1.164400
s.s	1.356800	3.192400	19.694000	42.181800
r	0.994000	0.991000	0.984000	0.965000

Table 9.1 Coefficients of Prediction Equations using Uniaxial Compressive Strength as Rock Cuttability Index.

The accuracy of the prediction equation can be improved by including more rock parameters (McFeat-Smith and Fowell 1977). However, it is decided not to further the exercise as the rock types studied are not sufficient to justify the validity of a general prediction equation.

9.2.3 Discussion

The effect of traverse speed on the tool forces was found to exist in Grindleford Sandstone, Penrith Sandstone and Pennant Sandstone, but not in Dumfries Sandstone or Middleton Limestone (Section 7.2.2). When cutting at the fast speed, other rock properties in addition to the uniaxial compressive strength take effect which are yet to be determined. Although the effect of traverse speed is found to be highly correlated to the abrasivity, the number of rocks tested was not sufficient to indicate any relationship. A prediction equation without discriminating this effect is unsafe and inappropriate. Hence to predict tool forces at the fast cutting speed was not undertaken. Dedicated research is suggested to investigate the speed effect and the related rock properties as it is so important to drag tool cutting and thus tunnelling machine performance.

9.3 Prediction of Water Jet Penetration in Rocks

Because of the importance of the jet penetration to the force reductions due to water jet assistance, it is desirable to predict the jet penetration based on the jet parameters, operational parameters and the rock properties.

In this section, the published jet cutting equations, either empirical or theoretical, are critically assessed using the laboratory experimental data from this project. The cutting equations are modified where an improvement in the prediction accuracy could be achieved.

9.3.1 Rehbinder's Theory

Rehbinder (1976) developed a jet cutting equation which shows that jet penetration is a function of pressure, jet diameter, grain size, permeability of the rock and the time of exposure.

$$\frac{h}{d_o} = \begin{cases} \dfrac{D}{d_o \beta} \ln \left(1 + \dfrac{\beta k P_o}{\mu \bar{\ell} D} T\right) & T < T_o = \dfrac{\mu \bar{\ell} D}{\beta k P_o} \left(\dfrac{P_o}{P_{th}} - 1\right) \\ \\ \dfrac{D}{d_o \beta} \ln \dfrac{P_o}{P_{th}} & T > T_o = \dfrac{\mu \bar{\ell} D}{\beta k P_o} \left(\dfrac{P_o}{P_{th}} - 1\right) \end{cases}$$

where D = width of the slot

d_o = jet diameter

h = slot depth

$\bar{\ell}$ = average grain size of the rock

P_o = stagnation pressure of the jet

P_{th} = threshold pressure of the rock

T = time of exposure = d_o/v

T_o = critical time of exposure

v = traversing speed of the jet

β = coefficient of pressure drop in a slot

k = modified permeability

ρ = density of water

μ = viscosity of water

The rock is characterised by its erosion resistance, $\bar{\ell}/k$, and its threshold pressure P_{th} (Rehbinder 1978). When T is very small and the slot is shallow ($h/D < 10$).

$$h = \frac{k}{\mu \bar{\ell}} P_o \cdot T = \frac{k}{\mu \bar{\ell}} \cdot P \cdot \frac{d_o}{v}$$

The specific erodability $k/\mu\bar{\ell}$ can be determined from the experimental data. The results are shown in Appendix E . It showed that the specific erodability $k/\mu\bar{\ell}$ is not a constant. Instead, it changes with traverse speed.

A modified Rehbinder's solution is suggested by assuming the specific erodability is proportional to the traverse speed. A linear relationship is established by means of least square curve fitting of experimental data.

<u>Dumfries Sandstone</u>

$$\frac{k}{\mu\bar{\ell}} = [0.508 + 1.550 \times V\ (m/s)] \times 10^{-7}\ m^3/NS$$

correlation coefficient = 0.935

<u>Grindleford Sandstone</u>

$$\frac{k}{\mu\bar{\ell}} = [1.173 + 2.815 \times V\ (m/s)] \times 10^{-8}\ m^3/NS$$

correlation coefficient = 0.914

<u>Penrith Sandstone</u>

$$\frac{k}{\mu\bar{\ell}} = [1.186 + 3.621 \times V\ (m/s)] \times 10^{-8}\ m^3/NS$$

correlation coefficient = 0.918

The estimated jet penetrations using both methods are shown in Appendix E. For the Rehbinder solution, the mean specific erodability is used. For the modified Rehbinder solution, the specific erodabilities are estimated using the linear relationship with the traverse speed.

9.3.2 Hashish's Theory

Hashish and du Plessis (1978) developed a compact, non-dimensional equation to predict the jet penetration of a wide range of solid materials by continuous high velocity water jets. The theory was based on a control volume analysis to determine the hydrodynamic forces acting on the solid boundaries of the cutting slot.

$$\frac{h}{d_o} = \frac{1-(\frac{\sigma y}{\rho V_o^2})}{\frac{2Cf}{\sqrt{\pi}}} \left[1-e^{-(\frac{2Cf}{\sqrt{\pi}}) \cdot (\frac{\rho V_o}{\eta}) (\frac{V_o}{V})}\right]$$

where C_f = hydrodynamic coefficient of friction

d_o = nozzle diameter

h = depth of cut

V_o = jet speed

v = traverse speed

η = damping coefficient

σ_y = compressive yield strength

ρ = fluid density.

The model assumed the compressive failure of the material is the dominant cutting mechanism and the theory predicts that the jet cutting occurs when:

$$\text{Jet Pressure} = p > 0.5\sigma_c$$

where σ_c = compressive strength

However, the measured threshold pressures are much lower than those of the estimated values (Table 7.2). It implies cutting mechanisms may operate other than that of compressive failure.

A test was carried out to estimate the total skin friction coefficient, cf, for various rocks. The jet penetration at zero traverse speed is measured and the skin friction coefficient Cf, is determined using the equation:

$$\frac{h}{d_o} = \frac{1 - \left(\frac{\sigma \, cf}{\rho V_o^2}\right)}{\frac{2Cf}{\sqrt{\pi}}}$$

The total skin friction coefficients of various rocks are tabulated in Table 9.2. Negative skin frictions were obtained, usually at low jet pressure, when the depth of cuts in Grindleford Sandstone and Penrith Sandstone were substituted into the equation. Additionally, the friction coefficient is not constant and changes significantly with pressure. The inapplicability of the theory to these sandstones could well be due to the fact that this theory assumes the jet penetration is in the form of pure mechanical fracture and ignores the effect of pore pressure. In the water jet assisted rock cutting, the jet transmits the hydraulic pressure loading as well as pressurising the pore spaces. If pore pressurisation is impossible the threshold pressure is much higher even when the material is the same. The effect of pore pressure in wet rock cutting is verified (Foreman and Secor 1974) and the related rock properties, especially permeability, are recognised in other water jet rock cutting theories (Crow 1973; Rehbinder 1976, 1977). Furthermore, sandstones are usually composed of quartz grains cemented together. In the water jet cutting of weak to medium sandstones, it is most likely that stronger grains are eroded out

Rock Type	Compressive Strength (MPa)	Nozzle Dia. (mm)	Jet Pressure (MPa)	Jet Speed (m/s)	Jet Penetration (mm)	Skin Friction Coefficient, C_f
Dumfries Sandstone	22.7	0.9	18.5	192	14.0	0.0219
			44.2	297	39.0	0.0152
Grindleford Sandstone	58.9	0.6	17.3	186	2.0	-0.1868
			45.2	301	5.5	0.0338
			71.5	378	7.0	0.0446
		0.9	18.5	192	6.0	-0.0795
			44.2	297	13.0	0.0204
			69.9	374	18.0	0.0257
		1.2	19.2	196	5.0	-0.1134
			43.8	296	10.0	0.0349
			69.9	372	19.0	0.0321
Penrith Sandstone	82.9	0.9	18.5	192	4.5	-0.2213
			44.2	297	13.5	0.0036
			69.9	374	16.5	0.0197

Table 9.2 Total Skin Friction Coefficient C_f for Various Rocks.

from the weaker cementing materials. Hence the model of compressive failure may not be justified and the threshold pressure is much lower than expected.

Instead of calculating the skin friction coefficient, Cf, by means of slotting at zero or very slow speed, Cf is estimated together with the yield strength σ_y, and damping coefficient, η, by the optimisation technique using experimental data. The estimated Cf, σ_y, and η are tabulated in Table 9.3.

	Dumfries Sandstone	Grindleford Sandstone	Penrith Sandstone
Cf	0.0335	0.1327	0.1456
σ_y(MPa)	25.8772	32.0185	24.8349
η(kt/m^{2}s)	4.6981	26.7459	22.8901

Table 9.3 Estimated parameters of Hashish's Equation for Various Rocks.

The estimated skin friction coefficient Cf is higher than expected, due to the low threshold pressure. The predicted jet penetration using the estimated Cf, σ_y, and η, are set out in tabular form in Appendix E.

9.3.3 Empirical Cutting Theory

Kuzmich *et al*. (1982) summarised experimental data obtained by different authors and suggested a generalised formula.

for calculating the jet penetration for a single jet pass:

Kuzmich's Equation:

$$\frac{h}{d_o} = 0.11 \left(\frac{P_o}{\sigma_c}\right)^{0.75} \left(\frac{V_o}{V}\right)^{0.5}$$

where: h = jet penetration

d_o = nozzle diameter

P_o = stagnation pressure

σ_c = uniaxial compressive strength

V_o = jet velocity

V = jet traverse speed.

To enable Kuzmich's equation to be refined to suit different rock materials, a modified Kuzmich equation is suggested here as:

Modified Kuzmich's Equation:

$$\frac{h}{d_o} = B \left(\frac{P_o}{\sigma_c}\right)^m \left(\frac{V_o}{V}\right)^n$$

where: B, m and n are constants for each material and are determined by the technique of optimisation, using the University's NAG FORTRAN computer public file.

Cooley (1974) modified Nikonov's equation (1972) and found the following equation has applications in slotting tests in various materials:

Cooley's Equation:

$$\frac{h}{d_o} = B\left(\frac{P_o}{\sigma_c} - 0.2\right)\left(\frac{V}{V_o}\right)^{-m}$$

where:

B = constant for each material

m = constant, equal to 0.5 for coal and 0.5-1.0 for other materials.

Both B and m are determined by the technique of optimisation.

The least square estimated constant coefficients for the modified Kuzmich's equation and Cooley's equation are shown in Table 9.4.

Sandstone	Modified Kuzmich's Equation			Cooley's Equation	
	B	m	n	B	m
Dumfries	0.8451	0.9530	0.3117	0.9967	0.2921
Grindleford	0.3164	1.1474	0.3624	0.5406	0.3183
Penrith	0.5522	0.9984	0.3438	1.0895	0.2922

Table 9.4 Estimated coefficients of Modified Kuzmich's and Cooley's equations for various rocks.

9.3.4 Results and Discussion

The actual jet penetrations, together with the predicted values, using various equations, are tabulated in Appendix E for the rock types with significant jet penetration, i.e. Dumfries, Grindleford and Penrith sandstones. The accuracy of the prediction is compared using the sum of squares of the residuals, while the linear correlation coefficient for actual and predicted jet penetrations is used to judge the appropriateness of the equation.

A small sum of squares of the residuals implies an accurate prediction, while the nearer the correlation coefficient is to 1.0 indicates the better the form of the prediction equation, as the prediction has the same trend as the actual results. The correlation coefficient of each prediction equation is included in the table for each rock.

Among these six prediction equations, Kuzmich's equation gave probably the worst prediction, as reflected by the large sum of squares of the residuals in these rocks. However, the equation form is good because the correlation coefficient is high, which is around 0.97, despite its simplicity. It highlights the problem of using prediction equations with coefficients 'fixed' in the field of water jet cutting. Water jet cutting is a very complicated action with so many factors capable of affecting the results. Hence the prediction equation should have a sufficient degree of flexibility to suit different situations, and that possibly accounts for the best predictions in both the trend and accuracy of the modified Kuzmich's equation. Cooley's equation performs inferior to the modified Kuzmich's equation, due probably to having only two estimated coefficients rather than three.

If the mean specific erodability is used, the Rehbinder's equation gives a poor prediction, indicated by the small correlation coefficient and the large sum of square of the residuals. The problem is the inconsistency of the specific erodability for different traverse speeds. When the specific erodability is assumed to have a linear relationship with the traverse speed and the specific erodability is estimated using the linear equation, the modified Rehbinder's equation produces improved results. The specific erodability is observed to change with traverse speed in a similar manner to the hydraulic specific energy, which tends to become constant when the traverse speed is over a critical speed which is in the region of 0.7-0.8 m/s. It is suspected that the jet cutting mechanism may be changing and resulting in a better erodability of the jet at higher speed. Hashish's prediction equation is complex and does not show an improved goodness of fit.

Basically all prediction equations, including Hashish's equation and Rehbinder's equation, involve an exercise in curve fitting using the results of 'reference' experiments. This approach is inevitable as it is impossible to embody so many parameters that are capable of affecting the results and quantify them in one single prediction equation. The failure of Crow's equation is partly attributed to his attempt to quantify the variables using laboratory determined parameters rather than estimating them using experimental data. In an overall assessment, the modified Kuzmich's equation gives the best correlation result. However, like all the curve-fitting equations, care must be exercised when extrapolating the results beyond the experiment conditions upon which the prediction equation is based.

9.4 Prediction of Force Reductions in Water Jet Assisted Rock Cutting : Rocks with Significant Jet Penetration

Although research has been carried out worldwide to investigate water jet assisted rock cutting, it is still impossible to produce a theory that can predict force reductions achieved with water jet assistance. The difficulty is obvious. There are four types of variables; namely, jet variables, tool variables, operational variables and rock variables. Infinitive combinations can be formed by the variation of these variables. Hence it is impractical, as well as impossible, to try to formulate a general theory that can predict force reduction.

The most common approach is the use of an empirical equation to summarise the results for the limited range of variables that are most relevant. The validity of published empirical equations are first examined. Based on an analysis of experimental data and the proposed hybrid cutting model, an empirical function is established.

9.4.1 Assessment of Kuzmich's Equation

Kuzmich *et al*. (1982) investigated hydromechanical rock cutting and considered the role of the jet as providing a slot to relieve the tool mechanically. When the jet was positioned in line and before the tool, a simple equation was proposed which characterised the decrease of cutting force in hybrid cutting, as compared with mechanical cutting.

$$\frac{F_c\ (h-m)}{F_c(m)} = 1 - 0.4\ \left(\frac{h}{d}\right)^{0.5}$$

where $F_c\ (h-m)$ = hydromechanical cutting force

$F_c\ (m)$ = mechanical cutting force

h = slot depth

d = mechanical depth of cut

Based on an analysis of the experimental data, the depth of slot is considered as having a functional relationship with jet velocity, nozzle diameter, traverse speed and uniaxial compressive strength of the rock. Slot depth can be estimated using an empirical equation:

$$\frac{h}{d_o} = 0.11 \left(\frac{P_o}{\sigma_c}\right)^{0.75} \left(\frac{V_o}{V}\right)^{0.5}$$

where h = slot depth

d_o = nozzle diameter

P_o = stagnation pressure

σ_c = uniaxial compressive strength

V_o = jet velocity

V = jet traverse speed.

Hence, if both equations are correct, force reductions achieved with water jet assistance can be predicted by knowing the appropriate jet parameters, operational parameters and rock strength. The potential practical advantages are significant.

In order to assess the applicability of the equations, experimental results obtained during the present study are compared with predicted values. The results are tabulated in Appendix E. Only rocks with significant jet penetration were analysed, including Dumfries Sandstone, Grindleford Sandstone and Penrith Sandstone.

The predicted force reductions are based on the predicted slot depth as well as actual slot depth. For the Penrith Sandstone, the jet penetrations during hybrid cutting are estimated by linear interpolation of slot testing data.

The predicted force reductions in percentage are compared with actual force reductions measured, both in mean cutting force and the 95% mean peak cutting force. The linear relationship between predicted and measured reductions is estimated by the correlation coefficient r. A perfect relationship exists when $r = \pm 1$, and a weak relationship when r is close to zero. The index of determination $= r^2$, which measures variation in the values of the predicted reductions that is accountable for the linear relationship with the measured values is enclosed in brackets and given in tabular form in Table 9.5, together with the correlation coefficient r.

Obviously these predictions do not have a strong relationship with the measured values. The index of determination is usually below 50%, indicating that less than half of the predictions are accountable for the linear relationship. A higher value was obtained between predicted and measured mean peak cutting force reductions in Grindleford Sandstone, but the values of less than 58% are still unsatisfactory.

Although this theory recognises the importance of jet penetration, the simplicity of the approach fails to provide a model capable of application to a wider range of rocks in different cutting conditions. The prediction of unlimited force reductions with slot depth is clearly unjustified.

	Dumfries Sandstone	Grindleford Sandstone	Penrith Sandstone
(1) and (3)	0.17 (0.03)	0.52 (0.27)	0.53 (0.28)
(1) and (4)	0.49 (0.24)	0.76 (0.58)	0.70 (0.48)
(2) and (3)	0.18 (0.03)	0.67 (0.45)	0.52 (0.27)
(2) and (4)	0.34 (0.12)	0.78 (0.60)	0.63 (0.40)

(1) = Predicted Cutting Force Reduction based on predicted Jet Penetration.

(2) = Predicted Cutting Force Reduction based on Actual Jet Penetration.

(3) = Actual Mean Cutting Force Reduction.

(4) = Actual Mean Peak Cutting Force Reduction.

Table 9.5 Correlation Coefficients between Actual and Predicted Force Reductions.

9.4.2 Suggested Empirical Equation

Based on the proposed hybrid cutting model and an analysis of experimental results, it is suggested that force reductions could be expressed as a function of jet penetration, depth of cut, traverse speed and tool bluntness.

$$\frac{F\ (h-m)}{F(m)} = f\ (h,d,V,\omega)$$

where: F(h-m) = tool force with water jet assistance

F(m) = tool force without water jet assistance

h = jet penetration

d = depth of cut

V = traverse speed

ω = tool wear

The functional dependence of force reductions on different parameters can be generalised with respect to jet penetration (Figure 9.1). Basically, maximum force reductions are dependent on tool bluntness, traverse speed, depth of cut and tool component considered. Optimum jet penetration, however, would seem to be independent of traverse speed. Some of the other variables are capable of influencing the performance of the water jet, but have not been investigated in the present study due to their lesser importance when compared with other factors.

After identification of several important parameters, the functional relationship of each parameter has been evaluated. In order to simplify the investigation, only one parameter has been

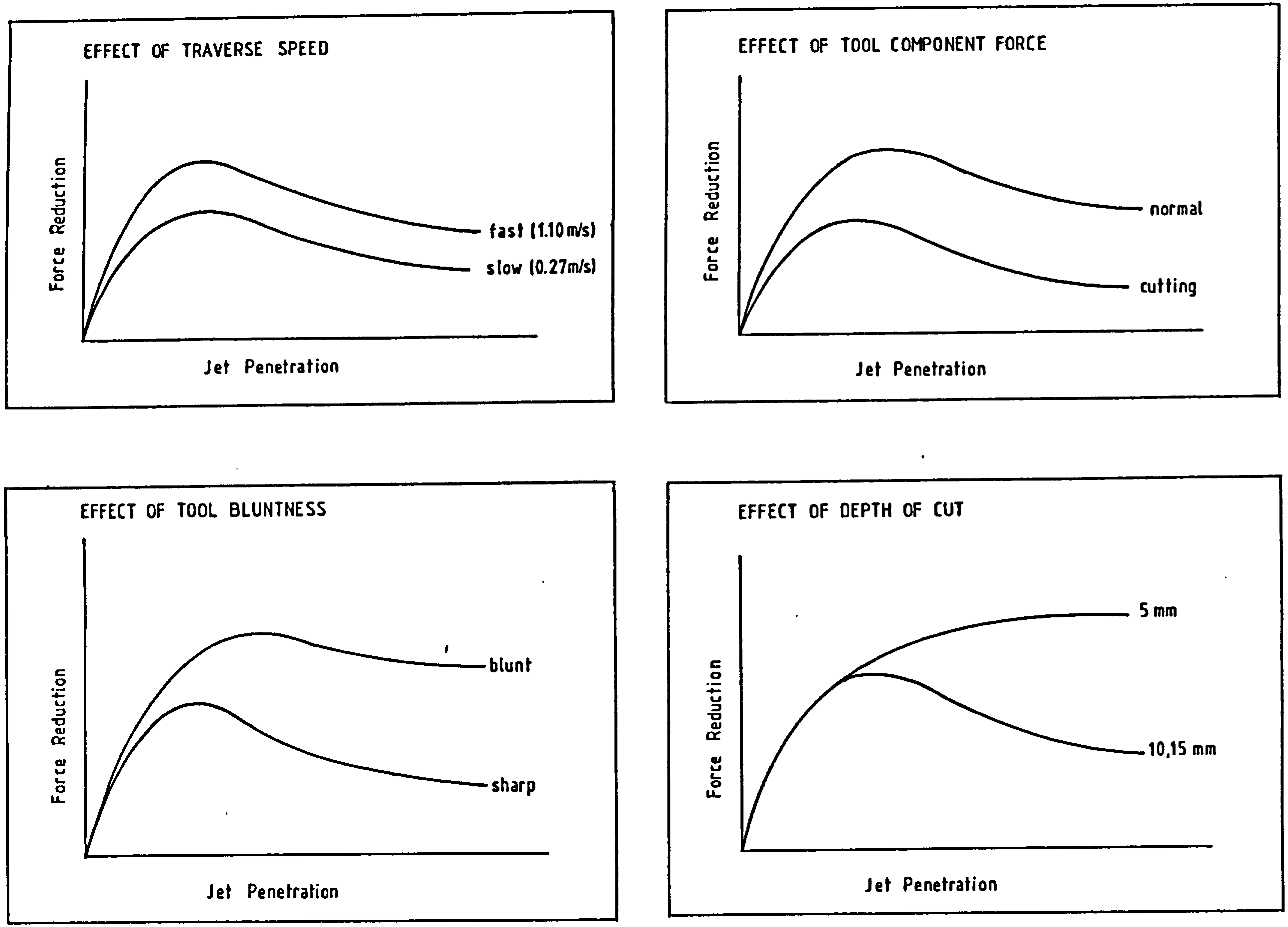

Figure 9.1 Generalised relationship between Force Reduction and Jet Penetration for various Parameters.

studied at one time, while other parameters were kept constant. If the functional relationship of this parameter is established, its validity can be proved by extending its application by including other variables.

For rocks with significant jet penetration, the importance of jet penetration is recognised as a unique parameter, capable of integrating effects of jet pressure, flow rate, nozzle design, stand-off distance and traverse speed, and is ideal to be used to quantify the water jet assistance for a particular rock. The functional relationship between force reduction and jet penetration $\phi(h)$ is first investigated:

$$\frac{F(h-m)}{F(m)} = f\ (d,\ v,\omega)\ \phi\,(h)$$

9.4.2.1 <u>Effect of Jet Penetration ($\phi(h)$)</u>

From the general shape of the force reduction-jet penetration curve (Figure 9.1), it can be seen that, with the exception of 5mm cuts, force reductions increase up to a maximum at optimal jet penetration and then decrease in a parabolic shaped curve. The force reductions tend to show a relatively constant residual value after excessive jet penetration.

Assuming $F_R = F_{Rmax}\ \phi\ (h)$

where: F_R = force reduction

F_{Rmax} = maximum force reduction

h = slot depth.

Actual force reduction curves are complex. However, they have a parabolic shape where slot depth is not excessive (i.e. <50% mechanical depth of cut). Assuming force reduction curves can be generalised using the parabolic function, then:

$$(x-k)^2 = 4a(b-y)$$

where x = jet penetration, h

y = force reduction, F_R

For boundary condition, assuming force reduction is negligible when slot depth is zero, i.e. $x = 0$, $y = 0$,

$$(0-k)^2 = 4a(b-0)$$

$$k^2 = 4ab$$

$$\therefore \quad (x-k)^2 = \frac{b}{k^2}(b-y)$$

Or, $$y = b - b\left(\frac{x-k}{k}\right)^2 = b\left(1 - \left(\frac{x-k}{k}\right)^2\right)$$

In this case, b will represent the maximum force reduction, F_{Rmax}, and K the optimal jet penetration, h_k.

$$F_R = F_{Rmax}\left(1 - \left(\frac{h-h_k}{h_k}\right)^2\right)$$

F_{Rmax} and h_k are estimated using the least squares optimisation technique based on the jet penetration characteristics of the rock and the actual force reductions at different traverse speeds and depths of cut. The analysis covers the primary experimental results in both Grindleford and Penrith sandstones. Only the jet-before-tool configuration is considered.

Evaluation of maximum force reductions and optimal jet penetrations are tabulated in Tables 9.6 and 9.7 for Grindleford Sandstone and Penrith Sandstone respectively. The optimum situation for 15mm cuts of Penrith Sandstone at 1.10 m/s is not located as described in Section 7.4.1. The cuts at 5mm depth, as discussed in Section 7.4.2 tend to have a much larger optimum jet penetration. These results are omitted in the analysis of optimal jet penetration.

Optimum Jet Penetration

It was observed from the analysed results that there is a consistent optimum jet penetration which is located within a narrow range of 20%-40% of the mechanical depth of cut for the sharp tools despite the different rocks tested, different traverse speeds and depths of cut. If all the results are pooled together then mean optimum jet penetration can be estimated as 25.1 ± 6.2% and 31.1 ± 9.4% of mechanical depth of cut for cutting and normal force reductions respectively. This difference shows quantitatively that optimum jet penetration is higher for the normal force than for cutting force, as observed previously (Section 7.4.1). The difference is statistically significant with a 95% confidence level.

The optimum jet penetrations obtained here are found to correlate closely with profiling depth measured in the chip shape analysis (Section 6.1.2). Table 9.8 presents optimum jet penetrations and profiling depths for each depth of cut for sharp tool cutting.

Depth of Cut (mm)	Cutting Speed (m/s)	Cutting Force		Normal Force	
		FRmax (%)	hk/d	FRmax(%)	hk/d
5	0.27	33.4	0.64	46.5	0.61
5	1.10	23.0	0.41	46.5	0.42
10	0.27	17.9	0.24	39.8	0.30
10	1.10	23.8	0.19	47.6	0.23
15	0.27	14.9	0.21	31.4	0.25
15	1.10	26.3	0.13	45.9	0.14

Table 9.6 Grindleford Sandstone : Maximum Force Reduction and Optimum Jet Penetration (Sharp Tool).

Depth of Cut (mm)	Cutting Speed (m/s)	Cutting Force		Normal Force	
		FRmax(%)	hk/d	FRmax(%)	hk/d
5	0.27	28.4	1.06	36.5	0.72
5	1.10	15.6	0.35	46.7	0.42
10	0.27	26.7	0.30	55.7	0.35
10	1.10	19.0	0.31	65.1	0.45
15	0.27	7.7	0.29	38.9	0.36
15	1.10	-	-	-	-

Table 9.7 Penrith Sandstone : Maximum Force Reduction and Optimum Jet Penetration (Sharp Tool).

Depth of Cut	Optimal Jet Penetration		Profiling Depth
	Cutting	Normal	
10 mm	2.7±0.5 (27%)	3.4±0.7 (34%)	2.8 (28%)
15 mm	3.2±1.2 (21%)	3.8±1.6 (25%)	3.5 (23%)

Table 9.8 Comparison between optimal jet penetration and profiling depth.

Profiling depth has a value somewhere between optimum jet penetration for cutting and normal force reductions. The comparatively higher optimum jet penetration for the normal force reduction means that the jet must penetrate and relieve the tool tip during profiling action in the zone of stable median cracks (Figure 6.2) and before the more productive chipping events occur.

Statistically there is no difference between profiling depths and optimum jet penetrations. Hence an analysis of chip depth during dry cutting may provide an estimate of optimum jet penetration in hybrid cutting. The practical implication is that the effects of different tool types on optimum jet pressure may be estimated. For example, a drag tool of large positive rake angle will tend to have a larger chip depth and a smaller profiling depth, hence smaller optimum jet penetration and thus smaller optimum jet pressure.

Further laboratory investigations are required to substantiate this postulation.

Maximum Tool Force Reductions

Maximum tool force reductions were found to be a function of rock type, traverse speed and depth of cut. If all the results for both Grindleford Sandstone and Penrith Sandstone are pooled together, maximum force reductions are 21.5 ± 7.3% and 45.5 ± 9.2% for mean cutting and mean normal force components respectively. The higher normal force reduction which is more than double the cutting force reduction in this case has been reported in all published works on water jet assisted cutting.

Goodness of Fit

In order to examine the suitability of using the parabolic function to characterise force reduction against jet penetration curves, the force reductions at different jet penetrations are estimated using the established maximum force reductions (FR_{max} and optimum jet penetrations, h_k, in Table 9.5). The actual force reductions and estimated force reductions are presented in tabular form in Appendix E, and are plotted in Figures 9.2 and 9.3 for cutting and normal force components respectively. A linear correlation is established between actual and estimated force reductions, with the correlation coefficient r = 0.954 and 0.975 for cutting and normal force reductions respectively. The high correlation coefficients imply that the parabolic function satisfactorily characterises the force reduction curves. Although

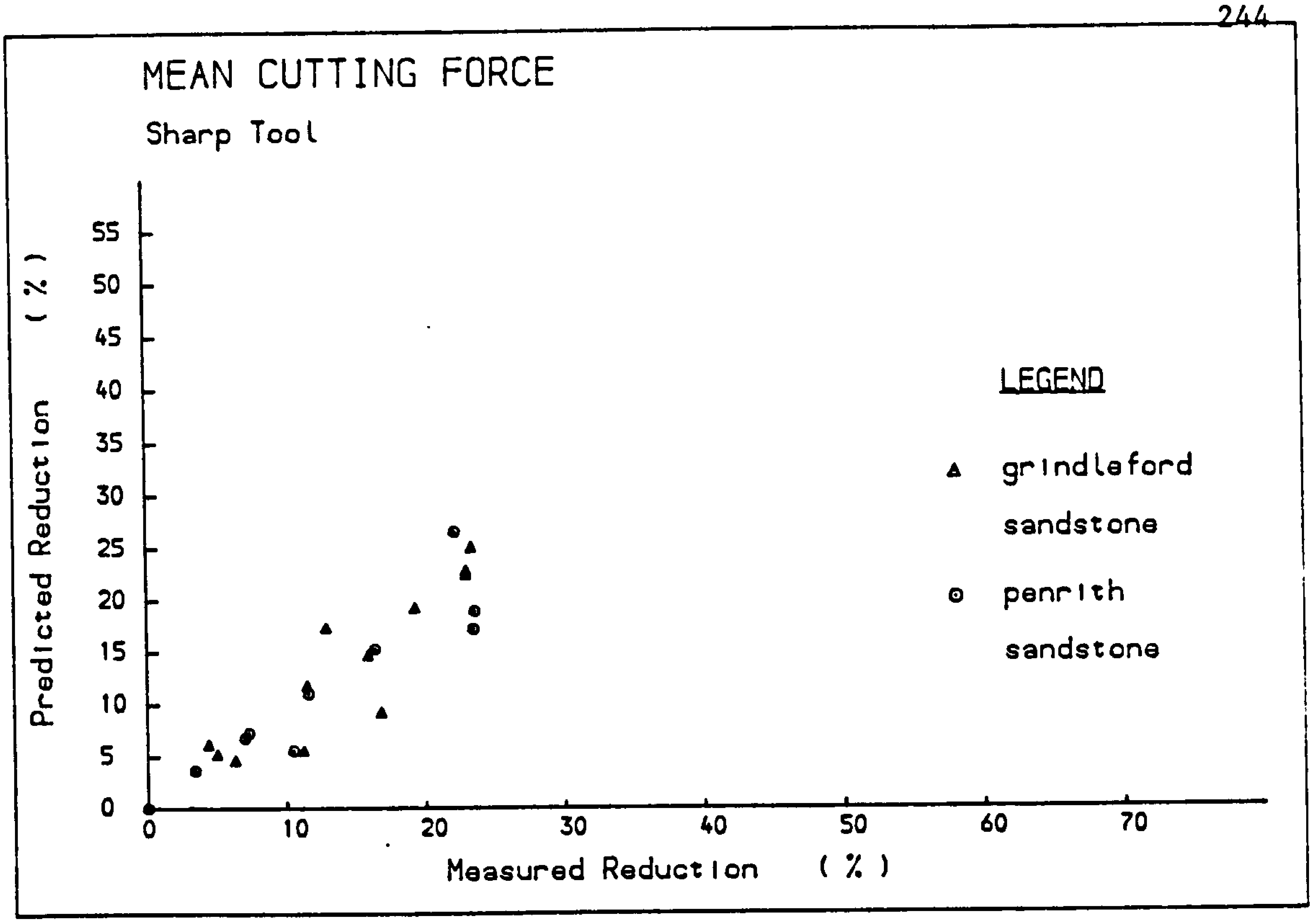

Figure 9.2 Measured and Predicted Mean Cutting Force Reduction; Grindleford and Penrith sandstones.

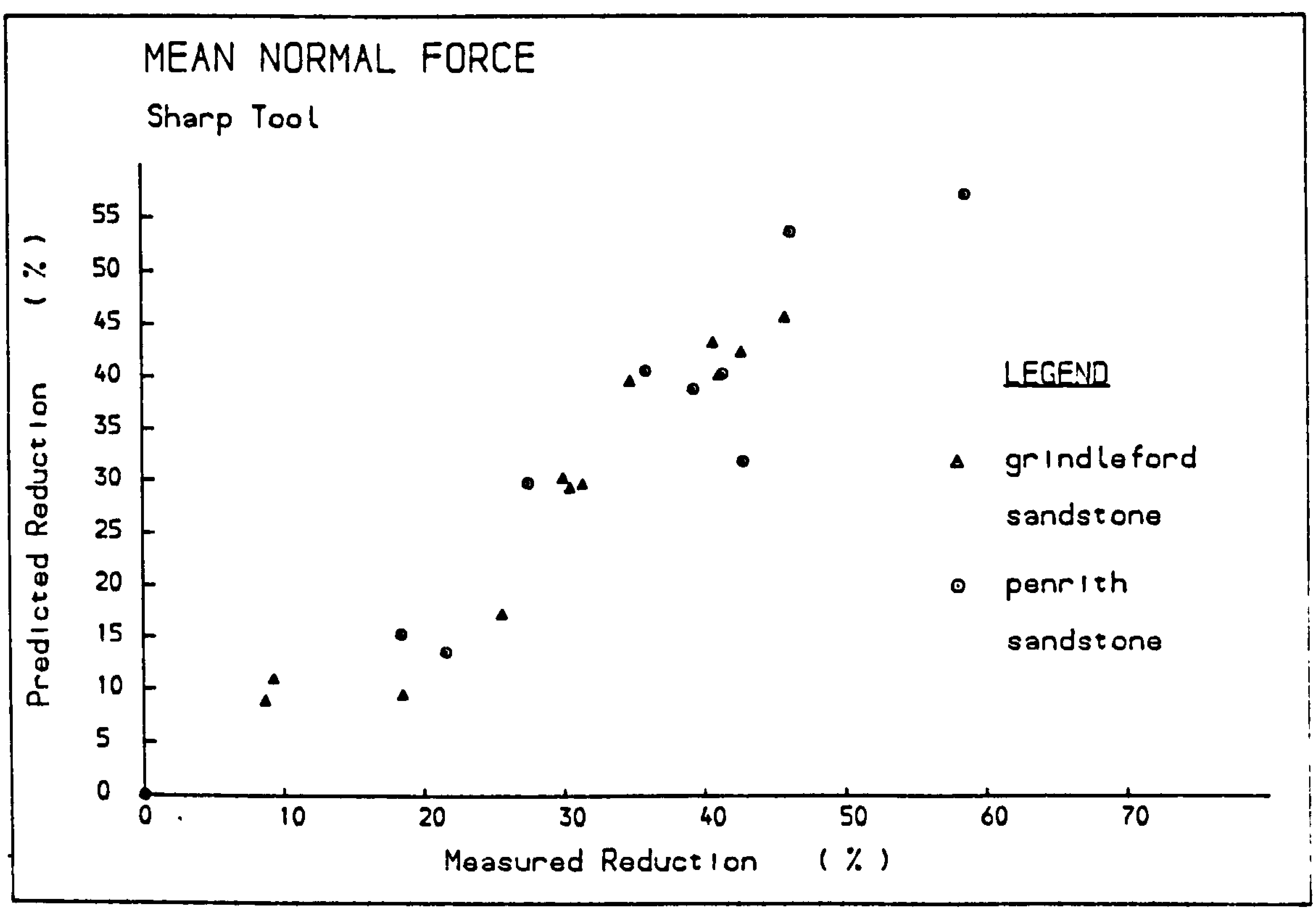

Figure 9.3 Measured and Predicted Mean Normal Force Reduction; Grindleford and Penrith sandstones.

other functions are possible, the parabolic function is preferred for its simplicity and the inclusion of the terms of optimum jet penetration and maximum force reduction.

9.4.2.2 Effect of Depth of Cut

The effect of depth of cut is the most difficult variable to quantify in a numerical expression. The difficulty is the need to find out the proportion of tool force spent in the events of crushing, profiling and chipping at different depths of cut. Only when this constitutive model is known can the net effect of the jet be estimated in a rational way. Hence maximum force reductions vary widely and no relationship was found.

The predominant profiling actions in the 5mm cuts favour a higher than expected value for the optimum jet penetration. For the 10mm and 15mm cuts, optimum jet penetration can be related to the depth of cut by means of chip depth.

9.4.2.3 Effect of Traverse Speed

As only two levels of traverse speed have been studied, it is impossible to derive any functional relationship between force reduction and traverse speed. Traverse speed is not an independent variable, and its effect is dependent on rock type as well. The speed effect may be due to rate of crushing underneath the wearflat (Section 7.2.2). The possible existence of a critical traverse speed that marks the commencement of the speed effect is also very difficult to determine using the present experimental design. Hence the effect of traverse speed on drag tool only cutting should be carefully studied before its effect on hybrid cutting can be estimated.

9.4.2.4 Effect of Tool Bluntness

From Table 9.6 it can be seen that optimum jet penetration and maximum force reductions are higher with blunt rather than with sharp tools. As only two levels of tool bluntness have been studied, no functional relationship between tool bluntness and optimum penetration or maximum force reduction has been established. However, it is expected that the blunter the tool, the higher the optimum jet penetration and maximum force reductions (Section 8.3.1).

An exercise in linear correlation of actual force reductions and predicted force reductions, using the values of maximum force reductions and optimum jet penetration as determined by the technique of least squares optimisation (Table 9.9), gave correlation coefficients of 0.961 and 0.979 for cutting and normal force reductions respectively. This implies that force reductions follow the same function as for a sharp tool, except a higher maximum force reduction and optimum jet penetration are required.

9.5 Prediction of Force Reductions in Water Jet Assisted Rock Cutting : Rocks with Insignificant Jet Penetration

9.5.1 Suggested Empirical Equation

When jet energy is too low, the water jet serves the purpose of flushing loosened debris to improve tool-rock force transmission, which contributes to a marginal reduction in tool force. If jet energy is sufficiently high, the water jet can penetrate and relieve the tool tip, which can reduce total tool force significantly when jet penetration is around the optimum.

Tool	Depth of Cut (mm)	Cutting Speed (m/s)	Cutting Force		Normal Force	
			F_{Rmax} (%)	hk/d	F_{Rmax} (%)	hk/d
Sharp	10	0.27	17.9	0.24	39.8	0.30
	10	1.10	23.8	0.19	47.6	0.23
Blunt	10	0.27	40.6	0.34	66.8	0.36
	10	1.10	29.5	0.30	69.0	0.24

Table 9.9 Grindleford Sandstone : Maximum Force Reduction and Optimum Jet Penetration (Sharp and Blunt Tool).

value. However, the threshold jet power for strong rocks can be very high. Before the threshold jet power is attained, a critical jet power may be reached with which the jet can gain access to the fracture system in the vicinity of the tool tip and help in chip spalling. As all strong rocks are very brittle and the cracking systems are quite extensive, the potential assistance from the water jet is substantial. The very encouraging results from 5mm hybrid cutting of Pennant Sandstone at 0.27 m/s traverse speed provides supporting evidence.

In this section, a conceptual model is developed to predict the critical jet power rather than the generally marginal force reductions before the critical jet power.

As described in Section 7.5, the critical jet power is the jet power required to break the finite rock thickness between the rock surface where the jet impinges and the crushed zone before the tip. This critical jet power is not considered an intrinsic constant, but depends on other variables.

(1) traverse speed which affects the jet energy available to the rock;

(2) depth of cut which affects the finite rock thickness between the rock surface and the crushed zone; and

(3) tensile strength of the rock which controls the ability of the jet to fracture the finite rock thickness.

Although the exact relationships between critical jet power and the above variables are not yet known, a linear relationship is regarded as a reasonable approximation, although other more detailed functions are also possible.

Hence:

Critical jet power (kW)

$$= K \times [\sigma_t] \times [d] \times [V]$$

where: K = proportionality constant (m)

σ_t = tensile strength (MPa)

d = depth of cut (mm)

V = traverse speed (m/s)

Now there is difficulty in determining the critical jet power. Ideally, critical jet power should be defined as the onset of hydraulic fracturing. However, this exact position is difficult to determine. Furthermore, force reductions are observed well before the occurrence of hydraulic fracturing, due to the jet's flushing power. Because of the substantial force reduction when hydraulic fracturing is significant, critical jet power is here defined as the jet power when the normal force reduction is 50%.

To examine the validity of the expression, the constant K is evaluated using the results for Pennant Sandstone and the published results of Dubugnon (1981). The results are tabulated in Table 9.10. The most striking results are the relatively

Researcher	Rock and Tensile Strength (MPa)	Depth of cut (mm)	Traverse Speed (m/s)	Critical Jet Power (kW)	Constant K (m)	Remarks
Dubugnon (1981)	Bohus Granite (22.2)**	6	0.15	7.6	0.38	
Dubugnon (1981)	Hohensyburg Sandstone (14.4-18.9)**	6	0.15	6.7	0.39 - 0.52	** The tensile strength is obtained by dividing the uniaxial compressive strength by 9, which is the average ratio for the rocks used in this project.
Ip (1986)	Pennant Sandstone (23.4)	5	0.27	12.4	0.39	

Table 9.10 Evaluation of Proportionality Constant, k, for prediction of Critical Jet Power.

invariant proportionality constant K. If the higher end of the quoted strength of Hokensyburg Sandstone is used, the constant K is essentially the same for all three rocks. Admittedly, only limited data are considered here, especially the lack of data for high speed cutting. However, the most encouraging results provide much scope for further research to prove or disprove the hypothesis. If the constant is relatively unchanged for a wide range of variables, the critical jet power (50% normal force reduction) can be estimated using the expression:

Critical jet power (kW)

$$= 0.39 \times \sigma_t \times d \times V$$

where σ_t = tensile strength (MPa)

h = depth of cut (mm)

V = traverse speed (m/s).

Hood's (1976) results when cutting norite (UCS = 300 MPa) are not included in this analysis as the force reductions were plotted against depth of cut rather than jet power and jet pressure. As a matter of interest, the maximum depth of cut at which jet power is equal to critical jet power (expected 50% normal force reduction), is evaluated.

Conditions:	Cutting Speed	= 0.15 m/s
	Jet Pressure	= 50 MPa
	Flow Rate	= 0.50 litre/sec
	Rock	= norite (UCS = 300 MPa)
	Tensile Strength	= $\frac{300 \text{ MPa}}{9}$ (assumed)

Using the equation:

Critical jet power

$$= 0.39 \times \sigma_t \times d \times V$$

$$\therefore \quad 50 \times 0.50 = 0.39 \times \frac{300}{9} \times d \times 0.15$$

$$h_{max} = 13 \text{ mm.}$$

The estimated maximum depth of cut at which hydraulic fracturing is significant is 13mm, which is beyond Hood's experimental conditions (Figure 2.7). The slow traverse speed is the reason behind the very encouraging results reported when jet pressure of only 50 MPa was used during the cutting of very hard norite. However, such encouraging results are not expected when the rock is cut at a realistic traverse speed which is over 1.0 m/s for a typical roadheader.

9.5.2 Discussion

As a matter of interst critical jet power for the Pennant Sandstone at different depths of cut and different traverse speeds are evaluated using the proposed equation. The results are set out in Table 9.11. The critical jet pressures are calculated using the following equation, assuming a 0.9mm diameter nozzle is used:

$$\text{Jet Power} = C_d \left(\frac{\pi}{4}\right) \left(\frac{2}{\rho}\right)^{\frac{1}{2}} d_o^{\,2}\, p^{\,3/2}$$

Cutting Speed (m/s)	Depth of Cut (mm)	Predicted Critical Jet Power (kW)	Predicted Critical Jet Pressure (0.9mm Jet) (MPa)
0.27	5	12.3	65
	10	24.6	103
	15	37.0	135
1.10	5	50.2	165
	10	100.4	262
	15	150.6	343

<u>Table 9.11</u> Predicted Critical Jet Power for Pennant Sandstone.

where: C_d = discharge coefficient

assume 0.832

ρ = fluid density

d_o = nozzle diameter

P = jet pressure.

The general impression gained is of the much higher jet power required at the 1.10 m/s traverse speed if significant force reductions are to be achieved from the hydraulic fracturing mechanism. Before this critical value is reached, the jet pressure may already be high enough to penetrate and slot the rock. If this is true, the proposed force reduction prediction for the rocks with significant jet penetration should be used instead.

The higher critical jet power required during higher traverse speed highlights the potential erroneous results if the laboratory findings for the slow traverse speed are extrapolated beyond laboratory conditions. This is very important, as most of the work published has been carried out at very slow speeds of less than 0.25 m/s (Hood 1976; Dubugnon 1981; Ozdemir *et al*. 1983), while the tool speed in a production tunnelling machine is over 1.0 m/s.

9.6 Summary

In this chapter, experimental results are analysed in an attempt to establish correlation equations capable of summarising the functional relationship between tool force reductions and water jet assistance in various rocks.

For the unassisted drag tool rock cutting, the uniaxial compressive strength is found to be the most informative rock cuttability index when the cutting speed is low, i.e. 0.27 m/s. In this case, the tool forces can be estimated using the following equations:

$$MCF = 0.008777\ (UCS)^{0.6299}(d)^{1.4027}$$

$$MNF = 0.002815\ (UCS)^{1.0755}(d)^{1.0752}$$

When the traverse speed is high (1.10 m/s), additional rock properties to uniaxial compressive strength should be included which are yet to be determined.

Because of the importance of jet penetration in water jet assisted cutting of rocks with significant jet penetration, published jet cutting theories are critically assessed. The modified Kuzmich's equation is found to be the best in correlating laboratory data of experimental rocks:

Modified Kuzmich's Equation:

$$\frac{h}{d_o} = B\left(\frac{P_o}{\sigma_c}\right)^m\left(\frac{V_o}{V}\right)^n$$

where B, m and n are constants obtained by least squares optimisation on experimental results.

For rocks with significant jet penetration, the jet penetration is the most appropriate parameter to summarise the water jet assistance to tool force reductions. The force reductions are found to have a parabolic function with the jet penetration, with maximum force reduction at optimum jet penetration. The functional relationship can be expressed as:

Force Reduction, F_R

$$= F_{Rmax} \left(1 - \left(\frac{h-hk}{hk}\right)^2\right)$$

Optimum jet penetration can be estimated by the profiling depth which is the difference between mechanical depth of cut and chip depth. The maximum force reduction is a function of traverse speed, depth of cut and rock type. The effect of bluntness is to increase both optimum jet penetration and maximum force reductions.

For the rocks without significant jet penetration, substantial tool force reductions are possible when hydraulic fracturing is operating. In this case, the critical jet power, which is defined here as when the normal force reduction is 50%, is less than the threshold jet power for jet penetration. Based on limited data from this project and published works, the critical jet power can be estimated using the following expression:

Critical Jet Power (kW)

$$= 0.39 \times \sigma_t \text{ (MPa)} \times d \text{ (mm)} \times V \text{ (m/s)}.$$

*　　*　　*

CHAPTER TEN

CHAPTER TEN

GENERAL DISCUSSION : THE EFFECT OF HIGH PRESSURE WATER JETS ON THE PERFORMANCE OF BOOM-TYPE TUNNELLING MACHINES

10.1 Introduction

The cutting efficiency of a tunnelling machine is always judged in terms of specific energy which measures the energy input per unit volume of rock output. However, this is not an appropriate variable to be used in the overall assessment of a tunnelling machine equipped with high pressure water jets. A high pressure water pump with reasonable flow rate provides up to a power of 75 kW, which is equivalent to the cutting head power of a medium roadheader. In a practical application, the increase in advance rate may not totally justify the increase of energy input, especially when cutting strong rock. However, there are other considerations in making water jet assisted cutting attractive.

In this chapter, effects of water jet assistance on various aspects of a practical boom-type tunnelling machine (roadheader) performance are discussed. Finally, the potential of the water jet equipped tunnelling machine is assessed overall.

10.2 General Machine Performance

Normal force increases rapidly once the wearflat is generated. A moderately blunt tool cutting Grindleford Sandstone showed a more than fourfold increase in normal force and a twofold increase in cutting force when compared with sharp tool cutting.

Since the tunnelling machine is cutting the rock with blunt tools in a field situation it is quite obvious that the majority of roadheaders are arcing force limited.

When insufficient arcing force is available in hard rock conditions, inefficient rubbing cuts result, or the head bounces out of the cut and does not regain its former cut depth. This produces ridges between the arrays of tools, impeding the progress of the head through the rock. The normal force component is the most important component relating to the arcing force. The reduced normal forces obtained with water jet assistance allow machines to maintain higher depths of cut and hence more efficient cutting. This is due to relieving breakout between lines of tools rather than the groove deepening mode of cutting resulting from shallow depths of cut.

The design of cutting heads should take into account the deeper cutting depths possible, allowing increased spacing between tools and hence fewer tools on the head. This increases the available hold-in force per tool, promoting efficient cutting and improved performance.

The above description applies to new cutting tools, although in a field situation, a wearflat soon develops on the tool. Higher slewing forces are required to maintain the 'as new depth of cut'. However, in practice, there is insufficient slewing force and shallower depths of cut, resulting in a lower performance.

With water jet assistance, not only is the tool force reduced, but the rate of development of wearflat is reduced and good performance is maintained for much longer periods. In hard rock where jet penetration is insignificant, it is this reduced rate of wear that accounts for much of the improved performance.

10.3 Jet Power and Nozzle Position

The major function of the water jet in terms of force reduction is to penetrate and relieve the tool tip from crushing and grinding. Optimum jet penetration is about 20% to 30% of mechanical depth of cut, which is closely related to the profiling depth. Thus the jet must be sufficiently powerful to penetrate to the profiling depth of the rock before it can effectively reduce the inefficient crushing events underneath the wearflat. The blunter the tool, the deeper the jet penetration required. If higher jet power is desired, jet pressure or flow rate must increase. Practical problems exist for both approaches. Firstly, present technology is not yet sufficiently advanced to solve the problems of the rotary seal (Kogelmann 1985). Hence the present commercial water jet assistance system in a tunnelling machine is limited to a maximum jet pressure of 70 MPa. Secondly, increase in jet flow rates is not encouraged as excessive amounts of water already cause practical problems in the mine (Straughan 1985). A water flow rate of 4 litre/min/tool is suggested as a realistic maximum for use in a mining environment (Morris and MacAndrew 1986). In a practical water jet assisted roadheader, 0.4mm diameter nozzles used in selected tool positions are reported by Straughan (1985).

As small diameter nozzles are not powerful enough to provide significant jet penetration, maximum benefits from jet assistance are not derived. Bit-force actuated phasing systems and phased rotary water seals are suggested as being two ways of keeping the problem of excessive water under control without jeopardising the jet power. A bit-force actuated system has the advantage of being able to operate the jet only when the tool is cutting the rock. However, the tool is very expensive and the mechanism is not reliable. The phased rotary seals can only be applied in ripper-type cutting heads and are also difficult and costly to manufacture (Kogelmann 1985).

Based on the assessment of the different systems as above, it seems that a system to optimise the water jet assistance has yet to be found. A potentially improved system is suggested as 'the jet-through-tip' configuration; this offers the following benefits:

(1) Shorter stand-off distance means better jet penetration characteristics;

(2) Lower jet pressure is required. Now the jet does not need to penetrate the profiling depth before relieving the tool tip from crushing events and a jet pressure slightly higher than the threshold pressure is sufficient. For example, a jet pressure around 20 MPa is sufficient, regardless of whether or not the tool is blunt, compared with the 70 MPa

for the sharp tool and higher pressure for the blunt tool in the Grindleford Sandstone cutting. Hence more nozzles can be afforded without problems of sealing or excessive floor water.

(3) The jet can keep the sharp tool tip geometry as soon as jet penetration is possible.

The nozzle hole should be slightly behind the tip. This position has the following advantages:

(1) By positioning the jet impingement slightly behind the cutting tip, the cutting face of the tool can preserve its role to promote the crushing zone ahead of the tool tip which is essential for the chipping events, while the jet can beneficially minimise crushing events underneath the wearflat. Tool force reductions are expected to be improved (Figure 6.6).

(2) The cutting edge can form a barrier to prevent the possibility of debris and quartz grains gaining access to the nozzle, thus reducing the chance of the jet becoming clogged.

(3) The track left by the tool is cooled, reducing the possibility of a methane ignition.

The possible disadvantages are:

(1) When the rock is very strong, the rock may not be penetrated. In this case, the jet flow may stop and the jet may lose its cooling ability, while the outside nozzle can manage to cool the tip once the chip is formed.

(2) The nozzle may become blocked as the jet is unable to flush out the debris beneath the wearflat.

(3) The tool tip is subjected to very high stress levels during the rock cutting operation. The introduction of a nozzle hole may create a weakness in the tool tip which may result in premature tip failure.

The idea of integrating the nozzle and the tool tip is very attractive in concept, particularly when jet penetration is possible. However, there is little published work relative to water jet assisted cutting using this type of tool. Further work is strongly recommended to see whether the potential advantages can be gained.

10.4 Cutting Head Speed (Tool Traverse Speed)

The slow and deep cut principle has been proposed and the advantage of lower specific energy and lower dust levels have been proved (Barker *et al*. 1966; Pomeroy 1966). However, this principle is not implemented in the roadheader design and the present production roadheaders usually have a high head speed with equivalent tool traverse speed well over 1.0 m/s. High speed is preferred as the excavation rate is directly related to the cutting speed (Hurt and MacAndrew 1981).

However, the benefits of higher cutting speed may not be justified for the following reasons:

(1) The wear rate and then tool force increase rapidly with cutting speed when cutting abrasive rocks.

(2) The normal force increases with cutting speed in strong sandstones.

Unless the rock is weak and non-abrasive, too high a cutting speed is not recommended.

There are more advantages in cutting deeper and slower from a water jet assistance viewpoint. The profiling depth is increasing proportional to the logarithmic scale of depth of cut, and tends to be a constant if the cutting is sufficiently deep. Hence optimum jet penetration only increases slightly with depth of cut. Additionally, the water jet can penetrate further at slow speed.

The reduction of tool traverse speed can be carried out in several ways. One possible method is to lower the head speed by gearbox. At present it is usual to have a two-speed gearbox in a typical roadheader. It is believed that more speed control in the gearbox is preferable. The high speed can be used for productivity when favourable conditions are met and low speed when the rock is strong.

10.5 Tool Life

In extending the applicability of roadheaders to strong rocks in which jet penetration is impossible, the force reduction due to the introduction of water jet is expected to be limited. For a practical tunnelling machine, all the cutting tools have some degree of bluntness as no tool will be changed unless it is very blunt. The crushing force underneath the wearflat of a blunt tool will dominate the tool force and is responsible for most of the arcing force and cutting torque. If the water jet cannot penetrate and relieve the cutting tip, improvement of the performance of the tunnelling machine is only marginal. Hydraulic fracturing which is so attractive in laboratory slow cutting is not expected to be of any assistance for a practical machine as the tool speeds are so fast.

The most practical help provided by the water jet is, in this case, to cool the cutting tip and thus keep its most efficient cutting geometry for a longer period of time. This means less wear rate and longer tool life. Not only is tool consumption rate lowered, but less down time for tool changing and hence improved performance is achieved.

Because of the beneficial effect of water in cooling the tool tip and extending tool life (Morris and MacAndrew 1986), the use of low pressure water jets is recommended, even when the cuttability of rocks is within the capacity of the roadheader.

10.6 Methane Ignition

The major cause of ignition of methane-air mixtures by machine tools is a hot spot on the rock. The hot spot is composed of a surface layer of either molten rock or metal which is the result of frictional sliding on the rock by the travelling tool. Trueman (1985) and Pearey (1985)provide an adequate summary on this particular subject.

Although the best position for the jet spray is behind the tools so far as the prevention of damp ignition is concerned, the jet-before-tool is also helpful in reducing or even eliminating methane ignition. Practical trials of two roadheaders equipped with high pressure water jet assisted cutting have proved the effectiveness of the water jet to reduce incendive sparking (Anon 1984; Clark 1984). The active cooling of the cutting tool by the water jet is regarded as the reason behind these observations.

10.7 Dust Suppression

An undisputed advantage of using water jets is the suppression of dust. Normally, 70% reduction in respirable dust has been obtained (MacNary et al. 1976; Calrk 1984; Morris et al. 1984). Although no dust measurement has been carried out in the present work, Plate 10.1 shows the effectiveness of the water jet in suppressing dust during the cutting of Pennant Sandstone. It is suggested that the better efficiency of fine particle collection when water jets are employed is the reason for dust suppression by the jets (Tutluoglu et al. 1983).

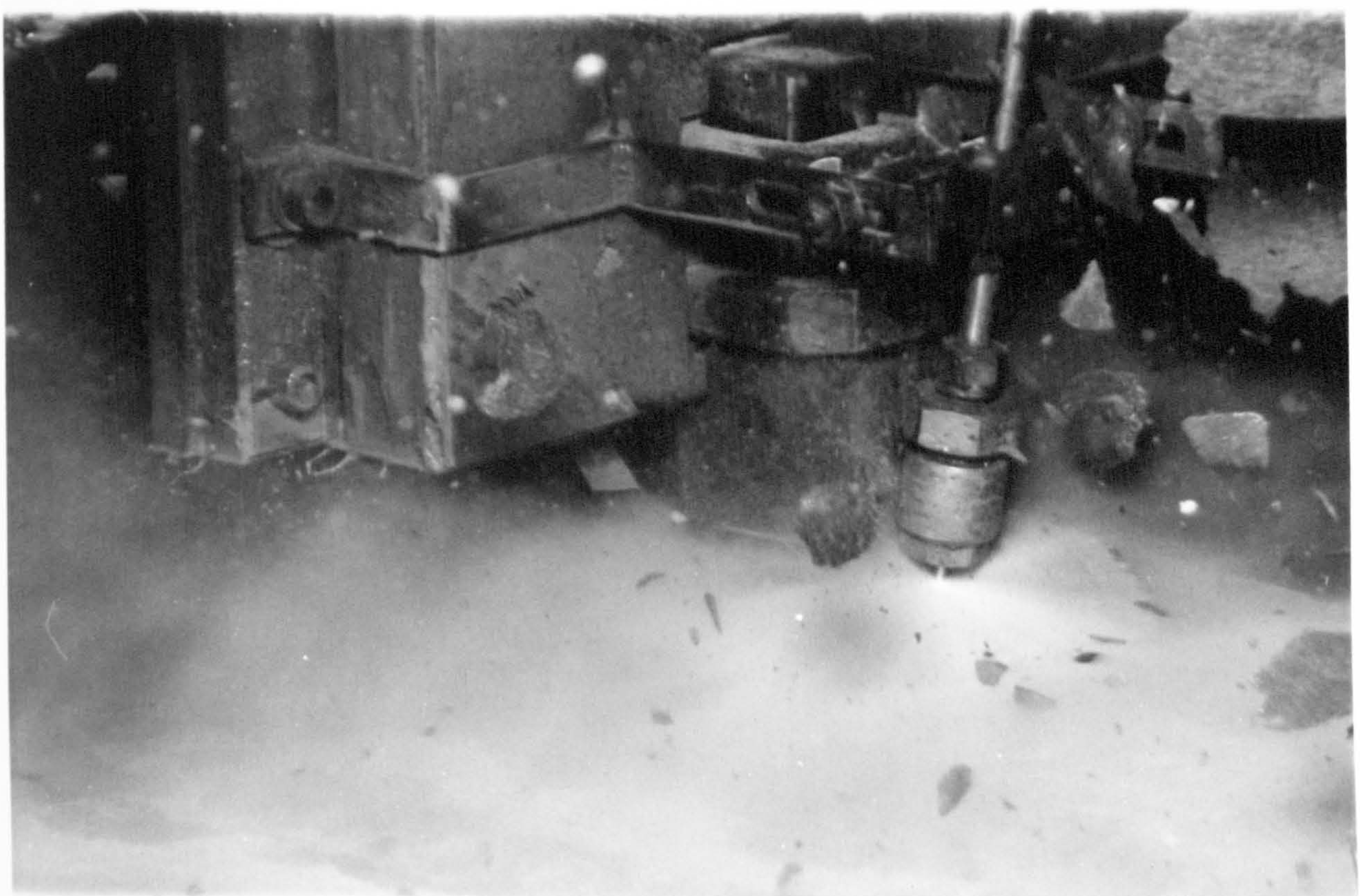

Plate 10.1

10.8 Flexibility and Manoeuvrability

Heavier and more powerful roadheaders are required to cut strong rocks. This involves not only a higher capital investment, but a bulky machine with less manoeuvrability. Additionally, a big roadheader is not favourable in some mines where a smaller tunnel section may be proved more economical.

A smaller size of roadheader equipped with high pressure water jet may be a better alternative. The addition of water jet can reduce the mechanical tool force required so that a small roadheader can provide reasonable advance rates when even stronger rocks are encountered which are normally outside the cuttability range of a small machine. This type of roadheader is particualrly useful in a tunnel of mixed rocks. Good performance is expected in weak rocks, with reasonable advance rates and acceptable pick consumption in cutting stronger rocks using water jet assistance. This may provide a better overall economic return than use of a heavier and more powerful machine throughout the total length of the tunnel or an unassisted machine with occasional hold-up when strong rocks are met and drill and blast techniques are necessary.

10.9 Overall Assessment

The success of water jet assisted rock cutting should be evaluated in terms of economy and health and safety considerations.

So far as economic considerations are concerned, specific energy provides only one of many yardsticks that are available.

Improvement in advance rate may well be proved to be of more practical importance. In tunnelling activities the cost of operating the machine accounts for only a small portion of total costs. Hence improved advance rate may shorten the total time of tunnelling and provide an overall saving. Extended tool life and less down time for changing cutting tools also contribute to overall economy against the possible unfavourable higher specific energy when water jets are operating.

With regard to the health and safety of the workforce underground, the water jet equipped tunnelling machine is proving unanimously superior in its ability to suppress dust and incendive sparking. Sometimes the use of water jets is the only way of suppressing dust levels to within limits permitted by the Health and Safety Regulations (Wilson 1984).

The water jet equipped tunnelling machine has proved to be very desirable with regard to its superiority in aspects of economy, health and safety. It is now required that new technology should provide a reliable rotary seal and phasing system for the successful implementation of the high pressure water jet to the tunnelling machine.

Because of the limited impact force the carbide tip of a drag tool can withstand, care must be exercised in applying the roadheader to very strong and abrasive rocks, even when the machine is equipped with high pressure water jets. Furthermore, the wear rate may still be unacceptably high if the tool speed is too high. Unless the water jet power can be increased significantly, which is unlikely at the present time for the problems of rotary seals and excessive amounts of floor water, dramatically improved machine performance is not expected. The best performance may be found in medium strength rocks (UCS < 120 MPa) where force reductions are obtained from direct jet assistance, as well as reduced wear rate.

*　　*　　*

CHAPTER ELEVEN

CHAPTER ELEVEN

SUMMARY AND CONCLUSIONS

During the course of this 3-year research project, the basic cutting mechanisms of high pressure water jet assisted drag tool rock cutting have been investigated.

Because of the large number of variables involved it was impossible to include all variables in this research programme. In addition, the potential wide range of all variables exclude the possibility of a detailed investigation. Selected variables have been studied at different levels, dependent on the importance of each variable. Hence any conclusions drawn in this thesis are applicable only to the conditions in the laboratory as observed. This must be borne in mind when these results are applied to conditions not modelled in the laboratory.

Basically, over one thousand cuts have been carried out in the five rock types under study, which cover a wide range of rocks cuttable or expected to be cuttable by a roadheader equipped with water jets. Very weak and very strong rocks have been included to ensure that the results are representative and the conclusions are quantitative.

A modified 50-tonne linear cutting rig was used for the cutting experiments. Modification enabled a cutting speed up to 1.10 m/s, representing a typical cutting speed for a production tunnelling machine cutting hard rocks. Jet pressures can vary up to 70 MPa and depths of cut used were 5mm, 10mm and 15mm.

The main objective of this project was to investigate the mechanisms for reduction in tool force under the assistance of high pressure water jets at realistic traverse speeds by laboratory experiments.

The research programme was divided into two phases. In the primary experimental programme, the major variables of jet pressure, depth of cut and traverse speed were investigated. A factorial experimental suite was applied to all five rock types. The influence of wearflat was minimised by using a pristine tool for each rock, except in the case of Pennant Sandstone, and the cutting sequence was randomised.

In the secondary experimental programme, various variables including jet position, nozzle diameter, tool bluntness, wear rate and slot depth were studied, using smaller but dedicated experimental designs on selected rock types. Typical depth of cut was 10mm and typical traverse speed 1.10 m/s. Jet pressure is the most important parameter in this project and this was studied in both programmes.

11.1 Drag Tool Rock Cutting

For drag tool rock cutting, the tool is found to perform four functions during the course of cutting:

Tool Force = Crushing + Profiling + Primary
Chipping + Secondary Chipping.

The force proportions of each event are dependent on the mechanical depth of cut, traverse speed, tool bluntness, rock type and are different for the cutting force and normal force components. The cutting force is composed of more chipping force and less crushing force, and vice versa for the normal force. Most of the events take place in the bottom few millimetres of the cutting.

The effect of traverse speed on tool forces was observed when Grindleford Sandstone and Penrith Sandstone were cut at two speeds with the same degree of tool bluntness. At a cutting speed of 0.27 m/s, the tool forces can be correlated using the uniaxial compressive strength as the rock cuttability index. For the fast cutting speed (1.10 m/s), extra rock indices should be included which are yet to be determined.

11.2 Water Jet Rock Cutting

During jet slotting experiments with jet pressures up to 70 MPa and a traverse speed up to 1.10 m/s, the water jet penetrated the rock by an erosive action rather than by gross internal fracture.

Significant jet penetrations were observed only in Dumfries Sandstone, Grindleford Sandstone and Penrith Sandstone, whilst there was no jet penetration in Pennant Sandstone and Middleton Limestone (even at 70 MPa pressure and 0.27 m/s traverse speed). Threshold jet pressures were found to exist, but poorly predicted, using published equations. When jet cutting efficiency is considered, the higher the traverse speed, the lower the hydraulic specific energy.

For the nozzle used in this project, the modified Kuzmich's equation provides the best correlation with the experimental results:

$$\frac{h}{d_o} = B \left(\frac{P_o}{\sigma c}\right)^m \left(\frac{V_o}{V}\right)^n$$

where: h = jet penetration

d_o = nozzle diameter

P_o = jet pressure

σc = uniaxial compressive strength

V_o = jet speed

V = jet traverse speed

B, m, n = constants.

11.3 Hybrid Cutting Model

Based on observations of a single representative cutting cycle by a drag tool, together with the effect of water jet impinging 1-2mm ahead of the tool tip, a phenomenological hybrid cutting model was proposed. Depending on the magnitude of jet penetration, three stages were identified in which the water jet played a different role. The effects of water jet assistance at different jet penetrations are described as follows:

(1) Insignificant Jet Penetration : As the water jet is incapable of penetrating and relieving the tool tip, the purpose of the jet is to flush out debris to reduce secondary comminution and improve tool-rock force transmisison. The force reduction is marginal.

(2) Optimum Jet Penetration : In optimum conditions, the jet penetration is sufficiently deep to relieve the tool tip from crushing events under the wearflat most of the time, but not too deep to remove the crushed zone essential for the chipping events. This optimum jet penetration represents the best compromise between the further tool force reduction due to lesser crushing events and the force increase due to more profiling events when jet penetration is deeper.

(3) Excessive Jet Penetration : When jet penetration is too deep, the water jet flushes out the crushed zone before the tool tip and eliminates chipping events. Although the tool tip is completely relieved, force reduction is outweighed by the force increase due to increase in profiling events and the net gain is reduced from optimum condition.

Dependent on jet penetration, rocks can be divided into two groups. One group of rocks are those with significant jet penetration which include Dumfries Sandstone, Grindleford Sandstone and Penrith Sandstone. Pennant Sandstone and Middleton Limestone belong to another group in which jet penetration is insignificant. The main difference is the ability of the jet to penetrate and relieve the tool tip in the former group but not in the latter. The difference which is not very clear when a new tool is used becomes obvious with the use of a blunt tool. Secondly, there exists an optimum jet penetration and thus 'optimum jet pressure' in the rocks with significant jet penetration with which the maximum force reduction is obtained.

11.4 Water Jet Assisted Drag Tool Rock Cutting : Rocks with Significant Jet Penetration

In this group of rocks, the proposed hybrid cutting model is generally applied. The major benefit from water jet assistance is to slot the rock ahead of the tool and to relieve the tool tip from confinement and crushing events. Hydraulic fracturing is not found to operate. Jet penetration is established as the most important parameter to evaluate jet assistance for its uniqueness to integrate the effects of jet pressure, nozzle diameter, nozzle design, stand-off distance and traverse speed.

Optimum jet penetration is about 25%-30% of mechanical depth of cut and maximum force reduction is on average 22% and 46% for mean cutting and mean normal force components respectively. The more crushing force component in the normal force leads to both higher optimum jet penetration and higher maximum force reduction. The optimum jet penetration is found to be closely related to profiling depth, which is relatively independent of rock type and traverse speed and can be estimated using the expression:

$$\text{Profiling depth} = 1.455 \times \ln(\text{depth of cut}) - 0.544.$$

When the jet penetration is not excessive (typically less than 50% mechanical depth of cut), the tool force reductions are related to jet penetration and the relationship can be generalised using a parabolic function of a form:

$$F_R = F_{Rmax} \left(1 - \left(\frac{h - h_k}{h_k}\right)^2\right)$$

where: F_R = force reduction

F_{Rmax} = maximum force reduction

h = jet penetration

h_k = optimal jet penetration

Due to the high proportion of tool force contributed by the crushing and profiling events in the 5mm depth of cut, the optimum jet penetration is higher than expected and approaches the mechanical depth of cut.

The validity of the proposed hybrid cutting model is fully proven by successfully explaining laboratory test results.

Traverse Speed : Force reductions in Grindleford Sandstone and Penrith Sandstone at the fast cutting speed are higher than at the slow speed as the effect of traverse speed to tool forces is operative in these rocks.

Nozzle Diameter: The effect of nozzle diameter is implied in the jet penetration. Slot width has little effect on tool force reductions.

Tool Bluntness : Higher force reductions and deeper optimum jet penetration were obtained with a blunt tool than when using a sharp tool, due to the higher proportion of tool force contributed by crushing events.

Jet Position : The jet-before-tool configuration invariably performs better than the jet-after-tool configuration in which the tool tip is not completely relieved even when jet penetration is significant.

Cutting Mode : Slightly higher force reductions are obtained in relieved cutting than in unrelieved cutting. This improvement could result from the slender chips formed in relieved cutting and hence more crushing events.

Unassisted Cutting with Slot : Force reduction only commences when the slot depth is more than 70% of mechanical depth of cut, indicating the relieving effect of the slot is possible only when the slot depth is deeper than chip depth. The small optimum jet penetration in hybrid cutting indicates that jet impingement must be as near to the tool tip as possible.

11.5 Water Jet Assisted Drag Tool Rock Cutting : Rocks with Insignificant Jet Penetration

For rocks with insignificant jet penetration, the main purpose of the water jet is to flush out loosened debris and improve the tool-rock force transmission efficiency. Tool force reductions are usually small. Substantial force reductions are possible when hydraulic fracturing is operating, which was observed when Pennant Sandstone was cut at 5mm depth of cut at 0.27 m/s cutting speed and the jet pressure was 70 MPa. The critical jet power, defined as when the mean normal force reduction due to hydraulic fracturing is 50%, can be estimated tentatively using the following equation:

$$\text{Critical jet power (kW)} = 0.39 \times \sigma_t \times d \times v$$

where: σ_t = tensile strength (MPa)

d = depth of cut (mm)

v = traverse speed (m/s).

Hydraulic fracturing was not observed at all in the Middleton Limestone; it was not observed in Pennant Sandstone at the higher cutting speed and/or higher depth of cut.

Tool Bluntness : Tool force reductions are smaller with a blunt tool than with a sharp tool as the contribution of the jet is to aid debris clearance which contributes much less to tool forces using a blunt tool than with a sharp tool.

Jet Position : No force reduction was derived from the jet-after-tool configuration as the beneficial effects of debris clearance were not obtained.

Cutting Mode : There was a slight improvement in water jet assistance in the relieved mode as compared with unrelieved cutting, although force reductions in both cases are marginal.

Wear Rate : After 16 metres of cutting in Pennant Sandstone at 1.10 m/s, normal force reductions were 40% using a jet of 70 MPa. This force reduction was obtained for water jets of different diameters and different positions, implying the cooling of the tungsten carbide tip is the main purpose of the jet in cutting this strong rock.

11.6 Summary

In order to obtain significant tool force reductions, the jet power must be either greater than the threshold jet power for slotting, or critical jet power for hydraulic fracturing. If the jet power is less than these values, the benefit derived from the water jet is to cool the tool tip. The wear rate is reduced and the tool tip can maintain its efficient geometry longer. Other benefits such as flushing of debris only contribute marginal force reductions.

With the 70 MPa water jet assistance, most benefits can be found in cutting medium strong rocks (UCS<120MPa) in which tool forces are reduced directly from water jet assistance, and indirectly from extended tool life.

* * *

CHAPTER TWELVE

CHAPTER TWELVE

RECOMMENDATIONS FOR FURTHER WORK

In this project, the basic cutting mechanism of water jet assisted drag tool rock cutting was investigated. Unfortunately, it is impossible to investigate every aspect of hybrid cutting. Indeed, in common with all research, many questions are often posed by the research results themselves.

The following is a list of topics recommended for further studies which, in the light of the findings of this project, are deemed to be essential to further the understanding of water jet assisted rock cutting using drag tools.

12.1 Tool Force

Four tool actions are identified in a typical cycle of drag tool rock cutting which include the crushing, profiling, primary and secondary chipping. Depending on the tool tip geometry, operational variables such as traverse speed and depth of cut, as well as rock type, different component forces are contributed from these four tool actions which combine to give the tool forces measured. Work is recommended to formulate a constitutive equation in order that proportions of tool forces by each tool action can be estimated. Particular emphasis is placed on the relationship between tool bluntness and the increase of tool force. If successful, this constitutive model can help to predict the absolute cutting and normal forces as well as the force reductions when water jets are applied.

12.2 Effect of Traverse Speed

The effect of traverse speed on the tool forces is observed for certain rock types but not others. Other researchers have attributed this to the wearflat, though this is rejected as the rocks were cut with the tool having some degree of bluntness. The effect of traverse speed is mostly reflected in the large increase in the normal force component, for both sharp tool and blunt tool rock cutting,when the traverse speed is fast. The normal force increase could be more than 100% when traverse speed is increased from 0.27 to 1.10 m/s. The cutting force increase is comparatively smaller. Normally a boom-type tunnelling machine cuts at a fast speed (>1.0 m/s), hence it is most important to determine whether the effect of traverse speed exists in the rock to be cut and, if so, how this effect can be quantified. Further research is suggested to establish the rock properties that define traverse speed effect. The possible existence of a critical cutting speed should also be investigated.

12.3 Optimum Jet Penetration

For the drag tool used in this project, the optimum jet penetration was found to correlate highly with profiling depth, which is the difference between the mechanical depth of cut and chip depth. If the equivalence between the optimum jet penetration and profiling depth is established, the optimum jet penetration for a particular tool can be estimated by measuring chip depth obtained in a simple unassisted cutting test. The hypothesis can be tested and proved by using several drag tools of different tip geometry and the optimum jet penetration measured can be compared with the chip depth.

12.4 Threshold Jet Pressure

The threshold jet pressure is the pressure when the hydraulic force of the jet on the rock grains exceeds the mechanical binding strength. It marks the lower limit of the jet pressure at which the jet erosion occurs. Unless hydraulic fracturing prevails, substantial tool force reductions are only possible when the jet can penetrate. This is especially important when the tool is blunt. Hence, to know the threshold jet pressures for the rocks to be cut is a matter of importance, as the capacity of the pumping system can be estimated. The existing prediction equation using the uniaxial compressive strength as the only rock parameter is proved experimentally to be insufficient. Further work is suggested so that a better prediction equation can be established to predict the threshold pressure with reasonable accuracy, based on the physical and mechanical properties of the rock, determined by small scale laboratory tests.

12.5 Higher Jet Power System

The 70 MPa jet system used during this project provides substantial assistance in the reduction of tool forces when medium strength sandstones are cut. However, higher jet power is required before the economical use of drag tools in harder rocks is feasible. Further experiments are proposed to increase the jet power in the hard rocks in order to determine whether these hard rocks will follow the general model of force reductions when jet slotting is possible. Additionally, the higher jet power provides an opportunity to investigate the relative merits to promote the force reduction by means of hydraulic fracturing or by jet slotting.

12.6 Critical Jet Power

The occurrence of significant force reductions before the water jet is powerful enough to slot the hard rock is very encouraging. The relative magnitude between the critical jet power and the threshold jet power marks the different mechanisms of water jet assistance. If the critical jet power is lower than the threshold jet power, the water jet assistance is mainly in a form of hydraulic fracturing. Otherwise, the water jet assistance is by penetrating the rock and relieving the tool tip. It is informative and desirable to evalute the relative values of both jet powers for the rock to be cut so that force reductions with water jet assistance can be estimated. The threshold jet power, as well as the optimum jet power giving the optimum jet penetration, is obtainable from slotting tests. An empirical equation is proposed in this thesis to estimate the critical jet power, which is based on limited experimental data. Further work is suggested to provide more data so that the prediction equation can be improved or substantiated and its accuracy improved.

12.7 Tool Bluntness

For the sake of comparison, pristine tools are usually used in most laboratory investigations. However, a production tunnelling machine always cuts the rock with tools of varying degrees of bluntness. Although the parabolic relationship between the force reduction and jet penetration is also applicable to blunt tools for rocks with significant jet penetration, the maximum force reduction and optimum jet penetration are different. Future research is recommended to investigate the change of maximum force reduction and optimum jet penetration for varying degrees of tool bluntness. It is suggested that tool bluntness can be quantified and the tool force can be related to the tool bluntness using a numerical function. The functional relationship between the tool bluntness and the maximum force reduction as well as optimum jet penetration should be established. These functions, if successful, could provide a means of estimating the force reduction when water jets are used on a tunnelling machine.

12.8 New Cutting Tool

When the nozzle is independent of the cutting tool, the jet-before-tool configuration gives better results with respect to the jet-after-tool configuration. However, the jet-through-tool, especially the jet-through-tip, provides attractive potential advantages. Unfortunately, most of the possible potentials are yet to be proved and published work is scarce. The basic principles and findings from this project should be applied to the design of this new generation of cutting tool. The new designs can be tested by laboratory experiments and their relative advantages and disadvantages can be evaluated.

12.9 Full-Scale Trials

The results presented earlier in this thesis show that jet penetration is a useful predictor of the benefits to be derived from water jet assistance and jet pressure and nozzle diameter should be matched to provide optimum penetration. The presence of an optimum provides a useful starting point for full-scale trials on an instrumented boom-type tunnelling machine to be undertaken in the University of Newcastle upon Tyne (Plate 12.1). The use of arrays of cutting tools with water jets under controlled laboratory conditions will allow the benefits of water jet assistance to be fully explored and the model proposed in this paper to be fully validated. Extra effects of the water jet which cannot be modelled by the linear cutting tests can also be studied.

* * *

Plate 12.1

REFERENCES

REFERENCES

Adam, R.F.J. "Retro Fitting Shearers and Continuous Miners with Water Jet Assisted Cutting" Proceedings 3rd US Water Jet Symposium, Pittsburg, May 1985.

Allington, A.V. "The Machining of Rock Materials" Unpublished Ph.D. Thesis, Univ. of Newcastle upon Tyne 1969.

Anon "Dosco experience of High Pressure Water Assisted Cutting Trials at Bentinck Colliery" Colliery Guardian Jul/Aug. 1984, pp. 258-59.

Barker, J.S. "A Laboratory Investigation of Rock Cutting using Large Picks" Int. J. Rock Mech. Min. Sci. Vol.1, 1964, pp. 519-34.

Barker, J.S., Pomeroy, C.D. and Whittaker, D. "The MRDE Large Pick Shearer Drum" The Mining Engineer Feb. 1966, pp. 323-33.

Barnes, J.W. "Roadway Drivage and Shaft Sinking" Colliery Guardian Aug. 1981, pp. 405-12.

Barton, C.C. "Variables in Fracture Energy and Toughness Testing of Rock" Proceedings 23rd US Symposium on Rock Mechanics, Society of Mining Engineers, Univ. of California, Berkeley, Aug. 1982, pp. 449-62.

Baumann, L. and Koppers, M. "State of Investigations on High Pressure Water-Jet Assisted Road Profile Cutting Technology" Proceedings 6th International Symposium on Jet Cutting Technology, 6-8 April 1982, pp. 283-300, Surrey, UK.

Bowden, F.P. and Brunton, J.H. "Deformation of Solids by Liquid Jet Impact" Proceedings Roy. Soc. London, Vol. 236A 1961, pp. 433.

Brace, W.F. "Behavior of Rock Salt, Limestone and Anhydrite during Indentation" Journal of Geophysical Research Vol. 65, No.6. June 1960, pp. 1773-789.

Bresee, J. C., Cristy, G.A. and McClain, W.C. "Some Comparisons of Continuous and Pulsed Jets for Excavation" Proceedings 1st International Symposium on Jet Cutting Technology, 5-7 April 1972, Coventry.

Brook, N. and Summers, D.A. "The Penetration of Rock by High Speed Water Jets" Int. J. Rock Mech. Min. Sci. Vol.6, pp. 249-58, 1969.

Brook, N. and Page, C.H. "Energy Requirements for Rock Cutting by High Speed Water Jets" Proceedings 1st International Symposium on Jet Cutting Technology, 5-7 April 1972, Coventry.

Brown, E.T. "Rock Characterization Testing and Monitoring" Int. Soc. for Rock. Mech., Pergamon Press, London 1981.

Brown, R. "Jet Cutting Technology; a Review and Bibliography" BHRA Fluid Engineering Series, V.9 1982.

Brunton, J.H. "The Physics of Impact and Deformation Single Impact" Proc. Roy. Soc. London, A260 1966, pp. 79-85.

Clark, R.A. "Success for Anderson Strathclyde High-Pressure-Water Roadheader" Colliery Guardian Jul/Aug 1984, pp.255-56.

Colback, P.S.B. and Wiid, B.L. "The Influence of Moisture Content on the Compressive Strength of Rocks" Proceedings 3rd Rock Mech. Symposium, Toronto, Canada 1965, pp. 65-83.

Cook, N.G.W. "Wear on Drag Bits in Hard Rock" Proceedings 14th Canadian Rock Mech. Symposium, May 1982, pp. 39-43.

Cook, N.G.W., Hood M., and Tsai, F. "Observations of Crack Growth in Hard Rock Loaded by an Indenter" Int. J. Rock Mech. Min Sci. 21 (2) 1984, pp.97-107.

Cooley, W.C. "Correlation of Data on Jet Cutting by Water Jets Using Dimensionless Parameters" Proceedings 2nd International Symposium on Jet Cutting Technology 2-4 April 1974, pp.H4-39/H4-48. Cambridge.

Crow, S.C. "A Theory of Hydraulic Rock Cutting" Int. J. Rock Mech. Min. Sci. & Geomech. Abstr. Vol.10, 1973, pp. 567-84.

Crow, S.C. "The effect of Porosity on Hydraulic Rock Cutting" Int. J. Rock Mech. Min. Sci. & Geomech. Abstr. Vol.11 1974, pp.103-05.

Crow, S.C., Lade, P.V. and Hurlburt, G.H. "The Mechanics of Hydraulic Rock Cutting" Proceedings 2nd International Symposium on Jet Cutting Technology 2-4 April 1974, Cambridge.

Department of Energy, The US., and UK National Coal Board
"Water Jet Assisted Roadheaders for Rock Excavation"
Pittsburgh US 1982.

Dubugnon, O. "An Experimental Study of Water Assisted Drag Bit Cutting of Rocks"
Proceedings of 1st US Water Jet Symposium, Golden Colorado April 1981, pp. II-4. 1. I-II-4.11.

Evans, I. and Murrell, S.A.F. "The Forces required to Penetrate a Brittle Material with a Wedge-Shaped Tool"
Proceedings Conf. on Non-Metallic Brittle Materials 1958. Butterworths, pp. 432-50.

Evans, I. "A Theory of the Basic Mechanics of Coal Ploughing"
Proceedings of the Int.Symposium on Mining Research, London, Pergamon, Vol.2 1962, pp.761-98.

Evans, I. "The Force Required to Cut Coal with Blunt Wedges"
Int. J. Rock Mech. Min. Sci. Vol.2 1965, pp.1-12.

Evans, I. and Pomeroy, C.D. "The Strength, Fracture and Workability of Coal"
Pergamon Press 1966.

Evans, I. "A Theory of the Cutting Force for Point-Attack Picks"
Int. J. of Mining Engineering 1984, Vol.2, pp.63-71.

Evans, R.J., Handewith, H.J. and Hood, M. "Cutting Trials with a Water-Jet-Assisted In-Seam Tester"
Proceedings 25th US Rock Mech. Symposium 1984, pp. 767-73.

Farmer, I.W. "Rock Fracture by Water Jet Impact"
Colliery Engineering Jan. 1967, pp.23-6.

Farmer, I.W. and Attewell, P.B. "Rock Penetration by High Velocity Water Jet"
Int. J. Rock Mech. Min. Sci. Vol.2 1964 , pp. 135-53.

Fauvel, O.R. "Implications of Laboratory Rock Cutting for the Design of a Tunnel Boring Machine Cutter Head"
Unpublished Ph.D. Thesis, Univ. of Newcastle upon Tyne 1981.

Field, J.E. "Stress Waves, Deformation and Fracture caused by Liquid Impact"
Proc. Roy. Soc. London, A260 1966, pp.86-93.

Forman, S. and Secor, G. "The Mechanics of Rock Failure Due to Water-Jet Impingement"
AIME Soc. of Pet. Engs. Paper SPE 4247 1973 pp. 163-74.

Fowell, R.J., Ip, C.K. and Johnson, S.T. "Water Jet Assisted Drag Tool Cutting : Parameters for Success" Proceedings 8th Int. Water Jet Cutting Technology Symposium, Durham, England. 9-11 Spet. 1986.

Fowell, R.J., Johnson, S.T. and Ip, C.K. "Further Studies in Water Jet Assisted Drag Tool Cutting in Rock" Proceedings 3rd US Water Jet Symposium, Pittsburgh 1985.

Fowell, R.J. and Pycroft, A.S. "Rock Machineability Studies for the Assessment of Selective Tunnelling Machine Performance" Proceedings 21st US Rock Mech. Symposium 1980 pp. 149-58.

Fowell, R.J. and Tecen, O. "Studies in Water Jet Assisted Drag Tool Rock Excavation" Proceedings 5th Int. Congress on Rock Mech. Melbourne, Australia, April 1983, pp. E207-E213.

Friedman, M. and Ford, L.M. "Analysis of Rock Deformation and Fractures Induced by Rock Cutting Tools used in Coal Mining" Proceedings 24th US Symposium on Rock Mech, Texas. June 1983, pp. 713-23.

Gregor, M. "Der Einfluss der Schnittgeschwindigkeit auf Schnitt-und Audruckkraft beim Zerspannen von Kohle" Gluckauf Forsch-HT Vol.29, pp.179-88.

Harris, H.D. and Mellor, M. "Cutting Rock with Water Jets" Int. J. Rock Mech. Min. Sci. & Geomech. Abstr. Vol.11 1974, pp. 343-58.

Harris, H.D. and Mellor, M. "Penetration of Rocks by Continuous Water Jets" Proceedings 2nd Int. Symposium on Jet Cutting Technology 2-4 April 1974, pp. H1-1/H1-14. Cambridge.

Hashish, M. and du Plessis, M.P. "Theoretical and Experimental Investigation of Continuous Jet Penetration of Solids" Journal of Engineering for Industry Feb. 1978 Vol.100, pp. 88-94.

Hashish, M. and du Plessis, M.P. "The Application of a Generalized Jet Cutting Equation" Proceedings 4th Int. Symposium on Jet Cutting Technology 12-14 April 1978, pp. F1-1 - F1-16. Canterbury.

Hashish, M. and du Plessis, M.P. "Prediction Equations Relating High Velocity Jet Cutting Performance to Stand Off Distance and Multipasses" Journal of Engineering for Industry Aug. 1979, Vol. 101, pp. 311-18.

Hashish, M. "Critical and Optimum Traverse Rates in Jet Cutting" Proceedings 1st US Water Jet Symposium Colorado 1981, pp. II-3.1 - II-3.14.

Hekimoglu, O.Z. "Studies in the Excavation of Selected Rock Materials with Mechanical Tools" Unpublished Ph.D. Thesis, Univ. of Newcastle upon Tyne 1984.

Henkel, E.H. "Jet-Miner Surface and In-Seam Trials Run by Berbau-Forshung GMBH, Germany" Proceedings US Water Jet Symposium, Missouri-Rolla May 1983.

Hewitt, K.S. "Aspects of the Design and Application of Cutting Systems for Rock Excavation" Unpublished Ph.D. Thesis, Univ. of Newcastle upon Tyne 1975.

Hood, M. "Cutting Strong Rock with a Drag Bit Assisted by High Pressure Water Jets" Journal of the South African Institute of Mining and Metallurgy 1976 77 (4), pp. 79-90.

Hood, M. "A Study of Methods to Improve the Performance of Drag Bits used to cut Hard Rocks" Ph.D. Thesis, Dept. of Mining Engineering, Univ. of Witwatersrand, Republic of S. Africa 1978.

Hood, M. and Tutluoglu, L. "Technological Advances with Water Jet Assisted Cutting Systems" Lawrence Berkeley Laboratory Report to the US Bureau of Mines. Oct. 1983, p.72.

Hood, M. "Waterjet-assisted Rock Cutting Systems - the Present State of the Art" International Journal of Mining Engineering 1985, 3, pp. 91-111.

Hurlburt, G.H., Crow, S.C. and Lade, P.V. "Experiments in Hydraulic Rock Cutting" Int. J. Rock Mech. Min. Sci & Geomech. Abstr. Vol.12 1975, pp. 203-12.

Hurt, K.G. and Laidlaw, D.D. "A Comparison of the Performance in Sandstone of Various Rock and Coal Cutting Tools: 1: Unrelieved Cutting" MRDE Report No.79 1979.

Hurt, K.G. and Laidlaw, D.D. "Laboratory Comparison of Three Rock Cutting Tools"
Tunnels and Tunnelling May 1979, pp.13-6.

Hurt, K.G. and Evans, I. "Point Attack Tools : an Evaluation of Function and Use for Rock Cutting"
The Mining Engineer March 1981, pp.673-75.

Hurt, K.G. and MacAndrew, K.M. "Designing Roadheader Cutter Heads"
The Mining Engineer Sept. 1981, pp.167-70.

Hurt, K.G. and MacAndrew, K.M. "Cutting Efficiency and Life of Rock-cutting Picks"
Mining Science and Technology 2 1985, pp.139-51.

Ip, C.K., Johnson, S.T. and Fowell, R.J. "Water Jet Rock Cutting and its Application to Tunnelling Machine Performance"
Proceedings 27th US Rock. Mech. Symposium, Alabama, June 1986.

Jaeger, J. C. and Cook, N.G.W. "Fundamentals of Rock Mechanics"
Chapman and Hall, 3rd Ed. 1979, pp.593.

Janach, W. "The Role of Bulking in Brittle Failure of Rocks under Rapid Compression"
Int. J. Rock Mech. Min. Sci & Geomech. Abstra. Vol.13 1976, pp. 177-86.

Johnson, S.T. "Studies in the Performance and use of Boom-Type Tunnelling Machines"
Unpublished Ph.D. Thesis, Univ. of Newcastle upon Tyne 1984.

Johnson, V.E., Kohl, R.A., Thiruvengadam, A. and Conn, A.F. "Tunnelling, Fracturing, Drilling and Mining with High Speed Water Jets Utilizing Cavitation Damage" Proceedings
1st Int. Symposium on Jet Cutting Technology 5-7 April 1972, Coventry, pp. A3-37 - A3-55.

Kenny, P. and Johnson, S.N. "An Investigation of the Abrasive Wear of Mineral Cutting Tools"
WEAR 36 (1976), pp. 337-61.

Kenny, P. and Johnson, S.N. "The Effect of Wear on the Performance of Mineral-Cutting Tools"
Colliery Guardian Vol.224 No.6, June 1976 pp. 246-52.

Kögelmann, W. "Safer and More Productive Mining and Tunnelling with Computer-Controlled Water-Jet Assisted Roadheaders and Shearers"
Proceedings 3rd US Water Jet Symposium, Pittsburgh, 21-23 May 1985.

Kovscek, P.D., Evans, R.J. and Taylor, C.D. "Test Results from a Longwall Shearer Retrofitted with Water Jet Assisted Cutting"
Proceedings 3rd US Water Jet Symposium 21-23 May 1985.

Kuzmich, I.A., Goldin, J.A., Ruthberg, M.I. and Frolov, V.S. "A Combined Method for Rock Breakage"
Proceedings 6th Int. Symposium on Jet Cutting Technology 6-8 April 1982, pp.301-21
Surrey, UK.

Labus, T.J. "Energy Requirements for Rock Penetration by Water Jets"
Proceedings 3rd Int. Symposium on Jet Cutting Technology 11-13 May 1976, Chicago, USA, pp. E3-29 - E3-40.

Lawn, B.R. and Swain M.V. "Microfracture Beneath Point Indentations in Brittle Solids"
Journal of Materials Science 10 1975, pp. 113-22.

Lawn, B. and Wilshaw, R. "Review Indentation Fracture : Principles and Applications"
Journal of Materials Science Vol.10 1975, pp. 1049-081.

Leach, S.J. and Walker, G.L. "The Application of High Speed Liquid Jets to Cutting"
Proceedings Roy. Soc. London Vol.260A 1966 pp. 295-315.

Lebrun, M. "Etude Theoretique at Experimentale de L'Abattage Mechanique, Application a la Conception de Machines D'abbattage et de Creusement"
Thesis presented at the Ecole National Seperieune des Mines de Paris, July 1978.

Lindqvist, P.A. and Lai, H.H. "Behaviour of the Crushed Zone in Rock Indentation"
Rock Mechanics and Rock Engineering 16 1983 pp. 199-207

Lindqvist, P.A. "Stress Fields and Subsurface Crack Propagation of Single and Multiple Rock Indentation and Disc Cutting"
Rock Mechanics Vol. 17/2 1984, pp. 97-112.

Lindqvist, P.A., Lai, H.H. and Alm, O. "Indentation Fracture Development in Rock Continuously Observed with a Scanning Electron Microscope" Int. J. Rock Mech. Min. Sci. & Geomech. Abstr. Vol. 21, No.4. pp. 165-82 1984.

Mann, R.L. and Fatt, I. "Effect of Pore Fluids on the Elastic Properties of Sandstone"
Geophysics Vol. 25 1960 No.2, pp. 433-44.

Merchant, M.E. "Basic Mechanics of the Metal Cutting Process"
J. Appl. Mech. Vol. 11 1945 P.A. 168.

McFeat-Smith, I. "Correlation of Rock Properties and Tunnel Machine Performance in Selected Sedimentary Rocks" Unpublished Ph.D. Thesis, Univ. of Newcastle upon Tyne, June 1975.

McFeat-Smith, I. "Rock Property Testing for the Assessment of Tunnelling Machine Performance" Tunnels and Tunnelling March 1977, pp. 29-33.

McFeat-Smith, I. and Fowell, R.J. "The Selection and Application of Roadheaders for Rock Tunnelling" Proceedings Rapid Excavation and Tunnelling Conference, 1979. Vol.1, pp. 261-79.

McNary, R.O., Blair, J.R., Novak, D.D. and Johnson, D.I. "Augmentation of a Mining Machine with a High-Pressure Jet" Proceedings 3rd Int. Symposium on Jet Cutting Technology 11-13 May 1976, Chicago, USA, pp. D2-13 - D2-20.

Morris, C.J. and MacAndrew, K.M. "A Laboratory Study of High Pressure Water Jet Assisted Cutting" 8th Int. Symposium on Jet Cutting Technology, Durham, UK 1986.

Morris, R., Agbede, R.O. and Thorpe, J.D. "Effects of Water-Through-Bit in Underground Mining Operations" Proceedings Coal Mine Dust Conference, Morgantown, W. Va. Oct. 8-10 1984, pp.110-18.

National Coal Board "NCB Cone Indenter" MRDE Handbook No.5. Revised 1977.

Nikonov, G.P. "Research into the Cutting of Coal by Small Diameter High Pressure Water Jets" Dynamic Rock Mechanics, Soc. of Mining Engineers Chap. 34, New York 1971.

Nikonov, G.P. and Goldin, Y.A. "Coal and Rock Penetration by Fine Continuous High Pressure Water Jets" Proceedings 1st Int. Symposium on Jet Cutting Technology, Coventry, England 1972, Paper E2.

Nishimatsu, Y. "The Mechanics of Rock Cutting" Int. J. Rock Mech. Min. Sci. Vol.9 1972, pp. 261-70.

Nishimatsu, Y. "On the Effect of Tool Velocity in the Rock Cutting" Mining and Machinery Brisbane, Australia 2-6 Jul, 1979, pp. 314-19.

Nishimatsu, Y., Akiyama, M., Suzuki, M., Watanabe, Y. and Miwa, S. "A Rock Machinability Testing System and Prediction of Productivity of Tunnelling Machines" Int. J. Rock Mech. Min. Sci. & Geomech. Abstr. Vol.16, 1979, pp.329-33.

Obert, L., Windes, S.L. and Duvall, W.I. "Standardized Tests for Determining the Physical Properties of Mine Rock" US Bureau of Mines RI 3891 1946, pp.67.

O'Dogherty, M.J. and Burney, A.C. " Laboratory Study of the Effect of Cutting Speed on the Performance of Two Coal Cutter Picks" Colliery Engineering Feb. 1963, pp. 51-4, Mar. 1963, pp. 111-14.

Ozdemir, L. and Evans, R.J. "Development of a Water Jet Assisted Drag Bit Cutting Head for Coal Measures Rocks" Proceedings Rapid Excavation and Tunnelling Conference, 1983 Vol.2, pp. 701-19.

Parate, N.S. "Influence of Water on the Strength of Limestone" Trans. AIME Vol. 254 1973, pp. 127-31.

Pearey, J.T. "Precautions against Frictional Ignitions Associated with Coal Cutting and Tunnelling" The Mining Engineer April 1985, pp. 517-25.

Plessis du, M.P. and Hashish, M. "Experimental and Theoretical Investigation of Hydraulic Cutting of a Western Canadian Coal" Proceedings 5th Int. Symposium on Jet Cutting Technology, Hanover June 2-4 1980, pp. 269-86.

Plumpton, N.A. and Tomlin, M.G. "The Development of a Water Jet System to Improve the Performance of a Boom-Type Roadheader" Proceedings 6th Int. Symposium on Jet Cutting Technology 6-8 April 1982, Surrey, pp. 267-82.

Pomeroy, C.D. "The Breakage of Coal by Wedge Action" Colliery Guardian Nov. 21 1963, pp. 642-77.

Pomery, C.D. "Mining Applications of the Deep Cut Principle" The Mining Engineer June 1968, pp. 506-17.

Price, N.J. "The Compressive Strength of Coal Measures Rocks" Colliery Engineer Vol. 37 1960, pp. 283-92.

Protodyakonov, M.M. and Teder, R.I. "Rational Methods of Planning Experiments" Dynamic Rock Mechanics. Proceedings 12th US Symposium on Rock Mechanics, New York 1971, pp. 129-49.

Rambanda, P.M.H.G. "An Investigation into the Effect of Moisture on Cuttability of Rocks"
Unpublished M.Sc. Dissertation, Univ. of Newcastle upon Tyne 1984.

Ranman, K.E. "A Model Describing Rock Cutting with Conical Picks"
Rock Mechanics Vol. 18 (2) 1985, pp. 131-40.

Rehbinder, G. "Some Aspects on the Mechanism of Erosion of Rock with a High Speed Water Jet"
Proceedings 3rd Int. Symposium on Jet Cutting Technology 11-13 May 1976, Chicago, USA, pp. E1-1 - E1-20.

Rehbinder, G. "Slot Cutting in Rock with a High Speed Water Jet"
Int. J. Rock Mech. Min. Sci. & Geomech Abstr. Vol.14 1977, pp. 229-34.

Rehbinder, G. "A Water Zone Propagating Through a Permeable Rock"
Rock Mechanics Vol. 9, 1977, pp. 245-53.

Rehbinder, G. "Erosion Resistance of Rock"
Proceedings 4th Int. Symposium on Jet Cutting Technology 12-14 April 1978, Canterbury, UK. pp. E1-1 - E1-10.

Rehbinder, G. "A Theory about Cutting Rock with a Water Jet"
Rock Mechanics Vol. 12 1980, pp. 247-57.

Rispin, A. and Bilgin, N. "Prediction of Disk Cutter Performance from Laboratory Rock Cutting Experiments"
Trans. IMM, Section A.
Vol. 86 1977, pp. A28-A34.

Ropchan, D., Wang, F.D., Wolgamott, H.J. "Application of Water-Jet-Assisted Drag Bit and Pick Cutter for the Cutting of Coal Measures Rocks"
Colorado School of Mines, DoE Contract No. ET-77-6-01-9082 April 1980, pp. 82.

Roxborough, F.F. and Rispin, A. "The Mechanical Cutting Characteristics of the Lower Chalk"
Tunnels and Tunnelling, Jan/Feb 1973.

Roxborough, F.F. and Rispin, A. "A Laboratory Investigation into the Application of Picks for Mechanized Tunnel Boring in the Lower Chalk"
The Mining Engineer Oct. 1973, No. 156, pp. 1-13.

Roxborough, F.F. "Cutting Rock with Picks"
The Mining Engineer June1973, pp. 445-55.

Roxborough, F.F. and Phillips, H.R. "Experimental Studies on the Excavation of Rock using Picks"
Proceedings 3rd Congr. Int. Soc. Rock Mech.
1974, pp. 1407-12.

Roxborough, F.F. and Phillips, H.R. "The Mechanical Properties and Cutting Characteristics of the Bunter Sandstone"
Report to TRRL, DoE, Univ. of Newcastle upon Tyne 1975.

Straughan, J. "High Pressure Water Jet Application to Roadheaders"
Proceedings 3rd US Water Jet Symposium,
Pittsburgh, USA, May 1985.

Summers, D.A. and Barker, C.R. "Surface Trials of the Hydrominer"
Proceedings 4th Int. Symposium on Jet Cutting Technology, Canterbury, UK April 1978, pp. J2-13 - J2-14.

Swain, M.V. and Lawn, B.R. "Indentation Fracture in Brittle Rocks and Glasses"
Int. J. Rock Mech. Min. Sci. & Geomech. Abstr.
Vol.13 1976, pp. 311-19.

Szlavin, J. "Relationships between some Physical Properties of Rock Determined by Laboratory Tests"
Int. J. Rock Mech. Min. Sci. & Geomech. Abstr.
Vol.11 1974, pp. 57-66.

Tecen, O. "High Pressure Waterjet Assisted Drag Tool Cutting of Rock Materials"
Unpublished Ph.D. Thesis, Univ. of Newcastle upon Tyne, UK 1982.

Trueman, R. "A Literature Review of the Ignition of Methane-Air Mixtures by Coal-Cutting Picks"
J. S.Afr. Inst. Min. Metall., Vol. 85, No.7.
Jul. 1985, pp. 209-15.

Tutluoglu, L., Hood, M. and Barton, C. "An Investigation of the Mechanisms of Water Jet Assistance on the Rock Cutting Process"
Proceedings 24th US Symposium on Rock Mechanics.
June 1983, pp. 743-49.

Wang, F.D. and Wolgamott, J. "Application of Water Jet Assisted Pick Cutter for Rock Fragmentation"
Proceedings 4th Int. Symposium on Jet Cutting Technology 12-14 April 1978, pp. C1-1 - C1-6,
Canterbury, UK.

Whittaker, D. "Effect of Pick Shape on Cutting Forces" Colliery Guardian Aug. 23 1962, pp. 242-44.

Whittaker, B.N. and Szwilski, A.B. "Rock Cutting by Impact Action" Int. J. Rock Mech. Min. Sci & Geomech. Abstr. Vol.10 1973, pp. 659-71.

Wilson, R.L. "Water-through-Bit Controls Dust" Coal Age March 1984, pp. 41-3.

* * *

APPENDICES

APPENDIX A

LABORATORY EQUIPMENT AND INSTRUMENTS

A.1 Linear Cutting Rig

A.2 High Pressure Water Pump

A.3 Drag Tool

A.4 Dynamometer

A.5 Amplifier

A.6 Tape Recorder

A.7 Galvonometer Amplifier

A.8 UV Recorder

A.9 Pressure Transducer

A.10 Analogue Filter

A.11 Analogue/Digital Converter

A.12 Microcomputer

* * *

A.1 LINEAR CUTTING RIG

Maximum specimen size	...	1m x 1m x 0.7m
Maximum table travel	...	0.90m
Speed of table travel	...	0.34 m/minute
Maximum cutter slide travel	...	1.2m
Speed of cutter slide assembly travel (up/down)	...	0.03 m/minute
Cutting Speed	...	0 - 1.10 m/s
Maximum Normal Force	...	50 kN
Maximum Cutting Force	...	50 kN

*   *   *

A.2 HIGH PRESSURE WATER PUMP

Presswell Engineerig Hydroflo High Pressure Pump.

Motor Power			75 kW
Intensifier (1)	Diameter	=	60mm
Maximum Jet Pressure		=	70 MPa
Maximum Flow Rate		=	45 litre/min
Intensifier (2)	Diameter	=	32mm
Maximum Jet Pressure		=	207 MPa
Maximum Flow Rate		=	15 litre/min.

* * *

A.3 DRAG TOOL

Wimet SS 41/2/HW Heavy Duty Radial Tool

Steel	BS970 EN24 Hardened and Tempered to 341/388 HB
Carbide	Grade CXT
Cobalt Content	9.5%
Hardness	1210 HV30
Grain Size	3.5 micron.
Braze Strength	15.0 tons/in² minimum

*   *   *

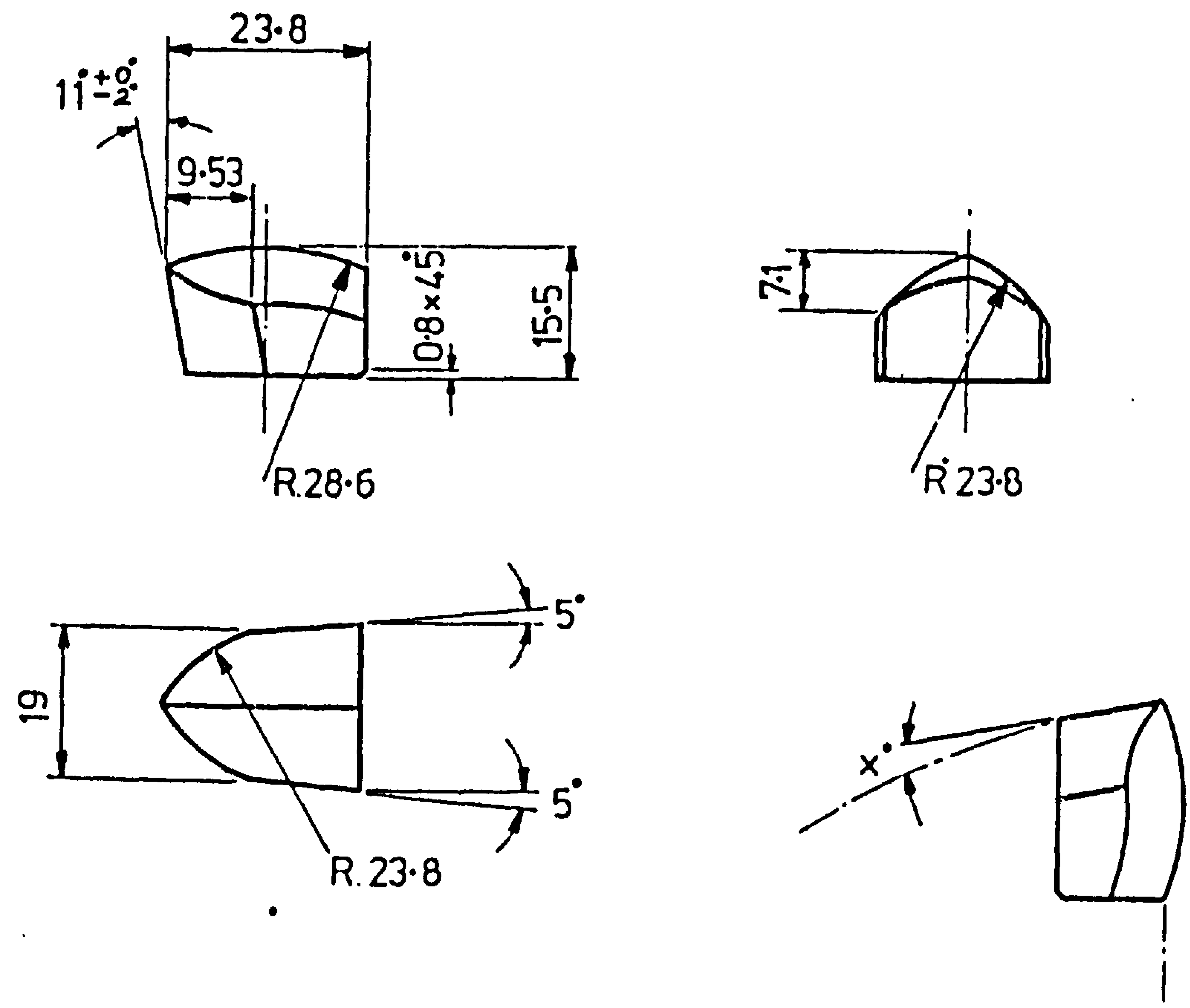

Size in mm

TS 9155

Tool Tip

A.4 DYNAMOMETER

Four-Post Triaxial Steel Dynamometer
(Allington 1969)

Maximum Force :	Cutting	=	100 kN
	Normal	=	50 kN
	Sideway	=	20 kN
Natural Frequency :	Cutting	=	7800 Hz
	Normal	=	6180 Hz
	Sideway	=	6180 Hz

* * *

A.5 AMPLIFIER

EMI SE4300 Carrier Amplifier

Carrier Frequency	3 or 10 KHz
Frequency Response	500 Hz for 3 KHz Carrier
	1750 Hz for 10 KHz Carrier
Maximum Gain	10,000
Full-Scale Output	± 1.4 v

* * *

A.6 TAPE RECORDER

Thorn EMI SE3000 7-Channel Precision FM Tape Recorder

Tape Speed	8-speed from $^{15}/_{32}$ in/sec to 60 in/sec.
Carrier Centre Frequency	216 KHz maximum
Playback band width	40 KHz maximum at 60 in/sec tape speed and pro-rata at other speeds.

* * *

A.7 GALVONOMETER AMPLIFIER

Thorn EMI Galvonometer Drive Module SE1052

Range	10 mv/cm to 100 v/cm in 13 steps.
Frequency Response	DC to 15 KHz ± 3dB
Output	DC to 10 KHz ± 1 dB

* * *

A.8 UV RECORDER

SE Laboratories SE3006 UV Recorder

Channels	6
Galvonometer	SE A1000
Paper Speed	10 to 1250 mm/s in 7 speeds.

* * *

A.9 PRESSURE TRANSDUCER

Intersonde K3020 Pressure Transducer

Range	0-207 MPa
Excitation Voltage	0-20v maximum
Dynamic Frequency Range	7 KHz to 65 KHz maximum (depending on the setting of gain).

* * *

A.10 ANALOGUE FILTER

Barr and Stroud EF4-03 Low Pass/High Pass Analogue Filter

Cut-Off Frequency Range 1 Hz to 100 KHz

Attenuation Response:

Normal:

Attenuation at cut-off frequency

= 3 dB ± 0.5 dB

Damped:

Attenuation at cut-off frequency

= 8 dB ± 0.5 dB

Final Attenuation Rate

= 24 dB/Octave.

* * *

A.11 ANALOGUE/DIGITAL CONVERTER

EDC Photonic Analogue 1208 Multichannel
Analogue Data Acquisition Interface

Inputs	8 differential channels
Sensitivity	0 to +10v or -5v to +5v.
Gain	1, 10, 100 to 1000 or software programmable.
Conversion	15 μs minimum
	35 μs maximum
Resolution	12 bits
Speed	1.08 KHz for 3 channels when PASCAL logging program developed during this project is used.

* * *

A.12 MICROCOMPUTER

Sirius - 1 Computer

Operating System	CPM-86
Ram Capacity	256 k
Clock Rate	1 MHz
Disk Drive	2

*   *   *

APPENDIX B

Jet Characteristics of Newcastle Nozzles.

APPENDIX B

JET CHARACTERISTICS OF NEWCASTLE NOZZLES

Nozzle Dia. (mm)	Jet Pressure (MPa)	Jet Speed (m/s)	Flow Rate (litre/min)	Jet Power (kW)	Discharge Coefficient (Cd)
0.6	17.3	186.0	2.6	0.75	0.823
0.6	29.9	244.5	3.4	1.69	0.820
0.6	45.2	300.7	4.2	3.16	0.823
0.6	71.5	378.2	5.3	6.32	0.826
0.9	18.5	192.4	6.0	1.85	0.817
0.9	30.4	246.6	7.9	4.00	0.839
0.9	44.2	297.3	9.4	6.92	0.828
0.9	69.9	373.9	12.0	13.98	0.841
1.2	19.2	196.0	10.4	3.33	0.782
1.2	29.7	243.7	12.8	6.34	0.774
1.2	43.8	296.0	15.7	11.46	0.782
1.2	69.0	371.5	19.6	22.54	0.778
1.5	16.8	183.3	16.0	4.48	0.823
1.5	29.5	242.9	21.8	10.72	0.846
1.5	43.0	293.3	26.4	18.92	0.849
1.5	67.2	366.6	33.0	36.96	0.849

APPENDIX C

Primary Experimental Results

C.1 Dumfries Sandstone

C.2 Grindleford Sandstone

C.3 Penrith Sandstone

C.4 Pennant Sandstone

C.5 Middleton Limestone

* * *

C.1 DUMFRIES SANDSTONE

Mean Cutting Force (kN)

	0.27 m/s				1.10 m/s			
	0 MPa	18 MPa	44 MPa	70 MPa	0 MPa	18 MPa	44 MPa	70 MPa
5mm	0.59	0.40	0.29	0.42	0.61	0.56	0.59	0.55
10mm	1.21	0.85	1.01	1.12	1.16	0.99	1.23	1.10
15mm	2.19	1.37	1.73	2.00	2.28	1.79	1.72	1.94

Mean Normal Force (kN)

	0.27 m/s				1.10 m/s			
	0 MPa	18 MPa	44 MPa	70 MPa	0 MPa	18 MPa	44 MPa	70 MPa
5mm	0.53	0.31	0.21	0.29	0.54	0.54	0.55	0.49
10mm	0.85	0.48	0.62	0.62	0.88	0.77	0.87	0.72
15mm	1.41	0.66	0.76	0.95	1.52	1.16	1.03	1.25

Mean Peak Cutting Force (kN)

	0.27 m/s				1.10 m/s			
	0 MPa	18 MPa	44 MPa	70 MPa	0 MPa	18 MPa	44 MPa	70 MPa
5mm	1.29	0.86	0.53	0.70	1.34	1.19	1.10	0.94
10mm	2.69	2.04	1.87	2.03	2.74	2.64	2.57	2.24
15mm	4.97	3.54	3.29	3.64	5.55	4.62	4.34	4.18

Mean Peak Normal Force (kN)

	0.27 m/s				1.10 m/s			
	0 MPa	18 MPa	44 MPa	70 MPa	0 MPa	18 MPa	44 MPa	70 MPa
5mm	1.01	0.59	0.36	0.48	1.01	0.97	0.90	0.76
10mm	1.77	1.03	1.02	1.02	1.75	1.70	1.57	1.31
15mm	2.95	1.46	1.29	1.57	3.14	2.56	2.25	2.17

C.2 GRINDLEFORD SANDSTONE

Mean Cutting Force (kN)

	0.27 m/s				1.10 m/s			
	0 MPa	18 MPa	44MPa	70MPa	0 MPa	18 MPa	44 MPa	70 MPa
5mm	1.27	1.00	0.91	0.89	1.49	1.37	1.18	1.19
10mm	3.03	2.52	2.64	2.84	3.57	3.39	2.75	2.88
15mm	5.72	5.74	4.81	5.06	7.34	6.52	5.62	5.65

Mean Normal Force (kN)

	0.27 m/s				1.10 m/s			
	0 MPa	18 MPa	44 MPa	70MPa	0 MPa	18 MPa	44 MPa	70 MPa
5mm	0.90	0.61	0.55	0.55	1.74	1.31	1.06	1.00
10mm	2.07	1.54	1.35	1.42	3.58	3.27	2.05	1.94
15mm	3.67	3.33	2.55	2.57	7.52	6.13	4.46	4.43

Mean Peak Cutting Force (kN).

	0.27 m/s				1.10 m/s			
	0 MPa	18 MPa	44 MPa	70 MPa	0 MPa	18 MPa	44 MPa	70 MPa
5mm	2.63	2.37	2.19	2.02	3.20	2.87	2.78	2.80
10mm	6.91	6.67	6.42	6.16	7.86	7.42	7.14	7.21
15mm	12.97	13.21	11.99	12.19	15.16	13.79	13.58	13.80

Mean Peak Normal Force (kN)

	0.27 m/s				1.10 m/s			
	0 MPa	18 MPa	44 MPa	70 MPa	0 MPa	18 MPa	44 MPa	70 MPa
5mm	1.75	1.35	1.24	1.16	3.14	2.47	2.13	2.00
10mm	4.19	3.45	3.00	2.80	6.58	6.08	4.48	4.35
15mm	7.53	6.76	5.94	5.61	12.95	11.08	9.54	8.67

C.3 PENRITH SANDSTONE

Mean Cutting Force (kN)

	0.27 m/s				1.10 m/s			
	0 MPa	18 MPa	44MPa	70 MPa	0 MPa	18 MPa	44 MPa	70 MPa
5mm	1.37	1.14	1.12	0.97	1.55	1.31	1.38	1.40
10mm	3.78	2.89	2.94	3.34	3.90	3.49	3.26	2.98
15mm	6.71	6.48	6.24	6.22	6.06	6.30	5.88	5.66

Mean Normal Force (kN)

	0.27 m/s				1.10 m/s			
	0 MPa	18 MPa	44 MPa	70 MPa	0 MPa	18 MPa	44 MPa	70 MPa
5mm	1.68	1.14	1.24	1.16	2.76	1.96	1.66	1.64
10mm	4.35	2.49	2.34	2.55	6.86	5.38	4.40	2.84
15mm	7.32	5.97	5.31	4.44	8.88	8.53	7.71	6.28

Mean Peak Cutting Force (kN)

	0.27 m/s				1.10 m/s			
	0 MPa	18 MPa	44 MPa	70 MPa	0 MPa	18 MPa	44 MPa	70 MPa
5mm	3.39	3.76	3.18	2.22	3.76	3.55	3.75	3.66
10mm	10.27	10.03	10.05	9.85	8.94	9.03	8.84	9.38
15mm	17.74	19.36	19.46	19.51	15.27	16.29	16.53	15.38

Mean Peak Normal Force (kN)

	0.27 m/s				1.10 m/s			
	0 MPa	18 MPa	44 MPa	70 MPa	0 MPa	18 MPa	44 MPa	70 MPa
5mm	3.71	3.20	3.05	2.25	5.52	4.52	4.07	3.79
10mm	10.39	8.61	8.07	7.28	13.21	11.24	10.19	8.56
15mm	17.54	16.75	16.08	14.99	18.97	18.73	17.35	15.16

C.4 PENNANT SANDSTONE

Mean Cutting Force (kN)

	0.27 m/s				1.10 m/s			
	0 MPa	18MPa	44 MPa	70MPa	0 MPa	18MPa	44MPa	70 MPa
5mm	2.24	2.54	2,15	1.77	3:75	3.65	3.59	3.51
10mm	5.53	5.49	5.96	6.17	14.38	15.09	14.21	13.76
15mm	10.06	10.42	11.43	11.59	-	-	-	-

Mean Normal Force (kN)

	0.27 m/s				1.10 m/s			
	0 MPa	18MPa	44MPa	70 MPa	0 MPa	18 MPa	44 MPa	70 MPa
5mm	4.09	4.35	3.12	1.79	8.74	8.83	8.42	8.22
10mm	8.79	8.32	8.08	7.85	44.73	47.32	44.52	43.32
15mm	13.02	13.22	13.40	12.91	-	-	-	-

Mean Peak Cutting Force (kN)

	0.27 m/s				1.10 m/s			
	0 MPa	18MPa	44 MPa	70 MPa	0 MPa	18 MPa	44 MPa	70 MPa
5mm	4.18	4.57	4.61	4.24	5.14	4.96	4.95	4.86
10mm	12.54	12.55	13.44	13.73	17.25	17.74	16.62	16.56
15mm	21.80	24.20	25.09	25.87	-	-	-	-

Mean Peak Normal Force (kN)

	0.27 m/s				1.10 m/s			
	0 MPa	18MPa	44 MPa	70 MPa	0 MPa	18 MPa	44 MPa	70 MPa
5mm	6.56	7.04	7.04	4.89	11.59	11.21	11.02	11.01
10mm	14.58	14.75	14.91	14.72	50.60	52.84	49.51	49.41
15mm	22.10	22.53	22.61	22.68	-	-	-	-

C.5 MIDDLETON LIMESTONE

Mean Cutting Force (kN)

	0.27 m/s				1.10 m/s			
	0 MPa	18 MPa	44 MPa	70 MPa	0 MPa	18 MPa	44 MPa	70 MPa
5mm	1.59	1.58	1.43	1.32	1.52	1.69	1.60	1.63
10mm	4.28	4.00	3.54	4.18	3.78	3.77	3.61	3.44
15mm	7.27	7.10	6.43	6.78	6.60	6.31	5.92	5.27

Mean Normal Force (kN)

	0.27 m/s				1.10 m/s			
	0 MPa	18 MPa	44 MPa	70 MPa	0 MPa	18 MPa	44 MPa	70 MPa
5mm	2.55	2.51	2.12	1.78	3.02	3.17	2.93	2.92
10mm	5.31	4.61	3.97	3.92	5.64	5.32	5.34	4.68
15mm	7.83	7.01	6.30	6.27	8.27	7.64	7.12	6.47

Mean Peak Cutting Force (kN)

	0.27 m/s				1.10 m/s			
	0 MPa	18 MPa	44 MPa	70 MPa	0 MPa	18 MPa	44 MPa	70 MPa
5mm	3.40	3.33	3.36	3.42	3.20	3.26	3.37	3.37
10mm	10.65	10.06	9.73	11.19	8.97	8.64	8.74	8.43
15mm	18.51	18.98	17.75	19.37	16.29	15.63	15.65	14.33

Mean Peak Normal Force (kN)

	0.27 m/s				1.10 m/s			
	0 MPa	18 MPa	44 MPa	70MPa	0 MPa	18 MPa	44 MPa	70 MPa
5mm	4.51	4.34	4.07	3.76	5.26	5.17	5.19	5.12
10mm	10.44	9.24	8.57	9.23	10.37	9.81	9.97	9.14
15mm	16.11	15.90	14.48	15.16	16.27	14.73	14.74	13.77

APPENDIX D

SECONDARY EXPERIMENTAL RESULTS

D.1 Effect of Nozzle Diameter

- D.1.1 Grindleford Sandstone
- D.1.2 Pennant Sandstone

D.2 Effect of Tool Bluntness and Jet Position

- D.2.1 Grindleford Sandstone
- D.2.2 Middleton Limestone

D.3 Effect of Wear Rate

D.4 Effect of Cutting Mode

- D.4.1 Grindleford Sandstone
- D.4.2 Pennant Sandstone

D.5 Effect of Slot Depth.

* * *

D.1 Effect of Nozzle Diameter

D.1.1 GRINDLEFORD SANDSTONE (DEPTH OF CUT = 10mm; TRAVERSE SPEED = 1.10 m/s)

Mean Cutting Force (kN)

Nozzle Diameter	0 MPa	18 MPa	44 MPa	70 MPa
0.6mm	4.06	4.19	3.93	3.52
0.9mm	3.57	3.39	2.75	2.88
1.2mm	4.00	3.55	3.18	3.34
1.5mm	4.44	3.93	3.26	3.49

Mean Normal Force (kN)

Nozzle Diameter	0 MPa	18 MPa	44 MPa	70 MPa
0.6mm	4.24	4.92	3.79	3.25
0.9mm	3.58	3.27	2.05	1.94
1.2mm	4.06	3.51	2.47	2.37
1.5mm	4.29	3.88	2.48	2.43

Mean Peak Cutting Force (kN)

Nozzle Diameter	0 MPa	18 MPa	44 MPa	70 MPa
0.6mm	8.13	8.45	7.86	7.61
0.9mm	7.86	7.42	7.12	7.21
1.2mm	8.01	7.49	7.60	8.01
1.5mm	8.76	8.01	8.27	8.53

Mean Peak Normal Force (kN)

Nozzle Diameter	0 MPa	18 MPa	44 MPa	70 MPa
0.6mm	7.37	8.05	6.87	6.30
0.9mm	6.58	6.08	4.48	4.35
1.2mm	7.06	6.36	5.00	4.91
1.5mm	7.56	6.97	5.21	5.08

D.1.2 PENNANT SANDSTONE - Relieved cutting (Sharp Tool)

Depth of cut = 10 mm

Traverse speed = 0.27 m/s

Mean Cutting Force (KN)

Nozzle Diameter	0 MPa	18.5 MPa	44.2 MPa	69.9 MPa
0.6 mm	6.62	7.07	7.40	7.07
0.9 mm	6.71	6.40	6.57	6.71

Mean Normal Force (KN)

Nozzle Diameter	0 MPa	18.5 MPa	44.2 MPa	69.9 MPa
0.6 mm	9.79	9.09	9.37	9.21
0.9 mm	8.75	8.14	7.62	7.42

Mean Peak Cutting Force (KN)

Nozzle Diameter	0 MPa	18.5 MPa	44.2 MPa	69.9 MPa
0.6 mm	18.23	18.14	18.62	18.52
0.9 mm	17.61	17.92	17.46	18.06

Mean Peak Normal Force (KN)

Nozzle Diameter	0 MPa	18.5 MPa	44.2 MPa	69.9 MPa
0.6 mm	18.37	17.98	17.43	18.23
0.9 mm	16.64	15.92	15.52	15.81

D.2 EFFECT OF TOOL BLUNTNESS AND JET POSITION

D.2.1 GRINDLEFORD SANDSTONE (Depth of cut = 10mm)

(i) Mean Cutting Force (kN)

	0.27 m/s				1.10 m/s			
	0 MPa	18 MPa	44 MPa	70 MPa	0 MPa	18 MPa	44 MPa	70 MPa
Jet Ahead								
Sharp	3.03	2.52	2.64	2.84	3.57	3.39	2.75	2.88
Blunt	5.93	4.56	3.85	3.67	6.65	6.25	5.16	4.69
Jet Behind								
Sharp	3.52	3.69	3.62	3.84	3.76	3.83	3.96	4.02
Blunt	5.69	5.31	4.59	4.61	6.29	5.95	5.61	5.03

(ii) Mean Normal Force (kN)

	0.27 m/s				1.10 m/s			
	0 MPa	18 MPa	44 MPa	70 MPa	0 MPa	18 MPa	44 MPa	70 MPa
Jet Ahead								
Sharp	2.07	1.54	1.35	1.42	3.58	3.27	2.05	1.94
Blunt	5.85	3.74	2.49	2.07	16.20	12.70	6.91	5.10
Jet Behind								
Sharp	2.55	2.61	2.36	2.17	3.49	3.79	3.20	3.11
Blunt	5.70	4.81	3.66	2.97	11.97	9.60	6.90	5.17

(iii) Mean Peak Cutting Force (kN)

	0.27 m/s				1.10 m/s			
	0 MPa	18 MPa	44 MPa	70 MPa	0 MPa	18 MPa	44 MPa	70 MPa
Jet Ahead								
Sharp	6.91	6.67	6.42	6.16	7.86	7.42	7.14	7.21
Blunt	11.07	9.54	8.39	7.23	10.15	10.12	9.53	9.13
Jet Behind								
Sharp	7.71	7.91	7.71	7.23	7.49	7.75	7.95	8.09
Blunt	10.83	10.32	9.00	8.36	9.72	9.75	9,38	8.88

(iv) Mean Peak Normal Force (kN)

	0.27 m/s				1.10 m/s			
	0 MPa	18 MPa	44 MPa	70 MPa	0 MPa	18 MPa	44 MPa	70 MPa
Jet Ahead								
Sharp	4.19	3.45	3.00	2.80	6.58	6.08	4.48	4.35
Blunt	9.87	7.21	5.14	3.81	20.08	17.55	12.28	9.99
Jet Behind								
Sharp	5.21	5.19	4.87	4.19	6.28	6.72	6.31	6.18
Blunt	9.77	8.81	6.94	5.27	15.43	13.42	10.31	8.46

D.2.2

MIDDLETON LIMESTONE (Depth of cut = 10mm; Traverse Speed = 1.10 m/s)

Mean Cutting Force (kN)

	0 MPa	18MPa	44 MPa	70MPa
Jet Ahead				
Sharp	4.28	4.00	3.54	4.18
Blunt	7.79	7.90	7.51	7.46
Jet Behind				
Sharp	3.89	3.64	3.49	3.60
Blunt	6.22	6.48	6.00	6.63

Mean Normal Force (kN)

	0 MPa	18 MPa	44 MPa	70 MPa
Jet Ahead				
Sharp	5.31	4.61	3.97	3.92
Blunt	24.92	24.27	22.45	21.63
Jet Behind				
Sharp	5.07	4.87	4.90	5.08
Blunt	22.20	22.69	21.56	22.08

Mean Peak Cutting Force (kN)

	0 MPa	18 MPa	44 MPa	70 MPa
Jet Ahead				
Sharp	10.65	10.06	9.73	11.19
Blunt	12.56	12.81	12.44	12.77
Jet Behind				
Sharp	8.79	8.67	8.37	8.46
Blunt	11.17	11.58	11.21	11.79

Mean Peak Normal Force (kN)

	0 MPa	18 MPa	44 MPa	70 MPa
Jet Ahead				
Sharp	10.44	9.24	8.57	9.23
Blunt	33.23	33.59	32.04	32.42
Jet Behind				
Sharp	9.09	9.00	9.00	9.07
Blunt	32.97	34.01	32.77	33.01

D.3 **Effect of Wear Rate**

Pennant Sandstone - Relieved Cutting (Depth of Cut = 10mm
Traverse Speed = 1.10m/s)

(i) Unassisted

Cut No.	Accumulative Length (m)	MCF (kN)	MNF (kN)	MPCF (kN)	MPNF (kN)
1	0.5	5.40	7.46	10.56	12.83
2	1.06	5.58	10.40	10.87	15.73
3	2.26	6.14	12.25	13.09	20.61
4	3.46	6.90	15.09	13.25	23.94
5	4.99	7.65	17.51	14.57	27.70
6	5.86	7.85	16.11	15.19	27.44
7	7.06	8.00	21.08	14.96	32.28
8	8.26	7.90	22.32	14.32	34.48
9	9.46	8.49	24.16	15.24	36.30
10	10.66	8.16	23.11	15.72	37.47
11	11.86	9.44	27.97	17.15	42.18
12	13.06	9.30	26.14	18.02	43.30
13	14.26	10.00	30.92	16.59	42.08
14	15.46	10.75	32.51	18.07	45.55

(ii) Jet - Before - Tool Configuration

Jet Pressure = 70 MPa

Nozzle Diameter = 0.6mm

Cut No.	Accumulative Length (m)	MCF (kN)	MNF (kN)	MPCF (kN)	MPNF (kN)
1	0.5	4.99	5.53	13.25	9.90
2	1.7	4.99	7.03	12.64	11.24
3	2.9	4.92	5.98	12.53	12.66
4	4.1	6.20	9.04	13.20	16.38
5	5.3	7.91	12.13	15.08	19.27
6	6.50	8.34	14.27	15.52	22.38
7	7.70	8.63	16.24	17.29	26.14
8	8.90	8.70	15.84	17.04	25.41
9	10.10	8.41	16.45	16.11	26.27
10	11.30	7.81	16.60	17.07	28.65
11	12.50	7.73	16.78	16.76	29.13
12	13.70	8.65	17.87	16.76	28.13
13	14.90	8.82	18.65	18.55	29.90

(iii) Jet - Before - Tool Configuration

Jet Pressure = 70 MPa

Jet Diameter = 0.9mm

Cut No.	Accumulative Length (m)	MCF (kN)	MNF (kN)	MPCF (kN)	MPNF (kN)
1	0.43	5.87	5.27	15.19	10.12
2	1.03	5.96	6.34	14.83	12.98
3	1.73	7.61	10.24	14.49	15.70
4	2.93	7.49	11.79	14.57	19.71
5	4.13	8.51	14.97	16.23	23.08
6	5.33	9.42	16.08	18.30	24.76
7	6.53	9.36	17.50	16.90	26.45
8	7.73	9.42	18.27	18.35	27.57
9	8.93	9.45	17.85	17.60	27.01
10	10.13	9.22	16.98	17.35	27.05
11	11.33	10.77	19.65	18.58	28.61
12	12.53	12.06	33.63	19.70	48.66
13	13.73	13.67	42.95	20.37	56.00
14	14.93	14.81	47.61	21.80	60.54

(iv) Jet - After - Tool Configuration

Jet Pressure = 70 MPa

Nozzle Diameter = 0.6mm

Cut No.	Accumulative Length (m)	MCF (kN)	MNF (kN)	MPCF (kN)	MPNF (kN)
1	0.54	4.36	4.66	11.07	9.38
2	1.74	5.79	7.11	13.90	13.22
3	2.94	7.20	9.85	15.19	16.29
4	4.14	6.20	7.85	15.56	16.03
5	5.34	7.48	10.95	14.68	17.50
6	6.54	7.43	11.10	15.69	19.06
7	7.74	8.11	13.18	16.39	21.35
8	8.94	7.79	12.94	15.89	21.30
9	10.14	8.47	15.63	15.44	22.86
10	11.34	8.60	15.87	15.83	23.96
11	12.54	8.29	15.88	15.83	24.29
12	13.74	8.70	17.16	16.93	25.28

(v) Jet - After - Tool Configuration

Jet Pressure = 70 MPa

Nozzle Diameter = 0.9mm

Cut No.	Accumulative Length (m)	MCF (kN)	MNF (kN)	MPCF (kN)	MPNF (kN)
1	0.3	5.89	6.65	13.68	12.10
2	0.85	5.29	8.95	12.64	14.56
3	1.29	7.61	9.87	13.23	14.30
4	2.49	8.01	11.00	15.36	18.15
5	3.69	7.67	13.04	14.49	19.71
6	4.89	7.51	12.52	15.66	21.09
7	6.09	7.01	13.87	13.96	21.61
8	7.29	8.00	13.91	15.30	22.47
9	9.49	7.69	14.79	14.85	22.17
10	9.69	9.24	16.53	16.03	24.07
11	10.89	8.69	15.86	16.14	24.85
12	12.09	9.34	17.16	15.83	24.93
13	13.29	10.15	18.78	17.01	26.53
14	14.49	11.70	20.32	17.91	27.48
15	15.69	11.61	19.78	19.08	27.35

D.4 EFFECT OF CUTTING MODE

D.4.1 Grindleford Sandstone - relieved cutting

Jet-before-tool configuration

Depth of cut = 10 mm

Traverse speed = 1.10 m/s

MEAN CUTTING FORCE (KN)

Nozzle Diameter	0 MPa	18.5 MPa	44.2 MPa	69.9 MPa
0.6 mm	4.58	4.90	4.69	4.38
0.9 mm	5.29	4.64	4.12	3.76
1.2 mm	4.93	4.99	3.90	3.57

MEAN NORMAL FORCE (KN)

Nozzle Diameter	0 MPa	18.5 MPa	44.2 MPa	69.9 MPa
0.6 mm	6.95	7.15	6.29	5.26
0.9 mm	7.36	6.10	4.06	3.52
1.2 mm	6.93	6.66	3.98	3.53

MEAN PEAK CUTTING FORCE (KN)

Nozzle Diameter	0 MPa	18.5 MPa	44.2 MPa	69.9 MPa
0.6 mm	9.87	10.09	10.16	10.10
0.9 mm	10.78	10.20	10.01	9.32
1.2 mm	10.17	10.22	9.42	8.91

MEAN PEAK NORMAL FORCE (KN)

Nozzle Diameter	0 MPa	18.5 MPa	44.2 MPa	69.9 MPa
0.6 mm	11.61	11.96	11.86	10.85
0.9 mm	12.24	11.15	8.85	7.59
1.2 mm	11.54	11.73	8.78	7.60

D.4.2 Pennant Sandstone - relieved cutting (blunt tool)

Jet-before-tool configuration

Depth of cut = 10 mm

Traverse speed = 0.27 m/s

Nozzle diameter = 0.9 mm

Jet Pressure (MPa)	MCF (kN)	MNF (kN)	MPCF (kN)	MPNF (kN)
0	9.25	17.79	21.40	29.85
18.5	10.36	18.85	22.89	30.84
44.2	9.71	17.38	22.19	30.42
69.9	10.20	17.57	24.22	31.14

D.5 Effect of slot depth

Grindleford Sandstone - dry cutting with slot (sharp tool)

Depth of cut = 10 mm

Traverse speed = 1.10 m/s

Slot Depth (mm)	MCF (kN)	MNF (kN)	MPCF (kN)	MPNF (kN)
0	4.38	6.01	8.07	9.14
3.71	4.32	5.98	7.90	9.02
5.91	4.53	6.16	7.62	9.03
7.36	4.28	5.06	7.50	8.31
10.87	3.71	3.62	6.74	6.84

APPENDIX E COMPARISON OF MEASUREMENTS AND PREDICTIONS

E.1	Rehbinder's Specific Erodability
E.1.1	Dumfries Sandstone
E.1.2	Grindleford Sandstone
E.1.3	Penrith Sandstone
E.2	Measured and Predicted Jet Penetration
E.2.1	Dumfries Sandstone
E.2.2	Grindleford Sandstone
E.2.3	Penrith Sandstone
E.3	Sum of squares of the Residuals for Tool Force Predictions using various Rock Property Indices
E.4	Measured and Predicted Force Reduction using Kuzmich's Equation.
E.4.1	Dumfries Sandstone
E.4.2	Grindleford Sandstone
E.4.3	Penrith Sandstone
E.5	Measured and Predicted Force Reduction using Proposed Expression
E.5.1	Grindleford Sandstone (sharp tool)
E.5.1	Penrith Sandstone (sharp tool)
E.5.3	Grindleford Sandstone (blunt tool)

E.1 REHBINDER'S SPECIFIC ERODABILITY

Nozzle Diameter (mm)	Stagnation Pressure (MPa)	Traverse Speed (m/s)	Jet Penetration (mm)	Specific Erodability $m^3/NS \times 10^{-8}$
0.9	18.5	0.27	4.51	7.3
		0.55	3.71	12.3
		0.82	3.53	17.4
		1.10	2.99	19.8
	44.2	0.27	12.11	8.2
		0.55	11.16	15.4
		0.82	10.14	20.9
		1.10	7.63	21.1
	69.9	0.27	21.08	9.0
		0.55	17.19	15.0
		0.82	16.05	20.9
		1.10	12.02	21.0
			Mean =	15.7 ± 5.3

E.1.1 Dumfries Sandstone.

Nozzle Diameter (mm)	Stagnation Pressure (MPa)	Traverse Speed (m/s)	Jet Penetration (mm)	Specific Erodability (m^3/NS) x 10^{-8}
0.9	18.5	0.27	0.74	1.20
		0.37	0.57	1.27
		0.55	0.55	1.82
		1.10	0.23	1.52
	30.4	0.27	1.66	1.64
		0.37	1.45	1.96
		0.55	1.12	2.25
		1.10	0.87	3.50
	44.2	0.27	2.83	1.92
		0.37	2.50	2.33
		0.55	1.99	2.75
		1.10	1.57	4.34
	69.9	0.27	4.48	1.92
		0.37	4.28	2.52
		0.55	3.91	3.42
		1.10	2.78	4.86
				Mean = 2.45 ± 1.07

E.1.2 Grindleford Sandstone.

Nozzle Diameter (mm)	Stagnation Pressure (MPa)	Traverse Speed (m/s)	Jet Penetration (mm)	Specific Erodability (m^3/NS) x 10^{-8}
0.9	14.7	0.25	0.99	1.87
		0.46	0.49	1.70
		0.73	0.40	2.21
		0.88	0.30	2.00
		1.04	0.10	0.79
	24.1	0.25	1.50	1.73
		0.46	1.28	2.71
		0.73	1.22	4.11
		0.88	1.00	4.06
		1.04	0.77	3.69
	36.4	0.25	2.36	1.80
		0.46	1.96	2.75
		0.73	2.19	4.88
		0.88	1.84	4.94
		1.04	1.47	4.67
	51.6	0.25	3.33	1.79
		0.46	2.97	2.94
		0.73	2.66	4.18
		0.88	2.30	4.36
		1.04	2.21	4.96
	69.9	0.25	5.29	2.10
		0.46	4.27	3.12
		0.73	3.53	4.10
		0.88	3.31	4.63
		1.04	2.95	4.88
			Mean =	3.34 ± 1.23

E.1.3 Penrith Sandstone.

E.2 MEASURED AND PREDICTED JET PENETRATION

Stagnation Pressure (MPa)	Jet Speed (m/s)	Traverse Speed (m/s)	Jet Penetration (mm)						
			Measured	Kuzmich	Modified Kuzmich	Cooley	Rehbinder	Modified Rehbinder	Hashish
18.5	192.4	0.27	4.51	2.27	4.85	3.76	9.68	5.71	4.78
		0.55	3.71	1.59	3.88	3.05	4.75	4.12	2.99
		0.82	3.53	1.30	3.43	2.72	3.19	3.61	3.18
		1.10	2.99	1.12	3.13	2.49	2.38	3.35	1.70
44.2	297.3	0.27	12.11	5.42	12.74	12.12	23.13	13.64	15.63
		0.55	11.16	3.79	10.20	9.85	11.36	9.84	12.22
		0.82	10.14	3.11	9.01	8.75	7.62	8.63	9.76
		1.10	7.63	2.68	8.22	8.04	5.68	7.99	8.02
69.9	373.9	0.27	21.08	8.56	21.17	21.36	36.58	21.38	19.10
		0.55	17.19	6.00	16.96	17.36	17.97	15.57	16.89
		0.82	16.05	4.91	14.98	15.44	12.04	13.65	14.48
		1.10	12.03	4.24	13.67	14.17	8.98	12.64	12.42
Sum of Squares of Residual ss			0.00	657.730	7.020	10.770	426.16	17.240	24.700
Correlation Coefficient, r			1.00	0.966	0.991	0.989	0.826	0.979	0.970
Index of Determination, r^2			1.00	0.933	0.982	0.979	0.693	0.958	0.940

E.2.1 Dumfries Sandstone.

Stagnation Pressure (MPa)	Jet Speed (m/s)	Traverse Speed (m/s)	Jet Penetration (mm)						
			Measured	Kuzmich	Modified Kuzmich	Cooley	Rehbinder	Modified Rehbinder	Hashish
18.5	192.4	0.27	0.74	1.11	0.82	0.45	1.51	1.19	0.43
		0.37	0.57	0.95	0.73	0.41	1.10	1.00	0.35
		0.55	0.55	0.78	0.63	0.36	0.74	0.82	0.25
		1.10	0.23	0.55	0.49	0.29	0.37	0.65	0.14
30.4	246.6	0.27	1.66	1.82	1.58	1.35	2.48	1.96	2.04
		0.37	1.45	1.56	1.41	1.22	1.81	1.64	1.71
		0.55	1.12	1.28	1.22	1.07	1.22	1.35	1.31
		1.10	0.87	0.90	0.95	0.86	0.61	1.06	0.76
44.2	297.3	0.27	2.83	2.65	2.59	2.49	3.61	2.85	3.22
		0.37	2.50	2.26	2.31	2.25	2.63	2.38	2.83
		0.55	1.99	1.86	2.00	1.98	1.77	1.97	2.27
		1.10	1.57	1.31	1.56	1.59	0.89	1.54	1.39
69.9	373.9	0.27	4.48	4.19	4.77	4.80	5.71	4.50	4.38
		0.37	4.28	3.58	4.25	4.34	4.17	3.77	4.07
		0.55	3.91	2.93	3.68	3.83	2.80	3.11	3.52
		1.10	2.78	2.08	2.87	3.07	1.40	2.44	2.36
Sum of Squares of Residuals,ss			0.00	2.700	0.360	0.680	7.610	1.880	1.260
Correlation Coefficient, r			1.00	0.978	0.994	0.992	0.876	0.982	0.978
Index of Determination, r^2			1.00	0.957	0.988	0.984	0.768	0.965	0.957

E.2.2 Grindleford Sandstone.

Stagnation Pressure (MPa)	Jet Speed (m/s)	Traverse Speed (m/s)	Jet Penetration (mm)						
			Measured	Kuzmich	Modified Kuzmich	Cooley	Rehbinder	Modified Rehbinder	Hashish
14.7	171.5	0.25	0.99	0.71	0.83	-0.15	1.77	1.10	0.48
		0.46	0.49	0.52	0.68	-0.13	0.96	0.82	0.31
		0.73	0.40	0.41	0.58	-0.11	0.61	0.69	0.21
		0.88	0.30	0.38	0.54	-0.10	0.50	0.66	0.18
		1.04	0.10	0.35	0.51	-0.10	0.42	0.63	0.16
24.1	219.5	0.25	1.50	1.16	1.49	0.64	2.90	1.81	1.99
		0.46	1.28	0.86	1.21	0.54	1.57	1.34	1.40
		0.73	1.22	0.68	1.03	0.47	0.99	1.14	1.00
		0.88	1.00	0.62	0.97	0.45	0.82	1.08	0.86
		1.04	0.77	0.57	0.91	0.42	0.70	1.03	0.75
36.4	269.8	0.25	2.36	1.75	2.41	1.80	4.38	2.74	3.16
		0.46	1.96	1.29	1.96	1.51	2.38	2.03	2.45
		0.73	2.19	1.03	1.67	1.32	1.50	1.72	1.83
		0.88	1.84	0.94	1.56	1.25	1.24	1.63	1.62
		1.04	1.47	0.86	1.48	1.19	1.05	1.56	1.43
51.6	321.2	0.25	3.33	2.49	3.63	3.35	6.20	3.88	3.94
		0.46	2.97	1.83	2.94	2.81	3.37	2.88	3.33
		0.73	2.66	1.46	2.51	2.45	2.12	2.44	2.65
		0.88	2.30	1.33	2.35	2.32	1.76	2.31	2.37
		1.04	2.21	1.22	2.22	2.21	1.49	2.28	2.12
69.9	373.9	0.25	5.29	3.37	5.17	5.34	8.40	5.26	4.42
		0.46	4.27	2.48	4.20	4.47	4.57	3.90	4.00
		0.73	3.53	1.97	3.58	3.90	2.88	3.30	3.36
		0.88	3.31	1.80	3.36	3.70	2.39	3.13	3.06
		1.04	2.95	1.65	3.17	3.52	2.02	3.00	2.79
Sum of Squares of Residuals,ss			0.00	22.93	0.960	6.830	29.47	1.780	3.180
Correlation Coefficient, r			1.00	0.967	0.989	0.958	0.835	0.981	0.954
Index of Determination, r^2			1.00	0.935	0.978	0.918	0.697	0.963	0.910

E.2.3 Penrith Sandstone.

E.3 Sum of Squares of the Residuals for Tool Force Predictions using various Rock Property Indices Cutting Speed = 0.27 m/s

Rock Index	MCF (kN)	MNF (kN)	MPCF (kN)	MPNF (kN)
1. Uniaxial Compressive Strength (MPa)	1.36	3.19	13.69	42.18
2. Uniaxial Tensile Strength (MPa)	2.13	12.98	37.90	91.26
3. Shore Hardness	1.46	9.45	48.18	143.08
4. Plasticity (%)	7.98	34.03	20.96	71.57
5. Porosity (%)	5.62	12.85	61.57	101.23
6. Cone Indenter Number	2.98	20.11	34.01	106.93
7. Dry Density (kg/m^3)	3.81	33.34	20.31	69.69
8. Newcastle Abrasivity (1/ 10mm)	17.71	73.44	53.87	137.81
9. Dynamic Young's Modulus (GPa)	27.38	83.18	152.44	270.97

E.4 ACTUAL AND PREDICTED CUTTING FORCE REDUCTIONS

Depth of Cut (mm)	Jet Pressure (MPa)	Predicted Jet Penetration hs (mm)	Actual Jet Penetration ha (mm)	Predicted Reduction (%)		Actual Reduction (%)	
				Based on hs	Based on ha	Mean	Mean Peak
5	18.5	2.27	4.51	27	38	32	33
	44.2	5.42	12.11	42	62	51	59
	69.9	8.56	21.08	52	82	29	46
10	18.5	2.27	4.51	19	27	30	24
	44.2	5.42	12.11	29	44	17	31
	69.9	8.56	21.08	37	58	7	25
15	18.5	2.27	4.51	22	22	47	40
	44.2	5.42	12.11	24	36	33	46
	69.9	8.56	21.08	30	47	23	40

E.4.1.1 Dumfries Sandstone : Traverse Speed = 0.27 m/s.

Depth of Cut (mm)	Jet Pressure (MPa)	Predicted Jet Penetration hs (mm)	Actual Jet Penetration ha (mm)	Predicted Reduction (%)		Actual Reduction (%)	
				Based on hs	Based on Ha	Mean	Mean Peak
5	18.5	1.12	2.99	19	31	8	0
	44.2	2.68	7.63	29	49	3	-2
	69.9	4.24	12.03	37	62	10	9
10	18.5	1.12	2.99	13	22	15	4
	44.2	2.68	7.63	21	35	-6	6
	69.9	4.24	12.03	26	44	5	18
15	18.5	1.12	2.99	11	18	22	17
	44.2	2.68	7.63	17	29	25	22
	69.9	4.24	12.03	21	36	15	25

E.4.1.2 Dumfries Sandstone : Traverse Speed = 1.10 m/s.

Depth of Cut (mm)	Jet Pressure (MPa)	Predicted Jet Penetration hs (mm)	Actual Jet Penetration ha (mm)	Predicted Reduction (%)		Actual Reduction (%)	
				Based on hs	Based on ha	Mean	Mean Peak
5	18.5	1.11	0.74	19	15	21	10
	44.2	2.65	2.83	29	30	28	17
	69.9	4.19	4.48	37	38	30	23
10	18.5	1.11	0.74	13	11	17	4
	44.2	2.65	2.83	21	21	13	7
	69.9	4.19	4.48	26	27	6	11
15	18.5	1.11	0.74	11	9	4	-2
	44.2	2.65	2.83	17	17	16	8
	69.9	4.19	4.48	21	22	12	6

E.4.2.1 Grindleford Sandstone : Traverse Speed = 0.27 m/s.

Depth of Cut (mm)	Jet Pressure (MPa)	Predicted Jet Penetration hs (mm)	Actual Jet Penetration ha (mm)	Predicted Reduction (%)		Actual Reduction (%)	
				Based on hs	Based on ha	Mean	Mean Peak
5	18.5	0.55	0.23	13	9	8	10
	44.2	1.31	1.57	20	22	21	13
	69.9	2.08	2.78	26	30	20	13
10	18.5	0.55	0.23	9	6	5	6
	44.2	1.31	1.57	14	16	23	9
	69.9	2.08	2.78	18	21	19	8
15	18.5	0.55	0.23	8	5	11	9
	44.2	1.31	1.57	12	13	23	10
	69.9	2.08	2.78	15	17	23	9

E.4.2.2 Grindleford Sandstone : Traverse Speed = 1.10 m/s.

Depth of Cut (mm)	Jet Pressure (MPa)	Predicted Jet Penetration hs (mm)	Actual Jet Penetration ha (mm)	Predicted Reduction (%)		Actual Reduction (%)	
				Based on hs	Based on ha	Mean	Mean Peak
5	18.5	0.89	1.20	17	20	17	-11
	44.2	2.13	2.86	26	30	18	16
	69.9	3.37	5.29	33	41	29	35
10	18.5	0.89	1.20	12	14	24	2
	44.2	2.13	2.86	18	21	22	2
	69.9	3.37	5.29	23	29	12	4
15	18.5	0.89	1.20	10	11	3	-9
	44.2	2.13	2.86	18	17	7	-10
	69.9	3.37	5.29	19	24	7	-10

E.4.3.1 Penrith Sandstone : Traverse Speed = 0.27 m/s.

Depth of Cut (mm)	Jet Pressure (MPa)	Predicted Jet Penetration hs (mm)	Actual Jet Penetration ha (mm)	Predicted Reduction (%)		Actual Reduction (%)	
				Based on hs	Based on ha	Mean	Mean Peak
5	18.5	0.44	0.37	12	11	16	6
	44.2	1.04	1.85	18	24	11	0
	69.9	1.65	2.95	23	31	10	3
10	18.5	0.44	0.37	8	8	11	-1
	44.2	1.04	1.85	13	17	16	1
	69.9	1.65	2.95	16	22	24	-5
15	18.5	0.44	0.37	7	6	-4	-7
	44.2	1.04	1.85	11	14	3	-8
	69.9	1.65	2.95	13	18	7	-1

E.4.3.2 Penrith Sandstone : Traverse Speed = 1.10 m/s.

E.5 Measured and Predicted Force Reductions

E.5.1 Grindleford Sandstone (sharp tool)

Depth of Cut (mm)	Traverse Speed (m/s)	Jet Pressure (MPa)	Measured (%)		Predicted (%)	
			cutting	normal	cutting	normal
5	0.27	18.5	21.3	32.2	13.6	19.8
		44.2	28.3	38.9	32.9	46.3
		69.9	29.9	38.9	28.3	36.3
	1.10	18.5	8.1	24.7	4.9	9.7
		44.2	20.8	39.1	21.8	43.7
		69.9	20.1	42.5	19.9	41.1
10	0.27	18.5	16.8	25.6	9.3	17.3
		44.2	12.9	34.8	17.4	39.7
		69.9	6.3	31.4	4.7	29.7
	1.10	18.5	5.0	8.7	5.3	8.9
		44.2	23.0	42.7	22.9	42.5
		69.9	19.3	45.7	19.3	45.8
15	0.27	18.5	4.4	9.3	6.2	11.0
		44.2	15.9	30.5	14.8	29.4
		69.9	11.5	30.0	11.9	30.3
	1.10	18.5	11.2	18.5	5.6	9.5
		44.2	23.4	40.7	25.1	43.4
		69.9	23.0	41.1	22.5	40.3

E.5.2 Penrith Sandstone (sharp tool)

Depth of Cut (mm)	Traverse Speed (m/s)	Jet Presure (MPa)	Measured (%)		Predicted (%)	
			Cutting	normal	cutting	normal
5	0.27	18.5	16.8	32.1	11.4	20.3
		44.2	18.2	26.2	22.1	34.7
		69.9	29.2	31.0	28.4	28.5
	1.10	18.5	15.5	29.0	7.6	19.6
		44.2	11.0	39.9	15.6	45.4
		69.9	9.7	40.6	8.3	38.9
10	0.27	18.5	23.5	42.8	17.2	32.0
		44.2	22.2	46.2	26.6	53.7
		69.9	11.6	41.4	11.1	40.4
	1.10	18.5	10.5	21.6	5.6	13.6
		44.2	16.4	35.6	15.3	40.6
		69.9	23.6	58.6	18.9	57.3
15	0.27	18.5	3.4	18.4	3.7	15.3
		44.2	7.0	27.5	6.8	29.8
		69.9	7.3	39.3	7.3	38.9

E. 5.3 Grindleford Sandtone (Blunt tool)

Depth of Cut (mm)	Traverse Speed (m/s)	Jet Pressure (MPa)	Measured (%)		Predicted (%)	
			Cutting	Normal	Cutting	Normal
10	0.27	18.5	23.1	36.1	15.7	24.9
		44.2	35.1	57.4	39.5	64.1
		69.9	38.1	64.6	36.5	62.2
	1.10	18.5	6.0	21.6	4.4	12.4
		44.2	22.4	57.3	22.9	60.2
		69.9	29.5	68.5	29.4	67.7

APPENDIX F

COMPUTER PROGRAMS FOR DIGITAL DATA LOGGING AND ANALYSIS

F.1 Listing of the Data Logging Program.

F.2 Listing of the Data Analysis Program.

*   *   *

APPENDIX F.1

```
PROGRAM LOGGING;
CONST
  NO OF CHANNELS=3;
  TOP=6000;

TYPE
  INTFILE=FILE OF INTEGER;
  RANGE=0  TOP;

VAR
  ORB  ABSOLUTE [$E808 00] BYTE;
  ORA  ABSOLUTE [$E808 01] BYTE;
  DDRB ABSOLUTE [$E808 02] BYTE;
  DDRA ABSOLUTE [$E808 03] BYTE;
  T1CL ABSOLUTE [$E808 04] BYTE;
  T1CH ABSOLUTE [$E808 05] BYTE;
  T1LL ABSOLUTE [$E808 06] BYTE;
  T1LH ABSOLUTE [$E808 07] BYTE;
  ACR  ABSOLUTE [$E808 11] BYTE;
  PCR  ABSOLUTE [$E808 12] BYTE;
  IFR  ABSOLUTE [$E808 13] BYTE;
  CH 0,CH 1,CH 2   ARRAY [0  TOP] OF INTEGER;
  IORESULT,TIME,PULSES INTEGER;
  LOGNUM,NSTART,NSTOP,NDATUM INTEGER;
  STIME,TTIME,SPEED,LLEN,LEN REAL;
  SAMPLES RANGE;
  ASCIICHAR,ANYCHAR CHAR;
  DATA FILE INTFILE;
  DATUM0,DATUM1 INTEGER;

PROCEDURE DELAY;
VAR
  I INTEGER;
BEGIN
  FOR I =0 TO 1 DO BEGIN END
END;

PROCEDURE INITIALISE;
VAR
  FILE1,FILE2 STRING;
BEGIN
  DDRB  = $FF;
  DDRA  = $00;
  PCR  = $AA;
  ORB  = $00;
  ACR  = $43;
  WRITELN;
  TIME =60;
  WRITE('Type length of cutting in metre          ');
  READLN(LEN);
  WRITE('Type logged length in metre              ');
  READLN(LLEN);
  WRITE('Type travel time in seconds (0 89m)      ');
  READLN(TTIME);
```

```
  SPEED =0 89/TTIME;
  SAMPLES =TRUNC((LEN/SPEED+0 75)*1E6/923);
  NSTART =TRUNC(0 05*1E6/SPEED/923);
  NSTOP =TRUNC((LLEN-0 10)*1E6/SPEED/923);
  NDATUM =SAMPLES-100;
  PULSES  = TIME DIV NO OF CHANNELS;
  T1CL =LO(PULSES);
  T1CH =HI(PULSES);
  WRITE('Type name of file to save on            ');
  READLN(FILE1);
  ASSIGN(DATA FILE,FILE1);
END;

PROCEDURE COLLECT;
VAR
  THRESHOLD,JUNK,POSITION INTEGER;
BEGIN
  POSITION  =0;
  JUNK =T1CL;
  ORB =1;
  DELAY;
  DELAY;
  JUNK = SHL(ORA,4) ! SHR(ORA,4);
  REPEAT;
    JUNK =T1CL;
    ORB =1;
    DELAY;
    THRESHOLD =SHL(ORA,4) ! SHR(ORA,4);
  UNTIL THRESHOLD > 2140;
  JUNK =T1CL; (* RESETS ANY INTERRUPT *)
  REPEAT
    REPEAT UNTIL (IFR & $40 > 0);
    JUNK =T1CL;
    ORB  = 0;
    DELAY;
    CH 0[POSITION]  = SHL(ORA,4) ! SHR(ORA,4);
    REPEAT UNTIL (IFR & $40 > 0);
    JUNK =T1CL;
    ORB  = 1;
    DELAY;
    CH 1[POSITION]  = SHL(ORA,4) ! SHR(ORA,4);
    REPEAT UNTIL (IFR & $40 > 0);
    JUNK =T1CL;
    ORB  = 2;
    DELAY;
    CH 2[POSITION]  = SHL(ORA,4) ! SHR(ORA,4);
    POSITION  = POSITION + 1
  UNTIL POSITION=SAMPLES
END;

PROCEDURE VIEW;
VAR
  I INTEGER;
  ANYCHAR CHAR;
BEGIN
  WRITELN('CHECK DATUM');
  WRITELN('-----------');
```

```
    WRITELN('This is the last 100 readings and the mean is datum');
    WRITELN;
    FOR I =(SAMPLES-99) TO (SAMPLES-81) DO
      WRITELN(I 5,CH 0[I] 10,CH 1[I] 10);
    WRITE('type <CR> to continue     1 of 5');
    READLN(ANYCHAR);
    WRITELN;
    FOR I =(SAMPLES-80) TO (SAMPLES-61) DO
      WRITELN(I 5,CH 0[I] 10,CH 1[I] 10);
    WRITE('type <CR> to continue     2 of 5');
    READLN(ANYCHAR);
    WRITELN;
    FOR I =(SAMPLES-60) TO (SAMPLES-41) DO
      WRITELN(I 5,CH 0[I] 10,CH 1[I] 10);
    WRITE('type <CR> to continue     3 of 5');
    READLN(ANYCHAR);
    WRITELN;
    FOR I =(SAMPLES-40) TO (SAMPLES-21) DO
      WRITELN(I 5,CH 0[I] 10,CH 1[I] 10);
    WRITE('type <CR> to continue     4 of 5');
    READLN(ANYCHAR);
    WRITELN;
    FOR I =(SAMPLES-20) TO (SAMPLES-1) DO
      WRITELN(I 5,CH 0[I] 10,CH 1[I] 10);
    WRITE('O K ? Type <CR> to continue or try again   ');
    READLN(ANYCHAR);
    WRITELN;
    WRITELN('CHECK PRE-RECORDING');
    WRITELN('-------------------');
    FOR I =NSTART TO NSTART+20 DO
      WRITELN(I 5,CH 0[I] 10,CH 1[I] 10);
    WRITE('type <CR> to continue   ');
    READLN(ANYCHAR);
    WRITELN;
    WRITELN('CHECK POST-RECORDING');
    WRITELN('--------------------');
    FOR I =NSTOP TO NSTOP+20 DO
      WRITELN(I 5,CH 0[I] 10,CH 1[I] 10);
    WRITE('type <CR> to continue   ');
    READLN(ANYCHAR);
  END;

  PROCEDURE  EROFIND;
  VAR
    SUM0,SUM1 REAL;
    I INTEGER;
  BEGIN
    SUM0 =0;
    SUM1 =0;
    FOR I =(SAMPLES-100) TO (SAMPLES-1) DO
    BEGIN
      SUM0 =SUM0+CH 0[I];
      SUM1 =SUM1+CH 1[I];
    END;
    DATUM0 =ROUND(SUM0/100);
    DATUM1 =ROUND(SUM1/100);
  END;
```

```
PROCEDURE CHECK;
CONST
  MAX0=0;
  MAX1=4095;
VAR
  I INTEGER;
  ANYCHAR CHAR;
BEGIN
  FOR I =NSTART TO NSTOP DO
  BEGIN
    IF (CH 0[I]=MAX0) OR (CH 1[I]=MAX1) THEN
    BEGIN
      WRITELN;
      WRITELN('Signal OVERFLOWS and GALVO AMP must be reset!');
      WRITE('RE-BOOT and try again    ');
      READLN(ANYCHAR);
    END;
  END;
END;

PROCEDURE STORE DATA;
VAR
  POSITION INTEGER;
BEGIN
  LOGNUM =NSTOP-NSTART+1;
  REWRITE(DATA FILE);
  WRITE(DATA FILE,LOGNUM,TIME);
  WRITE(DATA FILE,DATUM0,DATUM1);
  FOR POSITION =NSTART TO NSTOP DO
    WRITE(DATA FILE,CH 0[POSITION],CH 1[POSITION],CH 2[POSITION]);
  CLOSE(DATA FILE,IORESULT)
END;


BEGIN (* THIS IS THE MAIN PROGRAM *)
REPEAT
  INITIALISE;
  WRITELN('type any key to start    ');
  READ(ASCIICHAR);
  COLLECT;
  WRITELN;
  WRITELN(chr(7),'finished');
  WRITELN;
  VIEW;
  WRITELN;
   EROFIND;
  CHECK;
  WRITELN('data storing starts    ');
  STORE DATA;
  WRITELN('                finished');
  WRITELN;
  WRITE('anymore? y/n    ');
  READLN(ASCIICHAR);
UNTIL (ASCIICHAR='N') OR (ASCIICHAR='n')
END
```

APPENDIX F.2

```
program analysis; (*$R+*)
const
  maxdata=5000;
  datum2=2045;
  cf2=0 058337;
type
  ary=array [0  maxdata] of integer;
  intfile=file of integer;
var
  ch0,ch1,ch2 ary;
  mean0,mean1,mean2,mpcf,mpnf,sd0,sd1,cf0,cf1 real;
  ttime,ioresult,noofdata,datum0,datum1 integer;
  datafile intfile;
  result text;
  asciichar,anychar char;

PROCEDURE cfactor;
var
  factor0,factor1 integer;
BEGIN
  WRITE('Type cutting force conversion factor    ');
  READLN(Factor0);
  if factor0=1 then cf0 =-0 005884 else
  if factor0=2 then cf0 =-0 011723 else
  if factor0=3 then cf0 =-0 002389 else
  if factor0=4 then cf0 =-0 004759 else cf0 =0 02937;
  WRITE('Type normal force conversion factor     ');
  READLN(Factor1);
  if factor1=1 then cf1 =0 004534 else
  if factor1=2 then cf1 =0 009026 else
  if factor1=3 then cf1 =0 001963 else
  if factor1=4 then cf1 =0 003909 else cf1 =0 022645;
END;

procedure initiali ation;
var
  file1,file2 string;
begin
  write('type name of datafile             ');
  readln(file1);
  assign(datafile,file1);
  write('type name of result file          ');
  readln(file2);
  assign(result,file2);
end;

procedure readdata;
var
  count integer;
begin
  reset(datafile);
  read(datafile,noofdata,ttime);
  read(datafile,datum0,datum1);
  noofdata =trunc(noofdata/10)*10;
```

```
  writeln('data reading+analysis+sorting ');
  for count =1 to noofdata do
    read(datafile,ch0[count],ch1[count],ch2[count]);
end;

PROCEDURE calculation;
VAR
  N,I INTEGER;
  ANYCHAR CHAR;
  v0,v1,sumsq0,sumsq1,temp0,temp1,SUM0,SUM1,sum2 REAL;
BEGIN
  SUM0 =0;
  SUM1 =0;
  sum2 =0;
  FOR I =1 TO noofdata DO
  BEGIN
    sum0 =sum0+ch0[i];
    sum1 =sum1+ch1[i];
    sum2 =sum2+ch2[i];
  END;
  mean0 =(sum0/noofdata-datum0)*cf0;
  mean1 =(sum1/noofdata-datum1)*cf1;
  mean2 =(sum2/noofdata-datum2)*cf2;
END;

procedure swop(var p,q integer);
var
  hold integer;
begin
  hold =p;
  p =q;
  q =hold;
end(*swop*);

procedure (*quick*)sort(var x ary;nn integer);
var
  left,right array[1  500] of integer;
  i,j,sp,mid integer;
  pivot integer;
begin
  left[1] =1;
  right[1] =nn;
  sp =1;
  while sp>0 do
    begin
      if left[sp] >= right[sp] then sp =sp-1
      else
      begin
        i =left[sp];
        j =right[sp];
        pivot =x[j];
        mid =(i+j) div 2;
        if (j-i) > 5 then
          if ((x[mid] < pivot) and (x[mid] > x[i]))
            or
            ((x[mid] > pivot) and (x[mid] < x[i]))
          then swop(x[mid],x[j])
```

```
        else
          if ((x[i] < x[mid]) and (x[i] > pivot))
            or
            ((x[i] > x[mid]) and (x[i] < pivot))
          then swop(x[i],x[j]);
        pivot =x[j];
        while i < j do
          begin
            while x[i] < pivot do
              i =i+1;
              j =j-1;
            while (i < j) and (pivot < x[j]) do
              j =j-1; .
            if i < j then swop(x[i],x[j]);
          end(*while*);
        j =right[sp](*pivot to i*);
        swop(x[i],x[j]);
        if i-left[sp] >=right[sp] -i then
          begin(*put shorter part first*)
            left[sp+1] =left[sp];
            right[sp+1] =i-1;
            left[sp] =i+1;
          end
        else
          begin
            left[sp+1] =i+1;
            right[sp+1] =right[sp];
            right[sp] =i-1;
          end;
        sp =sp+1(*push stack*);
      end(*if*);
    end(*while*);
  end;

procedure meanpeak;
var
  j,k,p,q,i integer;
begin
  k =trunc(noofdata*0 05-0 5);
  j =trunc(noofdata*0 95+0 5);
  MPCF =(ch0[k]-datum0)*cf0;
  MPNF =(ch1[j]-datum1)*cf1;
end;

PROCEDURE VIEW;
BEGIN
  WRITELN('RESULT');
  WRITELN('======');
  WRITELN;
  WRITELN('DATA LOGGED                                  ',noofdata 10);
  WRITELN('M C F                                        ',MEAN0 10 2,' kN');
  WRITELN('M N F                                        ',MEAN1 10 2,' kN');
  WRITELN('95% M P C F                                  ',MPCF 10 2,' kN');
  WRITELN('95% M P N F                                  ',MPNF 10 2,' kN');
  writeln('PRESSURE                                     ',MEAN2 10 1,' MPa');
  WRITELN;
  WRITE('type <CR> to continue   ');
```

```
  READLN(ASCIICHAR);
  WRITELN;
END;

PROCEDURE RESULTOUT;
VAR
  P,I INTEGER;
BEGIN
  REWRITE(RESULT);
  WRITELN(RESULT,'LOGGED DATA                ',NOOFDATA 10);
  WRITELN(RESULT,'DATUM 0                    ',DATUM0 10);
  WRITELN(RESULT,'DATUM 1                    ',DATUM1 10);
  WRITELN(RESULT,'C F  0                     ',CF0 10 6);
  WRITELN(RESULT,'C F  1                     ',CF1 10 6);
  WRITELN(RESULT,'M C F                      ',MEAN0 10 2,' kN');
  WRITELN(RESULT,'M N F                      ',MEAN1 10 2,' kN');
  WRITELN(RESULT,'95% M P C F                ',MPCF 10 2,' kN');
  WRITELN(RESULT,'95% M P N F                ',MPNF 10 2,' kN');
  WRITELN(RESULT,'PRESSURE                   ',MEAN2 10 1,' MPa');
  CLOSE(RESULT,IORESULT);
END;

begin(*main program*);
CFACTOR;
 repeat
  writeln;
  initiali ation;
  readdata;
  calculation;
  sort(ch0,noofdata);
  sort(ch1,noofdata);
  meanpeak;
  writeln;
  view;
  resultout;
  writeln;
  write('continue? y/n   ');
  readln(anychar);
 until (anychar='n') or (anychar='N');
end
```

APPENDIX G

RESULTS OF THE STUDY OF THE EFFECTS OF MOISTURE CONTENT ON THE CUTTABILITY OF ROCKS

Rock	Density (kg/m^3)	Porosity (%)	Uniaxial Compressive Strength (MPa)	
			Dry	Wet
Gypsum	2114	-	22.0	8.3
Red Sandstone	2265	11.3	52.9	34.11
Marble	2590	0.4	69.3	65.5
Concrete	2180	-	20.8	14.9
Grey Sandstone	2440	7.2	77.8	32.1
Chalk	2227	14.0	58.2	17.8
Darney Sandstone	2094	16.0	47.9	18.8
Doddington Sandstone	2036	18.0	37.1	17.1
Anhydrite	2880	0.8	75.7	27.8

G.1 Physical and Mechanical Properties.

Rock Type	MPCF (kN)	MCF (kN)	MPNF (kN)	MNF (kN)	S.E. MJ/m^3	C.I.	Yield km/m^3
Gypsum	6.58	2.20	3.95	2.20	22.60	373.2	0.089
Red Sandstone	7.46	1.70	4.70	2.00	14.59	357.9	0.118
Marble	10.04	3.10	6.76	3.30	34.85	375.8	0.100
Concrete	5.96	1.20	3.42	1.30	12.47	389.4	0.104
Grey Sandstone	6.39	1.70	3.68	1.50	17.37	413.1	0.096
Chalk	6.26	1.80	3.88	1.80	13.05	439.8	0.139
Darney Sandstone	4.57	0.80	2.60	0.80	6.46	343.3	0.126
Sandstone	4.70	0.80	2.29	0.80	5.46	359.1	0.145
Anhydrite	17.42	3.21	10.68	5.85	34.25	369.3	0.094

G.2 <u>Summary of Results : Dry Cutting</u>

Rock Type	MPCF (kN)	MCF (kN)	MPNF (kN)	MNF (kN)	S.E. MJ/m^3	C.I.	Yield (kN/m^3)
Gypsum	4.26	1.30	2.54	1.30	20.78	350.3	0.063
Red Sandstone	6.91	1.60	4.38	2.10	16.94	326.1	0.104
Marble	9.67	3.13	6.48	3.55	34.69	374.9	0.099
Concrete	5.66	1.50	3.54	1.40	15.98	378.8	0.095
Grey Sandstone	5.11	1.40	3.00	1.20	14.71	410.6	0.099
Chalk	5.72	1.40	3.91	1.60	14.27	415.5	0.096
Darney Sandstone	3.38	1.10	2.12	0.90	10.28	335.3	0.105
Sandstone	3.35	0.90	2.39	0.70	5.36	358.1	0.173
Anhydrite	12.25	3.02	8.60	4.18	31.09	384.3	0.098

G.3 Summary of Results : Wet Cutting

Frontispiece	117/83
Plate 2.1	117/83
Plate 4.1	83/83
4.2	82/83
4.3	82/83
4.4	117/83
4.5	82/83
4.6	82/83
4.7	28/86
4.8	28/86
4.9	28/86
4.10	99/83
4.11	3/86
Plate 5.1	97/83
5.2	26/79
Plate 6.1	3/86
6.2	3/86
Plate 8.1	14/86
8.2	14/86
Plate 10.1	68/84
Plate 12.1	62/83